

JPTM

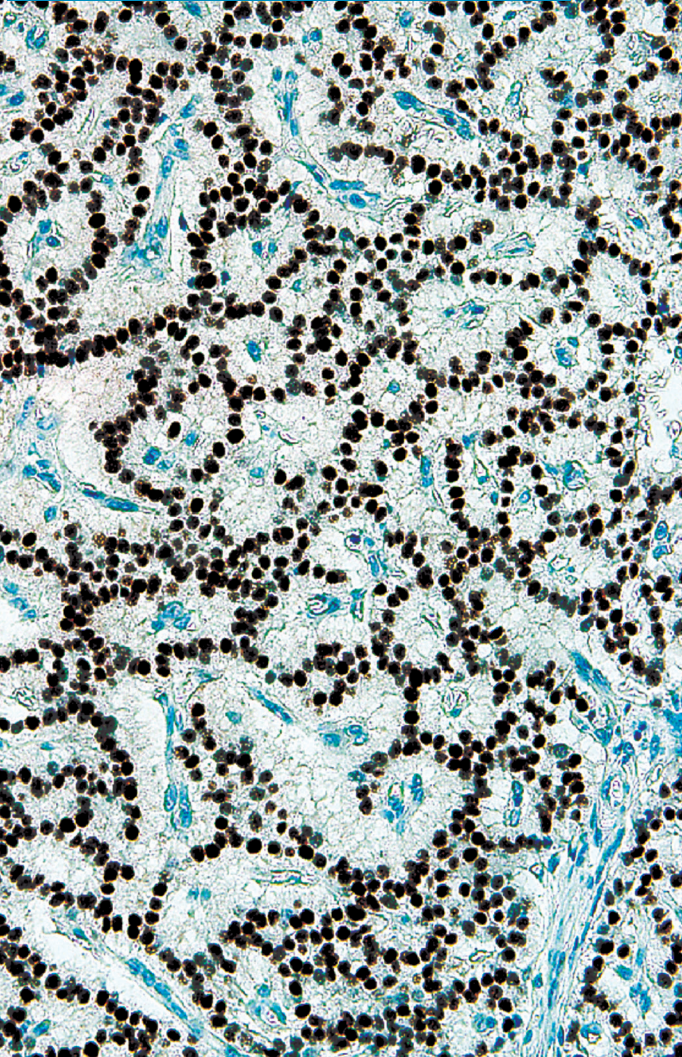
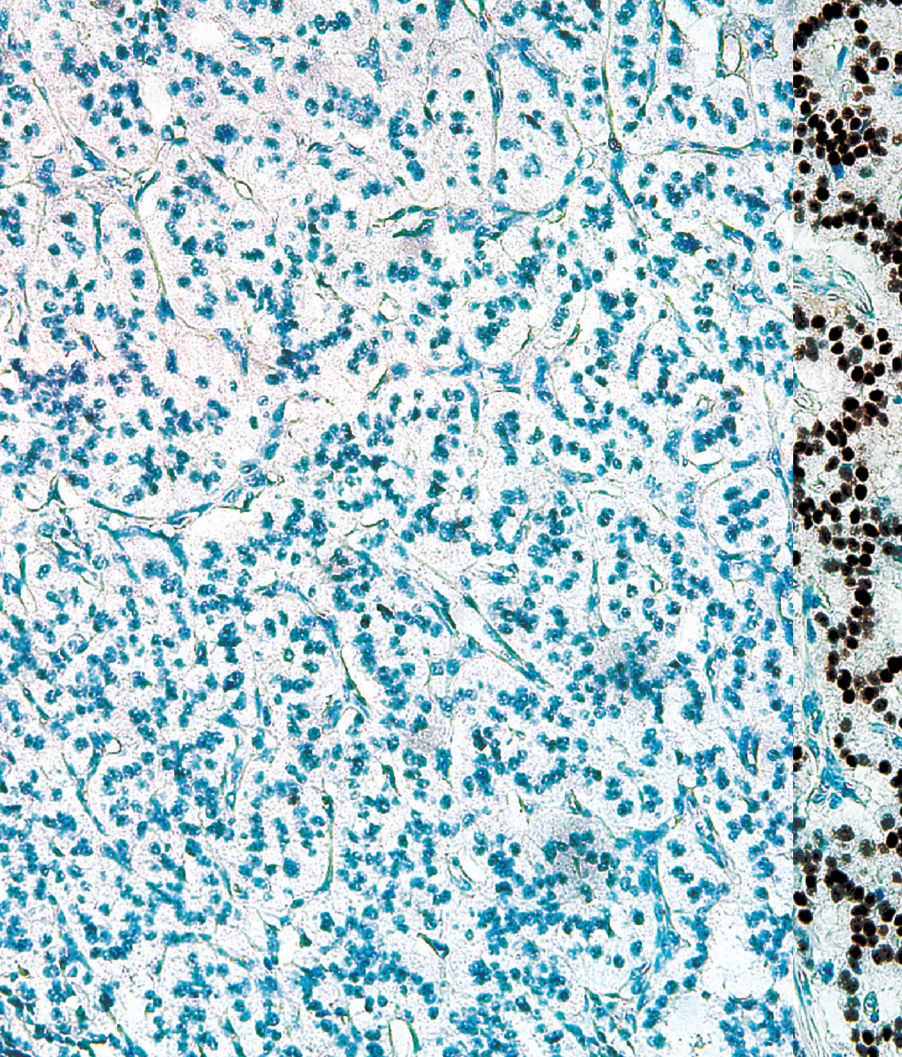
**Journal of Pathology
and Translational Medicine**

July 2017
Vol. 51 / No.4
jpatholtm.org
pISSN: 2383-7837
eISSN: 2383-7845



*Rare Gastric Lesions Associated
with Helicobacter pylori Infection:
A Histopathological Review*

*Epstein-Barr Virus-Associated
Lymphoproliferative Disorders:
Review and Update on 2016 WHO
Classification*



Aims & Scope

The *Journal of Pathology and Translational Medicine* is an open venue for the rapid publication of major achievements in various fields of pathology, cytopathology, and biomedical and translational research. The Journal aims to share new insights into the molecular and cellular mechanisms of human diseases and to report major advances in both experimental and clinical medicine, with a particular emphasis on translational research. The investigations of human cells and tissues using high-dimensional biology techniques such as genomics and proteomics will be given a high priority. Articles on stem cell biology are also welcome. The categories of manuscript include original articles, review and perspective articles, case studies, brief case reports, and letters to the editor.

Subscription Information

To subscribe to this journal, please contact the Korean Society of Pathologists/the Korean Society for Cytopathology. Full text PDF files are also available at the official website (<http://jpatholm.org>). *Journal of Pathology and Translational Medicine* is indexed by Emerging Sources Citation Index (ESCI), PubMed, PubMed Central, Scopus, KoreaMed, KoMCI, WPRIM, Directory of Open Access Journals (DOAJ), and CrossRef. Circulation number per issue is 700.

Editors-in-Chief

Hong, Soon Won, MD (*Yonsei University, Korea*)

Kim, Chong Jai, MD (*University of Ulsan, Korea*)

Associate Editors

Jung, Chan Kwon, MD (*The Catholic University of Korea, Korea*)

Park, So Yeon, MD (*Seoul National University, Korea*)

Shin, Eunah, MD (*CHA University, Korea*)

Kim, Haeryoung, MD (*Seoul National University, Korea*)

Editorial Board

Ali, Syed Z. (*Johns Hopkins Hospital, U.S.A.*)

Avila-Casado, Maria del Carmen (*University of Toronto, Toronto General Hospital UHN, Canada*)

Bae, Young Kyung (*Yeungnam University, Korea*)

Bongiovanni, Massimo (*Centre Hospitalier Universitaire Vaudois, Switzerland*)

Cho, Kyung-Ja (*University of Ulsan, Korea*)

Choi, Yeong-Jin (*The Catholic University of Korea, Korea*)

Choi, Yoo Duk (*Chonnam National University, Korea*)

Chung, Jin-Haeng (*Seoul National University, Korea*)

Gong, Gyungyub (*University of Ulsan, Korea*)

Fadda, Guido (*Catholic University of the Sacred Heart, Italy*)

Grignon, David J. (*Indiana University, U.S.A.*)

Ha, Seung Yeon (*Gachon University, Korea*)

Han, Jee Young (*Inha University, Korea*)

Jang, Se Jin (*University of Ulsan, Korea*)

Jeong, Jin Sook (*Dong-A University, Korea*)

Kang, Gyeong Hoon (*Seoul National University, Korea*)

Katoh, Ryohei (*University of Yamanashi, Japan*)

Kerr, Keith M. (*Aberdeen University Medical School, U.K.*)

Kim, Aeree (*Korea University, Korea*)

Kim, Jang-Hee (*Ajou University, Korea*)

Kim, Jung Ho (*Seoul National University, Korea*)

Kim, Kyoung Mee (*Sungkyunkwan University, Korea*)

Kim, Kyu Rae (*University of Ulsan, Korea*)

Kim, Se Hoon (*Yonsei University, Korea*)

Kim, Woo Ho (*Seoul National University, Korea*)

Kim, Youn Wha (*Kyung Hee University, Korea*)

Ko, Young Hye (*Sungkyunkwan University, Korea*)

Koo, Ja Seung (*Yonsei University, Korea*)

Lee, C. Soon (*University of Western Sydney, Australia*)

Lee, Hye Seung (*Seoul National University, Korea*)

Lee, Kyung Han (*Sungkyunkwan University, Korea*)

Lee, Sug Hyung (*The Catholic University of Korea, Korea*)

Lkhagvadorj, Sayamaa (*Mongolian National University of Medical Sciences, Mongolia*)

Moon, Woo Sung (*Chonbuk University, Korea*)

Ngo, Quoc Dat (*Ho Chi Minh University of Medicine and Pharmacy, VietNam*)

Park, Young Nyun (*Yonsei University, Korea*)

Ro, Jae Y. (*Cornell University, The Methodist Hospital, U.S.A.*)

Romero, Roberto (*National Institute of Child Health and Human Development, U.S.A.*)

Schmitt, Fernando (*IPATIMUP [Institute of Molecular Pathology and Immunology of the University of Porto], Portugal*)

Shahid, Pervez (*Aga Khan University, Pakistan*)

Sung, Chang Ohk (*University of Ulsan, Korea*)

Tan, Puay Hoon (*National University of Singapore, Singapore*)

Than, Nandor Gabor (*Semmelweis University, Hungary*)

Tse, Gary M. (*Prince of Wales Hospital, Hongkong*)

Vielh, Philippe (*International Academy of Cytology Gustave Roussy Cancer Campus Grand Paris, France*)

Wildman, Derek (*University of Illinois, U.S.A.*)

Yatabe, Yasushi (*Aichi Cancer Center, Japan*)

Yoon, Bo Hyun (*Seoul National University, Korea*)

Yoon, Sun Och (*Yonsei University, Korea*)

Statistics Editors

Kim, Dong Wook (*National Health Insurance Service Ilsan Hospital, Korea*)

Lee, Hye Sun (*Yonsei University, Korea*)

Manuscript Editor

Chang, Soo-Hee (*InfoLumi Co., Korea*)

Contact the Korean Society of Pathologists/the Korean Society for Cytopathology

Publishers: Han Kyeom Kim, MD, Hye Kyoung Yoon, MD

Editors-in-Chief: Soon Won Hong, MD, Chong Jai Kim, MD

Published by the Korean Society of Pathologists/the Korean Society for Cytopathology

Editorial Office

Room 1209 Gwanghwamun Officia, 92 Saemunan-ro, Jongno-gu, Seoul 03186, Korea

Tel: +82-2-795-3094 Fax: +82-2-790-6635 E-mail: office@jpatholm.org

#1508 Renaissancetower, 14 Mallijae-ro, Mapo-gu, Seoul 04195, Korea

Tel: +82-2-593-6943 Fax: +82-2-593-6944 E-mail: office@jpatholm.org

Printed by iMiS Company Co., Ltd. (JMC)

Jungang Bldg. 18-8 Wonhyo-ro 89-gil, Yongsan-gu, Seoul 04314, Korea

Tel: +82-2-717-5511 Fax: +82-2-717-5515 E-mail: ml@smilem.com

Manuscript Editing by InfoLumi Co.

210-202, 421 Pangyo-ro, Bundang-gu, Seongnam 13522, Korea

Tel: +82-70-8839-8800 E-mail: infolumi.chang@gmail.com

Front cover image: Progesterone receptor (PR) labeling in normal pancreas, neuroendocrine microadenoma, and pancreatic neuroendocrine tumor (PanNET) (Fig. 1). p390.

© Copyright 2017 by the Korean Society of Pathologists/the Korean Society for Cytopathology

© Journal of Pathology and Translational Medicine is an Open Access journal under the terms of the Creative Commons Attribution Non-Commercial License (<http://creativecommons.org/licenses/by-nc/4.0>).

© This paper meets the requirements of KS X ISO 9706, ISO 9706-1994 and ANSI/NISO Z.39.48-1992 (Permanence of Paper).

This journal was supported by the Korean Federation of Science and Technology Societies Grant funded by the Korean Government.

CONTENTS

REVIEWS

- 341 Rare Gastric Lesions Associated with *Helicobacter pylori* Infection: A Histopathological Review
Mee Joo
- 352 Epstein-Barr Virus-Associated Lymphoproliferative Disorders: Review and Update on 2016 WHO Classification
Hyun-Jung Kim, Young Hyeoh Ko, Ji Eun Kim, Seung-Sook Lee, Hyekyung Lee, Gyeongsin Park, Jin Ho Paik, Hee Jeong Cha, Yoo-Duk Choi, Jae Ho Han, Jooryung Huh, Hematopathology Study Group of the Korean Society of Pathologists

ORIGINAL ARTICLES

- 359 Implication of PHF2 Expression in Clear Cell Renal Cell Carcinoma
Cheol Lee, Bohyun Kim, Boram Song, Kyung Chul Moon
- 365 Yes-Associated Protein Expression Is Correlated to the Differentiation of Prostate Adenocarcinoma
Myung-Giun Noh, Sung Sun Kim, Eu Chang Hwang, Dong Deuk Kwon, Chan Choi
- 374 Basaloid Squamous Cell Carcinoma of the Head and Neck: Subclassification into Basal, Ductal, and Mixed Subtypes Based on Comparison of Clinico-pathologic Features and Expression of p53, Cyclin D1, Epidermal Growth Factor Receptor, p16, and Human Papillomavirus
Kyung-Ja Cho, Se-Un Jeong, Sung Bae Kim, Sang-wook Lee, Seung-Ho Choi, Soon Yuhl Nam, Sang Yoon Kim
- 381 Morphological Features and Immunohistochemical Expression of p57Kip2 in Early Molar Pregnancies and Their Relations to the Progression to Persistent Trophoblastic Disease
Marwa Khashaba, Mohammad Arafa, Eman Elsalkh, Reda Hemida, Wagiha Kandil
- 388 Loss of Progesterone Receptor Expression Is an Early Tumorigenesis Event Associated with Tumor Progression and Shorter Survival in Pancreatic Neuroendocrine Tumor Patients
Sung Joo Kim, Soyeon An, Jae Hoon Lee, Joo Young Kim, Ki-Byung Song, Dae Wook Hwang, Song Cheol Kim, Eunsil Yu, Seung-Mo Hong
- 396 HER2 Status and Its Heterogeneity in Gastric Carcinoma of Vietnamese Patient
Dang Anh Thu Phan, Vu Thien Nguyen, Thi Ngoc Ha Hua, Quoc Dat Ngo, Thi Phuong Thao Doan, Sao Trung Nguyen, Anh Tu Thai, Van Thanh Nguyen
- 403 Prognostic Significance of a Micropapillary Pattern in Pure Mucinous Carcinoma of the Breast: Comparative Analysis with Micropapillary Carcinoma
Hyun-Jung Kim, Kyeongmee Park, Jung Yeon Kim, Guhyun Kang, Geumhee Gwak, Inseok Park

-
- 410 **The Use of the Bethesda System for Reporting Thyroid Cytopathology in Korea: A Nationwide Multicenter Survey by the Korean Society of Endocrine Pathologists**
Mimi Kim, Hyo Jin Park, Hye Sook Min, Hyeong Ju Kwon, Chan Kwon Jung, Seoung Wan Chae, Hyun Ju Yoo, Yoo Duk Choi, Mi Ja Lee, Jeong Ja Kwak, Dong Eun Song, Dong Hoon Kim, Hye Kyung Lee, Ji Yeon Kim, Sook Hee Hong, Jang Sihm Sohn, Hyun Seung Lee, So Yeon Park, Soon Won Hong, Mi Kyung Shin

CASE REPORTS

- 418 **Metaplastic Carcinoma with Chondroid Differentiation Arising in Microglandular Adenosis**
Ga-Eon Kim, Nah Ihm Kim, Ji Shin Lee, Min Ho Park
- 422 **Mammary Carcinoma Arising in Microglandular Adenosis: A Report of Five Cases**
Mimi Kim, Milim Kim, Yul Ri Chung, So Yeon Park
- 428 **Perivascular Epithelioid Cell Tumor in the Stomach**
Sun Ah Shin, Jiwoon Choi, Kyung Chul Moon, Woo Ho Kim
- 433 **A Rare Case of Intramural Müllerian Adenosarcoma Arising from Adenomyosis of the Uterus**
Sun-Jae Lee, Ji Y. Park
- 441 **Metastatic Squamous Cell Carcinoma from Lung Adenocarcinoma after Epidermal Growth Factor Receptor Tyrosine Kinase Inhibitor Therapy**
Hyung Kyu Park, Youjeong Seo, Yoon-La Choi, Myung-Ju Ahn, Joungho Han
- 444 **Bronchial Washing Cytology of Pulmonary Langerhans Cell Histiocytosis: A Case Report**
Taeyoung Kim, Hyeong Ju Kwon, Minseob Eom, Sang Wook Kim, Min Hi Sin, Soon-Hee Jung

Instructions for Authors for *Journal of Pathology and Translational Medicine* are available at <http://jpatholm.org/authors/authors.php>

Rare Gastric Lesions Associated with *Helicobacter pylori* Infection: A Histopathological Review

Mee Joo

Department of Pathology, Inje University Ilsan Paik Hospital, Goyang, Korea

Received: November 10, 2016

Accepted: April 3, 2017

Corresponding Author

Mee Joo, MD, PhD

Department of Pathology, Inje University Ilsan Paik Hospital, 170 Juhwa-ro, Ilsanseo-gu, Goyang 10380, Korea
Tel: +82-31-910-7141
Fax: +82-31-910-7139
E-mail: mjoo@paik.ac.kr

Helicobacter pylori infection is associated with chronic gastritis, peptic ulcer disease, gastric adenocarcinoma, and mucosa-associated lymphoid tissue lymphoma. However, some rare gastric lesions exhibiting distinctive histological features may also be associated with *H. pylori* infection, including lymphocytic gastritis, granulomatous gastritis, Russell body gastritis, or crystal-storing histiocytosis. Although diverse factors can contribute to their development, there is convincing evidence that *H. pylori* infection may play a pathogenic role. These findings are mainly based on studies in patients with these lesions who exhibited clinical and histological improvements after *H. pylori* eradication therapy. Thus, *H. pylori* eradication therapy might be indicated in patients with no other underlying disease, particularly in countries with a high prevalence of *H. pylori* infection. This review describes the characteristic histological features of these rare lesions and evaluates the evidence regarding a causative role for *H. pylori* infection in their pathogenesis.

Key Words: *Helicobacter pylori*; Stomach; Gastritis; Rare; Immunoglobulins

Helicobacter pylori is a common gastric pathogen that causes gastritis, peptic ulcer disease, gastric adenocarcinoma, and mucosa-associated lymphoid tissue (MALT) lymphoma. *H. pylori* infection has been linked to a number of rare gastric mucosal lesions with distinctive histological features, including rare forms of gastritis, such as lymphocytic gastritis (LG)¹⁻⁵ or granulomatous gastritis (GG),^{3,4,6,7} and abnormal immunoglobulin deposits, such as Russell body gastritis (RBG)^{8,9} or crystal-storing histiocytosis (CSH).^{10,11} These lesions are easily diagnosed based on their distinctive histological features; however, their development can be attributed to various factors besides *H. pylori* infection. Therefore, the role of *H. pylori* as a causative organism remains debatable, and it has been suggested that *H. pylori* may be an “innocent bystander.”^{2,4,12} Nevertheless, *H. pylori* eradication therapy has been linked to clinical and histological improvements in a subset of these lesions,^{7,13-21} which supports the role of *H. pylori* infection in their development and implies that *H. pylori* eradication therapy could be an effective treatment. Therefore, in this review, we investigate the relationship between these rare gastric lesions and *H. pylori* infection, describe their characteristic histological features, and evaluate the role of *H. pylori* infection in their pathogenesis.

RARE FORMS OF GASTRITIS

LG and GG are not distinct clinicopathological entities, but rather morphologic patterns of injury that can be secondary to a variety of underlying etiologies.^{2-4,6} The histological identification of intraepithelial lymphocytosis and granuloma formation are key diagnostic features of LG and GG, respectively.¹⁻⁷ However, a morphological diagnosis of LG and GG should elicit clinical and laboratory workups to identify the underlying etiology. In Western countries, LG and GG are generally classified as special forms of *H. pylori*-negative gastritis.^{3,4} However, there is convincing evidence that *H. pylori* infection contributes to the pathogenesis of both LG^{1,5} and GG,^{6,7,22} and that *H. pylori* eradication therapy may be an effective treatment.^{7,13-15,17,23,24} Thus, it is possible that subsets of LG and GG could be categorized as *H. pylori*-associated gastritis. The potential role of *H. pylori* infection in the pathogenesis of each of these lesions is described below, along with their histopathological characteristics.

Lymphocytic gastritis

LG, first described by Haot *et al.*²⁵ in 1988, is a rare form of chronic gastritis that is characterized by a dense lymphocytic infiltration of the surface and pit gastric epithelium known as “intraepithelial lymphocytosis.” LG was initially considered to be

related to varioliform gastritis, which manifests as thickened mucosa with “octopus-sucker” targetoid erosions;^{25,26} however, the endoscopic features of LG vary according to its severity, ranging from normal to hypertrophic.^{2,27} Histologically, LG is defined by the presence of ≥ 25 intraepithelial lymphocytes (IELs) per 100 epithelial cells (Fig. 1). Gastric intraepithelial lymphocytosis is associated with a variety of conditions, including celiac disease, *H. pylori* infection, Crohn disease, syphilis, hypertrophic gastropathy, Ménétrier’s disease, human immunodeficiency virus, and lymphoma.²⁵ However, celiac disease and *H. pylori* infection are the main causes of LG, accounting for 38% and 29% of cases, respectively.^{5,13,28} The association between LG and celiac disease is relatively well established. Mild intraepithelial lymphocytosis with a low cut-off value (≥ 8 IELs/100 epithelial cells) has been observed in 84% of patients with celiac disease,²⁹ and LG occurs in up to 45% of patients, with resolution of LG in response to a gluten-free diet.^{5,13,28-30}

However, questions remain regarding the role of *H. pylori* infection in the development of LG due to the discrepancy between the prevalence of *H. pylori* in the general population and the inci-

dence of LG among patients with *H. pylori*-associated gastritis.^{2,4} Given the high global prevalence of *H. pylori* infection, it is unclear why the proportion of *H. pylori*-infected patients presenting with LG morphology ($< 5\%$) is so low.⁵ Nevertheless, *H. pylori* eradication therapy can resolve *H. pylori*-associated LG by reducing IEL levels, and has been shown to improve symptoms and/or lead to regression of the gastritis,¹³⁻¹⁶ which supports a causal role of *H. pylori* infection in the development of LG. Previous studies have reported that *H. pylori*-associated LG frequently exhibits significant neutrophilic activity in addition to intraepithelial lymphocytosis,^{2,3,16,27} which is distinct from celiac disease-associated LG that exhibits intraepithelial lymphocytosis without neutrophilic infiltration. In this context, Nielsen *et al.*²⁷ argued that *H. pylori*-associated intraepithelial lymphocytosis accompanied with significant neutrophilic infiltration should be considered “chronic active gastritis,” rather than LG. However, considering the fact that LG is a morphological diagnosis that is based on the presence of intraepithelial lymphocytosis (≥ 25 IELs per 100 epithelial cells), the use of the term “LG” remains relevant.

Interestingly, a considerable number of patients with LG and

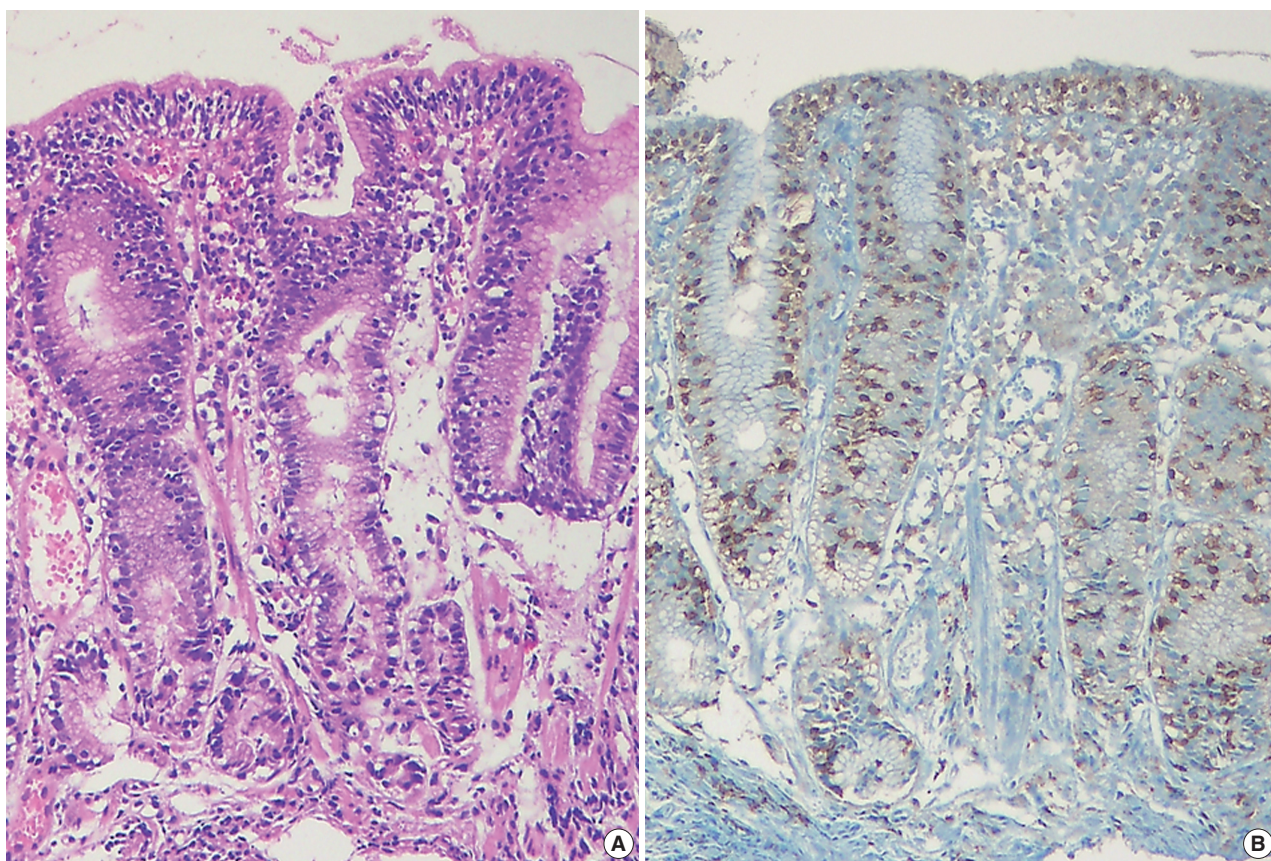


Fig. 1. Lymphocytic gastritis. (A) The biopsy specimen shows a marked increase in intraepithelial lymphocytes (IELs) (over 25 IELs per 100 epithelial cells) with a top-heavy distribution. (B) Most IELs are positive for CD3 immunostaining.

positive *H. pylori* serology did not exhibit histological evidence of *H. pylori* infection.^{1,14,15,27} In addition, the beneficial effects of *H. pylori* eradication therapy in LG have been observed in patients who had positive serology but negative histology for *H. pylori*.^{14,15} Furthermore, even when *H. pylori* infection has been histologically confirmed in patients with LG, colonization tends to be mild and focal.^{14,15} These results imply that failure to histologically detect *H. pylori* may be related to sampling error due to low-level infection.²⁷ Also, it is possible that LG development is a local, transient, or delayed immunological reaction to *H. pylori* infection, and is not a direct effect of the infection.^{1,13,14,27} Thus, if other causes can be excluded, *H. pylori* eradication therapy could be considered in symptomatic patients with LG who are histologically and/or serologically positive for *H. pylori*. This approach may be more appropriate in countries with a low prevalence of celiac disease and a high prevalence of *H. pylori* infection, even without histological detection of *H. pylori*.

IELs are functionally and phenotypically distinct from peripheral lymphocytes, and the majority of IELs in the gastrointestinal epithelium are CD3⁺/CD8⁺ T cells with cytotoxic potential.³¹ These IELs are thought to play an important role in mucosal immunity and have also been implicated in epithelial cell turnover by eliciting apoptosis through cytotoxic T-lymphocytes (CTLs).^{31,32} Recently, Han *et al.*³³ studied IEL subpopulations and their cytotoxicity in *H. pylori*-infected gastric mucosa using T-cell-restricted intracellular antigen-1 (TIA-1; a marker for resting and activated CTLs) and granzyme B (GrB; a marker for activated CTLs). They found that the IELs consisted of a mixture of TIA-1⁺/GrB⁻ CTLs, TIA-1⁺/GrB⁺ CTLs, and CD4⁺ T cells in the infected mucosa. In addition, they found that *H. pylori*-associated LG was distinct from *H. pylori* gastritis, based on the increased IEL levels and changes in the cytotoxicity and distribution of the subpopulations: *H. pylori*-associated LG had a higher proportion of activated GrB⁺ CTLs, compared to *H. pylori* gastritis. There was also a parallel increase in epithelial apoptosis. Meanwhile, in a study by Oberhuber *et al.*,³⁴ the proportion of GrB⁺ CTLs in *H. pylori*-associated LG (10.8%) was lower than that in idiopathic LG (12%) or celiac disease-associated LG (18.9%). Thus, although LG exhibits consistent histological features (regardless of etiology), IEL characteristics may vary depending on the underlying condition, which can lead to different clinical manifestations.

Granulomatous gastritis

GG is a rare disease that is characterized by the presence of granulomas, and is detected in 0.01%–0.35% of gastric biop-

sies.^{6,7,17,35} GG can be caused by a number of factors, including systemic disease (e.g., Crohn disease, sarcoidosis, or vasculitis), infection (e.g., tuberculosis, histoplasmosis, or syphilis), underlying malignancy, or foreign bodies.^{4,6,7,36} Crohn's disease and gastric sarcoidosis are the two leading causes of GG, accounting for 20%–50% of cases in Western countries.^{6,35} Isolated or idiopathic granulomatous gastritis (IGG) was first described by Fakhimi *et al.*³⁷ in 1965, and is diagnosed by the exclusion of other granulomatous diseases. However, whether IGG can be considered a discrete condition remains controversial, as it is possible that a clear etiology could be identified through a more meticulous clinical work-up and long-term follow-up.

Dhillon and Sawyerr²² first reported an association between GG and *H. pylori* infection in 1989. Since then a number of reports have been published that support their findings.^{6,7,17,18,23,24,38–42} These reports demonstrated that the mucosa surrounding granulomas in GG exhibits typical histological features of *H. pylori* gastritis, that features suggestive of other etiologies are absent, and that *H. pylori* eradication therapy can result in GG resolution. However, whether *H. pylori* plays a causative role in the pathogenesis of GG remains debatable. First, the incidence of GG is abnormally low relative to the *H. pylori* prevalence in the general population.^{6,7,12,35} Although Ectors *et al.*⁶ and Maeng *et al.*⁷ have reported the presence of *H. pylori* in 92% and 89% of GG cases, respectively, the overall incidences of GG were only 0.27% and 0.08%, respectively. Second, *H. pylori* organisms are rarely found within granulomas, implying *H. pylori* infection is a comorbidity rather than a cause in GG pathogenesis. Lastly, in cases of GG with *H. pylori* infection, granulomas often persist for 3–17 months after *H. pylori* eradication therapy,^{17,24,39} making its efficacy in GG questionable. It is plausible that although *H. pylori* can cause GG, granuloma formation is the result of a rare host response as opposed to a direct effect. Thus, *H. pylori* eradication therapy would be less effective in the resolution of GG, compared to its efficacy in conventional *H. pylori* gastritis.

Histologically, *H. pylori*-associated GG exhibits small non-necrotizing epithelioid granulomas with Langhans giant cells (Fig. 2), which are similar to those that are associated with sarcoidosis or Crohn disease. These granulomas tend to form in distinctive locations, such as the foveolar isthmi,⁶ with Maeng *et al.*⁷ reporting that the majority (66.7%) of granulomas were found there. They are also often in contact with a damaged pit (where *H. pylori* are commonly found) and are frequently accompanied by prominent neutrophilic infiltration, which distinguishes them from the granulomas that are observed in Crohn disease or sarcoidosis.^{6,7} However, this characteristic morphology and local-

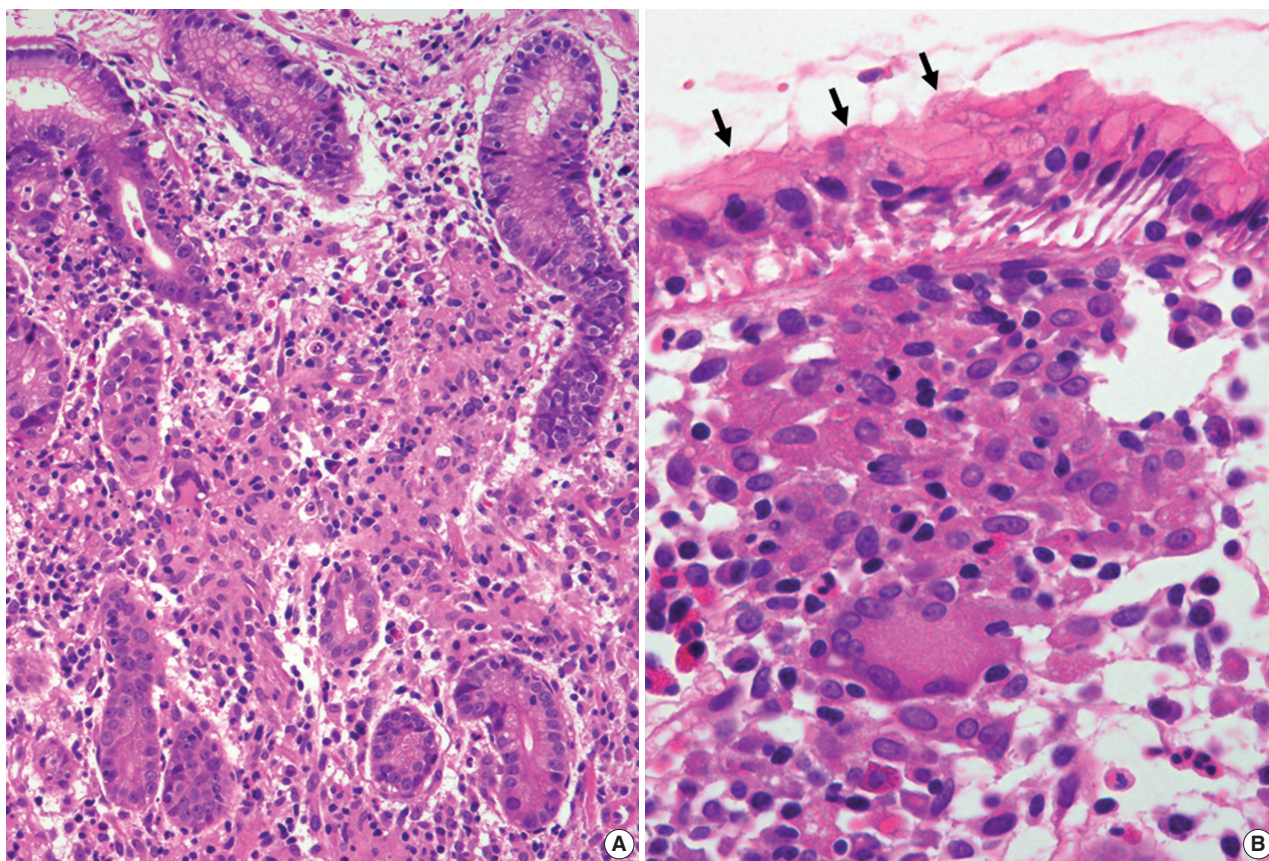


Fig. 2. Granulomatous gastritis. (A) The biopsy specimen demonstrates diffuse chronic active gastritis with confluent granulomas including multinucleated giant cells. (B) A well-defined granuloma is noted just below the surface foveolar epithelium. Some *Helicobacter pylori* organisms are seen (arrows).

ization has not been consistently reported in subsequent studies.^{18,23,24,40-42} Therefore, there are no distinct histologic features that could be used to confirm *H. pylori*-associated GG. Rather, it appears that the conditions in the mucosa surrounding granulomas are more informative,^{3,4,7} as the presence of *H. pylori* and neutrophil-rich chronic active gastritis (associated with glandular atrophy or intestinal metaplasia) increase the likelihood of *H. pylori* infection. Taken together, although the presence of *H. pylori* in the vicinity of granulomas does not imply a causative association, *H. pylori* eradication therapy should be considered when there are no other underlying disease except *H. pylori* infection.

INTRACELLULAR IMMUNOGLOBULIN ACCUMULATION IN ASSOCIATION WITH *HELICOBACTER PYLORI* INFECTION

Immunoglobulin accumulations can be found in reactive and neoplastic plasma cells and include large intracytoplasmic spheri-

cal inclusions (Russell bodies), small intracytoplasmic morular inclusions (Mott cells), intranuclear inclusions (Dutcher bodies), and rare angular- or needle-shaped intracytoplasmic crystalline inclusions. These accumulations are associated with chronic inflammation with plasmacytosis, autoimmune disease, multiple myeloma, or other B-cell lymphomas.⁴³⁻⁴⁵ Although the exact mechanism of immunoglobulin accumulation is unclear, it may be due to simple over-production, altered production, abnormal secretion, or impaired excretion.^{46,47} In the gastric mucosa, diffuse plasma cell infiltration with immunoglobulin overproduction may result from chronic over-stimulation of plasma cells by mucosal pathogens, especially *H. pylori*. Scattered Russell bodies are often observed with *H. pylori* gastritis, whereas Dutcher bodies are frequently associated with low-grade MALT lymphoma. However, RBG and CSH are rarely reported in the stomach.^{9,10} As the incidence of these lesions is low relative to *H. pylori*-associated gastritis, the contribution of *H. pylori* infection to their development is questionable. Furthermore, careful evaluation of their underlying cause is essential, as they can be associated with

monoclonal gammopathy or lymphoreticular neoplasms.^{20,43,48} The possible connections between *H. pylori* infection and these immunoglobulin accumulations, diagnostically relevant histological features, and biological significance are described below.

Russell body gastritis

The first case of RBG was reported by Tazawa and Tsutsumi in 1998.¹⁹ RBG is a rare form of chronic gastritis characterized by localized accumulation of Mott cells, which are plasma cells with a cytoplasm packed with small spherical inclusions (Fig. 3A, B). These lesions are rare, and only 30 cases of RBG have been published to date in the English literature.^{8,9,19-21,48-61} The clinical and pathological features of RBG are summarized in Table 1. Although its pathogenesis has not been fully elucidated, there is evidence to support a strong association between *H. pylori* infection

and RBG development. For example, *H. pylori* is detected in approximately two-thirds of patients with RBG.^{8,9,19-21,48,50,52,53,55,57,60,61} Few other infections that have been reported with RBG include human immunodeficiency virus (three patients),^{51,53,59} hepatitis C virus (one patient),⁵⁸ and candida esophagitis (one case).⁴⁹ In addition, more than 60% of patients with RBG exhibit lesion regression following *H. pylori* eradication therapy.^{19-21,53,60} Furthermore, it has been reported that highly virulent *H. pylori* genotypes (*vacA* and *cagA*) are associated with the formation of Russell bodies and Mott cells in the antral mucosa.⁶²

Immunoglobulin light chain restriction is generally considered to be proof of monoclonality and is an important indicator of B-cell neoplasia. Interestingly, light chain restriction was detected via immunohistochemistry in 12 out of 30 cases of RBG (kappa restriction in 11 cases and lambda restriction in one case).^{9,20,48,58,61}

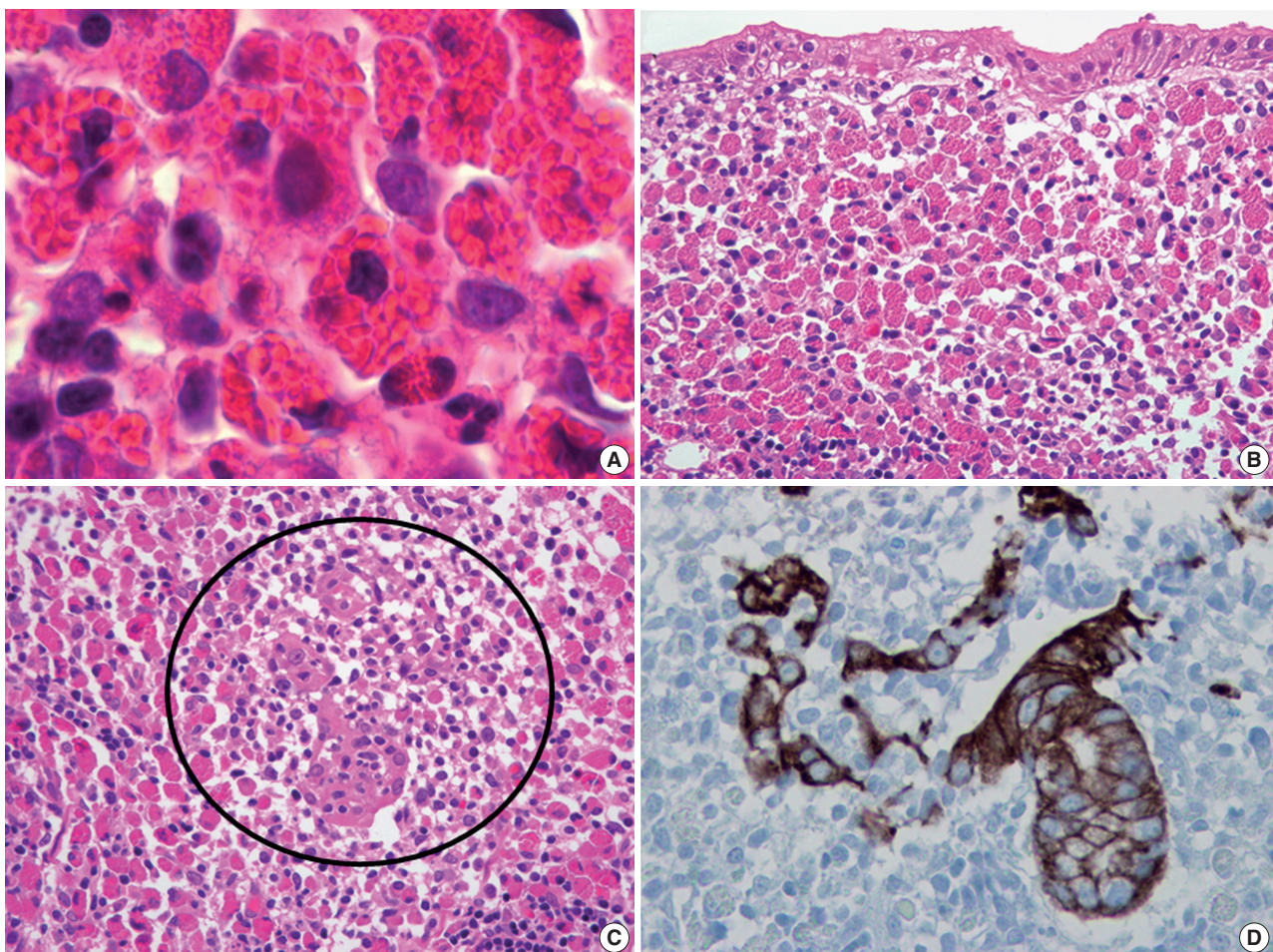


Fig. 3. Russell body gastritis with concomitant mucosa-associated lymphoid tissue lymphoma. (A) Mott cells are plasma cells in which the cytoplasm is packed with multiple variable-sized Russell bodies. (B) The lamina propria of the gastric mucosa is expanded by extensive infiltration of Mott cells, consistent with Russell body gastritis. (C) Small- to intermediate-sized atypical lymphoid cells, morphologically consistent with centrocyte-like cells are admixed with Mott cells and destroy adjacent gastric glands to form a lymphoepithelial lesion (circle). (D) Immunostaining for cytokeratin highlights a lymphoepithelial lesion.

Table 1. Clinical and pathologic findings of previously published cases of Russell body gastritis in the English literature

Case	Study	Age (yr)/Sex	Endoscopic finding	<i>Helicobacter pylori</i> infection	Ig light chain of Mott cells	Gastric lesion coexisted	HPET/Resolution of RBG	Others
1	Tazawa and Tsutsumi ¹⁹	53/M	Multiple ulcer scars	Yes	Polyclonal	None	Done/Yes	-
2	Erbersdobler <i>et al.</i> ⁴⁹	80/F	Irregular mucosal swelling	No	Polyclonal	None	NS	<i>Candida</i> esophagitis
3	Ensari <i>et al.</i> ⁵⁰	70/M	Flattened gastric folds	Yes	Polyclonal	None	Done/NS	-
4	Paik <i>et al.</i> ⁸	47/F	Erythematous swelling	Yes	Polyclonal	None	Done/NS	-
5	Paik <i>et al.</i> ⁸	53/F	Yellowish raised lesion	Yes	Polyclonal	None	Done/NS	-
6	Wolkersdörfer <i>et al.</i> ²⁰	54/M	Erythema and erosions	Yes	Monoclonal (λ)	None	Done/Yes	MGUS
7	Drut and Olenchuk ⁵¹	34/M	Elevation with central macule	No	Polyclonal	None	NS	HIV infection
8	Pizzolitto <i>et al.</i> ⁵²	60/F	Minute-raised granular areas	Yes	Polyclonal	None	Done/NS	-
9	Licci <i>et al.</i> ⁵³	59/M	Hyperemia	Yes	Polyclonal	None	Done/Yes	HIV infection
10	Habib <i>et al.</i> ⁵⁴	75/M	Nodular chronic active gastritis	No	Polyclonal	None	NS	-
11	Shinozaki <i>et al.</i> ⁵⁵	74/M	Centrally ulcerated bulky mass	Yes	Polyclonal	EBV-positive carcinoma	No	-
12	Shinozaki <i>et al.</i> ⁵⁵	29/F	Ulcerated mass	Yes	Polyclonal	EBV-positive carcinoma	No	-
13	Del Gobbo <i>et al.</i> ⁵⁶	78/F	Hyperemic gastric mucosa	No	Polyclonal	None	No	-
14	Wolf <i>et al.</i> ⁵⁷	67/M	Exophytic tumor	Yes	NS	Signet ring cell carcinoma	No	-
15	Coryne and Azadeh ⁵⁸	49/M	Severe raised erosive gastritis	No	Monoclonal (κ)	None	NS	HCV infection
16	Bhalla <i>et al.</i> ⁵⁹	82/M	Gastritis	No	Polyclonal	None	NS	HIV infection
17	Karabagli and Gokturk ⁶⁰	60/M	Large ulcerofungating mass	Yes	Polyclonal	None	Done/Yes	-
18	Yoon <i>et al.</i> ²¹	57/M	Elevation with central depression	Yes	Polyclonal	None	Done/Yes	-
19	Yoon <i>et al.</i> ²¹	43/M	Whitish flat lesion with nodularity	Yes	Polyclonal	None	Done/Yes	-
20	Araki <i>et al.</i> ⁶¹	74/F	Ulcer	Yes	Monoclonal (κ)	None	No	-
21	Zhang <i>et al.</i> ⁹	78/F	Gastritis with uneven mucosa	No	Monoclonal (κ)	None	No	-
22	Zhang <i>et al.</i> ⁹	77/F	Gastritis with uneven mucosa	Yes	Monoclonal (κ)	None	No	-
23	Zhang <i>et al.</i> ⁹	77/F	Punctiform erosion	Yes	Monoclonal (κ)	None	No	-
24	Zhang <i>et al.</i> ⁹	56/M	Raised erosion	Yes	Monoclonal (κ)	None	No	-
25	Zhang <i>et al.</i> ⁹	76/M	Erythema	Yes	Monoclonal (κ)	None	No	-
26	Zhang <i>et al.</i> ⁹	50/M	Flat and raised erosions	Yes	Monoclonal (κ)	None	No	-
27	Zhang <i>et al.</i> ⁹	28/M	Erythema	No	Monoclonal (κ)	None	No	-
28	Zhang <i>et al.</i> ⁹	24/F	Erythema	No	Monoclonal (κ)	None	No	-
29	Zhang <i>et al.</i> ⁹	66/M	Ulceration	No	NA	None	No	-
30	Joo ⁴⁸	56/M	Hyperemia and micronodularity	Yes	Monoclonal (κ)	MALT lymphoma	No	-

HPET, *Helicobacter pylori* eradication therapy; RBG, Russell body gastritis; M, male; F, female; NS, not stated; MGUS, monoclonal gammopathy of undetermined significance; HIV, human immunodeficiency virus; EBV, Epstein-Barr virus; HCV, hepatitis C virus; NA, not assessed; MALT, mucosa-associated lymphoid tissue.

Ten of these cases were localized gastric lesions with no associated lymphoid malignancy or plasma cell disorder, although one case was associated with low-grade MALT lymphoma,⁴⁸ and another with concomitant monoclonal gammopathy of undetermined significance.²⁰ This could be explained by the findings of Girón and Shah,⁶³ who reported that approximately 50% of patients with *H. pylori* infection exhibit either kappa or lambda light chain elevation, and suggested that *H. pylori* infection might contribute to immunoglobulin light chain dysfunction. Thus, RBG may be closely associated with *H. pylori* infection, and the majority of RBG cases may be reactive in nature, even when light

chain monoclonality is detected. Nevertheless, pathologists should be aware of the possibility of concomitant lymphoid neoplasms.

Given the strong association with *H. pylori* infection, it is possible that RBG, gastric carcinoma, or MALT lymphoma might occur simultaneously in the same patient. Previous reports describe Mott cell proliferation (features of RBG) in association with gastric carcinoma, including two cases of Epstein-Barr virus-positive lymphoepithelioma-like carcinoma,⁵⁵ and one case of signet ring cell carcinoma.⁵⁷ In these cases, Mott cell proliferation was likely a reactive paraneoplastic event, given that the carcinoma and Mott cells did not mix and that the Mott cells were

polyclonal. However, in the previously described case of RBG with concomitant MALT lymphoma,⁴⁸ the Mott cells were mixed with the neoplastic centrocyte-like cells (Fig. 3C) and exhibited IgM kappa monoclonality, which indicates the proliferating Mott cells were neoplastic components of MALT lymphoma.

Morphologically, Mott cells with eccentric nuclei and abundant eosinophilic cytoplasm are similar to poorly differentiated carcinoma cells or signet ring cells. In addition, in cases with abundant Mott cells and a few neoplastic cells, neoplastic cells may not be easily detected. Thus, immunostaining for cytokeratin should be conducted to exclude associated carcinoma.^{55,57} Furthermore, if light chain monoclonality is detected, pathologists should consider associated MALT lymphoma and perform ancillary immunostaining (e.g., for CD20 and cytokeratin) to identify centrocyte-like cells and lymphoepithelial lesions (Fig. 3D).⁴⁸

Crystal-storing histiocytosis

CSH is a rare condition, which often occurs with disorders such as monoclonal gammopathy, B-cell lymphoma, or plasma cell myeloma.^{43,64,65} Although many cases of CSH are systemic, organ-confined CSH has been described in the lung, lymph node, kidney, thyroid, thymus, parotid gland, and cornea.^{43,65-71} CSH is extremely rare in the stomach, and only eight cases of gastric CSH have been described to date in the English literature (Table 2).^{10,11,43,71,72} Among these, *H. pylori* infection was identified in four patients (50%) who did not exhibit concomitant gastric lesions (except for *H. pylori* gastritis) or a systemic disorder that might have caused monoclonal gammopathy.^{10,11} In the other four patients, there was no mention of *H. pylori* infection,^{43,71,72} and two of them were subsequently diagnosed with thymic lymphoma⁴³ and plasma cell myeloma,⁷¹ respectively. Therefore, although overproduction of immunoglobulin due to *H. pylori* infection could be a plausible cause of isolated gastric CSH, clinical workup is needed to exclude the possibility that it is a manifestation of underlying lymphoma or plasma cell myeloma. Light chain restriction was detected in five of seven cases (kappa restriction in two case and lambda restriction in three cases),^{10,71,72} all of

which except one had no associated B-cell/plasmacytic neoplasms. Thus, light chain restriction detected in isolated gastric CSH does not necessarily mean that it is associated with B-cell or plasmacytic neoplasm. Meanwhile, because no studies have reported CSH responding to *H. pylori* eradication therapy, its effectiveness is unclear.

Histologically, CSH is characterized by diffuse infiltrations of large, oval, polygonal, and, occasionally, spindle cells, with abundant eosinophilic cytoplasm and small eccentric nuclei. The eosinophilic cytoplasm is filled with elongated, rectangular, and needle-shaped/fibrillary crystalline inclusions (Fig. 4). These crystalline inclusions are approximately 5–20 nm long and are frequently arranged in parallel arrays.^{11,43,66} At low magnification, nodular aggregates of these cells can sometimes resemble adult rhabdomyomas or granular cell tumors in the way that they expand or displace normal structures, and proliferations of benign-looking histiocyte-like cells can also resemble Gaucher disease or malakoplakia.^{43,65,73,74} Therefore, immunostaining for desmin, smooth muscle actin, S100 protein, and immunoglobulin light chains can facilitate an accurate diagnosis.^{11,43,65,66,74}

CONCLUSION

This review examined several rare gastric lesions that have distinctive histological characteristics and are associated with a variety of conditions, including *H. pylori* infection. Although *H. pylori* may be a cause in many of these conditions, the association cannot be viewed as definite, given the low incidence of these lesions relative to the high prevalence of *H. pylori* infection, regional differences in the prevalence of *H. pylori* infection, and the possibility of other causative disorders. However, it is reasonable to consider *H. pylori* once other potential etiologies have been excluded. In addition, it is not advisable to consider *H. pylori* to be an “innocent bystander,” given the considerable proportion of these lesions that can be regressed or cured with *H. pylori* eradication therapy. Therefore, it is important that pathologists properly identify a lesion’s cause in order to ensure ap-

Table 2. Clinical and pathologic findings of six cases of gastric crystal-storing histiocytosis

Case No.	Study	Age (yr)/Sex	Endoscopic finding	Ig light chains	Crystal-storing cells	Helicobacter pylori infection
1	Jones <i>et al.</i> ⁴³	35/F	NS	Polyclonal	Histiocytes	NS
2	Stewart and Spagnolo ¹⁰	82/M	Gastritis	Monoclonal (IgA λ)	Plasma cells	Positive
3	Stewart and Spagnolo ¹⁰	81/M	Gastritis	NA	Plasma cells	Positive
4	Stewart and Spagnolo ¹⁰	52/F	Gastritis	Monoclonal (IgA λ)	Plasma cells	Positive
5	Joo <i>et al.</i> ¹¹	56/F	Polyps (three)	Polyclonal	Plasma cells and histiocytes	Positive
6	Vaid <i>et al.</i> ⁷²	NS	Submucosal tumor	Monoclonal (κ)	Histiocytes	NS

F, female; NS, not stated; M, male; NA, not assessed.

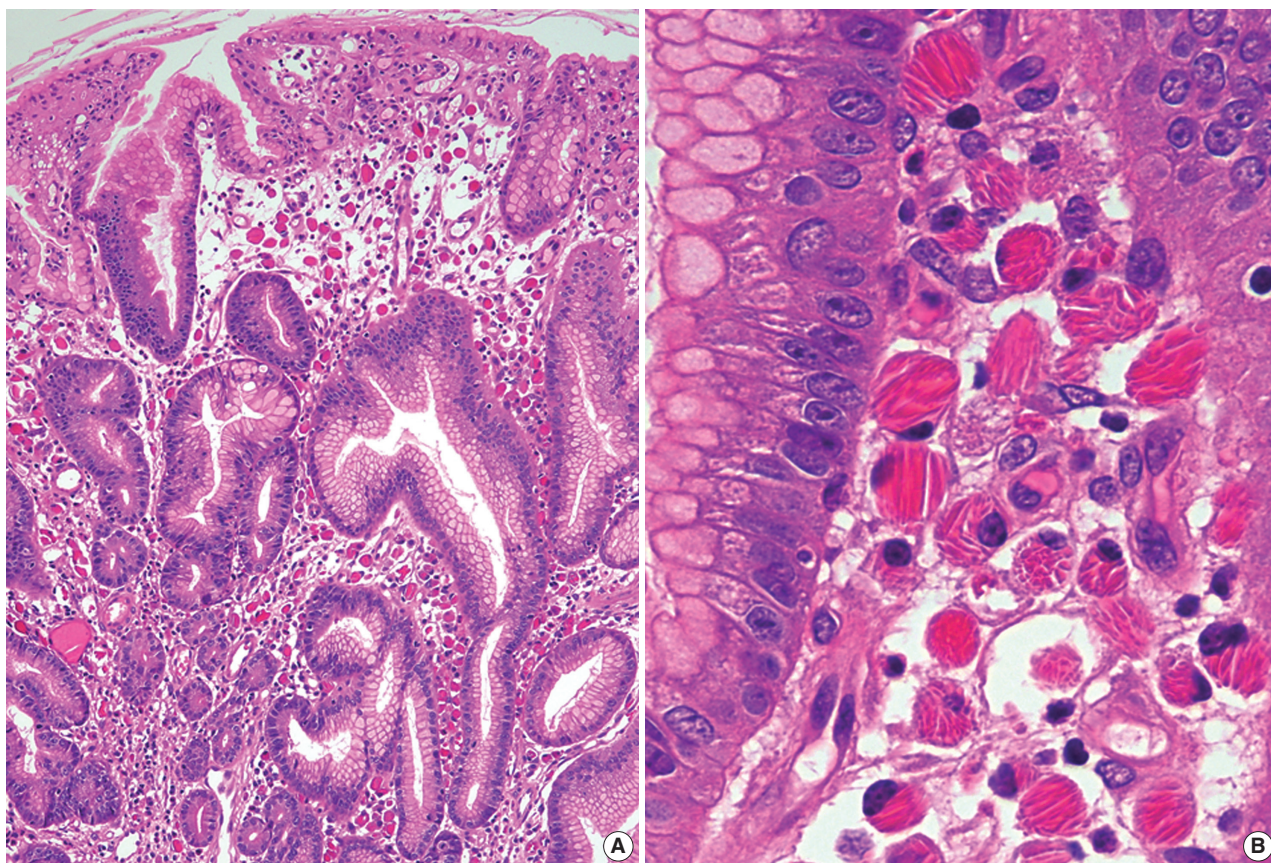


Fig. 4. Gastric crystal-storing histiocytosis. (A) The biopsy specimen demonstrates many large pinkish mononuclear cells in the lamina propria. (B) Higher magnification of mononuclear cells shows densely eosinophilic, refractile, needle-shaped, intracytoplasmic crystalline inclusions.

appropriate patient management. In this context, *H. pylori* should be considered as a possible cause in areas where it is prevalent. Further investigation is needed to confirm the role of *H. pylori* in the development of rare gastric lesions.

Conflicts of Interest

No potential conflict of interest relevant to this article was reported.

REFERENCES

- Dixon MF, Wyatt JI, Burke DA, Rathbone BJ. Lymphocytic gastritis—relationship to *Campylobacter pylori* infection. *J Pathol* 1988; 154: 125-32.
- Carmack SW, Lash RH, Gulizia JM, Genta RM. Lymphocytic disorders of the gastrointestinal tract: a review for the practicing pathologist. *Adv Anat Pathol* 2009; 16: 290-306.
- Genta RM, Lash RH. *Helicobacter pylori*-negative gastritis: seek, yet ye shall not always find. *Am J Surg Pathol* 2010; 34: e25-34.
- Srivastava A, Lauwers GY. Pathology of non-infective gastritis. *Histopathology* 2007; 50: 15-29.
- Wu TT, Hamilton SR. Lymphocytic gastritis: association with etiology and topology. *Am J Surg Pathol* 1999; 23: 153-8.
- Ectors NL, Dixon MF, Geboes KJ, Rutgeerts PJ, Desmet VJ, Vantrappen GR. Granulomatous gastritis: a morphological and diagnostic approach. *Histopathology* 1993; 23: 55-61.
- Maeng L, Lee A, Choi K, Kang CS, Kim KM. Granulomatous gastritis: a clinicopathologic analysis of 18 biopsy cases. *Am J Surg Pathol* 2004; 28: 941-5.
- Paik S, Kim SH, Kim JH, Yang WI, Lee YC. Russell body gastritis associated with *Helicobacter pylori* infection: a case report. *J Clin Pathol* 2006; 59: 1316-9.
- Zhang H, Jin Z, Cui R. Russell body gastritis/duodenitis: a case series and description of immunoglobulin light chain restriction. *Clin Res Hepatol Gastroenterol* 2014; 38: e89-97.
- Stewart CJ, Spagnolo DV. Crystalline plasma cell inclusions in *Helicobacter*-associated gastritis. *J Clin Pathol* 2006; 59: 851-4.

11. Joo M, Kwak JE, Chang SH, *et al.* Localized gastric crystal-storing histiocytosis. *Histopathology* 2007; 51: 116-9.
12. Renault M, Goodier A, Subramony C, Hood B, Bishop P, Nowicki M. Age-related differences in granulomatous gastritis: a retrospective, clinicopathological analysis. *J Clin Pathol* 2010; 63: 347-50.
13. Hayat M, Arora DS, Dixon MF, Clark B, O'Mahony S. Effects of *Helicobacter pylori* eradication on the natural history of lymphocytic gastritis. *Gut* 1999; 45: 495-8.
14. Madisch A, Miehlke S, Neuber F, *et al.* Healing of lymphocytic gastritis after *Helicobacter pylori* eradication therapy—a randomized, double-blind, placebo-controlled multicentre trial. *Aliment Pharmacol Ther* 2006; 23: 473-9.
15. Müller H, Volkholz H, Stolte M. Healing of lymphocytic gastritis by eradication of *Helicobacter pylori*. *Digestion* 2001; 63: 14-9.
16. Niemelä S, Karttunen T, Kerola T, Karttunen R. Ten year follow up study of lymphocytic gastritis: further evidence on *Helicobacter pylori* as a cause of lymphocytic gastritis and corpus gastritis. *J Clin Pathol* 1995; 48: 1111-6.
17. Miyamoto M, Haruma K, Yoshihara M, *et al.* Isolated granulomatous gastritis successfully treated by *Helicobacter pylori* eradication: a possible association between granulomatous gastritis and *Helicobacter pylori*. *J Gastroenterol* 2003; 38: 371-5.
18. Ozturk Y, Buyukgebiz B, Ozer E, Arslan N, Bekem O, Hizli S. Resolution of *Helicobacter pylori* associated granulomatous gastritis in a child after eradication therapy. *J Pediatr Gastroenterol Nutr* 2004; 39: 286-7.
19. Tazawa K, Tsutsumi Y. Localized accumulation of Russell body-containing plasma cells in gastric mucosa with *Helicobacter pylori* infection: 'Russell body gastritis'. *Pathol Int* 1998; 48: 242-4.
20. Wolkersdörfer GW, Haase M, Morgner A, Baretton G, Miehlke S. Monoclonal gammopathy of undetermined significance and Russell body formation in *Helicobacter pylori* gastritis. *Helicobacter* 2006; 11: 506-10.
21. Yoon JB, Lee TY, Lee JS, *et al.* Two cases of Russell body gastritis treated by *Helicobacter pylori* eradication. *Clin Endosc* 2012; 45: 412-6.
22. Dhillon AP, Sawyerr A. Granulomatous gastritis associated with *Campylobacter pylori*. *APMIS* 1989; 97: 723-7.
23. Delgado JS, Landa E, Ben-Dor D. Granulomatous gastritis and *Helicobacter pylori* infection. *Isr Med Assoc J* 2013; 15: 317-8.
24. Koyama S, Nagashima F. Idiopathic granulomatous gastritis with multiple aphthoid ulcers. *Intern Med* 2003; 42: 691-5.
25. Haot J, Hamichi L, Wallez L, Mainguet P. Lymphocytic gastritis: a newly described entity: a retrospective endoscopic and histological study. *Gut* 1988; 29: 1258-64.
26. Haot J, Jouret A, Willette M, Gossuin A, Mainguet P. Lymphocytic gastritis: prospective study of its relationship with varioliform gastritis. *Gut* 1990; 31: 282-5.
27. Nielsen JA, Roberts CA, Lager DJ, Putcha RV, Jain R, Lewin M. Lymphocytic gastritis is not associated with active *Helicobacter pylori* infection. *Helicobacter* 2014; 19: 349-55.
28. Feeley KM, Heneghan MA, Stevens FM, McCarthy CF. Lymphocytic gastritis and coeliac disease: evidence of a positive association. *J Clin Pathol* 1998; 51: 207-10.
29. Alsaigh N, Odze R, Goldman H, Antonioli D, Ott MJ, Leichtner A. Gastric and esophageal intraepithelial lymphocytes in pediatric celiac disease. *Am J Surg Pathol* 1996; 20: 865-70.
30. Bhatti TR, Jatla M, Verma R, Bierly P, Russo PA, Ruchelli ED. Lymphocytic gastritis in pediatric celiac disease. *Pediatr Dev Pathol* 2011; 14: 280-3.
31. Oberhuber G, Vogelsang H, Stolte M, Muthenthaler S, Kummer JA, Radaszkiewicz T. Evidence that intestinal intraepithelial lymphocytes are activated cytotoxic T cells in celiac disease but not in giardiasis. *Am J Pathol* 1996; 148: 1351-7.
32. Inagaki-Ohara K, Nishimura H, Sakai T, Lynch DH, Yoshikai Y. Potential for involvement of Fas antigen/Fas ligand interaction in apoptosis of epithelial cells by intraepithelial lymphocytes in murine small intestine. *Lab Invest* 1997; 77: 421-9.
33. Han SH, Joo M, Kim KM. High proportion of granzyme B+ intraepithelial lymphocytes contributes to epithelial apoptosis in *Helicobacter pylori*-associated lymphocytic gastritis. *Helicobacter* 2013; 18: 290-8.
34. Oberhuber G, Bodingbauer M, Mosberger I, Stolte M, Vogelsang H. High proportion of granzyme B-positive (activated) intraepithelial and lamina propria lymphocytes in lymphocytic gastritis. *Am J Surg Pathol* 1998; 22: 450-8.
35. Shapiro JL, Goldblum JR, Petras RE. A clinicopathologic study of 42 patients with granulomatous gastritis. Is there really an "idiopathic" granulomatous gastritis? *Am J Surg Pathol* 1996; 20: 462-70.
36. El Demellawy D, Otero C, Radhi J. Primary gastric lymphoma with florid granulomatous reaction. *J Gastrointest Liver Dis* 2009; 18: 99-101.
37. Fahimi HD, Deren JJ, Gottlieb LS, Zamcheck N. Isolated granulomatous gastritis: its relationship to disseminated sarcoidosis and regional enteritis. *Gastroenterology* 1963; 45: 161-75.
38. Sandmeier D, Bouzourene H. Does idiopathic granulomatous gastritis exist? *Histopathology* 2005; 46: 352-3.
39. Kim YS, Lee HK, Kim JO, *et al.* A case of *H. pylori*-associated granulomatous gastritis with hypertrophic gastropathy. *Gut Liver* 2009; 3: 137-40.
40. Fuentebella J, Bass D, Longacre T, Ro K. Abdominal pain, gastrointestinal bleeding, and weight loss in a 17-year-old male. *Dig Dis Sci*

- 2009; 54: 722-4.
41. Gonen C, Sarioglu S, Akpınar H. Magnifying endoscopic features of granulomatous gastritis. *Dig Dis Sci* 2009; 54: 1602-3.
 42. Yamane T, Uchiyama K, Ishii T, *et al.* Isolated granulomatous gastritis showing discoloration of lesions after *Helicobacter pylori* eradication. *Dig Endosc* 2010; 22: 140-3.
 43. Jones D, Bhatia VK, Krausz T, Pinkus GS. Crystal-storing histiocytosis: a disorder occurring in plasmacytic tumors expressing immunoglobulin kappa light chain. *Hum Pathol* 1999; 30: 1441-8.
 44. Gebbers JO, Otto HF. Plasma cell alterations in ulcerative colitis: an electron microscopic study. *Pathol Eur* 1976; 11: 271-9.
 45. van den Tweel JG, Taylor CR, Parker JW, Lukes RJ. Immunoglobulin inclusions in non-Hodgkin's lymphomas. *Am J Clin Pathol* 1978; 69: 306-13.
 46. Hasegawa H. Aggregates, crystals, gels, and amyloids: intracellular and extracellular phenotypes at the crossroads of immunoglobulin physicochemical property and cell physiology. *Int J Cell Biol* 2013; 2013: 604867.
 47. Valetti C, Grossi CE, Milstein C, Sitia R. Russell bodies: a general response of secretory cells to synthesis of a mutant immunoglobulin which can neither exit from, nor be degraded in, the endoplasmic reticulum. *J Cell Biol* 1991; 115: 983-94.
 48. Joo M. Gastric mucosa-associated lymphoid tissue lymphoma masquerading as Russell body gastritis. *Pathol Int* 2015; 65: 396-8.
 49. Erbersdobler A, Petri S, Lock G. Russell body gastritis: an unusual, tumor-like lesion of the gastric mucosa. *Arch Pathol Lab Med* 2004; 128: 915-7.
 50. Ensari A, Savas B, Okcu Heper A, Kuzu I, Idilman R. An unusual presentation of *Helicobacter pylori* infection: so-called "Russell body gastritis". *Virchows Arch* 2005; 446: 463-6.
 51. Drut R, Olenchuk AB. Images in pathology: Russell body gastritis in an HIV-positive patient. *Int J Surg Pathol* 2006; 14: 141-2.
 52. Pizzolitto S, Camilot D, DeMaglio G, Falconieri G. Russell body gastritis: expanding the spectrum of *Helicobacter pylori*-related diseases? *Pathol Res Pract* 2007; 203: 457-60.
 53. Licci S, Sette P, Del Nonno F, Ciarletti S, Antinori A, Morelli L. Russell body gastritis associated with *Helicobacter pylori* infection in an HIV-positive patient: case report and review of the literature. *Z Gastroenterol* 2009; 47: 357-60.
 54. Habib C, Gang DL, Ghaoui R, Pantanowitz L. Russell body gastritis. *Am J Hematol* 2010; 85: 951-2.
 55. Shinozaki A, Ushiku T, Fukayama M. Prominent Mott cell proliferation in Epstein-Barr virus-associated gastric carcinoma. *Hum Pathol* 2010; 41: 134-8.
 56. Del Gobbo A, Elli L, Braidotti P, Di Nuovo F, Bosari S, Romagnoli S. *Helicobacter pylori*-negative Russell body gastritis: case report. *World J Gastroenterol* 2011; 17: 1234-6.
 57. Wolf EM, Mrak K, Tschmelitsch J, Langner C. Signet ring cell cancer in a patient with Russell body gastritis: a possible diagnostic pitfall. *Histopathology* 2011; 58: 1178-80.
 58. Coyne JD, Azadeh B. Russell body gastritis: a case report. *Int J Surg Pathol* 2012; 20: 69-70.
 59. Bhalla A, Mosteanu D, Gorelick S, Hani el F. Russell body gastritis in an HIV positive patient: case report and review of literature. *Conn Med* 2012; 76: 261-5.
 60. Karabagli P, Gokturk HS. Russell body gastritis: case report and review of the literature. *J Gastrointestin Liver Dis* 2012; 21: 97-100.
 61. Araki D, Sudo Y, Imamura Y, Tsutsumi Y. Russell body gastritis showing IgM kappa-type monoclonality. *Pathol Int* 2013; 63: 565-7.
 62. Soltermann A, Koetzer S, Eigenmann F, Komminoth P. Correlation of *Helicobacter pylori* virulence genotypes vacA and cagA with histological parameters of gastritis and patient's age. *Mod Pathol* 2007; 20: 878-83.
 63. Giron JA, Shah SL. *Helicobacter pylori* infection and light chain gammopathy. *Clin Dev Immunol* 2013; 2013: 348562.
 64. Lebeau A, Zeindl-Eberhart E, Müller EC, *et al.* Generalized crystal-storing histiocytosis associated with monoclonal gammopathy: molecular analysis of a disorder with rapid clinical course and review of the literature. *Blood* 2002; 100: 1817-27.
 65. Dogan S, Barnes L, Cruz-Vetrano WP. Crystal-storing histiocytosis: report of a case, review of the literature (80 cases) and a proposed classification. *Head Neck Pathol* 2012; 6: 111-20.
 66. Ionescu DN, Pierson DM, Qing G, Li M, Colby TV, Leslie KO. Pulmonary crystal-storing histiocytoma. *Arch Pathol Lab Med* 2005; 129: 1159-63.
 67. Hirota S, Miyamoto M, Kasugai T, Kitamura Y, Morimura Y. Crystalline light-chain deposition and amyloidosis in the thyroid gland and kidneys of a patient with myeloma. *Arch Pathol Lab Med* 1990; 114: 429-31.
 68. Stirling JW, Henderson DW, Rozenbids MA, Skinner JM, Filipic M. Crystalloidal paraprotein deposits in the cornea: an ultrastructural study of two new cases with tubular crystalloids that contain IgG kappa light chains and IgG gamma heavy chains. *Ultrastruct Pathol* 1997; 21: 337-44.
 69. Papla B, Spólnik P, Rzenno E, *et al.* Generalized crystal-storing histiocytosis as a presentation of multiple myeloma: a case with a possible pro-aggregation defect in the immunoglobulin heavy chain. *Virchows Arch* 2004; 445: 83-9.
 70. Llobet M, Castro P, Barceló C, Trull JM, Campo E, Bernadó L. Massive crystal-storing histiocytosis associated with low-grade malignant B-cell lymphoma of MALT-type of the parotid gland. *Diagn Cytopathol* 1997; 17: 148-52.

71. Kanagal-Shamanna R, Xu-Monette ZY, Miranda RN, *et al.* Crystal-storing histiocytosis: a clinicopathological study of 13 cases. *Histopathology* 2016; 68: 482-91.
72. Vaid A, Caradine KD, Lai KK, Rego R. Isolated gastric crystal-storing histiocytosis: a rare marker of occult lymphoproliferative disorders. *J Clin Pathol* 2014; 67: 740-1.
73. Kapadia SB, Enzinger FM, Heffner DK, Hyams VJ, Frizzera G. Crystal-storing histiocytosis associated with lymphoplasmacytic neoplasms: report of three cases mimicking adult rhabdomyoma. *Am J Surg Pathol* 1993; 17: 461-7.
74. Kusakabe T, Watanabe K, Mori T, Iida T, Suzuki T. Crystal-storing histiocytosis associated with MALT lymphoma of the ocular adnexa: a case report with review of literature. *Virchows Arch* 2007; 450: 103-8.

Epstein-Barr Virus—Associated Lymphoproliferative Disorders: Review and Update on 2016 WHO Classification

Hyun-Jung Kim · Young Hyeon Ko¹
Ji Eun Kim² · Seung-Sook Lee³
Hyekyung Lee⁴ · Gyeongsin Park⁵
Jin Ho Paik⁶ · Hee Jeong Cha⁷
Yoo-Duk Choi⁸ · Jae Ho Han⁹
Jooryung Huh¹⁰ · Hematopathology
Study Group of the Korean Society
of Pathologists

Department of Pathology, Inje University, Sanggye Paik Hospital, Seoul; ¹Sungkyunkwan University, School of Medicine, Samsung Medical Center, Seoul; ²SMG-SNU Boramae Medical Center, Seoul National University, Seoul; ³Korea Cancer Center Hospital, Seoul; ⁴Eulji University Hospital, Eulji University School of Medicine, Daejeon; ⁵Gangnam St. Mary's Hospital, College of Medicine, The Catholic University of Korea, Seoul; ⁶Seoul National University Bundang Hospital, Seongnam; ⁷Ulsan University Hospital, Ulsan University School of Medicine, Ulsan; ⁸Chonnam National University Hospital, Chonnam National University, Gwangju; ⁹Ajou University Hospital, Suwon; ¹⁰Asan Medical Center, Ulsan University College of Medicine, Seoul, Korea

Received: January 6, 2017

Revised: March 11, 2017

Accepted: March 14, 2017

Corresponding Author

Jooryung Huh, MD
Department of Pathology, Asan Medical Center,
University of Ulsan College of Medicine, 88
Olympic-ro 43-gil, Songpa-gu, Seoul 05505, Korea
Tel: +82-2-3010-4553
Fax: +82-2-472-7898
E-mail: Jrhuh@amc.seoul.kr

Epstein-Barr virus (human herpesvirus-4) is very common virus that can be detected in more than 95% of the human population. Most people are asymptomatic and live their entire lives in a chronically infected state (IgG positive). However, in some populations, the Epstein-Barr virus (EBV) has been involved in the occurrence of a wide range of B-cell lymphoproliferative disorders (LPDs), including Burkitt lymphoma, classic Hodgkin's lymphoma, and immune-deficiency associated LPDs (post-transplant and human immunodeficiency virus-associated LPDs). T-cell LPDs have been reported to be associated with EBV with a subset of peripheral T-cell lymphomas, angioimmunoblastic T-cell lymphomas, extranodal nasal natural killer/T-cell lymphomas, and other rare histotypes. This article reviews the current evidence covering EBV-associated LPDs based on the 2016 classification of the World Health Organization. These LPD entities often pose diagnostic challenges, both clinically and pathologically, so it is important to understand their unique pathophysiology for correct diagnoses and optimal management.

Key Words: Epstein-Barr virus; Lymphoproliferative disorders

Epstein-Barr virus (EBV) is classified as a γ -herpes virus and contains a linear DNA molecule about 172 kb in length, which affects more than 90% of the worldwide adult population. If the infection does not become clinically silent, infectious mononucleosis is experienced by the exposed persons.¹ Although EBV

infection is lifelong, a long latency and reactivation of EBV results in various lymphoproliferative lesions including hematologic malignancies.² This article reviews the current understanding of EBV-associated lymphoproliferative disorders (LPDs) based on the 2016 classification of the World Health Organization

(WHO).³ Some LPDs exhibit a predisposition in Asian populations, including Koreans. These entities often pose diagnostic challenges, both clinically and pathologically, and it is important to understand their unique pathophysiology for correct diagnoses and optimal management. Generally intrinsic defects and post-transplant lymphoproliferative disorders (PTLDs) are excluded from this review, these are treated separately as immunodeficiency disorders by the WHO.

EPSTEIN-BARR VIRUS-ASSOCIATED B-CELL LYMPHOPROLIFERATIVE DISORDERS

The spectrum of EBV-associated B-cell LPDs is broad, ranging from reactive lymphoproliferative lymphadenitis to lymphomas. All the related disease entities are shown in Table 1. Well-defined lymphoma entities such as Burkitt lymphoma, classical Hodgkin lymphoma, and plasmablastic lymphoma are not included.⁴

Infectious mononucleosis

Primary EBV infection occurs most often in childhood and is generally asymptomatic. In adolescence, it is associated with a self-limiting infectious mononucleosis syndrome, manifested by fever, pharyngitis, malaise, and atypical lymphocytosis. Following primary infection, most individuals remain a life-long carrier of the virus without serious sequelae.⁵ However, a small population with the latent infection will develop various LPDs.

EBV is transmitted from the host by saliva and infected EBV replicates within oropharyngeal epithelium and is then exposed to circulating B-lymphocytes. Peripheral EBV-infected memory B-cells can return to the Waldeyer's ring, undergoing reactivation to produce an infectious virus that will be shed in the saliva. EBV-specific cytotoxic T-cells (CTL) destroy most infected cells.

The histologic features of infectious mononucleosis vary during the course of the disease. Early in the disorder, follicular hyperplasia occurs with monocytoid B-cell aggregates and epithelioid histiocytes. Later, the expansion of the paracortex predominates. The immunoblasts resemble classical Reed-Sternberg (RS) cells. The immunoblasts of predominantly B-cell types and partly T-cell types often express CD30. *In-situ* hybridization (ISH) of EBV-encoded small RNAs (EBERs) exhibit numerous positive immunoblasts in the paracortex but not in the germinal centers.⁶

Chronic active EBV of B-cell types

As first defined by Lekstrom-Himes *et al.*,⁷ chronic active EBV (CAEBV) of B-cell types refers to a chronic or persistent EBV in-

fection characterized by a severe illness lasting more than 6 months, persistent elevated EBV titers, and evidence of EBV-related organ damage. Currently, CAEBV is defined as (1) a severe progressive illness with a duration of more than 6 months, (2) lymphocytic infiltration of tissue (e.g., lymph nodes, lungs, liver, central nervous tissue, bone marrow, eye, and skin), (3) elevated EBV DNA and RNA in affected tissue, and (4) absence of any other immunosuppressive conditions.⁸

Histologically, the lymph nodes exhibits features resembling polymorphic PTLD, with paracortical expansion, plasmacytoid lymphoblastic proliferation, presence of plasma cells, and presence of occasional RS-like cells. EBV-ISH positive B-cells are noted in the paracortex. Among CAEBV patients, 63% had clonal immunoglobulin rearrangement.⁹

EBV-positive diffuse large B-cell lymphoma

EBV-positive diffuse large B-cell lymphoma (DLBCL), not otherwise specified was originally described as "senile EBV-associated B-cell LPD," or "EBV-positive DLBCL of the elderly" (older than 50 years) (WHO 4th edition).¹⁰ However, subsequent studies have shown that EBV-positive DLBCL is not limited to this older age group. In the elderly group, it is thought to be related to immunosenescence, which modifies T-cell homeostasis through a lack of thymic output of naïve T-cells and an accumulation of viral specific CD8⁺ T cells.

Histologically, four types have been described: monomorphic (DLBCL-like, monotonous sheets of large cells), polymorphic in the inflammatory background, T-cell/histiocyte-rich large cell lymphoma, and plasmacytoid differentiation. Immunophenotypically, the tumor cells express pan B-cell markers (CD20, PAX5, CD79a, OCT-2, and BOB-1), and are mostly CD30⁺, but lack CD15 expression.

This disease entity frequently involves extranodal sites including the skin, lung, tonsils, and stomach. Unfavorable prognostic factors include older age (> 70 years), high international prognostic index, and activated B-cell phenotype.¹¹

EBV mucocutaneous ulcer

This self-limited EBV positive B-cell proliferation is characterized by the presence of mucocutaneous ulcers with an indolent clinical course. This phenomenon is likely due to a more localized form of decreased immune surveillance, which is supported by a very low EBV viral load. The frequently involved sites includes the skin, oropharyngeal mucosa, and gastrointestinal tract.¹²

Histologically a sharply demarcated ulcer is lined by an inflammatory infiltrate with clusters of large atypical cells, often

with RS cell-like features. Phenotypically the large atypical cells are variably positive for CD20 and CD30, and uniformly positive for EBV-ISH and CD15⁺ in half of the cases (Fig. 1).

DLBCL associated with chronic inflammation

DLBCL associated with chronic inflammation develops in the setting of long-standing chronic inflammation with EBV association. It usually involves body cavities or enclosed spaces (like cysts). Pyothorax-associated lymphoma (PAL) represents the prototype of this entity.

Cases with PAL have long history of chronic pyothorax and may present with chest pain, fever, cough, dyspnea, and tumor mass. The prognosis of PAL is poor.

The morphology discloses a diffuse proliferation of large atypical lymphocytes with plasmacytoid cytology. Immunohistochemistry reveals neoplastic cells that represent pan-B cell markers, usually positive for IRF4/MUM1, and CD13. An aberrant expression of T-cell phenotypes is also seen.

The unique genomic instability has been reported as follows: A20 deletion, interferon-inducible 27 (*IFI27*), *TP53* mutation, and *MYC* amplification.¹³

Lymphomatoid granulomatosis

Katzstein *et al.*¹⁴ initially described a rare angiocentric and angiodestructive EBV-associated LPD, which was distinct from Wegener's granulomatosis.

Nearly all patients present with symptoms related to pulmonary involvement, followed by involved sites of the central nervous system, skin, liver, and kidney. Radiologically, bilateral variable sized lung nodules are noted in lymphomatoid granulomatosis (LYG).

The histologic features of LYG are observed in lung nodules. All the lesions are angioinvasive and angiocentric with fibrinoid necrosis of the vascular wall. The infiltrate is polymorphous with an admixture of small lymphocytes, histiocytes, and large lymphoid cells. The grading of LYG is based on the proportion of

Table 1. Epstein-Barr virus-associated B-cell lymphoproliferative diseases

Disease
Infectious mononucleosis
Chronic active Epstein-Barr virus of B-cell type
Epstein-Barr virus-positive diffuse large B-cell lymphoma
Epstein-Barr virus mucocutaneous ulcer
Diffuse large B-cell lymphoma associated with chronic inflammation
Lymphomatoid granulomatosis

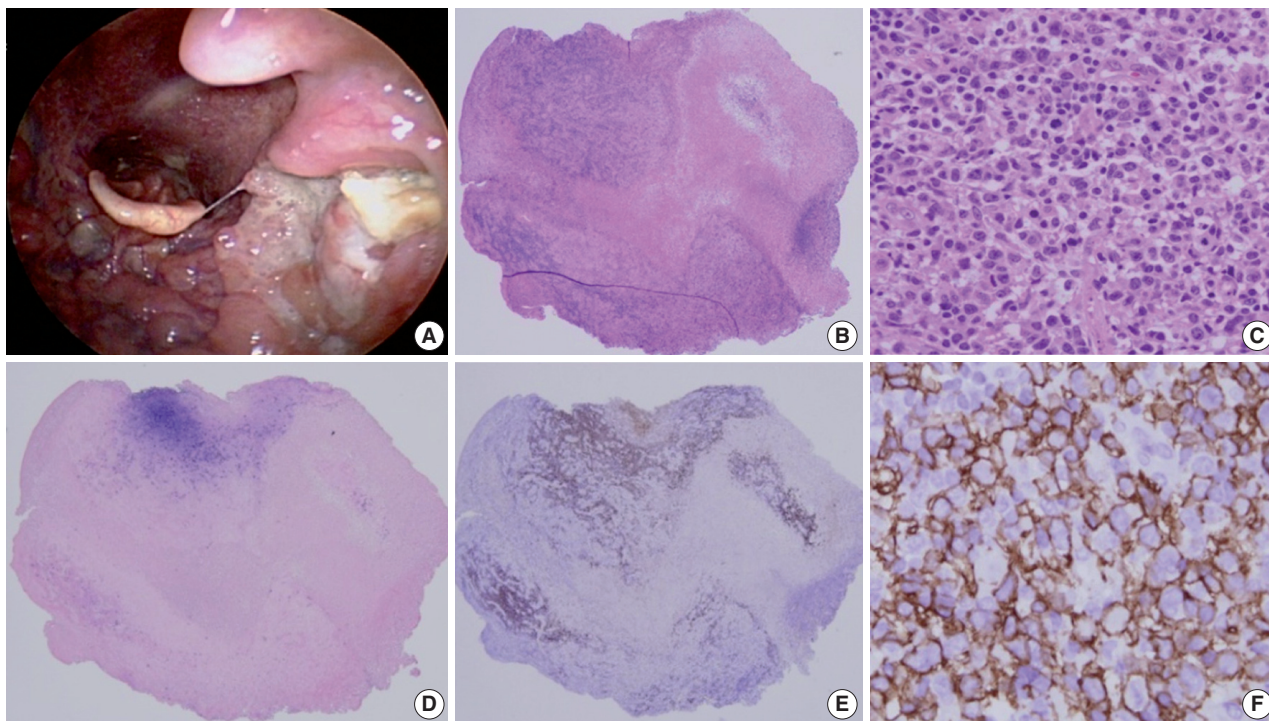


Fig. 1. Mucocutaneous ulcer (Courtesy of Dr. J.H. Paik). (A) This 70-year-old female presented with a sore throat, painful swelling saliva, and tonsillar enlargement with a discrete ulcer. (B) The scanning power view shows a dense infiltrate beneath the ulcer. (C) Medium sized atypical lymphocytes are observed. (D) Epstein-Barr virus (EBV)-*in-situ* hybridization positive cells are aggregated in the ulcer bed. (E) CD20 immunostaining disclosed overlapping with EBV-positive cells. (F) The large atypical cells are diffusely and strongly positive for CD20.

EBV positive cells. In general, grade 1 and grade 2 lesions are approached using strategies that are designed to improve the host's immune system, whereas grade 3 lesions require chemotherapy and do not respond to immunomodulatory therapies. Phenotypically, large atypical EBV-positive B cells express CD20, PAX5, CD79a, CD30⁺, and CD15⁻.¹⁵

EBV-ASSOCIATED T-CELL AND NATURAL KILLER CELL LPDS

EBV is a ubiquitous herpes virus with tropism for B cells, but the infection of T cells and natural killer (NK) cells may lead to several EBV-related LPDs. EBV-positive T/NK LPD encompasses disease entities with a broad clinicopathologic spectrum (Table 2).¹⁶

Table 2. EBV-associated T-cell and NK cell lymphoproliferative diseases

Disease
EBV-associated hyperinflammatory syndrome
EBV-associated hemophagocytic lymphohistiocytosis
CAEBV-type T/NK cell disease
Systemic chronic active EBV infection of T cell or NK cell type
Cutaneous forms of CAEBV
Severe mosquito bite allergy
Hydroa vacciniforme-like lymphoproliferative disease
Malignant T/NK cell disease
Systemic EBV-positive T-cell lymphoma
Extranodal NK/T cell lymphoma, nasal type
Extranodal NK/T cell lymphoma
Aggressive NK cell leukemia
EBV-positive nodal NK/T cell lymphoma (provisional)

EBV, Epstein-Barr virus; CAEBV, chronic active EBV; NK, natural killer.

EBV-associated hemophagocytic lymphohistiocytosis

Hemophagocytic lymphohistiocytosis (HLH) is a clinicopathologic syndrome encompassing a markedly dysregulated immune response and hypercytokinemia. HLH is characterized clinically by fever, splenomegaly, and cytopenias, and histologically by hemophagocytosis. The supportive laboratory findings for HLH are as follows: extremely high serum level of ferritin, lactate dehydrogenase, soluble CD25, and elevated viral capsid. EBV associated HLH accounts for 40% of HLH.

Histologically, EBV-positive T-cells and hemophagocytosing histiocytes are scattered in the sinusoids of the bone marrow and liver. The T-cells express CD8 and granzyme B. Even though it is uncommon, NK cells can be infiltrated in HLH.¹⁷

HLH can be effectively controlled in most patients (more than 90%), but the other 10% often die of fulminant disease.

CAEBV infection of T-cell or NK-cell types, systemic

CAEBV infection was initially defined as follows: (1) markedly abnormal EBV antibody titer; (2) histologic evidence of organ involved- interstitial pneumonia, hypoplasia of the bone marrow, uveitis, lymphadenitis, persistent hepatitis, or splenomegaly; and (3) increased EBV RNA in affected tissue.¹⁸

Clinically, CAEBV-T/NK is a disease of children but is also detected in young adults and even in middle-aged older adults with a mean age of 11.3 years.¹⁹ The symptoms are usually prolonged fever, hepatomegaly, splenomegaly, thrombocytopenia, anemia, and lymphadenopathy.¹⁹ Life-threatening complications include hemophagocytic syndrome, interstitial pneumonia, malignant lymphoma, coronary aneurysms, and central nervous system involvement. All patients have elevated levels of EBV DNA in their

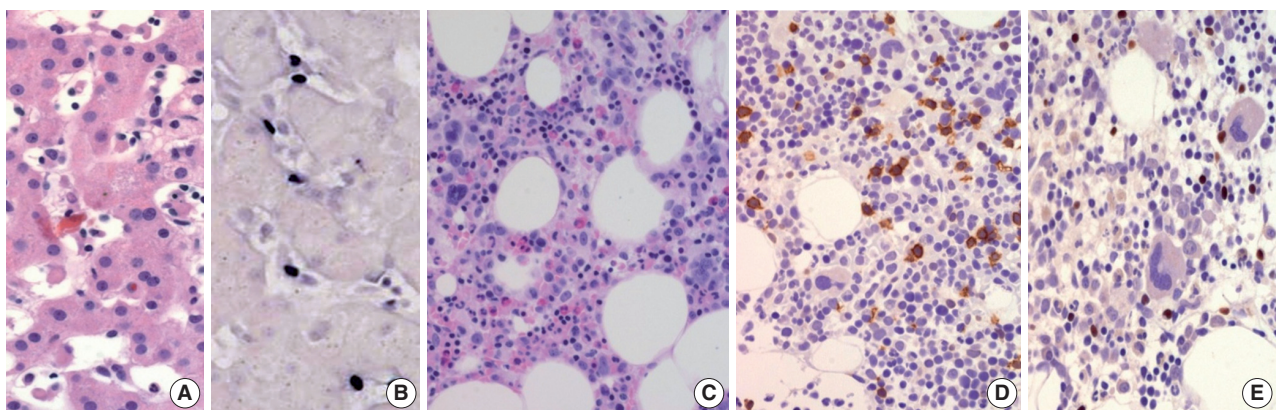


Fig. 2. Chronic active Epstein-Barr virus (EBV) infection of a T-cell or natural killer cell type, systemic (Courtesy of Dr. Y.H. Ko). (A) A 21-year-old man presented with severe oral ulcer, recurrent pneumonia, thrombocytopenia, and elevated liver enzymes for 2 years. Liver biopsy reveals atypical T lymphocytes infiltrating the sinusoidal and hepatic lobules. (B) EBV-encoded small RNA (EBER) *in-situ* hybridization exhibits positive signals in these T cells. (C) Bone marrow biopsy shows small lymphocytic infiltrate. (D) CD3 is expressed in most lymphocytes. (E) EBER *in-situ* hybridization also shows positive signals in T cells.

blood, which is well-correlated with clinical severity.¹⁹

Morphologically, in patients with CAEBV-T/NK the lymph nodes exhibit paracortical hyperplasia with polymorphic and polyclonal lymphoid proliferation and large numbers of EBV positive cells. The liver exhibits portal or sinusoidal infiltration by small lymphocytes with no definite atypia (Fig. 2).

Ohshima *et al.*¹⁸ proposed a three-tier classification as follows: category A1 is polymorphic LPD with polyclonal proliferation of EBV-infected T cells or NK cells; category A2 is polymorphic LPD with monoclonal T/NK cells; and category A3 is monomorphic LPD of monoclonal T cells.

Severe mosquito bite allergy

A severe mosquito bite allergy is a cutaneous manifestation of chronic EBV infection characterized by intense local skin symptoms, such as erythema, bullae, ulcers, and scarring. The systemic symptoms such as fever, lymphadenopathy, and liver dysfunction are developed after mosquito bites, vaccination, or injection.

The epidermis at the mosquito bite site exhibits necrosis and ulceration. The dermis reveals edema and infiltration of polymorphonuclear leukocytes, nuclear debris, and extravasated erythrocytes with fibrinoid necrosis of small vessels. The infiltrating small lymphocytes extend from the dermis to the subcutis in an angiocentric pattern. EBV-positive cells represent 3%–10% of infiltrating lymphocytes.²⁰

Hydroa vacciniforme-like LPD

Hydroa vacciniforme (HV)-like LPD is one of the cutaneous forms of CAEBV. It is initially described as an EBV positive polyclonal or monoclonal T/NK LPD, characterized by blistering photodermatoses in childhood and healed with vacciniform scarring.²¹ It is clinically divided into two types. The classic type is a self-limited disease with vesicles on sun-exposed areas in adolescence or young adulthood. Severe HV-type tends to exhibit more extensive skin lesions and systemic manifestations of fever, hepatomegaly, serologic abnormalities, and peripheral NK lymphocytosis. The severe type of HV often progresses to EBV-associated NK/T-cell malignancy.^{22,23}

Morphologic findings of HV are epidermal reticular degeneration to spongiotic vesiculation with perivascular and periappendiceal lymphocytic infiltration with no definite cytologic atypia. Severe HV and HV-like T-cell lymphomas mimic those of classic HV, but the dermal infiltrates are more extensive and deeper, composed of variably atypical lymphocytes.

The immunophenotype of the classic HV is CD4⁺ or CD8⁺ T-cells, but the severe form/lymphoma exhibits predominantly

CD8⁺ CTLs. The majority are $\alpha\beta$ T cells. A few cases involve $\alpha\beta$ T cells and rarely NK cells.

Systemic EBV-positive T-cell lymphoma

Systemic EBV-positive T-cell lymphoma of childhood and young adulthood is a fulminant illness of EBV-infected T cells with clonal proliferation and cytotoxic phenotype. The clinical manifestation of this lesion is a rapid clinical progression with multiple organ failure, sepsis, and death. A hemophagocytic syndrome is nearly always associated. Systemic EBV-positive T-cell lymphoma arising in patients with a history of CAEBV-T/NK develops in a median time of 35 months.²⁴

Hyperplasia of histiocytes and marked hemophagocytic syndrome are also noted with increased small T-cells in the bone marrow, spleen, and liver. The paracortical zone of the lymph node is expanded with the depletion of B-cell areas. The degree of cytologic atypia in EBV-positive lymphocytes is variable.

Extranodal NK/T cell lymphoma, nasal type

Extranodal NK/T cell lymphoma is a prototype of EBV-associated T-cell LPD, which is characterized by frequent necrosis, angiocentric growth, cytotoxic phenotype and a strong association with EBV. Since the nasal cavity is the most commonly involved site, the nasopharynx and upper aerodigestive areas including the nasal cavity disclose progressively destructive and ulcerative lesions or obstructive symptoms due to mass effects.²⁵

Extranasal NK/T cell lymphoma

Extranasal NK/T cell lymphomas frequently involve the skin, gastrointestinal tract, testis, and soft tissue. Most patients present at a higher stage with multiple areas of involvement.²⁶

The morphology of the involved sites is frequently ulcerated and necrotic. The cytologic composition varies ranging from small, medium, and large. Angiocentric growth accompanies diffuse necrosis, and vascular damage.

Aggressive NK cell leukemia

Aggressive NK-cell leukemia is a neoplasm of NK cells, which primarily involves peripheral blood and bone marrow. In contrast to conventional leukemia, the tumor cells may not be abundant in the peripheral blood and bone marrow. The average age of patients exhibiting this disorder is 39 years. The typical presentations include fever, hepatosplenomegaly, lymphadenopathy, and is complicated by hemophagocytic syndrome.

In histologic sections, there are diffuse, destructive and permeative infiltrates of monomorphic cells with a round to moderate

rim of pale or amphophilic cytoplasm. Interspersed apoptotic bodies and zonal cell death are common. Angioinvasive and angiodestructive growth is also frequently noted. The clinical course is fatal.

EBV-positive nodal NK/T cell lymphoma

EBV-positive nodal T/NK cell lymphoma may involve a limited number of extranodal organs except for the nasal cavity, but the main bulk of the tumor is located in the lymph nodes. This entity is very rare with fewer than 100 cases being reported in the literature.²⁷

The lymph nodes exhibit a diffuse infiltration of pleomorphic, variable sized cells. The cytomorphology of the tumor cells are more commonly centробlastoid, often anaplastic or plasmacytoid with some RS-like cells being noted. Some cases show extensive necrosis, many apoptotic bodies, and angiocentric growth patterns. The immunophenotype is as follows: CD3⁺, CD8⁺, TIA⁺, and granzyme B⁺.²⁸

The disease course is very aggressive, with a median survival of only 4 months.

CONCLUSION

Many new entities and concepts for EBV-positive LPDs have been added to the 2016 WHO classification, based on growing knowledge in the field of genetics and molecular virology. With this increased understanding of LPD the clinical and pathologic entities, we can perform EBV-ISH indicative of (1) clinically bordered between infection and neoplastic conditions; (2) past history of recurrent inappropriate immune response, especially in children/young adults or old age; and (3) a pathologically polymorphous inflammatory background (but not Hodgkin lymphoma). It helps that the final destination is the achievement of appropriate diagnosis and management of LPDs. Some entities are provisional and must wait for confirmation of additional data.

Conflicts of Interest

No potential conflict of interest relevant to this article was reported.

REFERENCES

1. Cohen JL. Epstein-Barr virus infection. *N Engl J Med* 2000; 343: 481-92.

2. Pittaluga S, Said J. Virally associated B cell lymphoproliferative disease. In: Jaffe E, Arbor DA, Campo E, Harris NL, Quintanilla-Fend L, eds. *Hematopathology*. 2nd ed. Philadelphia: Elsevier Health Science; 2016; 547-607.
3. Swerdlow SH, Campo E, Pileri SA, *et al*. The 2016 revision of the World Health Organization classification of lymphoid neoplasms. *Blood* 2016; 127: 2375-90.
4. Chaganti S, Heath EM, Bergler W, *et al*. Epstein-Barr virus colonization of tonsillar and peripheral blood B-cell subsets in primary infection and persistence. *Blood* 2009; 113: 6372-81.
5. Vouloumanou EK, Rafailidis PI, Falagas ME. Current diagnosis and management of infectious mononucleosis. *Curr Opin Hematol* 2012; 19: 14-20.
6. Fletcher C. *Diagnostic histopathology of tumors*. 3rd ed. Philadelphia: Churchill Livingstone/Elsevier, 2007; 1260-1.
7. Lekstrom-Himes JA, Dale JK, Kingma DW, Diaz PS, Jaffe ES, Straus SE. Periodic illness associated with Epstein-Barr virus infection. *Clin Infect Dis* 1996; 22: 22-7.
8. Cho EY, Kim KH, Kim WS, Yoo KH, Koo HH, Ko YH. The spectrum of Epstein-Barr virus-associated lymphoproliferative disease in Korea: incidence of disease entities by age groups. *J Korean Med Sci* 2008; 23: 185-92.
9. Cohen JL, Jaffe ES, Dale JK, *et al*. Characterization and treatment of chronic active Epstein-Barr virus disease: a 28-year experience in the United States. *Blood* 2011; 117: 5835-49.
10. Swerdlow SH, Campo E, Harris NL, *et al*. *WHO classification of tumors of hematopoietic and lymphoid tissues*. 4th ed. Lyon: IARC Press, 2008.
11. Nicolae A, Pittaluga S, Abdullah S, *et al*. EBV-positive large B-cell lymphomas in young patients: a nodal lymphoma with evidence for a tolerogenic immune environment. *Blood* 2015; 126: 863-72.
12. Dojcinov SD, Venkataraman G, Raffeld M, Pittaluga S, Jaffe ES. EBV positive mucocutaneous ulcer—a study of 26 cases associated with various sources of immunosuppression. *Am J Surg Pathol* 2010; 34: 405-17.
13. Hongyo T, Kurooka M, Taniguchi E, *et al*. Frequent p53 mutations at dipyrimidine sites in patients with pyothorax-associated lymphoma. *Cancer Res* 1998; 58: 1105-7.
14. Katzenstein AL, Carrington CB, Liebow AA. Lymphomatoid granulomatosis: a clinicopathologic study of 152 cases. *Cancer* 1979; 43: 360-73.
15. Song JY, Pittaluga S, Dunleavy K, *et al*. Lymphomatoid granulomatosis: a single institute experience: pathologic findings and clinical correlations. *Am J Surg Pathol* 2015; 39: 141-56.
16. Kimura H, Ito Y, Kawabe S, *et al*. EBV-associated T/NK-cell lymphoproliferative diseases in nonimmunocompromised hosts: prospec-

- tive analysis of 108 cases. *Blood* 2012; 119: 673-86.
17. Toga A, Wada T, Sakakibara Y, *et al.* Clinical significance of cloned expansion and CD5 down-regulation in Epstein-Barr Virus (EBV)-infected CD8+ T lymphocytes in EBV-associated hemophagocytic lymphohistiocytosis. *J Infect Dis* 2010; 201: 1923-32.
 18. Ohshima K, Kimura H, Yoshino T, *et al.* Proposed categorization of pathological states of EBV-associated T/natural killer-cell lymphoproliferative disorder (LPD) in children and young adults: overlap with chronic active EBV infection and infantile fulminant EBV T-LPD. *Pathol Int* 2008; 58: 209-17.
 19. Ko YH, Kim HJ, Oh YH, *et al.* EBV-associated T and NK cell lymphoproliferative disorders: consensus report of the 4th Asian Hematopathology Workshop. *J Hematopathol* 2012; 5: 319-24.
 20. Cohen JI, Kimura H, Nakamura S, Ko YH, Jaffe ES. Epstein-Barr virus-associated lymphoproliferative disease in non-immunocompromised hosts: a status report and summary of an international meeting, 8-9 September 2008. *Ann Oncol* 2009; 20: 1472-82.
 21. Park S, Ko YH. Epstein-Barr virus-associated T/natural killer-cell lymphoproliferative disorders. *J Dermatol* 2014; 41: 29-39.
 22. Miyake T, Yamamoto T, Hirai Y, *et al.* Survival rates and prognostic factors of Epstein-Barr virus-associated hydroa vacciniforme and hypersensitivity to mosquito bites. *Br J Dermatol* 2015; 172: 56-63.
 23. Cho KH, Kim CW, Heo DS, *et al.* Epstein-Barr virus-associated peripheral T-cell lymphoma in adults with hydroa vacciniforme-like lesions. *Clin Exp Dermatol* 2001; 26: 242-7.
 24. Quintanilla-Martinez L, Kumar S, Fend F, *et al.* Fulminant EBV(+) T-cell lymphoproliferative disorder following acute/chronic EBV infection: a distinct clinicopathologic syndrome. *Blood* 2000; 96: 443-51.
 25. Hong M, Lee T, Kang SY, Kim SJ, Kim W, Ko YH. Nasal-type NK/T-cell lymphomas are more frequently T rather than NK lineage based on T-cell receptor gene, RNA, and protein studies: lineage does not predict clinical behavior. *Mod Pathol* 2016; 29: 430-43.
 26. Chan JK, Sin VC, Wong KF, *et al.* Nonnasal lymphoma expressing the natural killer cell marker CD56: a clinicopathologic study of 49 cases of an uncommon aggressive neoplasm. *Blood* 1997; 89: 4501-13.
 27. Kato S, Asano N, Miyata-Takata T, *et al.* T-cell receptor (TCR) phenotype of nodal Epstein-Barr virus (EBV)-positive cytotoxic T-cell lymphoma (CTL): a clinicopathologic study of 39 cases. *Am J Surg Pathol* 2015; 39: 462-71.
 28. Jeon YK, Kim JH, Sung JY, Han JH, Ko YH; Hematopathology Study Group of the Korean Society of Pathologists. Epstein-Barr virus-positive nodal T/NK-cell lymphoma: an analysis of 15 cases with distinct clinicopathological features. *Hum Pathol* 2015; 46: 981-90.

Implication of PHF2 Expression in Clear Cell Renal Cell Carcinoma

Cheol Lee¹ · Bohyun Kim¹
Boram Song¹ · Kyung Chul Moon^{1,2}

¹Department of Pathology, Seoul National University College of Medicine, Seoul;
²Kidney Research Institute, Medical Research Center, Seoul National University College of Medicine, Seoul, Korea

Received: February 9, 2017
Revised: March 8, 2017
Accepted: March 14, 2017

Corresponding Author

Kyung Chul Moon, MD
Department of Pathology, Kidney Research Institute,
Medical Research Center, Seoul National University
College of Medicine, 103 Daehak-ro, Jongno-gu,
Seoul 03080, Korea
Tel: +82-2-2072-1767
Fax: +82-2-743-5530
E-mail: blue7270@snu.ac.kr

Background: Clear cell renal cell carcinoma (CCRCC) is presumed to be associated with adipogenic differentiation. Histone modification is known to be important for adipogenesis, and the function of histone demethylase plant homeodomain finger 2 (PHF2) has been noted. In addition, PHF2 may act as a tumor suppressor via epigenetic regulation of p53 and is reported to be reduced in colon cancer and stomach cancer tissues. In this study, we examined PHF2 expression in CCRCC specimens by immunohistochemistry. **Methods:** We studied 254 CCRCCs and 56 non-neoplastic renal tissues from patients who underwent radical or partial nephrectomy between 2000 and 2003 at the Seoul National University Hospital. Tissue microarray blocks were prepared, and immunohistochemical staining for PHF2 was performed. **Results:** Among 254 CCRCC cases, 150 cases (59.1%) showed high expression and 104 cases (40.1%) showed low expression. High expression of PHF2 was significantly correlated with a low Fuhrman nuclear grade ($p < .001$), smaller tumor size ($p < .001$), low overall stage ($p = .003$), longer cancer-specific survival ($p = .002$), and progression-free survival ($p < .001$) of the patients. However, it was not an independent prognostic factor in multivariate analysis adjusted for Fuhrman nuclear grade and overall stage. **Conclusions:** Our study showed that low expression of PHF2 is associated with aggressiveness and poor prognosis of CCRCC.

Key Words: PHF2 protein, human; Carcinoma, renal cell; Clear cell renal cell carcinoma; Immunohistochemistry; Adipogenesis

Renal cancer is one of the most common cancers in Korean males.¹ Among the types of renal cancer, clear cell renal cell carcinoma (CCRCC) is the most common. CCRCC can exhibit various histologic features,² but most tumors are golden yellow due to the abundant lipid contents of the cells, and microscopically, the tumor cells have a clear cytoplasm similar to adipocytes.³ The tumor cells have abundant cytoplasmic lipids in addition to glycogen, as revealed by an ultrastructural study.⁴ For this reason, CCRCC is presumed to be associated with adipogenic differentiation. Until recently, although three studies have shown that CCRCC is associated with adipogenic differentiation,⁵⁻⁷ the association of tumorigenesis with clear cell morphology is still required at the molecular level.

In recent studies, histone modification has been confirmed to be important in adipogenesis. In particular, the function of histone demethylase plant homeodomain finger 2 (PHF2), as it maps to human chromosome 9q22,⁸ has been noted.^{9,10} PHF2 is a dimethylated histone H3 lysine 9 (H3K9me2) demethylase¹⁰ that acts both in gluconeogenesis of hepatocytes and in signaling for regulation of immune and homeogenesis of macrophages *in vitro*.^{11,12}

The physiological role of PHF2 *in vivo* is not yet clear, but it

may be a co-activator with multiple transcription factors.¹⁰ To the best of our knowledge, only a few studies have investigated the association of PHF2 expression with human cancers, such as breast cancer, esophageal cancer and squamous cell carcinoma of the head and neck.¹³⁻¹⁵ A recent study has shown that PHF2 can act as a tumor suppressor through epigenetic regulation of p53 and shows reduced expression in colon cancer and stomach cancer tissues.¹⁶ However, there has been no report of PHF2 expression in CCRCC.

In this study, we investigated the relationship between the expression level of PHF2 and clinicopathological factors and prognosis in CCRCC patients using immunohistochemical staining of CCRCC specimens.

MATERIALS AND METHODS

Patients and tissue microarray

We examined 254 CCRCCs and 56 non-neoplastic renal tissues including the cortex and medulla from patients who underwent radical or partial nephrectomy between 2000 and 2003 in Seoul National University Hospital. Tissue microarray (TMA) blocks

containing representative tumor and non-neoplastic tissue core sections (2 mm in diameter) were prepared from each formalin-fixed paraffin block (SuperBioChips Laboratories, Seoul, Korea). All available hematoxylin and eosin-stained slides were reviewed to assess the validity of the diagnosis, and tumors were graded from 1 to 4 according to the Fuhrman nuclear grade system. Clinical and pathological information was collected from electronic medical records and pathological reports. The follow-up period ranged from 2 to 163 months, and the median follow-up period was 84.5 months. This study was approved by Seoul National University Hospital's Institutional Review Board (IRB).

Immunohistochemistry

Immunohistochemical staining for PHF2 was performed on 4 μm -thick sections taken from TMA. Immunohistochemistry (IHC) was performed using the Ventana Benchmark XT automated dyeing system (Ventana Medical Systems, Tucson, AZ, USA). Polyclonal rabbit anti-PHF2 antibody (Novus Biologicals,

Littleton, CO, USA) was diluted 1:200. Immunohistochemically stained TMA slides were individually reviewed by two pathologists without clinicopathological information.

In non-neoplastic renal tissue, PHF2 was commonly expressed in the nucleus and cytoplasm of the proximal tubular epithelium, but only in the nucleus of the distal tubular epithelium and podocytes of the glomerulus (Fig. 1). The expression of PHF2 was assessed in both the nucleus and cytoplasm of CCRCCs and classified as high when nuclear expression was observed in more than 10% of the tumor cells, regardless of cytoplasmic expression (Fig. 2).

Statistical analysis

Statistical analysis was performed using the statistical program SPSS ver. 21.0 (IBM Corp., Armonk, NY, USA). The chi-squared test was used to analyze the relationship between PHF2 expression and clinicopathological characteristics. Survival curves were generated using the Kaplan-Meier method, and survival rate differences were compared using the log-rank test.

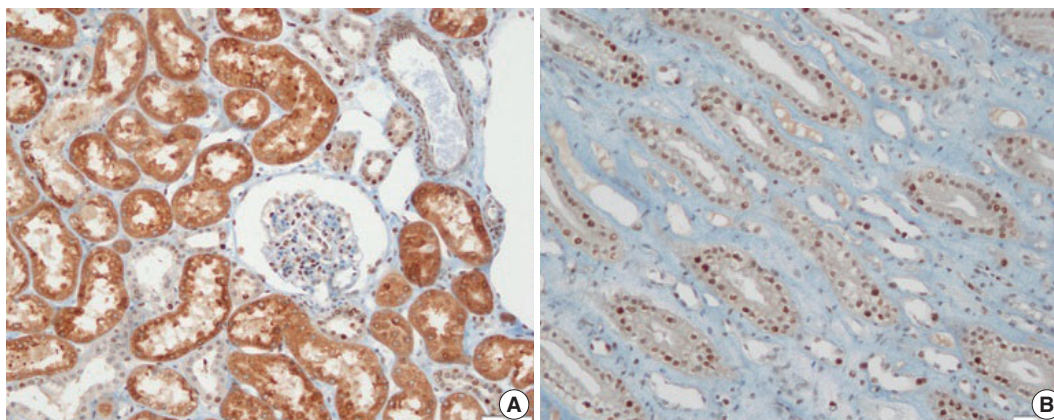


Fig. 1. Plant homeodomain finger 2 (PHF2) expression in non-neoplastic renal tissue. PHF2 is expressed in the nucleus and cytoplasm of the proximal tubular epithelium and in the nucleus of the distal tubular epithelium and podocytes in the glomerulus. (A) Cortex. (B) Medulla.

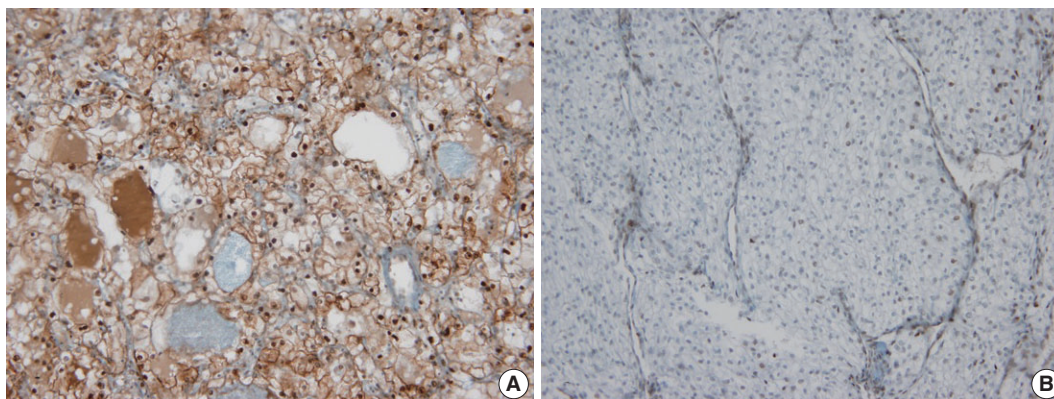


Fig. 2. Plant homeodomain finger 2 expression in clear cell renal cell carcinoma. (A) High expression (B) Low expression.

The multivariate Cox proportional hazard model was used to analyze the importance of various variables for survival. *p*-values less than .05 were considered statistically significant.

RESULTS

Basic clinicopathological characteristics

Of the 254 patients in this study, 187 (73.6%) were males and 67 (26.4%) were females. The age at diagnosis was between 28 and 82 years old. The mean age±standard deviation (SD) and median age were 56.2±11.3 years and 57 years, respectively. We have classified them into two groups: older than 57 years or not. The Fuhrman nuclear grade distribution was 16 cases in grade I (6.3%), 113 cases in grade II (44.5%), 93 cases in grade III (36.6%), and 32 cases in grade IV (12.6%). The tumor size ranged from 1.0 to 22.0 cm and the mean±SD size was 5.6±3.5 cm. At the time of diagnosis, 23 patients (9.1%) had metastatic cancers and 231 (90.9%) did not. According to the prognostic classification of the American Joint Committee on Cancer 7th edition,¹⁷ the T stage was as follows: T1 was 164 cases (64.6%), T2 was 38 cases (15.0%), T3 was 50 cases (19.7%), and T4 was

two cases (0.8%). Additionally, the overall stage was 162 cases in stage I (63.8%), 31 cases in stage II (12.2%), 37 cases in stage III (14.6%), and 24 cases in stage IV (9.4%) (Table 1).

Immunohistochemical result of PHF2 and relationship with clinicopathological characteristics

Of the 254 cases, 150 cases (59.1%) showed high expression, and 104 cases (40.1%) showed low expression. The high expression of PHF2 was associated with a younger age group (*p* = .006) and significantly correlated with low Fuhrman nuclear grade, small tumor size and low overall stage (*p* < .001, *p* < .001, and *p* = .003, respectively) (Table 1). However, there was no association with the patients' sex, T stage, or metastasis at diagnosis.

The association between PHF2 expression and survival time of the patients

To assess prognostic value, we evaluated the association between PHF2 expression and patient survival by a log-rank test using Kaplan-Meier analysis. We observed that high expression of PHF2 was significantly associated with longer cancer-specific survival (*p* = .002) and progression-free survival (*p* < .001) in CCRCC patients (Fig. 3).

Table 1. Relationship between PHF2 expression and clinicopathological characteristics

Characteristic	No. of cases (n=254)	PHF2 expression		p-value
		Low (n=104, 40.1%)	High (n=150, 59.1%)	
Age (yr)				.006
<57	124 (48.8)	40	84	
≥57	130 (51.2)	64	66	
Sex				.320
Male	187 (73.6)	80	107	
Female	67 (26.4)	24	43	
Fuhrman grade				<.001
1, 2	129 (50.8)	38	91	
3, 4	125 (49.2)	66	59	
Tumor size (cm)				<.001
<5	145 (57.1)	44	101	
≥5	109 (42.9)	60	49	
T stage				.071
1, 2	202 (79.5)	77	125	
3, 4	52 (20.5)	27	25	
Metastasis at diagnosis				.111
No	231 (90.9)	91	140	
Yes	23 (9.1)	13	10	
Overall stage				.003
I, II	193 (76.0)	69	124	
III, IV	61 (24.0)	35	26	

Values are presented as number (%).
PHF2, plant homeodomain finger 2.

Univariate and multivariate Cox regression analysis of cancer-specific survival and progression-free survival

Univariate cox regression analysis showed significant correlation with age (less than 57 or not), Fuhrman nuclear grade, tumor size (less than 5 cm or not), T stage, metastasis at diagnosis, overall stage, PHF2 expression status, cancer-specific survival (*p* = .009 for age, *p* = .003 for PHF2 expression status, and *p* < .001 for the others), and progression-free survival (*p* = .001 for age and *p* < .001 for the others) (Table 2). However, multivariate analysis adjusted for age, Fuhrman nuclear grade and overall stage showed that high expression of PHF2 was not an independent prognostic factor in CCRCC patients with cancer-specific survival (*p* = .566) and progression-free survival (*p* = .099) (Table 2).

DISCUSSION

In this study, we analyzed the association of PHF2 expression with other clinicopathological parameters and survival time of the CCRCC patients. High expression of PHF2 was associated with a young age group and correlated significantly with low Fuhrman nuclear grade and overall stage. We also observed that high expression of PHF2 was significantly correlated with longer cancer-specific survival and progression-free survival in patients.

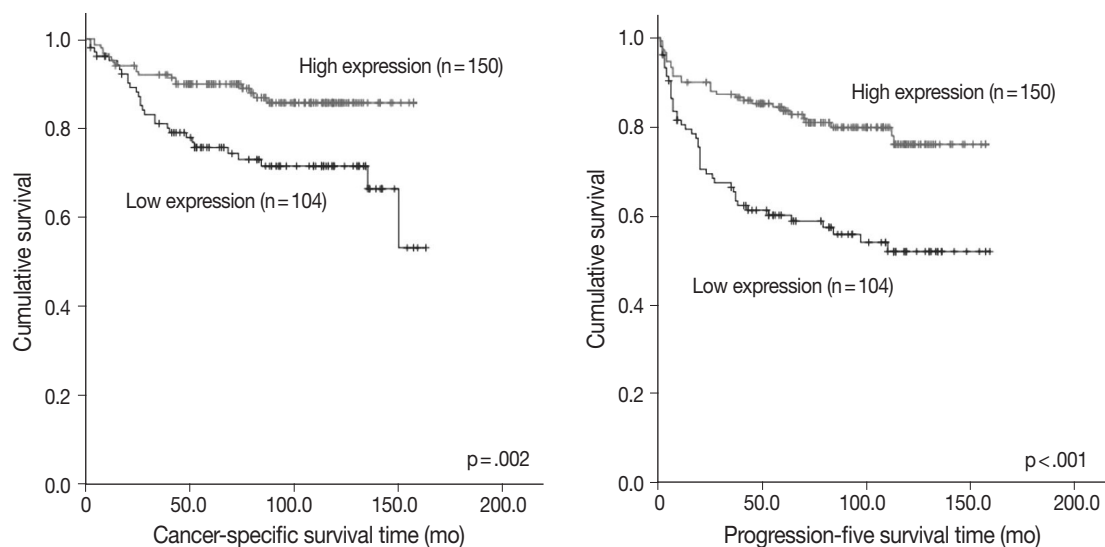


Fig. 3. Kaplan-Meier curves. Cancer-specific and progression-free survival according to plant homeodomain finger 2 (PHF2) expression.

Table 2. Univariate and multivariate Cox regression analysis of cancer-specific and progression-free survival

Parameter	Univariate analysis			Multivariate analysis		
	p-value	HR	95% CI	p-value	HR	95% CI
Cancer-specific survival						
Age (<57 yr vs ≥57 yr)	.009	2.239	1.227–4.088	.393	1.312	0.704–2.448
Sex (male vs female)	.870	0.947	0.492–1.821			
Fuhrman grade (1, 2 vs 3, 4)	<.001	7.754	3.463–17.363	<.001	4.391	1.911–10.089
Tumor size (<5 cm vs ≥5 cm)	<.001	8.130	3.801–17.391			
T stage (1, 2 vs 3, 4)	<.001	9.021	5.021–16.207			
Metastasis at diagnosis (no vs yes)	<.001	26.511	14.102–49.840			
Overall stage (I, II vs III, IV)	<.001	15.961	8.233–30.945	<.001	10.616	5.313–21.214
PHF2 expression (low vs high)	.003	0.419	0.235–0.749	.566	0.840	0.463–1.524
Progression-free survival						
Age (<57 yr vs ≥57 yr)	.001	2.324	1.436–3.762	.121	1.483	0.902–2.440
Sex (male vs female)	.959	0.987	0.586–1.660			
Fuhrman grade (1, 2 vs 3, 4)	<.001	3.972	2.357–6.692	.001	2.491	1.447–4.287
Tumor size (<5 cm vs ≥5 cm)	<.001	8.416	4.692–15.096			
T stage (1, 2 vs 3, 4)	<.001	6.573	4.121–10.484			
Metastasis at diagnosis (no vs yes)	<.001	19.269	11.058–33.578			
Overall stage (I, II vs III, IV)	<.001	9.230	5.744–14.832	<.001	6.470	3.933–10.643
PHF2 expression (low vs high)	<.001	0.385	0.242–0.611	.099	0.666	0.411–1.079

HR, hazard ratio; CI, confidence interval.

Multivariate analysis adjusted for age, Fuhrman nuclear grade and overall stage showed that high expression of PHF2 was not an independent prognostic factor for cancer-specific survival and progression-free survival in CCRCC patients.

PHF2 is a type of histone demethylase, and histone modification is known to be important in adipogenesis.^{9,10,18} PHF2 has been shown to play a role in gluconeogenesis in hepatocytes of fasted mice¹¹ and proinflammatory gene regulation in macrophages *in vitro*.¹² In a recent study, PHF2 was shown to play an important role in adipogenesis in transgenic mice.⁹ PHF2 de-

methylates the AT-rich interactive domain-containing protein 5B (ARID5B) and binds the promoter regions of target genes by forming a complex with demethylated ARID5B.^{10,11} PHF2 interacts with CCAAT/enhancer-binding protein alpha (CEBPA), one of the major regulators of adipogenesis, and promotes adipogenesis by demethylating H3K9me2 in the promoter region of CEBPA target gene. These results indicate that PHF2 promotes adipogenesis by coactivation of CEBPA and that PHF2 is a novel histone methylation-modifying enzyme that modulates adipogenesis.^{9,10}

As mentioned earlier, some studies have shown that adipogenic differentiation is associated with CCRCC.⁵⁻⁷ One study showed that gene expression patterns and IHC results in CCRCC tissues were associated with adipogenesis.⁷ They also found that CCRCC cells undergo adipogenic transdifferentiation, based on the observation that the clear cell morphology of CCRCC cells disappeared in standard cell culture media and was redeveloped in adipogenic media.⁷ This study concluded that adipogenesis was a type of epithelial mesenchymal transition.⁷ Another study has shown that adipose differentiation-related protein (ADFP) expression is increased at both mRNA and protein levels of CCRCC compared to non-neoplastic renal tissues and other types of renal cell carcinoma.⁵ ADFP was originally known as a protein associated with lipid metabolism, highly expressed in adipocytes and variably expressed in other cells.^{19,20} Higher ADFP levels in CCRCC were associated with a lower grade, lower stage and better prognosis, while higher ADFP levels were an independent good prognostic factor in multivariate analysis.^{5,6}

In previous studies, CCRCC with low nuclear grade showed a typical clear cell morphology, but CCRCC with a higher nuclear grade showed reduced clear cell morphology and other morphological features that are relatively frequently observed in metastatic renal cell carcinoma, such as eosinophilic cytoplasm and rhabdoid feature.^{2,21} These results suggest that clear cell morphology due to adipogenesis in CCRCC is associated with low nuclear grade and good prognosis. In this regard, our findings suggest that adipogenic differentiation by histone modification is a new tumorigenic mechanism that reflects the clear cell morphology in CCRCC. In addition, the loss of PHF2 expression seems to be correlated with tumor progression and a poor prognosis of CCRCC due to the loss of adipogenic differentiation.

The role of PHF2 in tumorigenesis is not yet well understood, and only a few studies have examined the association between human cancer and PHF2 expression. The expression of PHF2 in breast cancer was not correlated with patient prognosis.¹³ In esophageal squamous cell carcinoma, PHF2 was overexpressed in cancer cells compared to the non-neoplastic epithelium, and high cytoplasmic expression of PHF2 tended to be associated with decreased overall survival of the patients, but there was no statistical significance.¹⁴ In head and neck squamous cell carcinoma, loss of heterozygosity was observed in the chromosomal 9q22 locus located in the PHF2 gene in relation to dysplastic lesions, but it was not related to the clinicopathological index or patient survival rate.^{15,22}

A recent study showed that PHF2 can modulate p53 by demethylating H3K9me2, and down-regulation of PHF2 expression occurs in colon and stomach cancer.¹⁶ In the study, they suggested

that PHF2 acts as a tumor suppressor by regulating the function of p53.¹⁶ Even p53-positive colon cancer cells have a malignant phenotype associated with the suppression of p21, a downstream molecule of p53.¹⁶ They also suggested that PHF2 expression levels could help predict patient outcomes in tumors expressing functional p53.¹⁶ These results provide another perspective on the role of PHF2 in CCRCC, although the role of p53 in the progression of CCRCC remains controversial.²³⁻²⁵

Our study showed the clinicopathological significance of PHF2 expression in CCRCC. Low expression of PHF2 is associated with aggressiveness and poor prognosis of CCRCC, and this effect of PHF2 may be related to the role of PHF2 in adipogenesis or the regulation of p53. More functional studies will help clarify the role of PHF2 in the development and progression of CCRCC.

Conflicts of Interest

No potential conflict of interest relevant to this article was reported.

REFERENCES

- Jung KW, Won YJ, Kong HJ, Oh CM, Seo HG, Lee JS. Cancer statistics in Korea: incidence, mortality, survival and prevalence in 2010. *Cancer Res Treat* 2013; 45: 1-14.
- Lee C, Park JW, Suh JH, Nam KH, Moon KC. Histologic variations and immunohistochemical features of metastatic clear cell renal cell carcinoma. *Korean J Pathol* 2013; 47: 426-32.
- Eble JN, Sauter G, Epstein JI, Sesterhenn IA. *Pathology and genetics of tumours of the urinary system and male genital organs*. Lyon: IARC Press, 2004; 12-39.
- Rezende RB, Drachenberg CB, Kumar D, *et al*. Differential diagnosis between monomorphic clear cell adenocarcinoma of salivary glands and renal (clear) cell carcinoma. *Am J Surg Pathol* 1999; 23: 1532-8.
- Yao M, Tabuchi H, Nagashima Y, *et al*. Gene expression analysis of renal carcinoma: adipose differentiation-related protein as a potential diagnostic and prognostic biomarker for clear-cell renal carcinoma. *J Pathol* 2005; 205: 377-87.
- Yao M, Huang Y, Shioi K, *et al*. Expression of adipose differentiation-related protein: a predictor of cancer-specific survival in clear cell renal carcinoma. *Clin Cancer Res* 2007; 13: 152-60.
- Tun HW, Marlow LA, von Roemeling CA, *et al*. Pathway signature and cellular differentiation in clear cell renal cell carcinoma. *PLoS One* 2010; 5: e10696.
- Hasenpusch-Theil K, Chadwick BP, Theil T, Heath SK, Wilkinson DG, Frischauf AM. PHF2, a novel PHD finger gene located on human

- chromosome 9q22. *Mamm Genome* 1999; 10: 294-8.
9. Okuno Y, Ohtake F, Igarashi K, *et al.* Epigenetic regulation of adipogenesis by PHF2 histone demethylase. *Diabetes* 2013; 62: 1426-34.
 10. Okuno Y, Inoue K, Imai Y. Novel insights into histone modifiers in adipogenesis. *Adipocyte* 2013; 2: 285-8.
 11. Baba A, Ohtake F, Okuno Y, *et al.* PKA-dependent regulation of the histone lysine demethylase complex PHF2-ARID5B. *Nat Cell Biol* 2011; 13: 668-75.
 12. Stender JD, Pascual G, Liu W, *et al.* Control of proinflammatory gene programs by regulated trimethylation and demethylation of histone H4K20. *Mol Cell* 2012; 48: 28-38.
 13. Sinha S, Singh RK, Alam N, Roy A, Roychoudhury S, Panda CK. Alterations in candidate genes PHF2, FANCC, PTCH1 and XPA at chromosomal 9q22.3 region: pathological significance in early- and late-onset breast carcinoma. *Mol Cancer* 2008; 7: 84.
 14. Sun LL, Sun XX, Xu XE, *et al.* Overexpression of Jumonji AT-rich interactive domain 1B and PHD finger protein 2 is involved in the progression of esophageal squamous cell carcinoma. *Acta Histochem* 2013; 115: 56-62.
 15. Ghosh A, Maiti GP, Bandopadhyay MN, *et al.* Inactivation of 9q22.3 tumor suppressor genes predict outcome for patients with head and neck squamous cell carcinoma. *Anticancer Res* 2013; 33: 1215-20.
 16. Lee KH, Park JW, Sung HS, *et al.* PHF2 histone demethylase acts as a tumor suppressor in association with p53 in cancer. *Oncogene* 2015; 34: 2897-909.
 17. Edge SB, Byrd DR, Compton CC, Fritz AG, Greene FL, Trotti A 3rd. *AJCC cancer staging manual*. 7th ed. New York: Springer, 2010; 479-90.
 18. Musri MM, Carmona MC, Hanzu FA, Kaliman P, Gomis R, Párrizas M. Histone demethylase LSD1 regulates adipogenesis. *J Biol Chem* 2010; 285: 30034-41.
 19. Brasaemle DL, Barber T, Wolins NE, Serrero G, Blanchette-Mackie EJ, Londos C. Adipose differentiation-related protein is an ubiquitously expressed lipid storage droplet-associated protein. *J Lipid Res* 1997; 38: 2249-63.
 20. Gao J, Serrero G. Adipose differentiation related protein (ADRP) expressed in transfected COS-7 cells selectively stimulates long chain fatty acid uptake. *J Biol Chem* 1999; 274: 16825-30.
 21. Thoenes W, Störkel S, Rumpelt HJ. Histopathology and classification of renal cell tumors (adenomas, oncocytomas and carcinomas): the basic cytological and histopathological elements and their use for diagnostics. *Pathol Res Pract* 1986; 181: 125-43.
 22. Tripathi A, Dasgupta S, Roy A, *et al.* Sequential deletions in both arms of chromosome 9 are associated with the development of head and neck squamous cell carcinoma in Indian patients. *J Exp Clin Cancer Res* 2003; 22: 289-97.
 23. Baytekin F, Tuna B, Mungan U, Aslan G, Yorukoglu K. Significance of P-glycoprotein, p53, and survivin expression in renal cell carcinoma. *Urol Oncol* 2011; 29: 502-7.
 24. Noon AP, Polanski R, El-Fert AY, *et al.* Combined p53 and MDM2 biomarker analysis shows a unique pattern of expression associated with poor prognosis in patients with renal cell carcinoma undergoing radical nephrectomy. *BJU Int* 2012; 109: 1250-7.
 25. Noon AP, Vlatkovic N, Polanski R, *et al.* p53 and MDM2 in renal cell carcinoma: biomarkers for disease progression and future therapeutic targets? *Cancer* 2010; 116: 780-90.

Yes-Associated Protein Expression Is Correlated to the Differentiation of Prostate Adenocarcinoma

Myung-Giun Noh · Sung Sun Kim
Eu Chang Hwang¹
Dong Deuk Kwon¹ · Chan Choi

Departments of Pathology and ¹Urology,
Chonnam National University Hwasun Hospital,
Chonnam National University Medical School,
Hwasun, Korea

Received: March 15, 2017

Revised: April 17, 2017

Accepted: May 4, 2017

Corresponding Author

Chan Choi, MD, PhD
Department of Pathology, Chonnam National
University Hwasun Hospital, Chonnam National
University Medical School, 322 Seoyang-ro,
Hwasun 58128, Korea
Tel: +82-61-379-7071
Fax: +82-61-379-7099
E-mail: cchoi@chonnam.ac.kr

Background: Yes-associated protein (YAP) in the Hippo signaling pathway is a growth control pathway that regulates cell proliferation and stem cell functions. Abnormal regulation of YAP was reported in human cancers including liver, lung, breast, skin, colon, and ovarian cancer. However, the function of YAP is not known in prostate adenocarcinoma. The purpose of this study was to investigate the role of YAP in tumorigenesis, differentiation, and prognosis of prostate adenocarcinoma. **Methods:** The nuclear and cytoplasmic expression of YAP was examined in 188 cases of prostate adenocarcinoma using immunohistochemistry. YAP expression levels were evaluated in the nucleus and cytoplasm of the prostate adenocarcinoma and the adjacent normal prostate tissue. The presence of immunopositive tumor cells was evaluated and interpreted in comparison with the patients' clinicopathologic data. **Results:** YAP expression levels were not significantly different between normal epithelial cells and prostate adenocarcinoma. However, YAP expression level was significantly higher in carcinomas with a high Gleason grades (8–10) than in carcinomas with a low Gleason grades (6–7) ($p < .01$). There was no statistical correlation between YAP expression and stage, age, prostate-specific antigen level, and tumor volume. Biochemical recurrence (BCR)-free survival was significantly lower in patients with high YAP expressing cancers ($p = .02$). However high YAP expression was not an independent prognostic factor for BCR in the Cox proportional hazards model. **Conclusions:** The results suggested that YAP is not associated with prostate adenocarcinoma development, but it may be associated with the differentiation of the adenocarcinoma. YAP was not associated with BCR.

Key Words: Yes-associated protein (YAP); Prostate adenocarcinoma; Immunohistochemistry; Gleason score

Prostate cancer (PC) remains a leading cause of cancer-related death in North-American men¹ and is becoming an increasingly common cancer in South Korea.² Pathological stage and Gleason grade are important predictors of prognosis in patients with primary prostate adenocarcinoma who undergo a radical prostatectomy. The Gleason grading system is a well-established system for prostate adenocarcinoma that correlates with the differentiation of the prostate gland, pathological stage, disease progression, and recurrence.^{3,4} However, prostate adenocarcinoma is a remarkably heterogeneous disease. Distinguishing tumors associated with a poor outcome at the time of radical prostatectomy is problematic. The molecular mechanisms of prostate carcinogenesis remain poorly understood.⁵

The Hippo pathway, a vital growth regulator of cell proliferation and apoptosis, was first identified by mosaic screens in *Drosophila melanogaster*.⁶ Information about the Hippo pathway in *Drosophila* is likely applicable directly to mammalian systems, as it has been shown that mammalian homologues are capable

of rescuing *Drosophila* mutants defective in the Hippo signaling pathway.⁷ Yes-associated protein (YAP) is a transcriptional coactivator of the Hippo pathway and is a highly conserved component of this pathway in mammalian systems. In humans, amplification of the chromosomal region containing the YAP gene (11q22) has been reported in several tumor types.⁸ Recent genetic mouse models and studies with cancer patient demonstrated the critical roles of Hippo-YAP signaling in cancer development. For examples, immunohistochemistry studies have shown that an elevated expression/nuclear localization of YAP or transcriptional coactivator with a PDZ-binding domain (TAZ) correlates with malignant features in lung cancer.⁹ In datasets of breast cancer patients, elevated expression of gene signatures for YAP/TAZ activity correlates with high histological grade, enrichment of stem cell signatures, metastasis proclivity, and poor outcome.^{10,11} High expression of YAP activity has been found to be prognostic for bad outcome in four datasets of colorectal cancer patients and correlated with cetuximab resistance.¹² Immunohistochemistry

studies on human hepatocellular carcinoma samples showed that elevated expression of YAP or TAZ correlates with poor tumor differentiation and is prognostic of bad outcome.¹³ By immunohistochemistry on human pancreatic tissue samples, YAP and TAZ were found to be almost absent from normal acini, but moderately expressed and nuclearly localized in PanINs and in a subset of primary pancreatic ductal adenocarcinoma, whereas strong nuclear staining of YAP was found in metastases derived from pancreatic adenocarcinoma.¹⁴

Although the net effect of deregulated YAP and TAZ activities in many tissues is similar, their activities appear to be controlled by different regulatory mechanisms in different tissues.¹⁵ Previous studies demonstrated the biological significance of the Hippo-YAP signaling pathway in prostate adenocarcinoma, but large-scale studies have failed to identify YAP amplification and mutations in castration resistant PCs.¹⁶ Zhang *et al.*³ showed that the Hippo effector YAP regulates cell motility, invasion, and castration-resistant growth of prostate adenocarcinoma in rats. Hu *et al.*¹⁷ showed that YAP expression in PC is inversely correlated with increase in Gleason score. However, the clinical significance of YAP amplification in human prostate adenocarcinoma has largely remained unknown. This study investigates the role of YAP in the development, differentiation, and prognosis of prostate adenocarcinoma.

MATERIALS AND METHODS

Patients and tumor samples

Prostate acinar adenocarcinoma specimens were obtained from 188 patients who had undergone radical prostatectomy at Chonnam National University Hwasun Hospital from 2005 to 2012. The availability of adequate tissue material was the only inclusion criterion. Diagnostic criteria of prostate acinar adenocarcinoma were in agreement with the World Health Organization classification. Clinicopathologic data were collected from the medical records. All patients were advised to have prostate-specific antigen (PSA) follow-up every 3 months in the first year postoperation and at least biannually thereafter. Biochemical recurrence (BCR) was defined as two consecutive PSA measurements ≥ 0.2 ng/mL within an interval of more than 3 months. PSA progression-free survival time was defined as the time from radical prostatectomy to the first follow-up date showing PSA ≥ 0.2 ng/mL or until the last follow-up. This study was approved by the Institutional Review Board of Chonnam National University Hwasun Hospital (CNUHH-2017-022).

Immunohistochemistry for YAP

One representative slide of the prostate adenocarcinoma was selected for immunohistochemical staining. Tumor samples obtained during surgical treatment were fixed in formalin and embedded in paraffin for histologic studies. The slides of the tumor surgical specimens were stained with hematoxylin and eosin and were reviewed and representative tissue blocks were selected. YAP (1A12) mouse monoclonal antibody (Cell Signaling Technology, Danvers, MA, USA) at a dilution of 1:200 was used for immunohistochemical analysis. Immunostaining was performed using the avidin-biotin complex method. Briefly, representative paraffin blocks were cut consecutively at 4- μ m thickness, and immunohistochemical staining was carried out using a BOND-MAX Automated IHC/ISH Stainer (Leica Biosystems, Wetzlar, Germany).

Sections were deparaffinized in xylene and treated with 0.3% hydrogen peroxide in methanol for 20 minutes to block any endogenous peroxidase activity. Citrate buffer was used for antigen retrieval. Nonspecific binding was limited by using protein blocking buffer for 10 minutes. The sections were washed in phosphate-buffered saline and then incubated with the primary antibody for 20 minutes at room temperature. The samples were then incubated in secondary antibody (biotinylated) for 10 minutes, followed by incubation with streptavidin-horseradish peroxidase for 10 minutes, and exposed to diaminobenzidine, which was used as a chromogen. All labeled streptavidin-biotin-horseradish peroxidase system chemicals were obtained from Dako Cytomation Corp. (Carpinteria, CA, USA). Counterstaining was performed with Mayer's hematoxylin. Negative controls were treated similarly with the exception of incubation with the primary antibody (nonspecific staining control).

Assessment of protein expression

All immunostained slides were evaluated twice by two independent investigators blinded to the clinical details. Five views of the highest expression site were examined per slide, and 100 cells were observed per view at 400 \times magnification. In each slide, adjacent noncancerous basal cells of the prostate acinar tissue were available as internal positive controls and scattered lymphocyte were used as internal negative controls. YAP expression was graded according to the distribution, intensity, and percentage of positive cells as described previously.⁸ Both the tumor cells and noncancerous acinar cells were graded (Fig. 1). For the cytoplasmic distribution, weak cytoplasmic reactivity was considered as low expression regardless of the extent. Strong cytoplasmic reactivity with less than 50% positive cells was graded as low

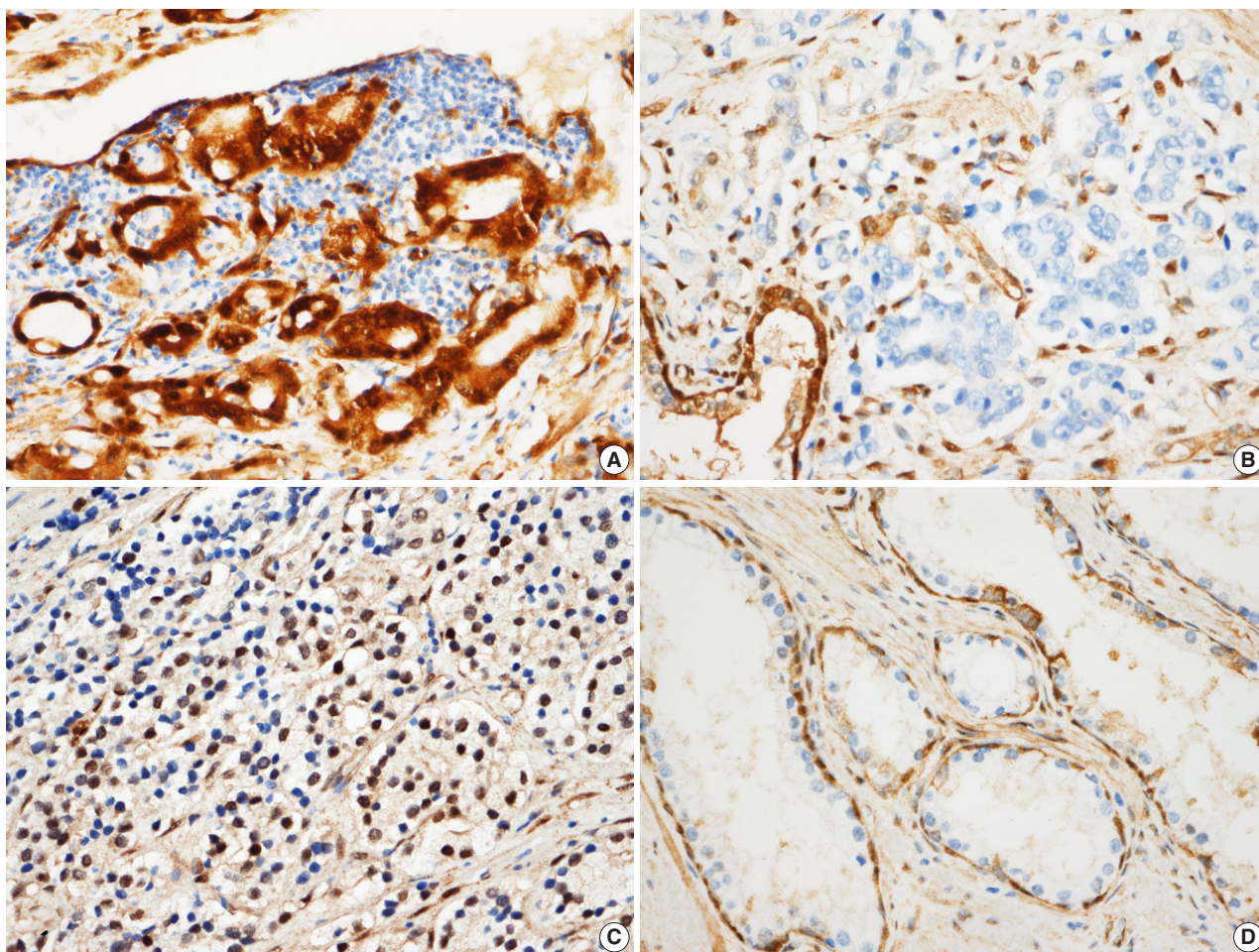


Fig. 1. Scoring according to the expression of Yes-associated protein (YAP) in prostate adenocarcinoma. (A) In prostate adenocarcinoma, both nuclei and cytoplasm are strongly positive for YAP, scored as high. (B) Negative expression is noted for YAP in prostate adenocarcinoma cells, which is scored as negative. (C) Nuclear expression in prostate adenocarcinoma cells, the nuclear stain over one tenth is scored as high. (D) YAP expression in normal prostate glands. Basal cells are strongly positive which were used as a positive control. Luminal cells did not show YAP expression. Stromal cells reveal mild expression of YAP.

expression; otherwise, it was graded as high expression if there were greater than 50% positive cells. For the nuclear distribution, samples with nuclear staining in less than 10% of cells were graded as low YAP expression, and samples with nuclear staining in more than 10% of cells were graded as high YAP high expression. YAP expression levels in prostate tissues were divided into high YAP expression and low/negative YAP expression. Two pathologists reviewed cases of inconclusive samples together and reached an agreement as to the YAP expression level.

Gene Expression Omnibus data

Microarray data of prostate adenocarcinoma deposited in the National Center for Biotechnology Information (NCBI) Gene Expression Omnibus (GEO) were analyzed.

Statistical analysis

Statistical analyses were performed with the statistical computing environment R (ver. 3.3.2, R Core Team) and the software program IBM SPSS (ver. 21.0 for Windows, IBM Corp., Armonk, NY, USA). Correlation with tumor and adjacent non-tumor tissue in prostate samples was assessed by the Spearman's rank correlation coefficient test. Association between the Gleason grade and clinical factors on radical prostatectomy specimens with YAP expression was calculated using chi-square test. Statistically significant trends associated with an increasing Gleason grade and YAP expression were analyzed by Cochran Armitage trend test. Multivariate logistic regression analysis was used to develop a trend score for tumor differentiation based on patient characteristics (age, initial PSA tumor volume, YAP expression, and pathologic stage). Kaplan-Meier survival curves were used to

assess the prognostic significance of YAP in predicting BCR. A multivariate analysis was performed using the Cox regression model to study the effects of different variables on BCR. All *p*-values were based on two-tailed statistical analyses and $p < .05$ was considered to be statistically significant. In GEO data, the Mann-Whitney and paired Wilcoxon tests were utilized when parameters were not normally distributed, while independent-samples and paired-sample *t* tests were used when parameters were normally distributed. The Kolmogorov-Smirnov test was employed to demonstrate deviation from the normal distribution.

RESULTS

YAP expression in 188 cases of prostate adenocarcinoma and their paired adjacent nontumor tissues was investigated by immunohistochemistry. In the cytoplasm of normal prostate luminal cells, 45 cases (23.9%) were completely negative, 125 cases (66.5%) showed low expression in cytoplasm, and 18 cases (9.6%) showed

high expression. In the nucleus, 140 cases (74.4%) were negative, 33 cases (17.6%) showed low expression, and 15 cases (8.0%) showed high expression (Table 1, Fig. 2A–D). In the nucleus of

Table 1. YAP expression in prostate adenocarcinoma and normal prostate tissue adjacent to the adenocarcinoma

Type	Prostate adenocarcinoma	Normal prostate glands adjacent to adenocarcinoma
Complete absence of reactivity	16/188 (8.5)	45/188 (23.9)
Nucleus		
Absent	44/188 (23.4)	95/188 (50.5)
Low	84/188 (44.7)	33/188 (17.6)
High	10/188 (5.3)	7/188 (3.7)
Cytoplasm		
Absent	9/188 (4.8)	0/188 (0)
Low	124/188 (66.0)	125/188 (66.5)
High	5/188 (2.7)	10/188 (5.3)
Nucleus and cytoplasm		
High	34/188 (18.1)	8/188 (4.3)

Values are presented as number (%).

YAP, Yes-associated protein.

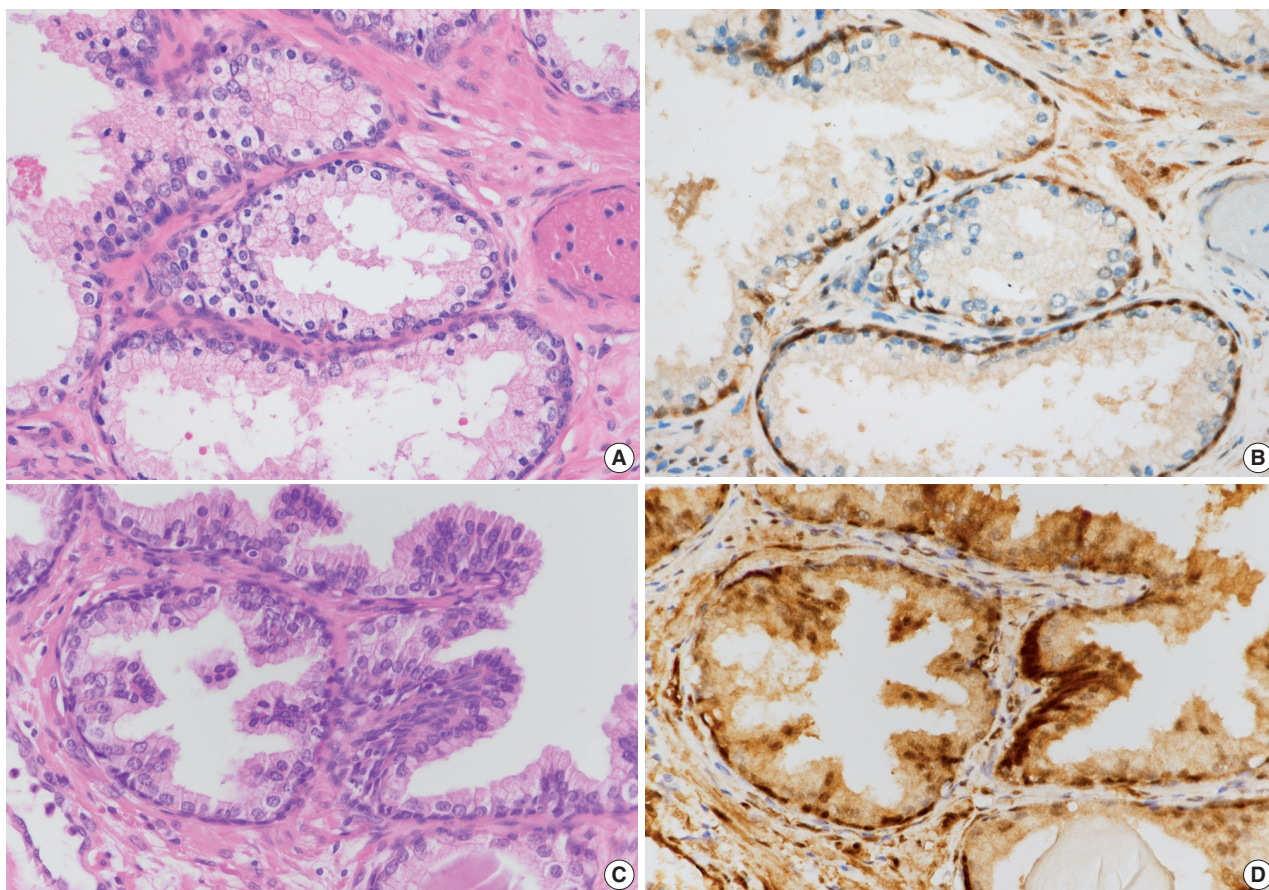


Fig. 2. Expression of Yes-associated protein (YAP) in prostate adenocarcinoma and normal prostate glands. (A–D) Hematoxylin and eosin (H&E)-stained section of benign glands and immunohistochemical stain of YAP in normal prostate glands. Luminal cells of normal prostate gland show no expression to mild expression of YAP in the cytoplasm. All of the basal cells and stroma show positive YAP.

(Continued to the next page)

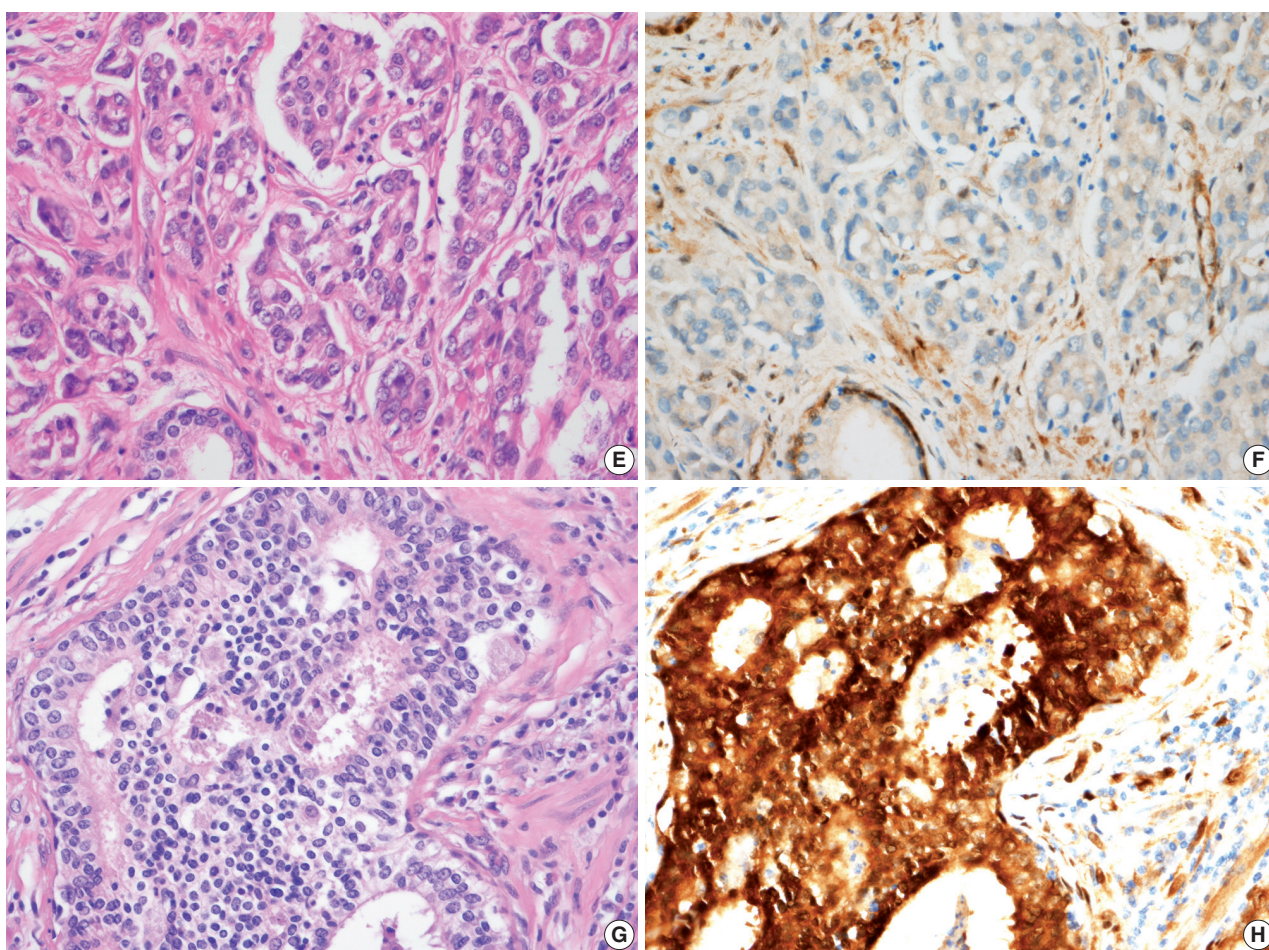


Fig. 2. (Continued from the previous page) (E) H&E-stained section of well-to-moderately differentiated prostate adenocarcinoma (Gleason score, 4+3=7). There are poorly formed glands and a few well-formed glands. (F) Expression of YAP in well-to-moderately differentiated prostate adenocarcinoma (Gleason score, 4+3=7). Tumor cells show either no or mild expression in the cytoplasm. (G) H&E-stained section of poorly differentiated prostate adenocarcinoma (Gleason score, 5+5=10). (H) Tumor cells display strong positivity in both nuclei and cytoplasm.

prostate adenocarcinoma, 60 cases (31.9%) were negative, 84 cases (44.7%) showed low expression and 44 cases (23.4%) were high expression. In the cytoplasm, 25 cases (13.3%) were negative, 124 cases (66.0%) showed low expression, and 39 cases (20.7%) showed high expression (Table 1, Fig. 2E–H). Basal cells and stroma were positive for YAP (Fig. 2).¹⁷

According to the YAP immunohistochemical scoring system used in this study, 49 cases of prostate adenocarcinoma tissues (26.1%) highly expressed YAP in both the nuclei and cytoplasm, whereas 139 cases of adenocarcinoma tissues (73.9%) were negative/low positive for YAP expression (Table 2). In contrast, 163 cases (86.7%) revealed low/negative expression of YAP and only 25 cases of these normal cells (13.3%) were highly positive for YAP expression (Table 2). The expression of YAP was not significantly different between tumor and adjacent normal tissues in the

prostate adenocarcinoma samples ($p > .05$) (Table 2).

YAP mRNA expression level in prostate adenocarcinoma available from GEO profiles was evaluated.^{18–24} Only one study found YAP expression to be higher in prostate adenocarcinoma than in normal tissue.¹⁹ In two other studies, YAP expression was lower in prostate adenocarcinoma than in normal tissue.^{20,23} There was no significant tendency of YAP RNA expression profiles between prostate adenocarcinoma and normal tissue (Table 3).

Next, the relationship between YAP expression and the clinicopathologic factors were analyzed. For well-to-moderately differentiated adenocarcinoma (Gleason score of 6–7), 118 cases (81.9%) were completely negative or weakly stained (intensity score of “low”) for YAP ($p < .01$) (Table 4, Fig. 2E, F). In comparison, 23 cases of poorly differentiated adenocarcinoma (52.3%) (Gleason score of 8–10) exhibited strong staining for YAP (intensity

Table 2. Comparison of YAP expression between adenocarcinoma and normal prostate tissue adjacent to the adenocarcinoma

Type	YAP negative/low expression	YAP high expression	p-value
Normal prostate glands adjacent to adenocarcinoma	163/188 (86.7)	25/188 (13.3)	> .05
Prostate adenocarcinoma	139/188 (73.9)	49/188 (26.1)	

Values are presented as number (%).

YAP, Yes-associated protein.

Table 3. YAP mRNA expression in normal tissues and prostate adenocarcinoma from GEO profiles

Study	Normal	No. of cases	Prostate cancer	No. of cases	p-value
Varambally <i>et al.</i> ¹⁸	3,797.54±2,444.70	18	3,017.58±2,076.74	21	.29
Chandran <i>et al.</i> ¹⁹	44.48±21.65	71	56.90±36.73	91	.01
Yu <i>et al.</i> ²⁰	1,280.71±445.43	71	878.24±414.46	91	< .01
Satake <i>et al.</i> ²¹	1,984.20±1,985.80	3	1,254.13±1,500.77	30	.42
Planche <i>et al.</i> ²²	8.43±1.54	18	8.05±1.75	18	.11
Arredouani <i>et al.</i> ²³	1,139.21±806.37	24	754.87±495.63	39	.02
Nanni <i>et al.</i> ²⁴	190.02±98.42	8	189.80±64.38	22	.98

Values are presented as mean±standard deviation.

YAP, Yes-associated protein; GEO, Gene Expression Omnibus.

Table 4. Clinicopathologic features of the patients

Characteristic	No. of patients	Low YAP expression	High YAP expression	p-value
Age (yr)				.74
<70	105	79 (75.2)	26 (24.8)	
≥70	83	60 (72.3)	23 (27.7)	
Initial PSA (ng/mL)				.44
≤4.0	7	5 (71.4)	2 (28.6)	
4.1–10.0	103	77 (74.8)	26 (25.2)	
10.1–20.0	44	29 (65.9)	15 (34.1)	
>20	34	28 (82.4)	6 (17.6)	
Tumor volume (g)				.22
<15	122	94 (77.0)	28 (23.0)	
≥15	66	45 (68.2)	21 (31.8)	
Tumor differentiation				< .01 ^a
Moderate to well differentiation (Gleason score 6–7)	144	118 (81.9)	26 (18.1)	
Poor differentiation (Gleason score 8–10)	44	21 (47.7)	23 (52.3)	
Pathologic stage				.69
pT2	146	109 (74.7)	37 (25.3)	
pT3	42	30 (71.4)	12 (28.6)	

Values are presented as number (%).

YAP, Yes-associated protein; PSA, prostate-specific antigen.

^aCochran Armitage trend test, $p < .01$.

score of “high”) ($p < .01$) (Table 4, Fig. 2G, H). However, no significant difference in YAP expression level was observed according to the age of the patient, tumor volume, preoperative serum PSA, or tumor stage (Table 4). A multivariate logistic regression model showed YAP expression (odds ratio [OR], 9.41; 95% confidence interval [CI], 3.76 to 53.51), initial PSA (OR, 1.10; 95% CI, 1.06 to 1.15), and pathologic stage (OR, 3.58; 95% CI, 1.40 to 9.42) to be significantly correlated with tumor differentiation (Table 5).

The BCR-free survival was significantly lower in patients with high YAP expressing cancers than those with negative/low YAP

expressing cancers ($p = .02$) (Fig. 3). In addition, univariate analysis showed that the Gleason grade (hazard ratio, 5.02; $p < .01$) and high YAP expression (hazard ratio, 1.919; $p = .02$) were associated with BCR. Furthermore, multivariate analysis using a Cox regression model demonstrated that the Gleason grade ($p < .01$) and T stage were independent prognostic factors for BCR. However YAP expression was not a significantly independent prognostic factor for BCR in the Cox proportional hazards model (Table 6).

DISCUSSION

YAP regulates cell proliferation, stem behavior and regeneration.¹⁵ Promotion of cell stemness and proliferation are important factors for cancer development and regeneration.¹⁵ YAP can be

Table 5. Significant risk factors for tumor differentiation in patients with prostate adenocarcinoma determined by multivariate logistic regression model

Factor	Multivariate	
	Odds ratio (95% CI)	p-value
Age	1.24 (0.54–2.89)	.61
Initial PSA	1.10 (1.06–1.15)	<.01
Tumor volume	1.08 (0.44–2.64)	.87
YAP expression	9.41 (3.76–23.51)	<.01
Pathologic stage	3.58 (1.40–9.42)	<.01

CI, confidence interval; PSA, prostate specific antigen; YAP, Yes-associated protein.

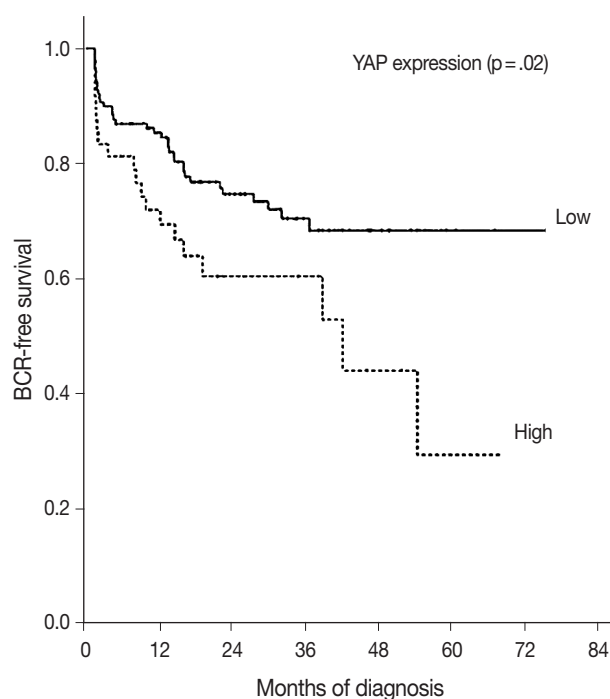


Fig. 3. Kaplan-Meier estimates of biochemical recurrence. Graph of the curve for progression-free survival in prostate adenocarcinoma patients, according to Yes-associated protein (YAP) expression (p = .02).

Table 6. Univariate and multivariate analyses for predictive factors in patients with prostate adenocarcinoma

Factor	Univariate		Multivariate	
	Hazard ratio (95% CI)	p-value	Hazard ratio (95% CI)	p-value
Gleason grade group	5.02 (2.97–8.50)	<.01	4.33 (0.56–1.87)	<.01
T stage	2.56 (1.49–4.39)	<.01	1.75 (2.39–7.85)	.05
High YAP expression	1.92 (1.11–3.32)	.02	1.03 (0.99–3.08)	.93

CI, confidence interval; YAP, Yes-associated protein.

used during the development of cancer and other phenotypes during reprogramming of mature and differentiated cells.¹⁵

As noted above, the expression of YAP via immunohistochemical staining showed no statistically significant difference between prostate adenocarcinoma and adjacent normal tissues. Similarly, in GEO data profiles, YAP mRNA was not statistically higher in prostate adenocarcinoma than in normal tissue. This suggested that YAP expression is not associated with tumorigenesis of prostate adenocarcinoma. YAP and/or TAZ knockdown in human colorectal cancer cell lines suppresses their growth and ability to trigger tumor formation after injection in mice.²⁵ On the other hand, YAP has been reported to be functionally implicated to tumorigenesis in other human cancers. Liver-specific YAP overexpression in transgenic mice leads to hepatomegaly and development of human hepatocellular carcinoma.²⁶ Similar results were obtained by delivering a phospho-mutant form of YAP in the mouse liver using transposon-mediated hydrodynamic transfection.²⁷ YAP or TAZ knockdown strongly reduces subcutaneous tumor growth of human and mouse hepatocellular carcinoma cell lines.²⁸ Functionally, pancreas-specific YAP knockout abrogates tumor progression from early pancreatic intraepithelial neoplasia lesions to pancreatic ductal adenocarcinoma in a mouse model of pancreatic cancer.²⁹

Poorly differentiated prostate adenocarcinoma cells stained more strongly for YAP than in moderately to well-to-moderately differentiated prostate adenocarcinoma. YAP immunoreactivity was inversely associated with the differentiation of prostate adenocarcinoma. In addition, YAP expression was found to be a factor affecting tumor differentiation. This finding indicates that there is a meaningful inverse relationship between YAP expression and differentiation of prostate adenocarcinoma, which suggests that YAP may play a role in the differentiation of prostate adenocarcinoma.

Hu *et al.*¹⁷ showed that down-regulation of YAP expression in prostate adenocarcinoma correlates with an increase in Gleason score, and this study showed differences from the results. It can be explained for several factors. First, the expression of YAP showed intratumoral heterogeneity in prostate adenocarcinoma. In tumors with heterogeneous expression, many tissue cores are

required to get comprehensive information. Hu *et al.*¹⁷ used tissue microarray (TMA) slides with two cores of intratumoral and peritumoral tissue per slide. In this study, we used we used a representative slide instead of TMA slide. Second, the interpretation method of YAP expression was different. It was estimated according to the distribution and intensity of positive staining in this study according to Steinhardt *et al.*⁸ However Hu *et al.*¹⁷ interpreted it as three categories, only cytoplasmic, only nuclear, both nuclear and cytoplasmic. Those factors might affect the difference of the results of this study and Hu *et al.*¹⁷

Enhanced YAP activity tends to promote stem cells and progenitor cells, while inhibiting differentiation.³⁰ Immunohistochemical studies on human hepatocellular carcinoma samples showed that elevated expression of YAP or TAZ correlates with poor differentiation of cancer cells and poor outcomes.³¹ In datasets of patients with breast cancer, an elevated expression of gene signatures for YAP/TAZ activity correlate with high histological grades, enrichment of stem cell signatures, tendency to metastasize, and poor outcomes.^{10,32} Prostate stem cell antigen expression identified through immunohistochemical staining and in situ hybridization is significantly increased in human PCs with a high Gleason score.³³ Considering that YAP is generally associated with cancer stem cells, we can further compare the expression of YAP and prostate stem cell antigens with differentiation stages of prostate adenocarcinoma. Once the relationship between PC stem cells and YAP and its mechanisms of action are revealed, it could be further explored as a new therapeutic target.

In this study, YAP immunoreactivity was not associated with the BCR of prostate adenocarcinoma. The univariate analysis was statistically significant, but not the multivariate analysis. This difference between the univariate and multivariate analyses might be attributed to the contribution of the Gleason score. Therefore, YAP immunoreactivity for prostate adenocarcinoma was not useful for predicting adverse outcomes. Expression of YAP in a variety of human cancers has been reported to be associated with a poor prognosis. High levels of YAP expression were found to be associated with poor outcomes in four datasets of colorectal cancer patients, and were positively correlated with cetuximab resistance.³⁴ YAP mRNA and protein levels have been shown to be upregulated in gastric adenocarcinoma, and YAP protein expression and nuclear localization were associated with poor patient outcomes.³⁵

There are several limitations to this study. First, this study investigated the relationship between YAP expression and clinicopathologic factors in prostate adenocarcinoma based on the morphological expression of the cancer. No functional studies of YAP

have been performed in relation to tumorigenesis of prostate adenocarcinoma. In addition, this study did not show a direct functional relationship between YAP expression and the differentiation pathway of prostate adenocarcinoma. The second limitation was that the tumor differentiation was interpreted in a two-tier system: well to moderate differentiation (Gleason score of 6–7) or poorly-differentiation (Gleason score of 8–10). The reason for this was that the number of patients subclassified by their Gleason score was largely uneven. The number of patients with Gleason score of 6 was 39, of 7 was 105, of 8 was 26, of 9 was 17, and of 10 was 1. If a larger cohort of patients was included in this study, the study might have had more specific results.

This study demonstrates that YAP is highly expressed in poorly differentiated prostate adenocarcinoma compared to well-differentiated or moderately differentiated prostate adenocarcinoma. However, YAP expression was not associated with BCR in the Cox proportional hazards model.

Conflicts of Interest

No potential conflict of interest relevant to this article was reported.

REFERENCES

1. Diallo JS, Aldejmah A, Mouhim AF, *et al.* Co-assessment of cytoplasmic and nuclear androgen receptor location in prostate specimens: potential implications for prostate cancer development and prognosis. *BJU Int* 2008; 101: 1302-9.
2. Joung JY, Lim J, Oh CM, *et al.* Current trends in the incidence and survival rate of urological cancers in Korea. *Cancer Res Treat* 2016 Sep 23 [Epub]. <https://doi.org/10.4143/crt.2016.139>.
3. Zhang L, Yang S, Chen X, *et al.* The hippo pathway effector YAP regulates motility, invasion, and castration-resistant growth of prostate cancer cells. *Mol Cell Biol* 2015; 35: 1350-62.
4. Epstein JI, Allsbrook WC Jr, Amin MB, Egevad LL; ISUP Grading Committee. The 2005 International Society of Urological Pathology (ISUP) Consensus Conference on Gleason Grading of Prostatic Carcinoma. *Am J Surg Pathol* 2005; 29: 1228-42.
5. McMenamin ME, Soung P, Perera S, Kaplan I, Loda M, Sellers WR. Loss of PTEN expression in paraffin-embedded primary prostate cancer correlates with high Gleason score and advanced stage. *Cancer Res* 1999; 59: 4291-6.
6. Edgar BA. From cell structure to transcription: Hippo forges a new path. *Cell* 2006; 124: 267-73.
7. Lai ZC, Wei X, Shimizu T, *et al.* Control of cell proliferation and

- apoptosis by mob as tumor suppressor, *mats*. *Cell* 2005; 120: 675-85.
8. Steinhardt AA, Gayyed MF, Klein AP, *et al*. Expression of Yes-associated protein in common solid tumors. *Hum Pathol* 2008; 39: 1582-9.
 9. Wang Y, Dong Q, Zhang Q, Li Z, Wang E, Qiu X. Overexpression of yes-associated protein contributes to progression and poor prognosis of non-small-cell lung cancer. *Cancer Sci* 2010; 101: 1279-85.
 10. Cordenonsi M, Zanconato F, Azzolin L, *et al*. The Hippo transducer TAZ confers cancer stem cell-related traits on breast cancer cells. *Cell* 2011; 147: 759-72.
 11. Di Agostino S, Sorrentino G, Ingallina E, *et al*. YAP enhances the proliferative transcriptional activity of mutant p53 proteins. *EMBO Rep* 2016; 17: 188-201.
 12. Lee KW, Lee SS, Kim SB, *et al*. Significant association of oncogene YAP1 with poor prognosis and cetuximab resistance in colorectal cancer patients. *Clin Cancer Res* 2015; 21: 357-64.
 13. Kim GJ, Kim H, Park YN. Increased expression of Yes-associated protein 1 in hepatocellular carcinoma with stemness and combined hepatocellular-cholangiocarcinoma. *PLoS One* 2013; 8: e75449.
 14. Morvaridi S, Dhall D, Greene MI, Pandol SJ, Wang Q. Role of YAP and TAZ in pancreatic ductal adenocarcinoma and in stellate cells associated with cancer and chronic pancreatitis. *Sci Rep* 2015; 5: 16759.
 15. Johnson R, Halder G. The two faces of Hippo: targeting the Hippo pathway for regenerative medicine and cancer treatment. *Nat Rev Drug Discov* 2014; 13: 63-79.
 16. Grasso CS, Wu YM, Robinson DR, *et al*. The mutational landscape of lethal castration-resistant prostate cancer. *Nature* 2012; 487: 239-43.
 17. Hu X, Jia Y, Yu J, Chen J, Fu Q. Loss of YAP protein in prostate cancer is associated with Gleason score increase. *Tumori* 2015; 101: 189-93.
 18. Varambally S, Yu J, Laxman B, *et al*. Integrative genomic and proteomic analysis of prostate cancer reveals signatures of metastatic progression. *Cancer Cell* 2005; 8: 393-406.
 19. Chandran UR, Ma C, Dhir R, *et al*. Gene expression profiles of prostate cancer reveal involvement of multiple molecular pathways in the metastatic process. *BMC Cancer* 2007; 7: 64.
 20. Yu YP, Landsittel D, Jing L, *et al*. Gene expression alterations in prostate cancer predicting tumor aggression and preceding development of malignancy. *J Clin Oncol* 2004; 22: 2790-9.
 21. Satake H, Tamura K, Furihata M, *et al*. The ubiquitin-like molecule interferon-stimulated gene 15 is overexpressed in human prostate cancer. *Oncol Rep* 2010; 23: 11-6.
 22. Planche A, Bacac M, Provero P, *et al*. Identification of prognostic molecular features in the reactive stroma of human breast and prostate cancer. *PLoS One* 2011; 6: e18640.
 23. Arredouani MS, Lu B, Bhasin M, *et al*. Identification of the transcription factor single-minded homologue 2 as a potential biomarker and immunotherapy target in prostate cancer. *Clin Cancer Res* 2009; 15: 5794-802.
 24. Nanni S, Priolo C, Grasselli A, *et al*. Epithelial-restricted gene profile of primary cultures from human prostate tumors: a molecular approach to predict clinical behavior of prostate cancer. *Mol Cancer Res* 2006; 4: 79-92.
 25. Rosenbluh J, Nijhawan D, Cox AG, *et al*. beta-Catenin-driven cancers require a YAP1 transcriptional complex for survival and tumorigenesis. *Cell* 2012; 151: 1457-73.
 26. Dong J, Feldmann G, Huang J, *et al*. Elucidation of a universal size-control mechanism in *Drosophila* and mammals. *Cell* 2007; 130: 1120-33.
 27. Shen S, Guo X, Yan H, *et al*. A miR-130a-YAP positive feedback loop promotes organ size and tumorigenesis. *Cell Res* 2015; 25: 997-1012.
 28. Xiao W, Wang J, Ou C, *et al*. Mutual interaction between YAP and c-Myc is critical for carcinogenesis in liver cancer. *Biochem Biophys Res Commun* 2013; 439: 167-72.
 29. Zhang W, Nandakumar N, Shi Y, *et al*. Downstream of mutant KRAS, the transcription regulator YAP is essential for neoplastic progression to pancreatic ductal adenocarcinoma. *Sci Signal* 2014; 7: ra42.
 30. Zanconato F, Cordenonsi M, Piccolo S. YAP/TAZ at the roots of cancer. *Cancer Cell* 2016; 29: 783-803.
 31. Guo Y, Pan Q, Zhang J, *et al*. Functional and clinical evidence that TAZ is a candidate oncogene in hepatocellular carcinoma. *J Cell Biochem* 2015; 116: 2465-75.
 32. Bartucci M, Dattilo R, Moriconi C, *et al*. TAZ is required for metastatic activity and chemoresistance of breast cancer stem cells. *Oncogene* 2015; 34: 681-90.
 33. Han KR, Seligson DB, Liu X, *et al*. Prostate stem cell antigen expression is associated with gleason score, seminal vesicle invasion and capsular invasion in prostate cancer. *J Urol* 2004; 171: 1117-21.
 34. Kim DH, Kim SH, Lee OJ, *et al*. Differential expression of Yes-associated protein and phosphorylated Yes-associated protein is correlated with expression of Ki-67 and phospho-ERK in colorectal adenocarcinoma. *Histol Histopathol* 2013; 28: 1483-90.
 35. Hu X, Xin Y, Xiao Y, Zhao J. Overexpression of YAP1 is correlated with progression, metastasis and poor prognosis in patients with gastric carcinoma. *Pathol Oncol Res* 2014; 20: 805-11.

Basaloid Squamous Cell Carcinoma of the Head and Neck: Subclassification into Basal, Ductal, and Mixed Subtypes Based on Comparison of Clinico-pathologic Features and Expression of p53, Cyclin D1, Epidermal Growth Factor Receptor, p16, and Human Papillomavirus

Kyung-Ja Cho · Se-Un Jeong
Sung Bae Kim¹ · Sang-wook Lee²
Seung-Ho Choi³ · Soon Yuhl Nam³
Sang Yoon Kim³

Departments of Pathology, ¹Medical Oncology, ²Radiation Oncology, and ³Otorhinolaryngology, Asan Medical Center, University of Ulsan College of Medicine, Seoul, Korea

Received: January 17, 2017
Revised: February 21, 2017
Accepted: March 3, 2017

Corresponding Author

Kyung-Ja Cho, MD
Department of Pathology, Asan Medical Center,
University of Ulsan College of Medicine,
88 Olympic-ro 43-gil, Songpa-gu, Seoul 05505,
Korea
Tel: +82-2-3010-4545
Fax: +82-2-472-7898
E-mail: kjc@amc.seoul.kr

Background: Basaloid squamous cell carcinoma (BSCC) is a rare variant of squamous cell carcinoma with distinct pathologic characteristics. The histogenesis of BSCC is not fully understood, and the cancer has been suggested to originate from a totipotent primitive cell in the basal cell layer of the surface epithelium or in the proximal duct of secretory glands. **Methods:** Twenty-six cases of head and neck BSCC from Asan Medical Center, Seoul, Korea, reported during a 14-year-period were subclassified into basal, ductal, and mixed subtypes according to the expression of basal (cytokeratin [CK] 5/6, p63) or ductal markers (CK7, CK8/18). The cases were also subject to immunohistochemical study for CK19, p53, cyclin D1, epidermal growth factor receptor (EGFR), and p16 and to *in situ* hybridization for human papillomavirus (HPV), and the results were clinico-pathologically compared. **Results:** Mixed subtype (12 cases) was the most common, and these cases showed hypopharyngeal predilection, older age, and higher expression of CK19, p53, and EGFR than other subtypes. The basal subtype (nine cases) showed frequent comedo-necrosis and high expression of cyclin D1. The ductal subtype (five cases) showed the lowest expression of p53, cyclin D1, and EGFR. A small number of p16- and/or HPV-positive cases were not restricted to one subtype. BSCC was the cause of death in 19 patients, and the average follow-up period for all patients was 79.5 months. Overall survival among the three subtypes was not significantly different. **Conclusions:** The results of this study suggest a heterogeneous pathogenesis of head and neck BSCC. Each subtype showed variable histology and immunoprofiles, although the clinical implication of heterogeneity was not determined in this study.

Key Words: Carcinoma, squamous cell; Keratins; Tumor suppressor protein p53; Receptor, epidermal growth factor; Cyclin D1

Basaloid squamous cell carcinoma (BSCC) of the head and neck is a rare variant of squamous cell carcinoma (SCC) with distinct pathologic characteristics with multipotential differentiation.¹ Histologic characteristics of BSCC include solid nesting, comedo-necrosis, cribriform pattern, trabecular arrangement, ductal differentiation, and associated conventional SCC, most frequently seen *in situ*. The histogenesis of BSCC is not fully understood, and the cancer has been suggested to originate from a totipotent primitive cell in the basal cell layer of the surface epithelium or in the proximal duct of secretory glands.² The incidence of ductal differentiation in BSCC has been reported to range from 27.5%–45%^{3,4} and was associated with significantly better survival than those without ductal differentiation in a study by Imamhasan *et al.*⁴

However, the clinical significance of the differentiation profiles of BSCC has not otherwise been studied. Most studies on BSCC cytokeratin (CK) immunoprofiles have focused on diagnostic value and the ability to distinguish BSCC from other carcinomas with basaloid features.⁵⁻¹² CK14 was the most consistently expressed CK in BSCC,^{3,5,6,10-12} which is similar to the pattern seen in conventional SCC.⁴ Nonetheless, considering the histologic diversity of BSCC, CK immunoprofiles of BSCC are expected to be heterogeneous and not unique. The aim of this study was to examine expression patterns of basal and ductal immunomarkers, including variable CKs, in BSCC of the head and neck; to subclassify them according to basal or ductal immunomarker expression; and to compare their histology, other oncogene expression, human pap-

illomavirus (HPV) status, and clinical features.

MATERIALS AND METHODS

Immunohistochemistry and *in situ* hybridization

Twenty-six cases of head and neck BSCC from Asan Medical Center, Seoul, Korea, reported during a 14-year period were subject to immunohistochemical study for CK5/6 (1:200, Zymed, San Francisco, CA, USA), CK7 (1:400, Dako, Glostrup, Denmark), CK8/18 (1:200, Cell Marque, Rocklin, CA, USA), CK19 (1:100, Cell Marque), p63 (1:200, Dako), p53 (1:3,000, Glostrup, cyclin D1 (1:100, Neomarkers, Fremont, CA, USA), epidermal growth factor receptor (EGFR; 1:200, Invitrogen, Carlsbad, CA, USA), p16^{INK4} (1:10, Pharmingen, Franklin Lakes, NJ, USA) and *in situ* hybridization for HPV. Immunostaining was carried out on 4- μ m sections using a Ventana autostainer and an ultra-view DAB detection kit (Ventana Medical Systems Inc., Tucson, AZ, USA), according to the manufacturer's instructions. Cytoplasmic staining of CK5/6, CK7, CK8/18, and CK19 and nuclear staining of p63, p53, cyclin D1, and p16^{INK4} were regarded as positive if diffusely or heterogeneously staining was noted in $\geq 20\%$ of the tumor cells. EGFR staining was regarded as positive if $\geq 10\%$ of tumor cells showed membranous staining with strong or intermediate intensity. For HPV *in situ* hybridization, the INFORM HPV III Family 16 Probe (B) was used in conjunction with the ISH iView Blue Plus Detection Kit (Ventana Medical Systems Inc.). The INFORM HPV III Family 16 Probe (B) detects the following high-risk HPV genotypes: 16, 18, 31, 33, 35, 39, 45, 51, 52, 56, 58, and 66. Light microscopy results were analyzed, and any blue nuclear dots in the tumor cells were regarded as positive staining.

Clinicopathologic analysis

Cases that expressed either one or two basal (CK5/6 and p63) or ductal (CK7 and CK8/18) markers were considered as basal or ductal subtypes, and expression of both basal and ductal markers was subclassified into a mixed subtype. The case histologies were re-evaluated for the presence of nuclear palisading, comedo-necrosis, cribriform pattern, ductal differentiation, mucin production, and desmoplasia. Clinical information, including survival period of the patients, was obtained via medical records. The average follow-up period for all patients was 79.5 months.

For descriptive statistics, all categorical data were compared with the chi-square test. Continuous data were expressed as mean values and were compared using ANOVA. A survival curve was estimated using the Kaplan-Meier method, and differences in

survival between groups were compared using the log-rank test. $p < .05$ was considered statistically significant.

RESULTS

Expression of basal and ductal markers

Positive rates for basal (CK5/6; p63) and ductal markers (CK7; CK8/18) in 26 BSCC are summarized in Table 1. Overall positive rates for CK5/6, p63, CK7, and CK8/18 were 65.4%, 73.1%, 34.6%, and 46.2%, respectively. Twelve combination patterns were observed, and BSCCs were subdivided into basal (nine cases), ductal (five cases), and mixed (12 cases) subtypes (Fig. 1). Clinical features of the 26 cases based on subtype are summarized in Table 2. Advanced age and male gender were more frequently observed in the mixed subtype than in the basal and ductal subtypes. While 60% of laryngeal or hypopharyngeal BSCC was classified as the mixed subtype, 60% of oropharyngeal BSCC was determined to be the basal subtype. BSCC was the cause of death in 19 of the 26 patients. Overall survival periods were not significantly different among the three subtypes (Fig. 2).

Histologic parameters

The relationships between histologic parameters and subtypes are listed in Table 3. Nuclear palisading was observed in both basal and ductal subtypes, but not in the mixed subtype ($p = .010$). Comedo-necrosis was most commonly observed in the basal subtype, followed by ductal and mixed subtypes ($p = .001$). Ductal differentiation or mucin production was observed not only in the ductal subtype but also in the basal and mixed subtypes. Desmoplasia was most common in the basal subtype, followed by ductal and mixed subtypes ($p = .021$). Representative histo-

Table 1. Combined expression patterns of basal and ductal markers in head and neck basaloid squamous cell carcinomas

	No. of cases	CK5/6	p63	CK7	CK8/18
Basal subtype	7	+	+	-	-
	1	+	-	-	-
	1	-	+	-	-
Ductal subtype	2	-	-	+	+
	2	-	-	+	-
	1	-	-	-	+
Mixed subtype	2	+	+	+	+
	1	+	+	+	-
	5	+	+	-	+
	1	+	-	-	+
	2	-	+	+	-
	1	-	+	-	+
Total, n (%)	26	17 (65.4)	19 (73.1)	9 (34.6)	12 (46.2)

CK, cytokeratin.

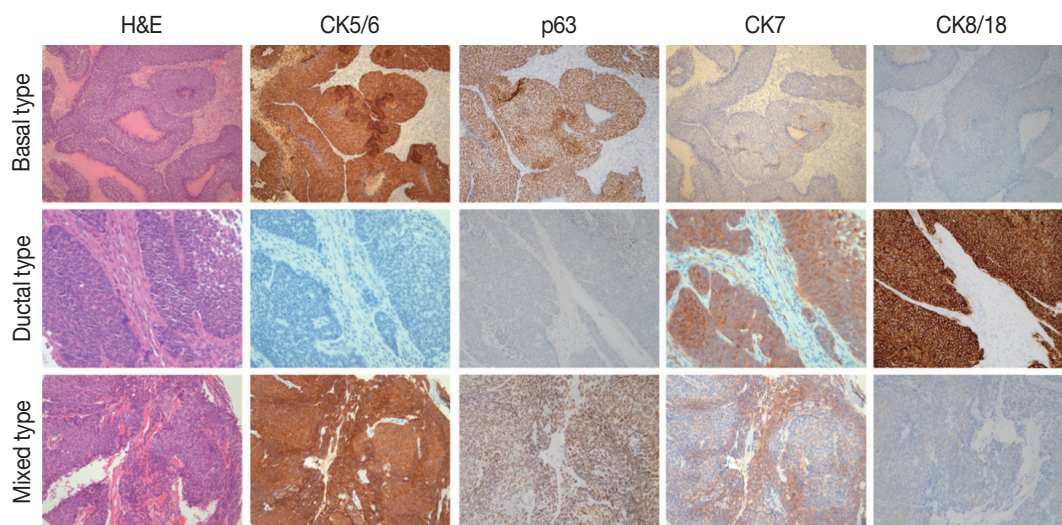


Fig. 1. Examples of combined expression patterns of basal and ductal immunomarkers in head and neck basaloid squamous cell carcinomas. CK, cytokeratin.

Table 2. Clinical features of head and neck basaloid squamous cell carcinoma according to subtype

Characteristic	Basal (n=9)	Ductal (n=5)	Mixed (n=12)
Age, mean (yr)	59.8	58.2	63.7
Male:Female	7:2	3:2	11:1
Location			
Larynx (n=5)	0	2	3
Hypopharynx (n=10)	3	1	6
Oropharynx (n=5)	3	1	1
Nasopharynx (n=1)	1	-	-
Sinonasal (n=2)	1	1	-
Oral cavity (n=1)	-	-	1
Salivary gland (n=1)	1	-	-
External auditory canal (n=1)	-	-	1
Outcome			
DOD (n=19)	6	4	9
AWD (n=3)	2	0	1
AUS (n=4)	1	1	2
Average survival period (mo)	65.8	59.2	52.5

DOD, died of disease; AWD, alive with disease; AUS, alive with unknown status.

logic features are shown in Fig. 3.

Expression of CK19, p53, cyclin D1, EGFR, p16, and HPV

The expression rates of other tested markers in the three subgroups are compared in Table 4 and illustrated in Fig. 4. CK19, which normally exists in the basal layers of both squamous epithelium and various ductal structures, was positive in 42.3% of cases and was most commonly identified in the mixed subtype, followed by ductal and basal subtypes ($p > .05$). Overexpression of p53 was observed in 34.6% of cases and was more commonly observed in mixed than in basal or ductal subtypes ($p > .05$). Cyclin

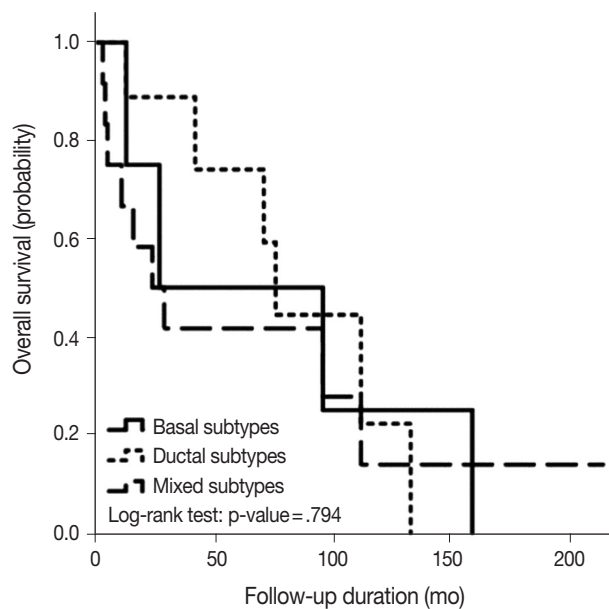


Fig. 2. Overall survival curves of basal, ductal, and mixed subtypes of head and neck basaloid squamous cell carcinomas.

D1 and EGFR expression were observed in 69.2% and 61.5%, respectively, and the ductal subtype showed the lowest expression rate for both proteins ($p > .05$). Four p16-positive cases and three HPV-positive cases showed no subtype tendencies.

DISCUSSION

BSCC is a type of squamous cell carcinoma that occurs in the supraglottic larynx, pyriform sinus, base of tongue, or esophagus. The main histologic components of BSCC are undifferentiated

cells, but there can be divergent differentiation, including ductal differentiation. The multipotency of BSCC has been described more often with an esophageal origin than in the head and neck.^{1,3,4}

Several studies on the CK immunoprofiles of BSCC have been reported, based on diagnoses in the head and neck region, and most of them focused on the diagnostic value and distinguishing BSCC from other carcinomas with basaloid features.^{5,6,8-12} The most frequently expressed CK subtype in BSCC was CK14 (53%–100%)^{5,6,8,10,11} and CK5/6 (100%),⁹ followed by CK19 and CK8/18 (80%),⁶ and CK17 (68%).⁵ These have been described as useful markers for differentiating BSCC from other histologically similar tumors including basal cell carcinoma with squamous metaplasia, adenoid cystic carcinoma, and neuroendocrine carcinoma. The CK7 expression rate has varied depending on the report (0%–53%).^{8,10,11,13,14}

Table 3. Histologic features of head and neck basaloid squamous cell carcinoma according to subtype

Histologic finding	Basal (n=9)	Ductal (n=5)	Mixed (n=12)	Total (n=26)
Palisading	4 (44.4)	3 (60.0)	0 ^a	7 (26.9)
Comedonecrosis	9 (100)	3 (60.0)	3 (25.0) ^b	15 (57.7)
Cribriform pattern	2 (22.2)	2 (40.0)	3 (25.0)	7 (26.9)
Ductal differentiation	4 (44.4)	2 (40.0)	2 (16.7)	8 (30.8)
Mucin production	2 (22.2)	2 (40.0)	3 (25.0)	7 (26.9)
Desmoplasia	4 (44.4)	2 (40.0)	0 ^c	6 (23.1)

Values are presented as number (%).

^ap = .010; ^bp = .001; ^cp = .021.

Based on the variable histology and CK expression of BSCC, we hypothesized that this tumor is heterogeneous and not homogenous. Kobayashi *et al.*⁵ also concentrated on the histologic diversity of esophageal BSCC. They analyzed expression patterns of CK7, CK14, and smooth muscle actin in relationship to different components of BSCCs. However, our attempt to subclassify BSCC according to the expression of basal (CK5/6, p63) or ductal markers (CK7, CK8/18) is novel.

Imamhasan *et al.*⁴ studied 22 esophageal BSCCs in comparison with conventional SCC. BSCC frequently manifested with ductal differentiation (27.5%), and cases with ductal differentiation were associated with better outcomes than cases without ductal differentiation, although this result was not statistically significant. Ductal differentiation was observed in eight of 26 cases (30.8%)

Table 4. Other immunomarker expression in head and neck basaloid squamous cell carcinoma according to subtype

Immunomarker	Basal (n=9)	Ductal (n=5)	Mixed (n=12)	Total (n=26)
CK19	2 (22.2)	2 (40.0)	7 (58.3)	11 (42.3)
p53	2 (22.2)	1 (20.0)	6 (50.0)	9 (34.6)
Cyclin D1	7 (77.8)	2 (40.0)	9 (75.0)	18 (69.2)
EGFR	6 (66.7)	1 (20.0)	9 (75.0)	16 (61.5)
p16	1	2	1	4 (15.4)
HPV	1	2	0	3 (11.5)

Values are presented as number (%).

CK, cytokeratin; EGFR, epidermal growth factor receptor; HPV, human papillomavirus.

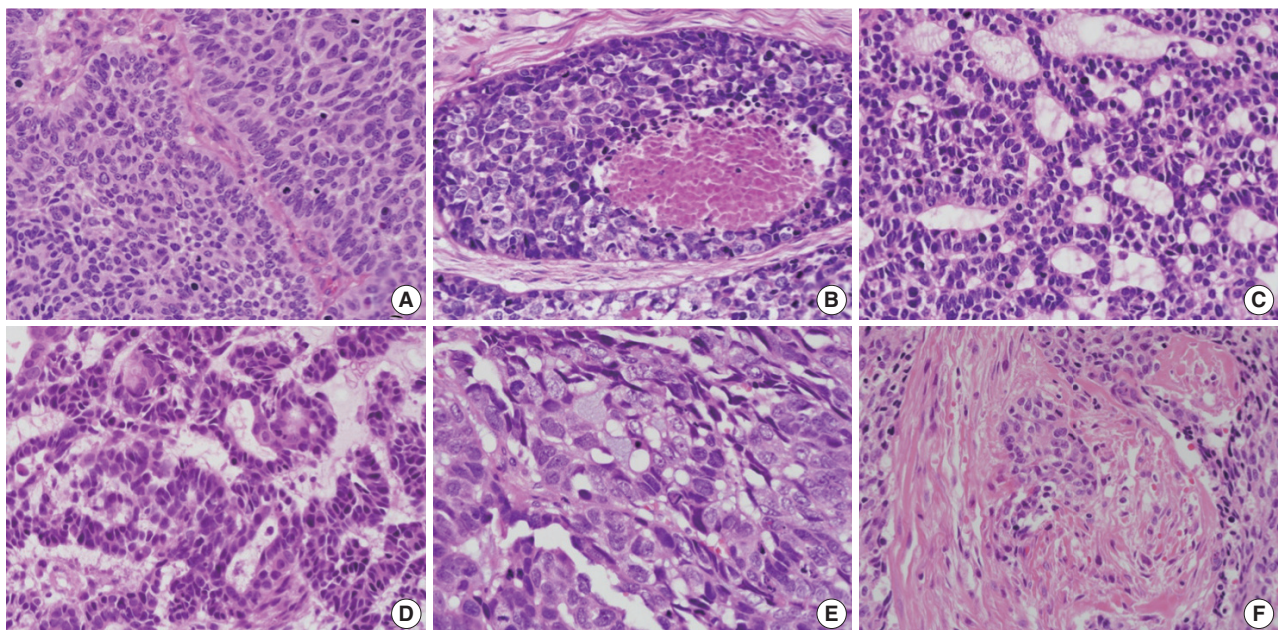


Fig. 3. Representative histologic parameters of basaloid squamous cell carcinomas. (A) Nuclear palisading. (B) Comedo-necrosis. (C) Cribriform pattern. (D) Ductal differentiation. (E) Mucin production. (F) Desmoplasia.

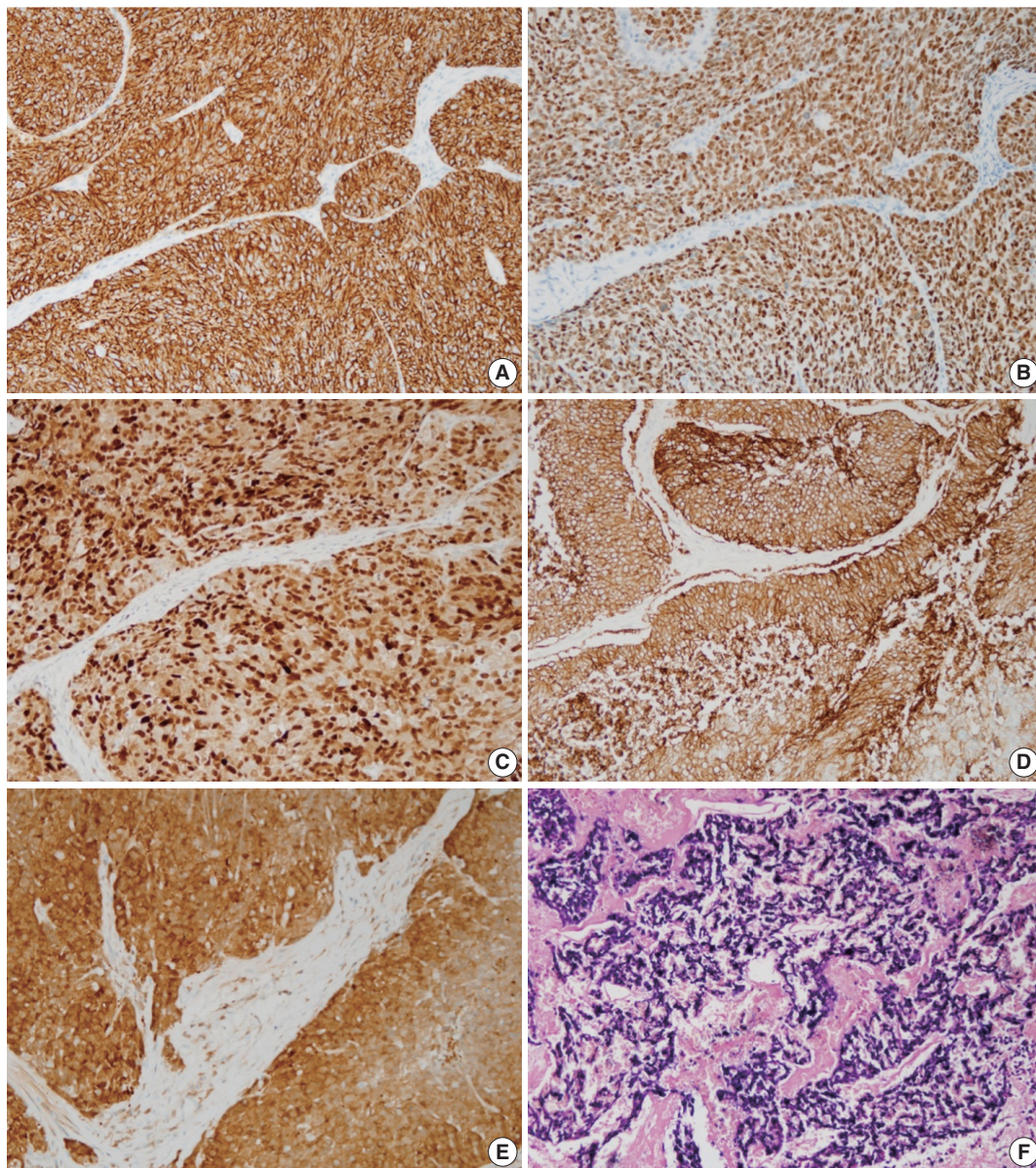


Fig. 4. Representative expression patterns of cytokeratin 19 (A), p53 (B), cyclinD1 (C), epidermal growth factor receptor (D), p16 (E), and human papillomavirus *in situ* hybridization (F).

in our study. Ductal differentiation or mucin production was not restricted to the ductal subtype but was associated with basal or mixed subtypes. Ductal differentiation and ductal phenotypes were not significantly associated with improved prognoses. There was no significant difference in overall survival among the three subtypes. Among other histologic parameters, peripheral nuclear palisading, comedo-necrosis, and desmoplasia were significantly less frequent in the mixed subtype than in the basal or ductal phenotype. However, the clinical significance of this result was not fully elucidated.

When expression rates for other immunomarkers were com-

pared, CK19, which can be both a basal and ductal marker, was positive in 42.3% of cases, which was lower than the rate of CK5/6 (65.4%) or CK8/18 (46.2%) expression. The p53 expression rate in head and neck BSCC was 34.6%, which was slightly lower than reported rates of 40%–100%.^{1,6,14,15} CyclinD1 and EGFR were positive in 69.2% and 61.5%, respectively. There are currently no reported data on expression patterns of these proteins in head and neck BSCC. A few studies on esophageal BSCC showed 25% cyclinD1 positivity and 56%–100% EGFR positivity.^{16,17} The ductal subtype tended to exhibit lower levels of p53, cyclinD1, and EGFR expression than basal or mixed subtypes; however,

based on the small number of cases in this study, the result was not statistically significant. A small number of p16- and/or HPV-positive cases were not restricted to one subtype. Three HPV-positive cases consisted of one basal subtype from the tonsil, one ductal subtype from the tonsil, and one ductal subtype from the nasal cavity. In the past, a relationship between HPV and basaloid morphology of head and neck squamous cell carcinoma has been suggested,^{18,19} but it is now accepted that not all BSCC cases are associated with HPV, and HPV status is more closely related to the location than histology of SCC.^{20,21} A recent study suggested a relationship between high-risk HPV and CK19 expression,²² but two of three HPV-positive cases in this study were negative for CK19.

In summary, BSCC consists of a heterogeneous group that contain tumors with basal, ductal, or mixed immunophenotypes, and this phenomenon suggests a complex histogenesis. Mixed subtypes showed fewer histological characteristics, and the ductal subtype showed less oncogenic protein expression (p53, cyclin D1, and EGFR), although the clinical implications of these findings have not been fully elucidated. The low expression rate of BSCC for CK19 contrasts with the high expression in conventional SCC and limits the diagnostic utility of CK19 mRNA detection in this entity.

Although this study suggested a heterogeneous pathogenesis of head and neck BSCC, there were some limitations to this study, including the retrospective design, small number of cases, and the fact that all patients came from a single institution. Extended or multi-institutional studies might produce more significant results. Furthermore, remarkable advances in investigative tools, such as genomic microarray technologies and next-generation sequencing, could help confirm the results.

Conflicts of Interest

No potential conflict of interest relevant to this article was reported.

REFERENCES

1. Cho KJ, Jang JJ, Lee SS, Zo JI. Basaloid squamous carcinoma of the oesophagus: a distinct neoplasm with multipotential differentiation. *Histopathology* 2000; 36: 331-40.
2. Raslan WF, Barnes L, Krause JR, Contis L, Killeen R, Kapadia SB. Basaloid squamous cell carcinoma of the head and neck: a clinicopathologic and flow cytometric study of 10 new cases with review of the English literature. *Am J Otolaryngol* 1994; 15: 204-11.
3. Kobayashi Y, Nakanishi Y, Taniguchi H, *et al.* Histological diversity in basaloid squamous cell carcinoma of the esophagus. *Dis Esophagus* 2009; 22: 231-8.
4. Imamhasan A, Mitomi H, Saito T, *et al.* Immunohistochemical and oncogenetic analyses of the esophageal basaloid squamous cell carcinoma in comparison with conventional squamous cell carcinomas. *Hum Pathol* 2012; 43: 2012-23.
5. Linskey KR, Gimbel DC, Zukerberg LR, Duncan LM, Sadow PM, Nazarian RM. BerEp4, cytokeratin 14, and cytokeratin 17 immunohistochemical staining aid in differentiation of basaloid squamous cell carcinoma from basal cell carcinoma with squamous metaplasia. *Arch Pathol Lab Med* 2013; 137: 1591-8.
6. Mane DR, Kale AD, Angadi P, Hallikerimath S. Expression of cytokeratin subtypes: MMP-9, p53, and alphaSMA to differentiate basaloid squamous cell carcinoma from other basaloid tumors of the oral cavity. *Appl Immunohistochem Mol Morphol* 2013; 21: 431-43.
7. Patil DT, Goldblum JR, Billings SD. Clinicopathological analysis of basal cell carcinoma of the anal region and its distinction from basaloid squamous cell carcinoma. *Mod Pathol* 2013; 26: 1382-9.
8. Winters R, Naud S, Evans MF, Trotman W, Kasznica P, Elhosseiny A. Ber-EP4, CK1, CK7 and CK14 are useful markers for basaloid squamous carcinoma: a study of 45 cases. *Head Neck Pathol* 2008; 2: 265-71.
9. Serrano MF, El-Mofty SK, Gnepp DR, Lewis JS Jr. Utility of high molecular weight cytokeratins, but not p63, in the differential diagnosis of neuroendocrine and basaloid carcinomas of the head and neck. *Hum Pathol* 2008; 39: 591-8.
10. Coletta RD, Almeida OP, Vargas PA. Cytokeratins 1, 7 and 14 immunoreexpression are helpful in the diagnosis of basaloid squamous carcinoma. *Histopathology* 2006; 48: 773-4.
11. Coletta RD, Cotrim P, Almeida OP, Alves VA, Wakamatsu A, Vargas PA. Basaloid squamous carcinoma of oral cavity: a histologic and immunohistochemical study. *Oral Oncol* 2002; 38: 723-9.
12. Tsubochi H, Suzuki T, Suzuki S, *et al.* Immunohistochemical study of basaloid squamous cell carcinoma, adenoid cystic and mucoepidermoid carcinoma in the upper aerodigestive tract. *Anticancer Res* 2000; 20: 1205-11.
13. Xie S, Bredell M, Yang H, Shen S, Yang H. Basaloid squamous cell carcinoma of the maxillary gingiva: a case report and review of the literature. *Oncol Lett* 2014; 8: 1287-90.
14. Yu GY, Gao Y, Peng X, Chen Y, Zhao FY, Wu MJ. A clinicopathologic study on basaloid squamous cell carcinoma in the oral and maxillofacial region. *Int J Oral Maxillofac Surg* 2008; 37: 1003-8.
15. Sampaio-Góes FC, Oliveira DT, Dorta RG, *et al.* Expression of PCNA, p53, Bax, and Bcl-X in oral poorly differentiated and basaloid squamous cell carcinoma: relationships with prognosis. *Head Neck*

- 2005; 27: 982-9.
16. Sato-Kuwabara Y, Fregnani JH, Jampietro J, *et al.* Comparative analysis of basaloid and conventional squamous cell carcinomas of the esophagus: prognostic relevance of clinicopathological features and protein expression. *Tumour Biol* 2016; 37: 6691-9.
 17. Abe K, Sasano H, Itakura Y, Nishihira T, Mori S, Nagura H. Basaloid-squamous carcinoma of the esophagus: a clinicopathologic, DNA ploidy, and immunohistochemical study of seven cases. *Am J Surg Pathol* 1996; 20: 453-61.
 18. Mendelsohn AH, Lai CK, Shintaku IP, *et al.* Histopathologic findings of HPV and p16 positive HNSCC. *Laryngoscope* 2010; 120: 1788-94.
 19. El-Mofty SK, Patil S. Human papillomavirus (HPV)-related oropharyngeal nonkeratinizing squamous cell carcinoma: characterization of a distinct phenotype. *Oral Surg Oral Med Oral Pathol Oral Radiol Endod* 2006; 101: 339-45.
 20. Begum S, Westra WH. Basaloid squamous cell carcinoma of the head and neck is a mixed variant that can be further resolved by HPV status. *Am J Surg Pathol* 2008; 32: 1044-50.
 21. Chernock RD, Lewis JS Jr, Zhang Q, El-Mofty SK. Human papillomavirus-positive basaloid squamous cell carcinomas of the upper aerodigestive tract: a distinct clinicopathologic and molecular subtype of basaloid squamous cell carcinoma. *Hum Pathol* 2010; 41: 1016-23.
 22. Santoro A, Pannone G, Ninivaggi R, *et al.* Relationship between CK19 expression, deregulation of normal keratinocyte differentiation pattern and high risk-human papilloma virus infection in oral and oropharyngeal squamous cell carcinoma. *Infect Agent Cancer* 2015; 10: 46.

Morphological Features and Immunohistochemical Expression of p57Kip2 in Early Molar Pregnancies and Their Relations to the Progression to Persistent Trophoblastic Disease

Marwa Khashaba
Mohammad Arafa¹
Eman Elsalkh¹ · Reda Hemida²
Wagiha Kandil¹

Department of Pathology, Faculty of Medicine, Port Said University, Port Said; Departments of ¹Pathology and ²Obstetrics and Gynecology, Faculty of Medicine, Mansoura University, Mansoura, Egypt

Received: January 31, 2017
Revised: April 19, 2017
Accepted: April 28, 2017

Corresponding Author
Mohammad Arafa, MD, PhD
Department of Pathology, Faculty of Medicine, Mansoura University, 35516 Mansoura, Egypt
Tel: +20-50-226-5922
Fax: +20-50-226-3717
E-mail: marafa8@yahoo.com

Background: Although the morphological features characteristic of products of conception specimens including molar pregnancies are well described, substantial histopathological similarities are observed between the different entities, especially in cases of early pregnancies. Furthermore, there are no current solid criteria that could predict cases with progression to persistent gestational trophoblastic disease. In this study, we aimed to determine the most specific histopathological and immunohistochemical features required for accurate diagnosis that can reliably predict the clinical behavior. **Methods:** Sixty-five cases of products of conception were reviewed clinically and pathologically, and any progression to persistent gestational trophoblastic disease (GTD), if present, was noted. Pathological assessment of the archival material included re-cut sections of 5 µm in thickness, routine staining with hematoxylin and eosin and immunohistochemical staining of p57Kip2. **Results:** Certain histopathological criteria were found to be significant in differentiation between complete hydatidiform mole (CHM) and partial hydatidiform mole including villous shape and outline, villous trophoblast hyperplasia, and atypia in extravillous trophoblasts. There were no significant differences in any morphological or immunohistochemical features between cases with or without subsequent development of GTD. **Conclusions:** Histopathological diagnosis of molar pregnancy remains problematic especially in early gestation. Their diagnosis should be stated after a constellation of specific histopathological criteria in order not to miss CHM. p57Kip2 immunohistochemistry is of great value in diagnosis of cases that had equivocal morphology by histopathological examination. However, there were no significant features to predict cases that subsequently developed persistent GTD.

Key Words: Hydatidiform mole; Complete hydatidiform mole, early; p57Kip2 immunohistochemistry

Hydatidiform mole (HM) is an abnormal gestation characterized by significant hydropic change and variable trophoblastic proliferation involving part or all of chorionic villi.^{1,2} HM is categorized into two separate entities, complete hydatidiform mole (CHM) and partial hydatidiform mole (PHM), according to morphology and cytogenetics. However, hydropic abortion (HA) could morphologically mimic HM.^{3,4}

Characteristic morphologic features have been proposed for the diagnosis of product of conception (POC) specimens including CHM, PHM, and HA. However, substantial histopathological similarities are observed between the three entities, especially in cases of early detection resulting in interobserver and intraobserver variability in the diagnosis of POC specimens.^{5,6} Thus, the diagnosis of POC on the basis of histopathology alone remains a challenge for pathologists, even those experienced.⁷

Persistent gestational trophoblastic disease (PGTD) develops

after CHM in 10% to 30% of cases,⁴ and after PHM in 0.5% to 5% whereas HA has no relation to PGTD.⁵ Thus, follow-up serum β-human chorionic gonadotropin (β-HCG) measurements aren't essential in cases of HA, whereas these measurements form part of surveillance for PGTD in cases of HM. Therefore, accurate distinction of CHM from PHM on one hand and of HM from HA on the other hand is important for appropriate clinical management and has prognostic implications.³

Difficult cases may require molecular techniques using the differences in DNA content of different POC cases.⁸ However, such molecular diagnostic methods are technically difficult, relatively costly, and non-available in most of pathology laboratories.² Detection of the expression of gene products such as p57Kip2 by the trophoblastic cells should be highlighted. The p57Kip2 gene (CDKN1C) is a strongly paternally imprinted gene expressed only by the maternal allele in most tissues and is involved in implan-

tation.⁹ In normal placenta, nuclear p57Kip2 expression is seen in villous cytotrophoblast, extravillous trophoblast, villous stromal cells, and deciduas.^{10,11} p57Kip2 can identify CHM (androgenetic diploidy) by the lack of its expression¹²⁻¹⁴ and can be helpful in distinguishing CHM from PHM and non molar HA,¹¹ but can't distinguish PHM (diandric monogynic triploidy) from nonmolar (biparental diploidy) specimens as both are positive.¹⁴ CHM mostly doesn't contain maternal genome. Therefore, p57Kip2 staining is unexpressed or greatly reduced in the nuclei of their cytotrophoblasts and stromal cells.¹¹ Products of conception containing maternal genetic material, PHM and nonmolar HA, show positive nuclear p57Kip2 staining in cytotrophoblast and villous stromal cells. p57Kip2 is also expressed in intermediate trophoblast islands and decidual cells, serving as positive internal control in all POC cases.^{12,13}

In this study, we aimed to define precise histopathological and immunohistochemical features to make a proper diagnosis of the different types of HMs especially in early gestational ages and to distinguish those from other mimics. Furthermore, specific features to predict prognosis and progression to PGTD were investigated.

MATERIALS AND METHODS

Sample collection

Archival materials of sixty five cases of POC specimens were retrieved from the department of Pathology, Faculty of Medicine, Mansoura University, between January 2013 and December 2014. The protocol was approved by the Ethical Committee of Mansoura University and informed consents were obtained from the patients.

Histopathological review

The paraffin blocks were re-cut in 5- μ m-thick sections and stained with hematoxylin and eosin stain and were independently reviewed by two pathologists for evaluation of the main morphological findings of HM.^{13,15}

Immunohistochemistry

Five-micrometer-thick tissue section from each case was subject to immunohistochemical staining using monoclonal antibody against the p57Kip2 protein (NeoMarkers/Lab Vision Corporation, Fremont, CA, USA) with dilution 1:200 and the Envision system (DakoCytomation, Glostrup, Denmark). All the steps were performed according to the manufacturers' instructions.

In all cases, p57Kip2 was assessed in the nuclei of the villous

cytotrophoblasts, extravillous trophoblasts, and villous stromal cells. Specimens were interpreted as positive for p57Kip2 staining when there was distinct nuclear staining of villous cytotrophoblasts and stromal cells. The p57Kip2 stain was interpreted as negative when there was no distinct staining or limited nuclear staining (< 10%) of villous cytotrophoblasts and stromal cells. Staining of intermediate trophoblasts and/or maternal decidua was considered as the positive internal control for these specimens.

Statistical methods

Data were analyzed using the program SPSS ver. 20 (IBM Corp., Armonk, NY, USA) to obtain descriptive statistics. Statistical significance was determined at 95% level of confidence (i.e., differences will be considered significant if $p < .05$).

RESULTS

Examination of clinical data

The age of patients ranged from 16 to 50 years with a mean of 26 ± 8 years and a median of 24 years. All cases were in the first or early second trimester. Their gestational age ranged from 6 to 14 weeks with a mean of 9 ± 2 weeks and a median of 8 weeks.

Histopathological examination

Significant histopathological criteria for the diagnosis and distinguishing different entities are shown in Table 1. Examples of the morphological features are demonstrated in Fig. 1.

Immunohistochemistry

Specimens that showed distinct nuclear staining of cytotrophoblasts and villous stromal cells were interpreted as positive for p57Kip2 (Fig. 1H). On the other hand, specimens that showed no or limited nuclear staining (in < 10%) of cytotrophoblasts

Table 1. Significant histopathological criteria according to the final diagnosis of the studied cases using p57Kip2 immunohistochemistry

Significant criteria differentiating between CHM and PHM	Significant criteria differentiating between molar and nonmolar pregnancy
Villous shape and outline: $p < .001$	Villous shape and outline: $p < .001$
Villous trophoblast hyperplasia: $p = .001$	Cistern formation: $p < .001$
Atypia at extravillous trophoblast: $p < .001$	Trophoblastic inclusion: $p = .001$
	Villous trophoblast hyperplasia: $p < .001$

CHM, complete hydatidiform mole; PHM, partial hydatidiform mole.

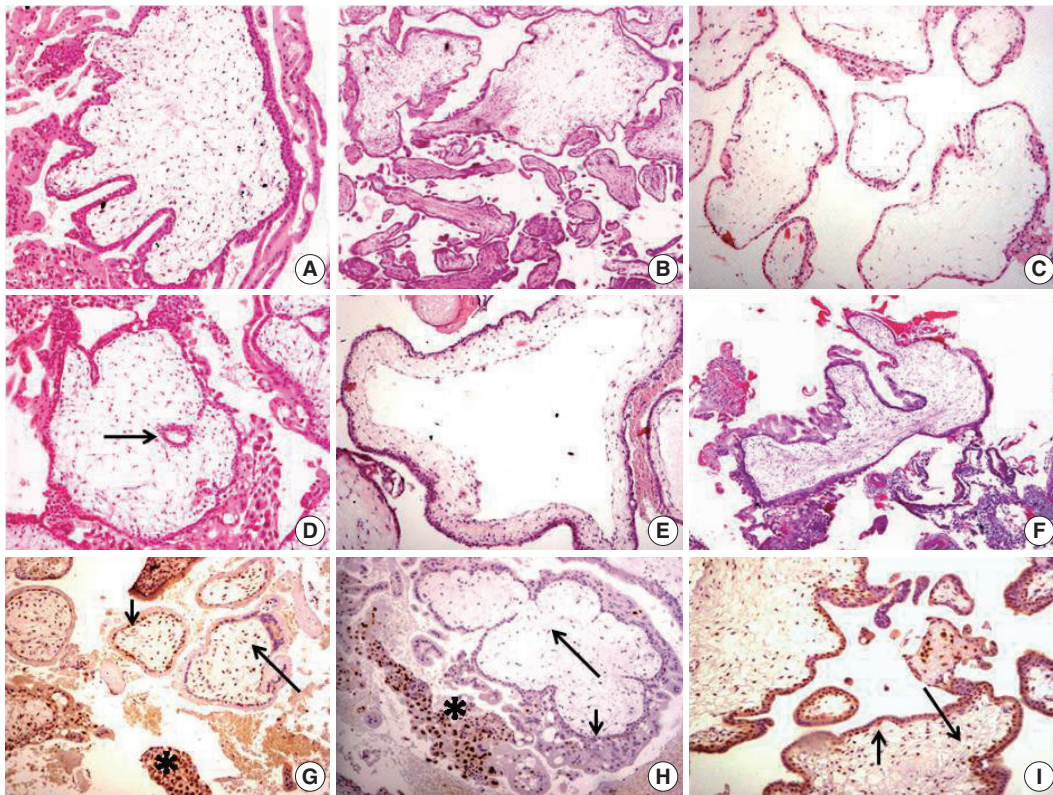


Fig. 1. (A) Complete hydatidiform mole (CHM): irregular villous outline (club shaped) with villous stromal karyorrhectic debris. (B) Partial hydatidiform mole (PHM). Two villous populations; large edematous villi with irregular outline and normal appearing nondistended ones. (C) Hydropic abortion (HA): distended villi with hydropic change. (D) CHM: trophoblastic inclusion (arrow). (E) CHM: cistern formation. (F) CHM: multifocal villous trophoblastic hyperplasia. (G) HA: positive p57Kip2 nuclear staining in intermediate trophoblast as positive internal control (asterisk). Positive p57Kip2 nuclear staining in villous cytotrophoblasts (CT) (short arrow) and villous stromal cells (long arrow) (immunoperoxidase). (H) CHM p57Kip2 immunohistochemistry: negative nuclear staining in villous CT (short arrow) and villous stromal cells (long arrow); positive p57Kip2 nuclear staining in intermediate trophoblast as positive internal control (asterisk) (immunoperoxidase). (I) PHM: positive p57Kip2 nuclear staining in villous CT (short arrow) and villous stromal cells (long arrow) (immunoperoxidase).

and villous stromal cells with positive internal control were considered negative for p57Kip2 stain (Fig. 1). Accordingly, the studied cases were redistributed as shown in Table 2.

CHM originally constituted 39 cases. However, after reevaluation based on the histopathological criteria and p57Kip2 immunohistochemistry, seven cases were added to CHM (previously diagnosed as PHM). On the other hand, one case originally diagnosed as CHM was converted to PHM. The final typing of the molar cases was, therefore, 45 cases of CHM and 11 cases of PHM.

Follow-up

By following the clinical history of all studied cases, nine cases (14% of total/16% of molar cases) were found to progress into gestational trophoblastic disease (GTD) based on persistence of symptoms and serum β -HCG level (Table 3). These represented 18% of CHM and 9% of PHM cases. As shown in Table 4, histopathological criteria of these cases were examined and compared

Table 2. Comparison of the diagnosis of the studied cases by histopathological examination and p57Kip2 immunohistochemistry (n=56)

Method of diagnosis	Case		p-value
	CHM	PHM	
Haematoxylin and eosin stain	39 (60)	17 (26)	<.001
p57Kip2 immunohistochemistry	45 (69)	11 (17)	

Values are presented as number (%).

CHM, complete hydatidiform mole; PHM, partial hydatidiform mole.

with the results of p57Kip2 immunohistochemistry to detect the most statistically significant histopathological feature that can predict the progression of molar disease into PGTD. According to the current study, none of the studied histopathological parameters could differentiate between cases with or without progression to GTD.

Table 3. Cases that developed gestational trophoblastic neoplasia (n=9)

Case	Age (yr)	GA (wk)	Histopathology	p57Kip2	β-HCG (mIU/mL)	MTX	Response	Second-line treatment
1	20	10	CHM	Negative	2907	2	Yes	-
2	28	4	CHM	Negative	1294	2	Yes	-
3	29	8	CHM	Negative	280	1	Yes	-
4	48	8	CHM	Negative	1328	3	No	Hysterectomy
5	20	12	CHM	Negative	4177	3	Yes	-
6	29	9	CHM	Negative	446	2	Yes	-
7	19	8	CHM	Negative	3260	2	Yes	-
8	42	10	CHM	Negative	5000	6	No	EMA/CO
9	24	8	PHM	Positive	4990	5	Yes	-

GA, gestational age; β-HCG, β-human chorionic gonadotropin; MTX, methotrexate; CHM, complete hydatidiform mole; EMA/CO, etoposide, methotrexate, actinomycin D, cyclophosphamide, vincristine/ovine; PHM, partial hydatidiform mole.

Table 4. Histopathological criteria of cases that clinically progressed to PGTD in comparison to the rest of the series

Parameters		PGTD (n=9)	Non-PGTD (n=56)	p-value
Villous shape and outline	Distended regular	1	9	>.99
	Distended irregular	5	24	
	Non-distended	1	8	
	Two population of villi (distended and nondistended)	2	15	
Cistern	Present	8	45	>.99
	Absent	1	11	
Trophoblastic inclusion	Present	6	34	>.99
	Absent	3	22	
Stromal myxoid change	Present	4	26	>.99
	Absent	5	30	
Villous trophoblast hyperplasia	Circumferential	4	21	>.99
	Multifocal	4	27	
	Polar	1	8	
Stromal karyorrhexis	Present	0	14	.186
	Absent	9	42	
Atypia at extravillous trophoblast	Mild	5	32	>.99
	Marked	4	24	

PGTD, persistent gestational trophoblastic disease.

DISCUSSION

The present study was performed to investigate histopathological parameters commonly used during routine histopathological examination in the differential diagnosis of POC cases, especially those with early gestational age. Also, we aimed to study the value of using these histopathological criteria for diagnosis of HM specimens by comparing them with the results of p57Kip2 immunohistochemical staining.

In agreement with previous reports, our results showed that examination of the villous shape was statistically significant in differentiation between CHM and PHM cases on one hand and between molar and nonmolar cases on the other hand.^{16,17} Most of our studied CHM cases (62%) had a population of distended villi with irregular outline. This was significant in differentiation between POC specimens and in favor of early CHM.^{15,18} Our

results were in contrast with the results of the study by Ishikawa *et al.*¹⁶ who found that enlarged villi with regular round outline was a good marker for the diagnosis of CHM. This disagreement can be explained by the fact that the gestational age of our cases was in the first trimester, and at this early gestational age, villi of CHM don't exhibit the well formed distended villi with regular outline and have more irregular outline.

Cistern formation is a major criterion in HM. Our study showed that cistern formation was found in CHM (96%) more common than in PHM cases (91%). It was significant in differentiation between molar and nonmolar pregnancy. On the other hand, it wasn't significant in differentiation between the CHM and PHM. This is in contrast to other studies that found it significant and in favor of diagnosis of PHM.^{17,18} This may be because of the difference in number of studied CHM cases.

We found that the presence of trophoblastic inclusion in the

villous core was present in 82% of PHM and in 67% of CHM. This was statistically significant in differentiation between cases of molar and nonmolar pregnancy but was insignificant in differentiation between the CHM and PHM as described in previous reports.^{16,17,19} Trophoblastic hyperplasia is an essential requirement for the diagnosis of molar pregnancy.²⁰ The results of this study demonstrated that 59% of CHM cases had circumferential villous trophoblastic hyperplasia, while 88% of PHM cases exhibited multifocal villous trophoblast hyperplasia. Polar trophoblast hyperplasia was in favor of nonmolar POC diagnosis. It was found to be statistically significant in differentiation between CHM and PHM on one hand and between molar and nonmolar POC on the other hand, in agreement with previous studies.^{19,20} On the other hand, our results disagreed with the study of Abdou *et al.*¹⁷ on 59 cases of POC specimens and found that trophoblast hyperplasia had no statistically significant value in that differentiation. This marked circumferential villous trophoblast hyperplasia which was found in CHM cases may be related to the absence of p57Kip2 expression by the villous cytotrophoblasts and villous stromal cells in CHM cases which lack the maternal genome. This results in loss of cell cycle control and hence increased trophoblast proliferation.

It is known that villi in CHM have a high level of stromal karyorrhectic debris.²¹ In this study, villous stromal karyorrhectic debris wasn't observed in any case diagnosed as PHM or nonmolar POC. Although the villous stromal karyorrhectic debris was found in 36% of CHM cases, it wasn't statistically significant in differentiation of the three entities; CHM vs PHM or molar vs nonmolar pregnancies. This was in agreement with the finding that stromal karyorrhexis couldn't differentiate between POC cases.¹⁷ This was in disagreement with the results of a study including 113 specimens of POC before 13th week gestation and found that the rate of stromal karyorrhexis was significantly higher in early CHM than in PHM ($p < .001$). They proved and confirmed that the frequent karyorrhexis in the villous stroma is a useful histopathologic parameter in the differential diagnosis of CHM from PHM and HA in early gestational age. However, the stromal karyorrhexis couldn't be used as a significant feature in cases showing diffuse hydropic change due to an absence of cellular components in the stroma.¹⁸

The current study showed that atypia (in the form of increased nucleocytoplasmic ratio, hyperchromasia, and pleomorphism) in extravillous trophoblast was mainly of marked degree in 74% of CHM, and of mild degree in 71% of PHM cases. Marked atypia was in favor of CHM diagnosis, while mild atypia was in favor of PHM and HA diagnosis. Marked degree of atypia was statistically significant in differentiation between CHM and

PHM specimens, while mild degree of atypia wasn't significant in differentiation between molar and nonmolar POC. It may be a useful histopathologic feature regarding the diagnosis and classification of HM. This was consistent with the observation that trophoblast atypia could differentiate between CHM and PHM where diffuse marked atypia was found in most CHM and focal mild atypia in most PHM.²² This was in contrast with others who found that atypia in extravillous trophoblast showed no significant value in differentiation between CHM and PHM.^{17,19}

In our study, seven cases diagnosed histopathologically as PHM were reclassified as CHM after p57Kip2 immunohistochemistry (showed no or scattered nuclear staining in villous CT and villous stromal cells). Six of these cases exhibited morphological features similar to PHM on histopathological examination in the form of two populations of villi; small and large distended villi with irregular outline and multifocal villous trophoblast hyperplasia. One case showed two villous populations, circumferential villous trophoblast hyperplasia and trophoblastic inclusion in the core of their villi without stromal karyorrhexis. In these cases, we can consider p57Kip2 as a gold standard for the diagnosis and classification of HM cases. This was similar to previous observations.¹⁰

In a retrospective study done by Landolsi *et al.*² on 220 specimens of HA, negative p57Kip2 expression was observed in 8 cases with a histopathological diagnosis of PHM, and in one case with a diagnosis of HA. Landolsi *et al.*² tried to explain this negative p57Kip2 expression either due to mis-diagnosis of CHM or lack of staining due to loss of antigenicity. They proved the mis-diagnosis of CHM by genotyping analysis of their discordant nine cases and found absence of their maternal allele.² Funkunaga *et al.*⁷ reported artifactual loss of staining due to loss of antigenicity in four HA and one PHM cases, but the presence of positive internal control in decidual and implantation site trophoblasts in our study excludes this explanation.¹²

In the current study, one case histopathologically diagnosed as CHM was inconsistent with the pattern of p57Kip2 immunostaining which showed positive nuclear staining in villous CT and villous stromal cells. This was also found in the results of previous studies in which one case out of 132 CHM cases was found to show positive p57Kip2 immunostaining in their CT and villous stromal cells.² This was explained by false-positive immunohistochemistry or a mis-diagnosis of PHM or HA. Another possibility is the presence of twin gestation, one of them normal and the other CHM. Furthermore, rare CHMs are biparental in origin and contain both maternal and paternal chromosomal components. They explained it as a mis-diagnosis, as no adequate

DNA material was available for genetic study to confirm. In such rare cases, we can't consider p57Kip2 as a gold standard for the diagnosis and the matter will require further studies including molecular techniques using the differences in DNA content.

Concerning the follow-up data, nine cases out of the 65 total cases (14%) developed PGTD. They were diagnosed based on persistence of their symptoms and their serum β -HCG level which didn't come down to the basal level. Eight cases of these were diagnosed as CHM (18% of total CHM). Similar results were found in a study performed by Van Cromvoirt *et al.*²³ to identify cases that developed PGTD after CHM; 89 cases (20%) of their total 448 CHM cases developed PGTD and required chemotherapy.²⁴⁻²⁶

According to our results, one case of PHM (9% of total PHM) had developed PGTD. But this was inconsistent with the percentage detected in a study done by Wielsma *et al.*²⁴ which detected cases of PHM that developed PGTD; only 6 out of 344 PHM cases (2%) were found to have developed PGTD and were treated successfully by methotrexate chemotherapy. Also, it was inconsistent with the percentage reported by Chen *et al.*³ who found that 2.5%–7.5% of PHM can progress to PGTD. We can attribute this difference between the two studies to the very limited number of the PHM cases studied in the current study. We reviewed these cases histopathologically and didn't find any specific morphological or immunohistochemical features associated with their progression to PGTD. In that regard, the current study was in agreement with the histopathological and immunohistochemical study done by Petts *et al.*²⁵ on 150 cases of molar pregnancy. To achieve this distinction, further studies are required using a larger number of cases and implementing further immunohistochemical markers that may have a benefit.

In conclusion, histopathological diagnosis of molar pregnancy remains problematic especially in early gestational age. The diagnosis requires a constellation of specific histopathological criteria in order not to miss the diagnosis of CHM. p57Kip2 immunohistochemistry is of great value in the diagnosis of cases that have equivocal morphology by histopathological examination. However, there are no significant features to predict cases that subsequently develop persistent trophoblastic disease. Further immunohistochemical markers should be studied to accurately distinguish PHM from CHM and also to predict patients' outcome.

Conflicts of Interest

No potential conflict of interest relevant to this article was reported.

REFERENCES

- Cheung AN. Gestational trophoblastic disease. In: Robboy SJ, Mutter GL, Prat J, Bentley RC, Russell P, Anderson MC, eds. Robboy's pathology of the female reproductive tract. Edinburgh: Churchill Livingstone Elsevier, 2009; 881-907.
- Landolsi H, Missaoui N, Brahem S, Hmissa S, Gribaa M, Yacoubi MT. The usefulness of p57(KIP2) immunohistochemical staining and genotyping test in the diagnosis of the hydatidiform mole. *Pathol Res Pract* 2011; 207: 498-504.
- Chen KH, Hsu SC, Chen HY, Ng KF, Chen TC. Utility of fluorescence in situ hybridization for ploidy and p57 immunostaining in discriminating hydatidiform moles. *Biochem Biophys Res Commun* 2014; 446: 555-60.
- Chiang S, Fazlollahi L, Nguyen A, Betensky RA, Roberts DJ, Iafrate AJ. Diagnosis of hydatidiform moles by polymorphic deletion probe fluorescence *in situ* hybridization. *J Mol Diagn* 2011; 13: 406-15.
- Berkowitz RS, Goldstein DP. Clinical practice: molar pregnancy. *N Engl J Med* 2009; 360: 1639-45.
- Vang R, Gupta M, Wu LS, *et al.* Diagnostic reproducibility of hydatidiform moles: ancillary techniques (p57 immunohistochemistry and molecular genotyping) improve morphologic diagnosis. *Am J Surg Pathol* 2012; 36: 443-53.
- Fukunaga M, Katabuchi H, Nagasaka T, Mikami Y, Minamiguchi S, Lage JM. Interobserver and intraobserver variability in the diagnosis of hydatidiform mole. *Am J Surg Pathol* 2005; 29: 942-7.
- Murphy KM, Ronnett BM. Molecular analysis of hydatidiform moles: utilizing p57 immunohistochemistry and molecular genotyping to refine morphologic diagnosis. *Pathol Case Rev* 2010; 15: 126-34.
- Popiolek DA, Yee H, Mittal K, *et al.* Multiplex short tandem repeat DNA analysis confirms the accuracy of p57(KIP2) immunostaining in the diagnosis of complete hydatidiform mole. *Hum Pathol* 2006; 37: 1426-34.
- Banet N, DeScipio C, Murphy KM, *et al.* Characteristics of hydatidiform moles: analysis of a prospective series with p57 immunohistochemistry and molecular genotyping. *Mod Pathol* 2014; 27: 238-54.
- Sarmadi S, Izadi-Mood N, Abbasi A, Sanii S. p57KIP2 immunohistochemical expression: a useful diagnostic tool in discrimination between complete hydatidiform mole and its mimics. *Arch Gynecol Obstet* 2011; 283: 743-8.
- Madi JM, Braga AR, Paganella MP, Litvin IE, Da Ros Wendland EM. Accuracy of p57KIP2 compared with genotyping for the diagnosis of complete hydatidiform mole: protocol for a systematic review and meta-analysis. *Syst Rev* 2016; 5: 169.

13. Buza N, Hui P. New diagnostic modalities in the histopathological diagnosis of hydatidiform moles. *Diagn Histopathol* 2012; 18: 201-9.
14. Khooei A, Atabaki Pasdar F, Fazel A, *et al.* Ki-67 expression in hydatidiform moles and hydropic abortions. *Iran Red Crescent Med J* 2013; 15: 590-4.
15. Clement PB, Young RH. *Atlas of gynaecologic surgical pathology*. 3rd ed. London: Elsevier, 2014; 271-97.
16. Ishikawa N, Harada Y, Tokuyasu Y, Nagasaki M, Maruyama R. Re-evaluation of the histological criteria for complete hydatidiform mole: comparison with the immunohistochemical diagnosis using p57KIP2 and CD34. *Biomed Res* 2009; 30: 141-7.
17. Abdou A, Kandil M, El-Wahed MA, Shabaan M, El-Sharkawy M. The diagnostic value of p27 in comparison to p57 in differentiation between different gestational trophoblastic diseases. *Fetal Pediatr Pathol* 2013; 32: 395-411.
18. Kim MJ, Kim KR, Ro JY, Lage JM, Lee HI. Diagnostic and pathogenetic significance of increased stromal apoptosis and incomplete vasculogenesis in complete hydatidiform moles in very early pregnancy periods. *Am J Surg Pathol* 2006; 30: 362-9.
19. Landolsi H, Missaoui N, Yacoubi MT, *et al.* Assessment of the role of histopathology and DNA image analysis in the diagnosis of molar and non-molar abortion: a study of 89 cases in the center of Tunisia. *Pathol Res Pract* 2009; 205: 789-96.
20. Bajaj MS, Mehta M, Kashyap S, *et al.* Clinical and pathologic profile of angiomyxomas of the orbit. *Ophthal Plast Reconstr Surg* 2011; 27: 76-80.
21. Chiu PM, Ngan YS, Khoo US, Cheung AN. Apoptotic activity in gestational trophoblastic disease correlates with clinical outcome: assessment by the caspase-related M30 CytoDeath antibody. *Histopathology* 2001; 38: 243-9.
22. Montes M, Roberts D, Berkowitz RS, Genest DR. Prevalence and significance of implantation site trophoblastic atypia in hydatidiform moles and spontaneous abortions. *Am J Clin Pathol* 1996; 105: 411-6.
23. van Cromvoirt SM, Thomas CM, Quinn MA, McNally OM, Bekkers RL. Identification of patients with persistent trophoblastic disease after complete hydatidiform mole by using a normal 24-hour urine hCG regression curve. *Gynecol Oncol* 2014; 133: 542-5.
24. Wielsma S, Kerkmeijer L, Bekkers R, Pyman J, Tan J, Quinn M. Persistent trophoblast disease following partial molar pregnancy. *Aust N Z J Obstet Gynaecol* 2006; 46: 119-23.
25. Petts G, Fisher RA, Short D, Lindsay I, Seckl MJ, Sebire NJ. Histopathological and immunohistochemical features of early hydatidiform mole in relation to subsequent development of persistent gestational trophoblastic disease. *J Reprod Med* 2014; 59: 213-20.
26. Hemida R, Arafa M, AbdElfattah H, Sharaf-Eldin D. Human chorionic gonadotropin (hCG) testing in specimens of tumor and myometrial tissues during surgical treatment of gestational trophoblastic tumors. *J Cancer Res Updates* 2015; 4: 122-6.

Loss of Progesterone Receptor Expression Is an Early Tumorigenesis Event Associated with Tumor Progression and Shorter Survival in Pancreatic Neuroendocrine Tumor Patients

Sung Joo Kim · Soyeon An
Jae Hoon Lee¹ · Joo Young Kim²
Ki-Byung Song¹ · Dae Wook Hwang¹
Song Cheol Kim¹ · Eunsil Yu
Seung-Mo Hong

Department of Pathology and
¹Division of Hepatobiliary and Pancreatic Surgery,
Asan Medical Center, University of Ulsan
College of Medicine, Seoul; ²Department of
Pathology, Korea University Anam Hospital, Korea
University College of Medicine, Seoul, Korea

Received: January 16, 2017
Revised: February 21, 2017
Accepted: March 19, 2017

Corresponding Author

Seung-Mo Hong, MD, PhD
Department of Pathology, Asan Medical Center,
University of Ulsan College of Medicine,
88 Olympic-ro 43-gil, Songpa-gu, Seoul 05505,
Korea
Tel: +82-2-3010-4558
Fax: +82-2-472-7898
E-mail: smhong28@gmail.com

Background: Pancreatic neuroendocrine tumors (PanNETs) are the second most common pancreatic neoplasms and there is no well-elucidated biomarker to stratify their detection and prognosis. Previous studies have reported that progesterone receptor (PR) expression status was associated with poorer survival in PanNET patients. **Methods:** To validate previous studies, PR protein expression was assessed in 21 neuroendocrine microadenomas and 277 PanNETs and compared with clinicopathologic factors including patient survival. **Results:** PR expression was gradually decreased from normal islets (49/49 cases, 100%) to neuroendocrine microadenoma (14/21, 66.6%) to PanNETs (60/277, 21.3%; $p < .001$). PanNETs with loss of PR expression were associated with increased tumor size ($p < .001$), World Health Organization grade ($p = .001$), pT classification ($p < .001$), perineural invasion ($p = .028$), lymph node metastasis ($p = .004$), activation of alternative lengthening of telomeres ($p = .005$), other peptide hormonal expression ($p < .001$) and ATRX/DAXX expression ($p = .015$). PanNET patients with loss of PR expression (5-year survival rate, 64.1%) had significantly poorer recurrence-free survival outcomes than those with intact PR expression (90%) by univariate ($p = .012$) but not multivariate analyses. Similarly, PanNET patients with PR expression loss (5-year survival rate, 76%) had significantly poorer overall survival by univariate ($p = .015$) but not multivariate analyses. **Conclusions:** Loss of PR expression was noted in neuroendocrine microadenomas and was observed in the majority of PanNETs. This was associated with increased grade, tumor size, and advanced pT and pN classification; and was correlated with decreased patient survival time by univariate but not multivariate analyses. Loss of PR expression can provide additional information on shorter disease-free survival in PanNET patients.

Key Words: Pancreas; Neuroendocrine tumors; Receptors, progesterone; Survival

Pancreatic neuroendocrine tumors (PanNETs) are rare, amounting to only 3% of pancreatic neoplasms^{1,2} and 9% of all gastroenteropancreatic neuroendocrine tumors in Korea.³ Although PanNET patients have better survival outcomes than pancreatic ductal adenocarcinoma patients, PanNETs are still malignant neoplasms with a 10-year survival rate of only 40%–50% after surgical resection.^{4–6} Surgical resection is the main curative treatment option for PanNET patients, although other therapies with somatostatin analogs, cytotoxic chemotherapies, and molecular targeted therapies have recently been used in metastatic or unresectable PanNET patients.^{7,8}

A better understanding of the molecular mechanisms of PanNETs is important to better predict clinical outcomes and identify patients who may benefit from therapies targeting PanNETs. A

previous whole-exome sequencing study revealed the genomic landscape of PanNETs including a higher mutational frequency in *MEN1*, *ATRX* (alpha thalassemia/mental retardation syndrome X-linked), and *DAXX* (death-domain associated protein) and a lower mutational frequency in several genes involving mammalian target of rapamycin pathways, including *PTEN*, *TSC2*, and *PIK3CA*.⁹ In that study also, less than half of PanNETs had inactivating mutations in either the *ATRX* or *DAXX* genes, in mutually exclusive ways.⁹ Alterations in the *ATRX* or *DAXX* proteins were closely associated with the alternative lengthening of telomeres (ALT) mechanism in PanNETs,¹⁰ and the loss of *ATRX* or *DAXX* expression and ALT activation were associated with poorer survival in primary PanNET patients.^{11–13}

The hormonal expression status in PanNETs has clinical im-

plications. Peptide hormonal expression is reported to have better prognostic implications for PanNET patients. Increased expression of insulin, GLP1, and other peptide hormones are associated with better overall survival in PanNET patients, whereas gastrin expression has been reported to be associated with worse survival.¹⁴ Among the steroid hormones, only progesterone receptors (PRs), but not estrogen receptors or androgen receptors, are expressed in normal islets.¹⁵⁻¹⁷ PR expression in normal pancreatic islets suggests a possible role for progesterone in pancreatic islet function. A study in mice with intact gonads demonstrated that progesterone treatment stimulated β -cell proliferation in pancreatic islets.¹ However, those proliferation effects were lost in gonadectomized mice. Those observations suggested that progesterone effects require intact gonadal function for normal β -cell proliferation.¹ In our present study, we determined the clinical and prognostic significances of PR expression in surgically resected PanNET patients using tissue microarray immunolabeling.

MATERIALS AND METHODS

Case selection

After approval (2015-0387) from the Institutional Review Board of Asan Medical Center, the records of 277 surgically resected primary PanNETs and 21 sporadic neuroendocrine microadenomas resected between January 1995 and December 2015 were retrieved from the Department of Pathology at Asan Medical Center. Primary PanNETs were defined as well-differentiated, nonfunctional neuroendocrine neoplasms with diameters ≥ 0.5 cm, while neuroendocrine microadenomas were defined as well-differentiated, nonfunctional NETs with diameters < 0.5 cm.^{1,18} All PanNET cases were classified using the 2010 World Health Organization (WHO) classification scheme with mitotic activity and the Ki-67 labeling index.¹ The Ki-67 labeling index was measured by manually assessing the tumor's hottest spot in high-power fields after printing the captured image, as previously described.¹⁹ A minimum of 500 tumor cells were included in the manual count. Poorly differentiated neuroendocrine carcinomas, such as small-cell carcinomas and large-cell carcinomas, were excluded. Pathological data, such as tumor size, extension, lymph node and distant metastases, and perineural and lymphovascular tumor invasion, were extracted from the pathology reports. The clinical data reviewed included patient age, gender, symptoms, and survival outcomes. The expression profiles of specific peptide hormones, including insulin, glucagon, gastrin, serotonin, somatostatin, and glucagon-like peptide 1; other proteins, such as ATRX and DAXX; and the ALT status were used as previously

reported.^{12,14}

Tissue microarray construction

Tissue microarrays were constructed from archived, formalin-fixed, paraffin-embedded tissue blocks with a manual tissue microarrayer (Uni TMA Co. Ltd., Seoul, Korea), as previously described.^{12,14,20} Briefly, three cores from the tumors and one core from the normal pancreatic parenchyma with a diameter of 2 mm were punched from donor blocks and placed in recipient blocks.

Immunohistochemical staining

Immunohistochemical labeling was performed at the immunohistochemical laboratory of the Department of Pathology, Asan Medical Center. In brief, 4-mm-thick tissue sections were deparaffinized and hydrated in xylene and serially diluted in ethanol. Endogenous peroxidase was blocked by incubation in 3% H₂O₂ for 10 minutes, and then heat-induced antigen retrieval was performed. Primary antibodies were used with a Benchmark autostainer (Ventana Medical Systems, Tucson, AZ, USA) in accordance with the manufacturer's protocol. Sections were incubated at room temperature for 32 minutes in primary antibodies for PR (1:200, NCL-L-PGR-312, Novocastra, Newcastle upon Tyne, UK), synaptophysin (1:200, DiNona, Seoul, Korea), chromogranin (1:200, DAK-A3, DakoCytomation, Glostrup, Denmark), and Ki-67 (1:100, 7B11, Zymed, San Francisco, CA, USA). The sections were then labeled with an automated immunostaining system and processed with an iView DAB detection kit (Benchmark XT, Ventana Medical Systems). Immunostained sections were lightly counterstained with hematoxylin, dehydrated in ethanol, and cleared in xylene. Immunoreactivity was interpreted by light microscopic examination and independently evaluated by two pathologists, coauthors of this study (S.J.K. and S.M.H.), who were blind to the clinicopathologic information.

Evaluation of PR labeling

Immunohistochemical labeling of the PR protein was scored using a previously described histological scoring system, which takes into account the size of the stained area and the intensity of the labeling. To be included in the analyses, a tumor had to have sufficient numbers of PR-labeled cells to permit quantification (> 100 PR-positive tumor cells). The labeled area was scored from 0 to 4 for having $< 5\%$, $5\%–25\%$, $26\%–50\%$, $51\%–75\%$, or $> 75\%$ PR-positive cells, respectively. The intensity scale ranged from 0 to 2 as follows: 0, no labeling of tumor cells; 1, weak labeling; and 2, intense labeling, as previously described.²¹

The total histological score (H-score) was calculated by multiplying the area score by the intensity score. The resulting H-score ranged from 0 to 8. We considered cases with an H-score below 2 to have loss of PR expression and cases with an H-score greater than or equal to 2 to have intact PR expression. PR labeling in normal islets was used as an internal positive control. Representative images of PR expression in normal islet and in PanNETs are depicted in Fig. 1. Immunohistochemical staining was evaluated by two independent pathologists (S.J.K. and S.M.H.).

Statistical analyses

SPSS software ver. 20.0 (IBM Corp., Chicago, IL, USA) was used for statistical analyses. The overall and recurrence-free survival times were calculated from the date of diagnosis of PanNET to that of death from any cause and from the date of diagnosis of PanNET to that of recurrence, respectively. Both overall and recurrence-free survival rates were calculated using the Kaplan-Meier method, and the association between overall survival rate and clinicopathologic factors was compared using the log-rank

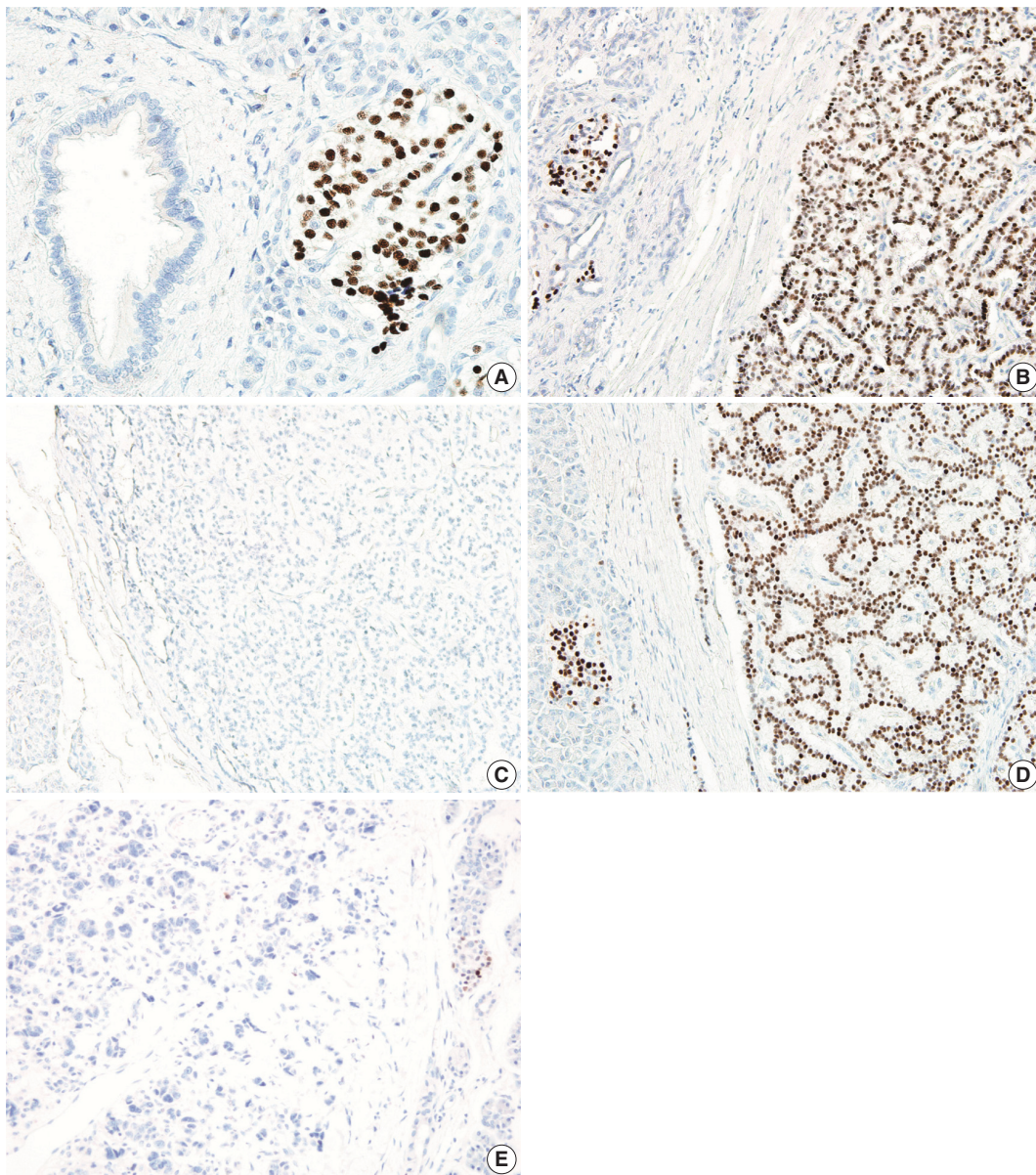


Fig. 1. Representative images of progesterone receptor (PR) labeling in normal pancreas, neuroendocrine microadenoma, and pancreatic neuroendocrine tumor (PanNET). (A) Islets are positive, while acinar and ductal epithelial cells are negative for PR staining in the normal pancreas. Some neuroendocrine microadenomas show intact PR labeling (B), while other neuroendocrine microadenomas demonstrate loss of PR labeling (C). Some PanNETs show intact PR labeling (D), while other PanNETs demonstrate loss of PR labeling (E).

test. The correlations between PR expression and other prognostic factors were analyzed using the chi-square and Fisher exact tests. Possible prognostic factors associated with survival probability were calculated using the Cox's proportional hazard regression model; $p < .05$ was considered statistically significant.

RESULTS

Patient characteristics

Patient characteristics are summarized in Table 1. In the total cohort, 134 patients (49%) were male and 143 (51%) were female. The mean age of the patients was 52.3 ± 12.7 years. According to the WHO classification, there were 85 G1, 95 G2, and 8 G3, respectively. The mean tumor size of the PanNETs and neuroendocrine microadenomas was 3.0 ± 2.2 cm and 0.3 ± 0.1 cm, respectively. In all, 126 cases were classified as pT1, while others had higher pT classifications (95 pT2, 52 pT3, and 4 pT4); 79 cases (28.5%) had lymphovascular invasion and 42 cases (15.2%) had perineural invasion. Metastasis to regional lymph nodes occurred in 39 cases (14.1%) and metastasis to distant organs at the surgical resection of PanNET was observed in 10 cases (3.6%). The median follow-up period was 38 ± 35 months (range, 1 to 188 months).

PR expression

All of the normal pancreatic islets in the patient samples expressed the PR protein in various proportions. PR protein expression was observed in $63.5 \pm 9.8\%$ of the endocrine cells in the islets. A representative image of PR expression in an islet is depicted in Fig. 1. This expression gradually decreased from normal islets (49/49, 100%) to neuroendocrine microadenoma (14/21, 66.6%) to PanNETs (60/277, 21.3%). The H-scores for PR in normal islets, neuroendocrine microadenomas, and PanNETs were 5.1 ± 2.3 , 3.0 ± 3.3 , and 1.3 ± 2.5 , respectively ($p < .001$) (Figs. 1, 2). The mean H-score of the PR expression loss group was 0.1 ± 0.3 , while that of the PR expression intact group was 5.8 ± 2.3 . The majority of PanNETs showed a loss of PR expression (218/277, 78.7%) (Fig. 1).

Correlations between PR expression and clinicopathologic factors

The associations between PR expression and clinicopathologic factors are summarized in Table 1. Loss of PR expression was more commonly observed in PanNETs with larger tumors ($p < .001$), a higher WHO grade ($p = .001$), higher Ki-67 labeling index ($p = .004$), higher pT classification ($p < .001$), frequent peri-

neural invasion ($p = .028$), and regional lymph node metastasis ($p = .004$). Loss of PR expression was also strongly associated with other peptide hormonal expression ($p < .001$), loss of ATRX/DAXX expression ($p = .015$), and activation of ALT ($p = .005$). In addition, the loss of PR expression was marginally associated with lymphovascular invasion ($p = .077$) but not with age, gender, or distant metastasis.

Table 1. Clinicopathologic factors associated with PR expression in PanNETs

Characteristic	PR loss	Intact PR	p-value
Age (yr)			.412
≤60	149 (78.0)	42 (22)	
>60	69 (80.2)	17 (19.8)	
Sex			.380
Male	107 (79.9)	27 (20.1)	
Female	111 (77.6)	32 (22.4)	
Tumor size (cm)			<.001
≤3	126 (71.2)	51 (28.8)	
>3	92 (86.4)	8 (13.6)	
WHO grade			.001
Grade 1	65 (76.5)	20 (23.5)	
Grade 2	83 (87.4)	12 (12.6)	
Grade 3	8 (100.0)	0	
pT classification			<.001
pT1	70 (62.5)	42 (27.5)	
pT2–T4	148 (89.7)	17 (10.3)	
Lymphovascular invasion			.077
Absent	151 (76.3)	47 (23.7)	
Present	67 (84.8)	12 (15.2)	
Perineural invasion			.028
Absent	180 (76.6)	55 (23.4)	
Present	38 (90.5)	4 (9.5)	
Lymph node metastasis			.004
Absent	181 (76.1)	57 (23.9)	
Present	37 (94.9)	2 (5.1)	
Distant metastasis			.639
Absent	210 (78.7)	57 (21.3)	
Present	8 (80.0)	2 (20.0)	
Ki-67 labeling index (%)			.004
<3	137 (73.3)	50 (26.7)	
≥3 and <20	57 (89.1)	7 (10.9)	
≥20	2 (100.0)	0	
Hormone expression			<.001
Absent	91 (94.8)	5 (5.2)	
Present	49 (68.1)	23 (31.9)	
ALT expression			.005
Absent	166 (75.7)	54 (24.5)	
Present	52 (91.2)	5 (8.8)	
ATRX/DAXX expression			.015
Absent	45 (90.0)	5 (10.0)	
Present	166 (75.5)	54 (24.5)	

Values are presented as number (%).

PR, progesterone receptor; PanNET, pancreatic neuroendocrine tumor; WHO, World Health Organization; ALT, alternative lengthening of telomeres.

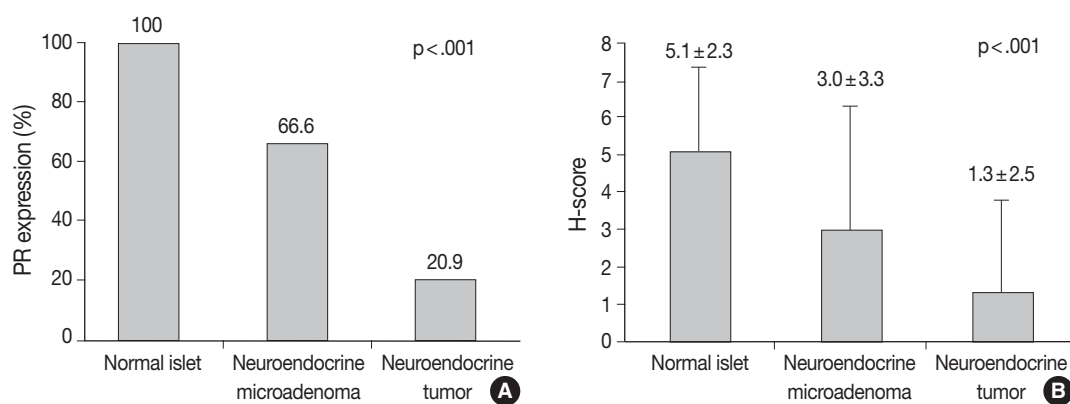


Fig. 2. Progesterone receptor (PR) expression status and the H-score in normal islets, neuroendocrine microadenomas, and pancreatic neuroendocrine tumors (PanNETs). (A) Comparison of PR expression in normal islets, neuroendocrine microadenomas, and PanNETs. (B) The H-score for PR in normal islets, neuroendocrine microadenomas, and PanNETs is 5.1 ± 2.3 , 3.0 ± 3.3 , and 1.3 ± 2.5 , respectively ($p < .001$).

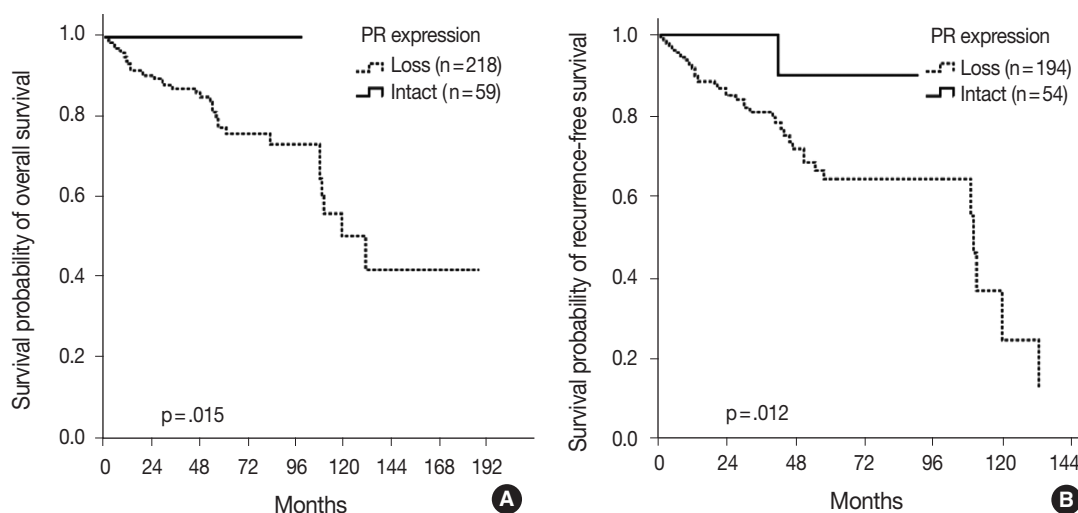


Fig. 3. Kaplan-Meier survival analyses of pancreatic neuroendocrine tumor (PanNET) patients according to progesterone receptor (PR) expression. (A) The 100% overall 5-year survival rate for PanNET patients with PR expression is significantly better than that for those without insulin expression (76%, $p = .015$). (B) The recurrence-free 5-year survival rate for PanNET patients with PR expression (90%) is significantly better than that for those without PR expression (64.1%, $p = .012$).

Survival analyses of PR expression

The overall 5-year survival rate of 100% among the PanNET patients with intact PR expression was significantly better than for patients with PR expression loss (76%, $p = .015$) (Fig. 3A). Similarly, the recurrence-free 5-year survival rate in the PanNET patients with intact PR expression (90%) was significantly better than that of those with PR expression loss (64.1%, $p = .012$) (Fig. 3B).

Univariate analyses of other clinicopathologic factors

The relationships found between survival and other clinicopathologic factors are summarized in Table 2. The clinicopathologic factors associated with poorer survival, according to univariate survival analyses, were older age ($p = .015$), larger tumor size ($p =$

.008), higher WHO grade ($p < .001$), higher pT classification ($p = .015$), and frequent lymphovascular ($p = .002$), perineural ($p < .001$), and regional lymph node metastasis ($p < .001$).

Multivariate analyses of clinicopathologic factors

The Cox proportional hazard model was employed with other significant clinicopathologic factors to determine the prognostic significance of PR expression as well as other clinicopathologic factors in PanNET patients. Only WHO grade ($p = .001$) and lymphovascular invasion ($p = .020$) were independently prognostic, but loss of PR expression was not a prognostic factor in our model ($p = .117$) (Table 2).

DISCUSSION

PR immunohistochemistry has been used to identify ovarian-type stroma for the diagnosis of mucinous cystic neoplasms of the pancreas in the field of pancreas pathology.¹⁸ A recent study demonstrated that loss of or decreases in PR expression in ovarian type stroma of invasive carcinoma with mucinous cystic neoplasm and mucinous cystic neoplasm with high-grade dysplasia were associated with decreased volumes of ovarian-type stroma in mucinous cystic neoplasms.²² These results suggest the possible utility of PR immunolabeling as a surrogate marker for invasion in the diagnosis of mucinous cystic neoplasms.

In addition to the use of PR expression for diagnosing mucinous cystic neoplasms, this expression has also been reported in all normal islets of Langerhans, and previous studies have detected PR in 40%–75% of islets.^{16,17} In our current study, PR expression was noted in 64% of normal islets, a similar proportion to that found in previous studies.

Neuroendocrine microadenomas are precursors and initiating lesions for PanNETs.^{23,24} Only a few previous studies have conducted biomarker evaluations for neuroendocrine microadenomas.^{12,25,26} Decreased menin expression and increased cytokeratin 19 expression have been reported in neuroendocrine microadenomas.^{25,26} However, controversy exists over the loss of ATRX or DAXX expression in these tumors.^{12,26,27} Confirming previous findings, we observed PR expression in 67% of neuroendocrine

microadenomas, and our observations suggest that PR expression loss can also be included as an early event in neuroendocrine tumorigenesis.

PR expression was present in only 21% of the PanNETs examined in our current study, and the majority of PanNETs showed loss of PR expression. Previous studies have found wide ranges of PR expression, from 46% to 76%.^{16,28,29} Plausible explanations for the lower PR expression in our study include different ethnic backgrounds (Western vs Korean), antibody clones, and the cutoff point used for positive expression. While previous studies examined European or American populations, the present study was performed on a Korean population. This difference in ethnic background could have affected PR expression. In addition, previous studies considered PR expression loss when the proportion of nuclear PR labeling was < 1% or < 5%,^{16,28,29} whereas we used the H-score, multiplying the intensity and proportion of PR expression. Different cutoff points for the evaluation of PR expression could explain the lower levels detected in our study.

Loss of PR expression was associated with larger tumor size, higher WHO grade, higher pT classification, and frequent lymphovascular and perineural invasion, and regional lymph node metastasis. Our current observations are thus concordant with the results of previous studies.^{16,28} Arnason *et al.*¹⁵ previously examined 40 PanNET cases and observed that PanNETs with strong PR expression were associated with fewer nodal or distant metastases of PanNETs. Viale *et al.*¹⁶ studied 96 PanNETs and reported that less

Table 2. Univariate and multivariate analyses of PR expression in PanNETs

Characteristic	Variables	Univariate analyses		Multivariate analyses		
		5-Year survival rate (%)	p-value	Hazard ratio	95% confidence interval	p-value
PR expression	Loss	64.1	.012	0.20	0.03–1.49	.117
	Intact	90				
Age (yr)	≤ 60	70.3	.015	1.58	0.76–3.23	.228
	> 60	62.1				
Sex	Male	59.1	.609	-	-	-
	Female	56.9				
Tumor size (cm)	≤ 3	74.6	.008	0.94	0.37–2.39	.879
	> 3	55.7				
WHO grade	Grade 1	76.9	< .001	1.00	-	.001
	Grade 2	65.8		1.24	0.60–2.56	.558
	Grade 3	0		10.74	3.79–30.45	< .001
pT classification	pT1	76.7	.015	1.14	0.39–3.35	.974
	pT2–T4	61.8				
Lymphovascular invasion	Absent	71.5	.002	2.19	1.13–4.23	.020
	Present	54				
Perineural invasion	Absent	71.5	< .001	1.12	0.40–3.16	.813
	Present	41				
Lymph node metastasis	Absent	73	< .001	1.65	0.60–4.55	.341
	Present	27.8				

PR, progesterone receptor; PanNET, pancreatic neuroendocrine tumor; WHO, World Health Organization.

PR immunoreactivity was more commonly associated with malignant behaviors, including metastasis, invasion of surrounding tissues, or larger vessel involvement. Estrella *et al.*²⁸ reviewed 160 PanNET cases and found that loss of PR expression was associated with larger tumor size and advanced American Joint Committee on Cancer tumor staging but was not correlated with age, gender, or WHO grade.

In our present study series, we observed that PanNET patients with PR expression loss had significantly poorer overall and disease-free survival outcomes by univariate but not multivariate analyses. Thus, PR status can provide additional survival information for PanNET patients but cannot be used as a prognostic indicator. Previous studies have also evaluated PanNETs with PR expression and patient survival.^{15,28} Arnason *et al.*¹⁵ reported that pancreas and small intestinal NET patients with intact PR expression had significantly better disease-free survival (median, 155 months) than those with decreased PR expression (median, 38 months). However, they further found that this was only marginally significant when they restricted their examination to only PanNET patients.¹⁵ Estrella *et al.*²⁸ observed no significant differences in overall survival based on PR expression status only. However, when they compared the survival of PanNET patients after combining PTEN and PR expression status, dual PR- and PTEN-negative PanNET patients showed shorter metastasis-free survival than either single PR- or PTEN-positive patients or dual PR- and PTEN-positive patients.²⁸

The biological roles of PR in normal islets and PanNETs have not been completely elucidated. One previous study demonstrated that the administration of progesterone to PR knock-out mice with intact gonads induced β -cell proliferation, which suggests anti-proliferation activity for PR.² PRs exist as two protein isoforms, PRA and PRB.³⁰ Recently, Yazdani *et al.*³¹ demonstrated that PanNET tumorigenesis occurred via activation of PRB after its binding to progesterone, which was induced by the activation of transcription factors FOS and Jun and followed by overexpression of CCND1. They also demonstrated that PRA in the progesterone signaling pathway inhibited PanNET tumorigenesis by suppressing the PRB promoter.³¹

In summary, we performed an immunohistochemical study of PR in 21 surgically resected neuroendocrine microadenomas and 277 PanNETs. Our key findings were loss of PR expression in neuroendocrine microadenomas and in the majority of PanNETs and associated with increased WHO grade, tumor size, and advanced pT and pN classification. The loss of PR expression also correlated with decreased patient survival time according to univariate, but not multivariate, analysis. In conclusion, the loss of

PR expression can provide additional information on shorter disease-free survival outcomes in PanNET patients.

Conflicts of Interest

No potential conflict of interest relevant to this article was reported.

Acknowledgments

This work was supported by the Basic Science Research Program through the National Research Foundation of Korea (NRF) funded by the Ministry of Education, Science and Technology (2016R1A2B4009381) and a grant (2013-554) from the Asan Institute for Life Sciences, Seoul, Republic of Korea.

REFERENCES

1. Bosman FT, Carneiro F, Hruban RH, Theise ND. WHO classification of tumours of the digestive system. 4th ed. Lyon: IARC Press, 2010.
2. Picard F, Wanatabe M, Schoonjans K, Lydon J, O'Malley BW, Auwerx J. Progesterone receptor knockout mice have an improved glucose homeostasis secondary to beta-cell proliferation. *Proc Natl Acad Sci U S A* 2002; 99: 15644-8.
3. Gastrointestinal Pathology Study Group of Korean Society of Pathologists, Cho MY, Kim JM, *et al.* Current trends of the incidence and pathological diagnosis of gastroenteropancreatic neuroendocrine tumors (GEP-NETs) in Korea 2000-2009: multicenter study. *Cancer Res Treat* 2012; 44: 157-65.
4. Bilimoria KY, Talamonti MS, Tomlinson JS, *et al.* Prognostic score predicting survival after resection of pancreatic neuroendocrine tumors: analysis of 3851 patients. *Ann Surg* 2008; 247: 490-500.
5. Fesinmeyer MD, Austin MA, Li CI, De Roos AJ, Bowen DJ. Differences in survival by histologic type of pancreatic cancer. *Cancer Epidemiol Biomarkers Prev* 2005; 14: 1766-73.
6. Halfdanarson TR, Rabe KG, Rubin J, Petersen GM. Pancreatic neuroendocrine tumors (PNETs): incidence, prognosis and recent trend toward improved survival. *Ann Oncol* 2008; 19: 1727-33.
7. Kulke MH, Shah MH, Benson AB 3rd, *et al.* Neuroendocrine tumors, version 1.2015. *J Natl Compr Canc Netw* 2015; 13: 78-108.
8. Amin S, Kim MK. Islet cell tumors of the pancreas. *Gastroenterol Clin North Am* 2016; 45: 83-100.
9. Jiao Y, Shi C, Edil BH, *et al.* DAXX/ATRX, MEN1, and mTOR pathway genes are frequently altered in pancreatic neuroendocrine tumors. *Science* 2011; 331: 1199-203.
10. Heaphy CM, de Wilde RF, Jiao Y, *et al.* Altered telomeres in tumors

- with *ATRX* and *DAXX* mutations. *Science* 2011; 333: 425.
11. Marinoni I, Kurrer AS, Vassella E, *et al.* Loss of *DAXX* and *ATRX* are associated with chromosome instability and reduced survival of patients with pancreatic neuroendocrine tumors. *Gastroenterology* 2014; 146: 453-60.
 12. Kim JY, Brosnan-Cashman JA, An S, *et al.* Alternative lengthening of telomeres in primary pancreatic neuroendocrine tumors is associated with aggressive clinical behavior and poor survival. *Clin Cancer Res* 2017; 23: 1598-606.
 13. Singhi AD, Liu TC, Roncaioli JL, *et al.* Alternative lengthening of telomeres and loss of *DAXX/ATRX* expression predicts metastatic disease and poor survival in patients with pancreatic neuroendocrine Tumors. *Clin Cancer Res* 2017; 23: 600-9.
 14. Kim JY, Kim MS, Kim KS, *et al.* Clinicopathologic and prognostic significance of multiple hormone expression in pancreatic neuroendocrine tumors. *Am J Surg Pathol* 2015; 39: 592-601.
 15. Arnason T, Sapp HL, Barnes PJ, Drewniak M, Abdolell M, Rayson D. Immunohistochemical expression and prognostic value of ER, PR and HER2/neu in pancreatic and small intestinal neuroendocrine tumors. *Neuroendocrinology* 2011; 93: 249-58.
 16. Viale G, Doglioni C, Gambacorta M, Zamboni G, Coggi G, Bordi C. Progesterone receptor immunoreactivity in pancreatic endocrine tumors: an immunocytochemical study of 156 neuroendocrine tumors of the pancreas, gastrointestinal and respiratory tracts, and skin. *Cancer* 1992; 70: 2268-77.
 17. Doglioni C, Gambacorta M, Zamboni G, Coggi G, Viale G. Immunocytochemical localization of progesterone receptors in endocrine cells of the human pancreas. *Am J Pathol* 1990; 137: 999-1005.
 18. Hruban RH, Pitman MB, Klimstra DS. Tumors of the pancreas. Washington, DC: American Registry of Pathology, 2007.
 19. Tang LH, Gonen M, Hedvat C, Modlin IM, Klimstra DS. Objective quantification of the Ki67 proliferative index in neuroendocrine tumors of the gastroenteropancreatic system: a comparison of digital image analysis with manual methods. *Am J Surg Pathol* 2012; 36: 1761-70.
 20. Son EM, Kim JY, An S, *et al.* Clinical and prognostic significances of cytokeratin 19 and KIT expression in surgically resectable pancreatic neuroendocrine tumors. *J Pathol Transl Med* 2015; 49: 30-6.
 21. Roh J, Knight S, Chung JY, *et al.* S100A4 expression is a prognostic indicator in small intestine adenocarcinoma. *J Clin Pathol* 2014; 67: 216-21.
 22. Jang KT, Park SM, Basturk O, *et al.* Clinicopathologic characteristics of 29 invasive carcinomas arising in 178 pancreatic mucinous cystic neoplasms with ovarian-type stroma: implications for management and prognosis. *Am J Surg Pathol* 2015; 39: 179-87.
 23. Anlauf M, Perren A, Klöppel G. Endocrine precursor lesions and microadenomas of the duodenum and pancreas with and without MEN1: criteria, molecular concepts and clinical significance. *Pathobiology* 2007; 74: 279-84.
 24. Anlauf M, Schlenger R, Perren A, *et al.* Microadenomatosis of the endocrine pancreas in patients with and without the multiple endocrine neoplasia type 1 syndrome. *Am J Surg Pathol* 2006; 30: 560-74.
 25. Hackeng WM, Brosens LA, Poruk KE, *et al.* Aberrant Menin expression is an early event in pancreatic neuroendocrine tumorigenesis. *Hum Pathol* 2016; 56: 93-100.
 26. Hadano A, Hirabayashi K, Yamada M, *et al.* Molecular alterations in sporadic pancreatic neuroendocrine microadenomas. *Pancreatol* 2016; 16: 411-5.
 27. de Wilde RF, Heaphy CM, Maitra A, *et al.* Loss of *ATRX* or *DAXX* expression and concomitant acquisition of the alternative lengthening of telomeres phenotype are late events in a small subset of MEN-1 syndrome pancreatic neuroendocrine tumors. *Mod Pathol* 2012; 25: 1033-9.
 28. Estrella JS, Broaddus RR, Mathews A, *et al.* Progesterone receptor and PTEN expression predict survival in patients with low- and intermediate-grade pancreatic neuroendocrine tumors. *Arch Pathol Lab Med* 2014; 138: 1027-36.
 29. Pelosi G, Bresaola E, Bogina G, *et al.* Endocrine tumors of the pancreas: Ki-67 immunoreactivity on paraffin sections is an independent predictor for malignancy: a comparative study with proliferating-cell nuclear antigen and progesterone receptor protein immunostaining, mitotic index, and other clinicopathologic variables. *Hum Pathol* 1996; 27: 1124-34.
 30. Li X, O'Malley BW. Unfolding the action of progesterone receptors. *J Biol Chem* 2003; 278: 39261-4.
 31. Yazdani S, Kasajima A, Ogata H, *et al.* Progesterone receptor isoforms A and B in pancreatic neuroendocrine tumor. *Neuroendocrinology* 2015; 101: 309-20.

HER2 Status and Its Heterogeneity in Gastric Carcinoma of Vietnamese Patient

Dang Anh Thu Phan
Vu Thien Nguyen · Thi Ngoc Ha Hua
Quoc Dat Ngo
Thi Phuong Thao Doan
Sao Trung Nguyen · Anh Tu Thai¹
Van Thanh Nguyen¹

Department of Pathology, University of Medicine and Pharmacy Ho Chi Minh City, Ho Chi Minh City; ¹Department of Pathology, Ho Chi Minh City Oncology Hospital, Ho Chi Minh City, Vietnam

Received: February 22, 2017
Revised: April 14, 2017
Accepted: April 24, 2017

Corresponding Author

Dang Anh Thu Phan, MD, PhD
Department of Pathology, University of Medicine and Pharmacy Ho Chi Minh City, 217 Hong Bang Street, Ward 11, District 5, Ho Chi Minh City, Vietnam
Tel: +84-8-38558411
Fax: +84-8-38552304
E-mail: phandanganhthu@yahoo.com

Background: Human epidermal growth factor receptor 2 (HER2) is related to the pathogenesis and poor outcome of numerous types of carcinomas, including gastric carcinoma. Gastric cancer patients with HER2 positivity have become potential candidates for targeted therapy with trastuzumab. **Methods:** We investigated 208 gastric cancer specimens using immunohistochemistry (IHC), fluorescence *in situ* hybridization and dual *in situ* hybridization (ISH). We also investigated the concordance between IHC and ISH. The correlation between HER2 status and various clinicopathological findings was also investigated. **Results:** In total, 15.9% (33/208) and 24.5% (51/208) of gastric cancers showed *HER2* gene amplification and protein overexpression, respectively. A high level of concordance between ISH and IHC analyses (91.3%, $\kappa=0.76$) was found. A significant correlation between HER2 status and intestinal-type ($p<.05$) and differentiated carcinomas ($p<.05$) was also noted. The HER2 heterogeneity was high in gastric cancers; we found 68.8% phenotypic heterogeneity and 57.6% genotypic heterogeneity. Heterogeneity in HER2 protein expression and gene amplification showed a close association with diffuse histologic type and IHC 2+. **Conclusions:** HER2 protein overexpression and gene amplification were detected in 24.5% and 15.9% of gastric cancer specimens, respectively. Intestinal-type showed a higher level of HER2 protein overexpression and gene amplification than diffuse type. HER2 status also showed a significant relationship with well- and moderately-differentiated carcinomas. The ratio of phenotypic and genotypic heterogeneity of HER2 was high in gastric carcinomas and was associated with HER2 IHC 2+ and diffuse histologic type.

Key Words: Protein HER2; Stomach neoplasms; Protein overexpression; Immunohistochemistry; Gene amplification; Fluorescence *in situ* hybridization; Dual-color silver *in situ* hybridization

According to global cancer statistics from 2012 (GLOBOCAN 2012), gastric cancer remains the fourth most frequent cause of cancer-related mortality in developing countries.¹ In Vietnam, the incidence of gastric cancer has been increasing in recent years and poor outcome was due to delayed diagnosis and advanced stage.

Conventional chemotherapy has not been very beneficial for gastric cancer. Targeted therapeutics, especially human epidermal growth factor receptor 2 (HER2) inhibitors, have recently shown more advantages in treating late-stage gastric cancer.² The Trastuzumab for Gastric Cancer trial has proven the efficacy of humanized monoclonal antibody against HER2 protein, so-called trastuzumab, in the treatment of advanced gastric cancer or gastroesophageal junction cancer with HER2 positivity.³

HER2 is a proto-oncogene encoded by ERBB2 on chromosome 17, also a member of the HER family. The intracellular domain of

HER2, a membrane-bound receptor tyrosine kinase, is responsible for extracellular signal transmission to initiate cellular signaling pathways such as mitogen-activated protein kinase, phosphoinositide 3-kinase, phospholipase C, and protein kinase C, leading to cell proliferation, cell survival, angiogenesis, migration, and invasion.⁴ HER2-positive status (protein overexpression and/or gene amplification) has been identified in several carcinomas, especially in breast cancer, where it has a frequency of 20%–25%, suggesting its prognostic and predictive value in this carcinoma.⁵ On the other hand, in gastric cancer, the reported level of HER2 overexpression and amplification varies widely from 7%–27%,^{6–10} and the prognostic value of HER2 status is not commonly accepted.

This study aimed to detect HER2 status including protein expression and gene amplification, as well as investigate HER2 heterogeneity and the concordance between two methods (immunohistochemistry [IHC] and *in situ* hybridization). We also

investigated the relationship between HER2 status and clinicopathological findings.

MATERIALS AND METHODS

Patients and tissue specimens

For this study, we retrospectively enrolled 208 gastric cancer patients who underwent curative gastrectomy at the University Medical Center, Ho Chi Minh City, Vietnam, from January 2012 to June 2015. No patients had received preoperative radiation or chemotherapy. All surgical specimens were promptly fixed in 10% buffered formalin, no longer than 30 minutes after resection, and for a fixing time of 8–48 hours. Clinicopathological features were recorded including age, sex, histologic type by Lauren, tumor differentiation, depth of invasion, lymph node status, and lymphovascular invasion.

IHC staining

We performed IHC staining for HER2 on the automated slide stainer (BenchMark XT), using monoclonal antibody 4B5 (Ventana Medical System, Tucson, AZ, USA) following the manufacturer's procedures. We incubated 5- μ m slices after antigen retrieval (10 mM citrate buffer at 98°C for 40 minutes) with 4B5 for 30 minutes. Subsequently 3,3'-diaminobenzidine was added for visualization. The sections were stained with hematoxylin for counterstaining and then cover-slipped. Negative controls (omission of primary antibody) and positive controls (gastric cancer tissue with known IHC HER2 3+) were included in each staining run.

Evaluation of IHC results

Slides were scored by a pathologist following the scoring system of Hofmann *et al.*⁶ The generally accepted cut-off definition for HER2 membranous positivity is 10% of the tumor cells. A score of 0 was defined as no reactivity or membrane staining in < 10% of the tumor cells. Faint membrane staining was defined as a score of 1+. Weak-to-moderate complete membrane staining was defined as a score of 2+, and moderate-to-strong complete membrane staining was defined as a score of 3+. Scores of 2+ and 3+ were defined as HER2 protein positive/over-expression. Phenotypic heterogeneity was defined as the proportion of tumor cells showing membranous staining in more than 10%, but less than 50% of tumor cells.

In situ hybridization

We performed *in-situ* hybridization (ISH) for 208 cases of gastric cancer using dual-color silver *in situ* hybridization (SISH) (28

cases randomly selected) and fluorescence in situ hybridization (FISH) (the remaining 180 cases).

Fluorescence *in situ* hybridization

HER2 gene amplification was detected by FISH using a Pathvision HER2 DNA probe kit (Vysis Inc., Downers Grove, IL, USA) according to the manufacturer's instructions. We heated hybridization buffer, DNA probe, and purified water to 73°C for 5 minutes. Slides were dipped in a denaturing bath (70% formamide 2 \times saline-sodium citrate [SSC]) for 5 minutes at 73°C, then dehydrated in increasing ethanol concentrations, and then covered with the probe mixture. We incubated all slides for 30 minutes at 42°C, then washed with 0.4 \times SSC/0.3% NP-40 for 2 minutes, air-dried in darkness, counterstained with 4',6-diamidino-2-phenylindole (DAPI), and lastly covered with a cover-slip. The signals were visualized under fluorescence microscope (BX51, Olympus, Tokyo, Japan) and the images were captured and saved with Spectral Imaging software (Applied Spectral Imaging Inc., Carlsbad, CA, USA). *HER2* gene expression is represented by discrete red signals or signal clusters and Chr17 as green signals.

Dual-color SISH

We performed automated SISH on the Ventana Benchmark XT platform (Ventana Medical Systems Inc.) following the manufacturer's protocols and using the INFORM HER2 DNA and Chromosome 17 probes. HER2 is identified by a dinitrophenyl (DNP) labeled probe and visualized utilizing ultraView SISH DNP Detection Kit. The Chr17 centromere is labeled with a digoxigenin (DIG) probe and detected using ultraView Red ISH DIG Detection Kit (Ventana Medical Systems Inc.). The signals were visualized under light microscopy (BX50, Olympus) in which HER2 expression appeared as discrete black signals (SISH) and Chr17 as red signals. The mean *HER2*/CEP17 ratio was calculated by counting signals in 20 tumor cells under high-power field (\times 600).

Evaluation of FISH and dual SISH results

HER2 gene status was based on the ratio of *HER2* gene copies and Chr17 copies in nuclei of tumor cells. *HER2* gene status was defined as non-amplified if the *HER2*/Chr17 ratio was under 2.0 or amplified if the *HER2*/Chr17 ratio was 2.0 or more. If the *HER2*/CEP17 ratio was 1.8 or more but less than 2.0, 20 more tumor cells were investigated to determine the *HER2* gene status. *HER2* amplification was further sub-classified into low-level amplification (*HER2*/CEP17 ratio 2–5) and high-level amplification

(*HER2*/CEP17 ratio ≥ 5).

Polysomy of chromosome 17 was set as more than 3 CEP17 signals per nuclei. Genotypic heterogeneity was defined by the existence of more than 5% but less than 50% of tumor cells with a *HER2*/CEP17 ratio higher than 2.0.

Statistical analysis

We used SPSS ver. 15.0 statistical software program (SPSS Inc., Chicago, IL, USA) for statistical analyses. The chi-square tests (Kappa chi-square test or chi-square test) were performed to analyze correlations between *HER2* status and clinicopathological features. *p*-values below .05 indicate statistically significant results.

RESULTS

Clinicopathological characteristics of patients

Patient age ranged widely from 30 to 81 years (median, 58.2 years). There was a higher number of male patients (*n* = 139) than female patients (*n* = 69), with a male/female ratio of 2:1. Clinicopathological features are noted in Table 1.

Overexpression of *HER2*

HER2 protein expression in 208 gastric tissue samples was investigated by IHC staining (Fig. 1). Of the 208 gastric carcinoma

Table 1. Clinical and pathologic features of 208 cases of gastric cancer

Parameter	No. (%)
Sex	
Male	139 (66.8)
Female	69 (33.2)
Age	
Range	30–82
Mean \pm standard deviation	58.2 \pm 11.6
Histologic type by Lauren	
Intestinal type	78 (37.5)
Diffuse type	109 (52.4)
Mixed	21 (10.1)
Tumor differentiation	
Differentiated	77 (37.0)
Undifferentiated	131 (63.0)
Depth of invasion (pT stage)	
T1	12 (5.8)
T2	36 (17.3)
T3	10 (4.8)
T4	150 (72.1)
Lymph node status (pN stage)	
N0	87 (41.8)
N1, 2, 3	121 (58.2)
Lymphovascular invasion	57 (27.4)

tissue samples, 148 (71.2%) were scored as 0, 9 (4.3%) scored as 1+, 23 (11.1%) scored as 2+, and 28 (13.4%) scored as 3+. In total, 24.5% were positive (51/208).

HER2 amplification

The amplification rate of the *HER2* gene was 15.9% (33/208) in all gastric carcinoma tissue samples, with 29 cases detected by FISH and four cases detected by dual SISH (Fig. 2). Of amplified cases, 27 cases (81.8%) showed low-level amplification (ratio *HER2*/CEP17, 2 to < 5) and only six cases (18.2%) showed a high ratio *HER2*/CEP17 (> 5). Polysomy of chromosome 17 was not found in any of the tissue samples.

The correlation between IHC and ISH in the surgical specimens is shown in Table 2. A concordance between IHC and ISH results was seen in 190/208 (157 IHC 0/1+ not amplified, 6 IHC 2+ amplified, and 27 IHC 3+ amplified) with a rate of 91.3% ($\kappa = 0.76$). Six out of 23 IHC 2+ cases (26.1%) showed amplification and one out of 28 IHC 3+ cases (3.6%), which showed signet ring cell carcinoma, was not-amplified.

Correlation between clinicopathological findings and *HER2* status

The clinicopathological differences were shown in gastric carcinoma with or without *HER2* protein expression or *HER2* gene amplification. The *HER2* protein expression and *HER2* gene amplification rates were 43.6% (34/78) and 29.5% (23/78) in intestinal type gastric carcinomas ($p < .05$). *HER2* status was also related to good differentiation ($p < .05$). However, no significant correlation was found between *HER2* status and other clinicopathological features including sex and age of the patients, depth of invasion, lymph node status, and lymphovascular invasion (Table 3).

Intratumor heterogeneity of *HER2*

HER2 showed phenotypic heterogeneity (IHC expression) and genotypic heterogeneity (gene amplification) (Fig. 3). Phenotypic heterogeneity was observed in 35 of 51 IHC cases (68.8%), in which 12 cases of 28 IHC 3+ cases (42.9%) and all 23 IHC 2+ cases (100%) demonstrated heterogeneity. Phenotypic heterogeneity of *HER2* expression was higher in the diffuse type than in the intestinal type (75% vs 67.6%). Genotypic heterogeneity was observed in 19 of 33 ISH cases (57.6%). Genotypic heterogeneity was higher in diffuse-type than in intestinal-type cancers (66.7% vs 52.2%).

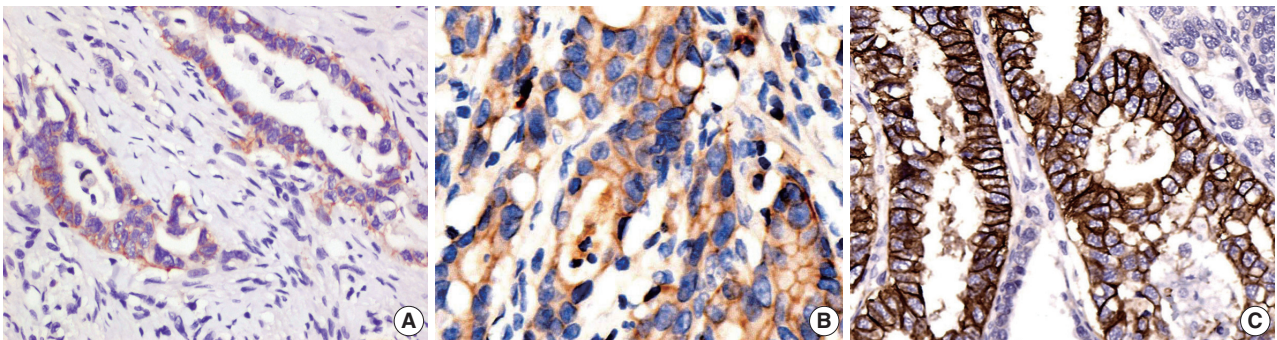


Fig. 1. The human epidermal growth factor receptor 2 (HER2) protein expression detected by immunohistochemistry (IHC). HER2 IHC scores of 1+ (A), 2+ (B), and 3+ (C).

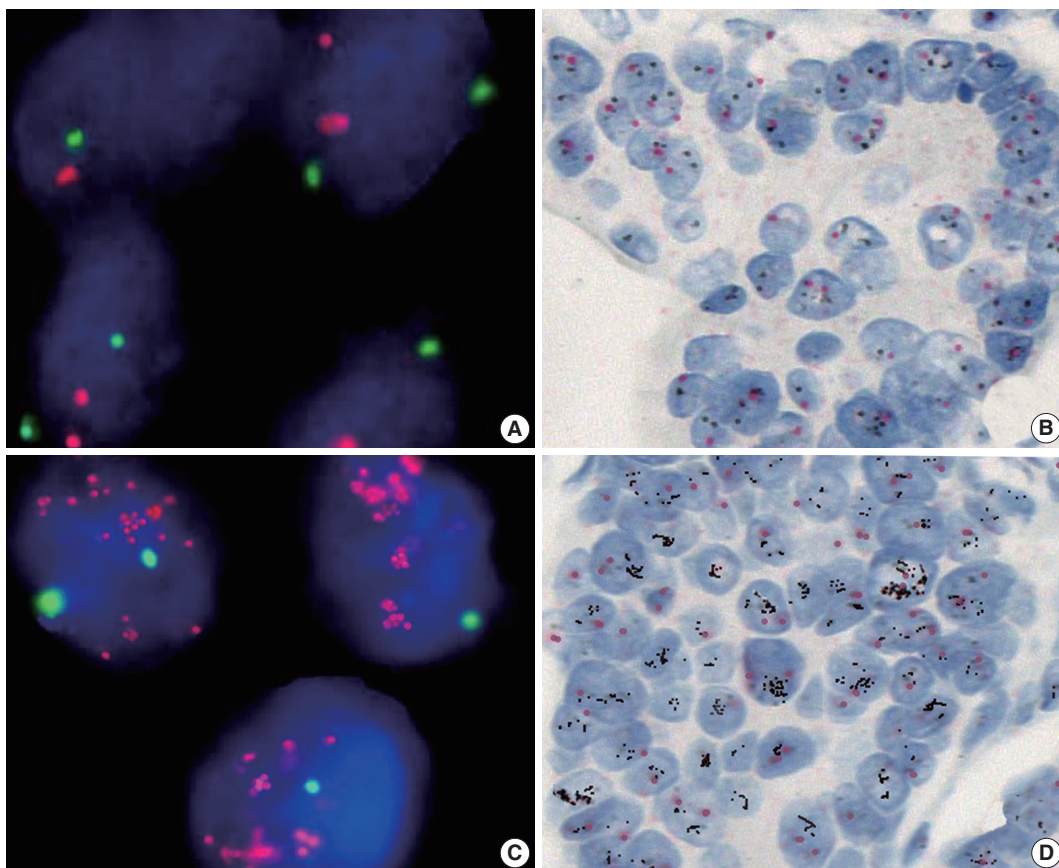


Fig. 2. The human epidermal growth factor receptor 2 (*HER2*) gene status detected by fluorescence *in situ* hybridization (FISH) and dual-color silver *in situ* hybridization (SISH). Representative photomicrographs of FISH (A, C) and dual-color SISH (B, D). Non-amplified cases detected by FISH (A) and dual-color SISH (B). Amplified cases detected by FISH (C) and dual-color SISH (D).

Table 2. Correlation between HER2 protein expression and *HER2* gene amplification

HER2 Dual ISH and FISH	Immunohistochemistry for HER2				Total
	3+ (n=28)	2+ (n=23)	1+ (n=9)	0 (n=148)	
Amplified	27	6	0	0	33
Not-amplified	1	17	9	148	175

HER2, human epidermal growth factor receptor 2; ISH, *in situ* hybridization; FISH, fluorescence *in situ* hybridization.

Table 3. Correlation between clinicopathologic findings and HER2 status

Clinicopathologic data	HER2 (IHC) positive	p-value	HER2 (ISH) amplification	p-value
Sex		NS		NS
Male	37 (26.6)		25 (18.0)	
Female	14 (20.3)		8 (11.6)	
Age (yr)		NS		NS
>60	29 (30.5)		18 (18.9)	
≤60	22 (19.5)		15 (13.3)	
Histologic type		< .05		< .05
Intestinal type	34 (43.6)		23 (29.5)	
Diffuse type	12 (11.0)		6 (5.5)	
Tumor differentiation		< .05		< .05
Grade 1, 2	34 (44.2)		22 (28.6)	
Grade 3, 4	17 (13.0)		11 (8.4)	
Depth of invasion		NS		NS
T1–2	13 (27.1)		8 (16.7)	
T3–4	38 (23.8)		25 (15.6)	
Lymph node metastasis		NS		NS
Negative	21 (24.1)		13 (14.9)	
Positive	30 (24.8)		20 (16.5)	
Lymphovascular invasion		NS		NS
Negative	37 (24.5)		23 (15.2)	
Positive	14 (24.6)		10 (17.5)	

Values are presented as number (%).

HER2, human epidermal growth factor receptor 2; IHC, immunohistochemistry; ISH, *in situ* hybridization; NS, not significant.

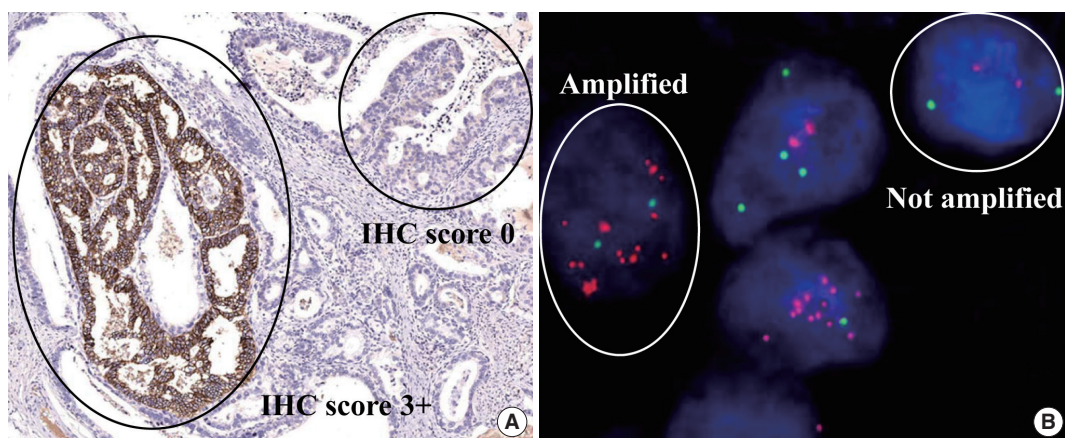


Fig. 3. Intratumoral heterogeneity of human epidermal growth factor receptor 2 (HER2). Heterogeneity of HER2 protein expression (A) and heterogeneity of *HER2* gene amplification (B).

DISCUSSION

We investigated HER2 protein overexpression and gene amplification in 208 surgical tissue samples of gastric carcinoma. HER2 protein positivity and *HER2* gene amplification were observed in 24.5% and 15.9% of cases, respectively. While HER2 protein positivity in gastric carcinoma was reported from 11 to 24%,^{6,8,11–13} *HER2* gene amplification varied from 7% to 27%.^{7–10} This variation was attributed to an inconsistent HER2 IHC scoring system, different methodologies including antibody selec-

tion and/or random selection of patients. Moreover, the interpretation of IHC or ISH can be influenced by subjective factors such as the prompt fixing time after removal, the volume of formalin, and the duration of fixation. In this study, all gastric specimens were fixed no later than 30 minutes after removal in 10% buffered formalin for 8–48 hours.

In our study, we used the HER2 scoring system proposed by Hofmann *et al.*,⁶ showing a high level of concordance (91.3%) between IHC and ISH. A number of studies investigated the relationship between IHC and FISH in gastric cancer specimens

and also reported a high level of concordance that varied from 86.9 to 93.5%.^{3,6} Our study also showed high concordance between IHC and ISH. We did not compare the concordance between dual SISH and FISH in this study. However, some studies have shown a high level of concordance between dual SISH and FISH, which ranged from 94.5% to 98.3%.^{3,9}

In this study, we recognized that one of 28 HER2 IHC 3+ cases showed non-amplification, and it was signet ring cell carcinoma. HER2 status may be found in this rare histologic type of gastric cancer with a very low rate of positivity. The HER2 protein expression in signet ring cell carcinoma may be misinterpreted due to strong nuclear/cytoplasmic staining, which was observed in the IHC staining method. Therefore, ISH confirmation should be considered in signet ring cell carcinoma.

The higher positive rates of HER2 in intestinal-type compared to other types of gastric carcinoma have been widely reported and our results were similar.^{8,11,13-16} It was also reported that HER2 overexpression is related to well-and-moderately differentiated gastric cancer but not with tumor stage or the age and sex of gastric cancer patients.^{13,17,18} On the other hand, the correlation of positive HER2 status with other clinicopathological factors, including age, sex, and TNM stage, remains controversial. It has been reported that a higher frequency of HER2 positivity is significantly correlated with older age, male gender, upper location of tumor, lymphatic or vascular invasion, higher T stage, lymph node metastasis, distant metastasis, and higher TNM stage.^{8,11,15,19-21} In our study, we demonstrated that there was no significant relationship between HER2 status and clinicopathological variables such as sex and age of the patients, depth of invasion, lymph node status and lymphovascular invasion.

Genotypic heterogeneity was defined by College of American Pathologists (CAP) in 2009 for breast cancers, in which the tumor showed at least 5% but fewer than 50% of nuclei with a *HER2/CEP17* ratio ≥ 2.0 .²² The 2013 American Society of Clinical Oncology/CAP HER2 guideline update⁵ recommends using an IHC HER2 test to define areas of potential amplification. In gastric cancer, there are no guidelines for tumor heterogeneity assessment. Yang *et al.*¹⁶ recognized 79.3% of cases with heterogeneous HER2 protein expression and 44.0% of cases with HER2 genetic heterogeneity. Our results also showed that frequency of phenotypic heterogeneity was higher than that of genotypic heterogeneity (68.8% vs 57.6%).

Kim *et al.*¹¹ found that heterogeneity was more prevalent in IHC 2+ cases than IHC 3+ cases (90.9% vs 40.9%). Nishida *et al.*²³ also reported that phenotypic heterogeneity was recognized in 63.5% of IHC 2+ cases, and in only 28.3% in IHC 3+ cases.

Our results are consistent with results from these studies, in which phenotypic heterogeneity and genotypic heterogeneity showed a higher rate in IHC 2+ cases than IHC 3+ cases.

Lee *et al.*²⁴ recognized that diffuse or mixed histological subtypes have a higher rate of heterogeneous HER2 expression. In our study, we also found that the diffuse type showed a higher rate of heterogeneity for HER2 expression or amplification than did the intestinal type. These results may be important for pathologists to consider when predicting HER2 heterogeneity in IHC and ISH results during routine histological examination.

In conclusion, our study demonstrates that HER2 protein expression and gene amplification were recognized in 24.5% and 15.9% of gastric cancer patients, respectively. Intestinal-type disease showed a higher rate of HER2 protein expression and gene amplification than diffuse type. HER2 status also showed a significant relationship with well and moderately differentiated carcinomas. The ratio of phenotypic and genotypic heterogeneity of HER2 was high in gastric carcinoma and related to HER2 IHC 2+ and diffuse histologic type.

Conflicts of Interest

No potential conflict of interest relevant to this article was reported.

Acknowledgments

We would like to give special thanks to Hoffmann La Roche Company and Roche Diagnostics Vietnam for HER2 IHC testing and dual-color SISH support and The Ho Chi Minh City Oncology Hospital, Vietnam, for HER2 FISH testing support.

REFERENCES

1. Ferlay J, Soerjomataram I, Dikshit R, *et al.* Cancer incidence and mortality worldwide: sources, methods and major patterns in GLOBOCAN 2012. *Int J Cancer* 2015; 136: E359-86.
2. Kuo CY, Chao Y, Li CP. Update on treatment of gastric cancer. *J Chin Med Assoc* 2014; 77: 345-53.
3. Bang YJ, Van Cutsem E, Feyereislova A, *et al.* Trastuzumab in combination with chemotherapy versus chemotherapy alone for treatment of HER2-positive advanced gastric or gastro-oesophageal junction cancer (ToGA): a phase 3, open-label, randomised controlled trial. *Lancet* 2010; 376: 687-97.
4. Zaczek A, Brandt B, Bielawski KP. The diverse signaling network of EGFR, HER2, HER3 and HER4 tyrosine kinase receptors and the consequences for therapeutic approaches. *Histol Histopathol* 2005;

- 20: 1005-15.
5. Wolff AC, Hammond ME, Hicks DG, *et al.* Recommendations for human epidermal growth factor receptor 2 testing in breast cancer: American Society of Clinical Oncology/College of American Pathologists clinical practice guideline update. *J Clin Oncol* 2013; 31: 3997-4013.
 6. Hofmann M, Stoss O, Shi D, *et al.* Assessment of a HER2 scoring system for gastric cancer: results from a validation study. *Histopathology* 2008; 52: 797-805.
 7. Takehana T, Kunitomo K, Kono K, *et al.* Status of c-erbB-2 in gastric adenocarcinoma: a comparative study of immunohistochemistry, fluorescence *in situ* hybridization and enzyme-linked immunosorbent assay. *Int J Cancer* 2002; 98: 833-7.
 8. Yan SY, Hu Y, Fan JG, *et al.* Clinicopathologic significance of HER-2/neu protein expression and gene amplification in gastric carcinoma. *World J Gastroenterol* 2011; 17: 1501-6.
 9. Park YS, Hwang HS, Park HJ, *et al.* Comprehensive analysis of HER2 expression and gene amplification in gastric cancers using immunohistochemistry and *in situ* hybridization: which scoring system should we use? *Hum Pathol* 2012; 43: 413-22.
 10. Yano T, Doi T, Ohtsu A, *et al.* Comparison of HER2 gene amplification assessed by fluorescence *in situ* hybridization and HER2 protein expression assessed by immunohistochemistry in gastric cancer. *Oncol Rep* 2006; 15: 65-71.
 11. Kim KC, Koh YW, Chang HM, *et al.* Evaluation of HER2 protein expression in gastric carcinomas: comparative analysis of 1,414 cases of whole-tissue sections and 595 cases of tissue microarrays. *Ann Surg Oncol* 2011; 18: 2833-40.
 12. Park DI, Yun JW, Park JH, *et al.* HER-2/neu amplification is an independent prognostic factor in gastric cancer. *Dig Dis Sci* 2006; 51: 1371-9.
 13. Shan L, Ying J, Lu N. HER2 expression and relevant clinicopathological features in gastric and gastroesophageal junction adenocarcinoma in a Chinese population. *Diagn Pathol* 2013; 8: 76.
 14. Barros-Silva JD, Leitao D, Afonso L, *et al.* Association of *ERBB2* gene status with histopathological parameters and disease-specific survival in gastric carcinoma patients. *Br J Cancer* 2009; 100: 487-93.
 15. Cho J, Jeong J, Sung J, *et al.* A large cohort of consecutive patients confirmed frequent HER2 positivity in gastric carcinomas with advanced stages. *Ann Surg Oncol* 2013; 20 Suppl 3: S477-84.
 16. Yang J, Luo H, Li Y, *et al.* Intratumoral heterogeneity determines discordant results of diagnostic tests for human epidermal growth factor receptor (HER) 2 in gastric cancer specimens. *Cell Biochem Biophys* 2012; 62: 221-8.
 17. Grabsch H, Sivakumar S, Gray S, Gabbert HE, Müller W. HER2 expression in gastric cancer: rare, heterogeneous and of no prognostic value: conclusions from 924 cases of two independent series. *Cell Oncol* 2010; 32: 57-65.
 18. He C, Bian XY, Ni XZ, *et al.* Correlation of human epidermal growth factor receptor 2 expression with clinicopathological characteristics and prognosis in gastric cancer. *World J Gastroenterol* 2013; 19: 2171-8.
 19. Moelans CB, Milne AN, Morsink FH, Offerhaus GJ, van Diest PJ. Low frequency of HER2 amplification and overexpression in early onset gastric cancer. *Cell Oncol (Dordr)* 2011; 34: 89-95.
 20. Zhang XL, Yang YS, Xu DP, *et al.* Comparative study on overexpression of HER2/neu and HER3 in gastric cancer. *World J Surg* 2009; 33: 2112-8.
 21. Yonemura Y, Ninomiya I, Yamaguchi A, *et al.* Evaluation of immunoreactivity for erbB-2 protein as a marker of poor short term prognosis in gastric cancer. *Cancer Res* 1991; 51: 1034-8.
 22. Vance GH, Barry TS, Bloom KJ, *et al.* Genetic heterogeneity in HER2 testing in breast cancer: panel summary and guidelines. *Arch Pathol Lab Med* 2009; 133: 611-2.
 23. Nishida Y, Kuwata T, Nitta H, *et al.* A novel gene-protein assay for evaluating HER2 status in gastric cancer: simultaneous analyses of HER2 protein overexpression and gene amplification reveal intratumoral heterogeneity. *Gastric Cancer* 2015; 18: 458-66.
 24. Lee S, de Boer WB, Fermoye S, Platten M, Kumarasinghe MP. Human epidermal growth factor receptor 2 testing in gastric carcinoma: issues related to heterogeneity in biopsies and resections. *Histopathology* 2011; 59: 832-40.

Prognostic Significance of a Micropapillary Pattern in Pure Mucinous Carcinoma of the Breast: Comparative Analysis with Micropapillary Carcinoma

Hyun-Jung Kim · Kyeongmee Park
Jung Yeon Kim · Guhyun Kang
Geumhee Gwak¹ · Inseok Park¹

Departments of Pathology and ¹Surgery, Inje University Sanggye Paik Hospital, Seoul, Korea

Received: January 15, 2017
Revised: February 27, 2017
Accepted: March 14, 2017

Corresponding Author

Kyeongmee Park, MD, PhD
Department of Pathology, Inje University Sanggye Paik Hospital, 1342 Donggil-ro, Nowon-gu, Seoul 01757, Korea
Tel: +82-2-950-1263
Fax: +82-2-951-6964
E-mail: kpark@paik.ac.kr

Background: Mucinous carcinoma of the breast is an indolent tumors with a favorable prognosis; however, micropapillary features tend to lead to aggressive behavior. Thus, mucinous carcinoma and micropapillary carcinoma exhibit contrasting biologic behaviors. Here, we review invasive mucinous carcinoma with a focus on micropapillary features and correlations with clinicopathological factors. **Methods:** A total of 64 patients with invasive breast cancer with mucinous or micropapillary features were enrolled in the study. Of 36 pure mucinous carcinomas, 17 (47.2%) had micropapillary features and were termed mucinous carcinoma with micropapillary features (MUMPC), and 19 (52.8%) had no micropapillary features and were termed mucinous carcinoma without micropapillary features. MUMPC were compared with 15 invasive micropapillary carcinomas (IMPC) and 13 invasive ductal and micropapillary carcinomas (IDMPC). **Results:** The clinicopathological factors of pure mucinous carcinoma and MUMPC were not significantly different. In contrast to IMPC and IDMPC, MUMPC had a low nuclear grade, lower mitotic rate, higher expression of hormone receptors, negative human epidermal growth factor receptor 2 (HER2) status, lower Ki-67 proliferating index, and less frequent lymph node metastasis ($p < .05$). According to univariate analyses, progesterone receptor, HER2, T-stage, and lymph node metastasis were significant risk factors for overall survival; however, only T-stage remained significant in a multivariate analysis ($p < .05$). **Conclusions:** In contrast to IMPC and IDMPC, the micropapillary pattern in mucinous carcinoma does not contribute to aggressive behavior. However, further analysis of a larger series of patients is required to clarify the prognostic significance of micropapillary patterns in mucinous carcinoma of the breast.

Key Words: Breast; Micropapillary; Mucinous; Prognosis

Mucinous carcinoma of the breast, believed to be an indolent tumor, affects older females. Pure mucinous carcinoma with a > 90% mucinous component has a better prognosis than that of mixed mucinous carcinoma. This carcinoma tends to follow an indolent course with infrequent lymphatic or hematogenic dissemination and to have a favorable prognosis.¹⁻⁴ Invasive micropapillary carcinoma (IMPC) was first reported by Siriaunkgul and Tavassoli⁵ in 1993 as a rare subtype of breast carcinoma. IMPC is characterized by tumor cells arranged in tubules with a small or obliterated lumen, which extensively penetrate the lymphatic or vascular space, leading to a high frequency of lymph node metastasis.⁶⁻¹⁴ In a previous study, axillary lymph node metastases were found in all of 27 patients at the initial diagnosis. Twelve of these patients were followed up, and six died at a mean of 22 months after the initial treatment.¹² It is important for pathologists to identify micropapillary formations, as they indicate the

potential for aggressive tumor behavior and influence the choice of therapy. Thus, the micropapillary and pure mucinous subtypes of invasive carcinoma are opposites in terms of their biological behavior.¹⁵ These two patterns sometimes coexist in the same tumor. Tumor cells in mucinous carcinoma can exhibit different patterns, such as cords, trabeculae, cribriform structures, and solid lobules. Previous studies have suggested that the micropapillary pattern in cases of mucinous carcinoma is associated with aggressive tumor behavior.¹⁶⁻¹⁸ The pathogenetic association of this mucinous micropapillary carcinoma (MUMPC) with pure mucinous carcinoma is unclear.

The aim of this study was to characterize the clinicopathological parameters of MUMPC and to compare them with those of pure mucinous carcinoma, IMPC, and invasive ductal and micropapillary carcinoma (IDMPC). Moreover, the prognostic significance of micropapillary features in breast carcinoma was

determined.

MATERIALS AND METHODS

We analyzed 64 patients diagnosed with MUMPC, IMPC, IDMPC, or mucinous carcinoma without micropapillary features (MUC). These 64 cases were diagnosed and treated for breast carcinoma at Inje University Sanggye Paik Hospital between 1997 and 2012. Only cases with tumors containing a $\geq 90\%$ mucinous component were defined as mucinous carcinoma. Morphologically, micropapillae were defined as clusters of tumor cells separated from surrounding stroma by clear spaces and that exhibited reverse polarity, also known as an “inside-out” growth pattern, whereby the apical pole of the cells faces the stroma rather than the luminal surface.¹⁹ MUMPC was defined as a tumor in which micropapillary features constituted $>50\%$ of the tumor epithelial components (Fig. 1). Patient age, tumor stage by TNM classification,²⁰ lymph node metastasis, nuclear grade, mitotic rate, estrogen receptor (ER) status, progesterone receptor (PR) status, human epidermal growth factor receptor 2 (HER2) status, Ki-67 proliferating index, molecular subtype, and survival were recorded. The following antibodies were used for immunohistochemistry (IHC): ER (SP1, Dako, Carpinteria, CA, USA), PR (SP2, Dako), HER2 (HercepTest, Dako), Ki-67 (MIB-1, Dako), cytokeratin (CK) 5/6 (D5/16, Dako), and epidermal growth factor receptor (EGFR; E30, Dako). Cases were classified as ER-, PR-, and HER2-positive or negative, and the latest American Society of Clinical Oncology guidelines for the detection and scoring of ER, PR, and HER2 were followed.^{21,22} Cases with a HER2 IHC grade of 2+ subsequently underwent evaluation of *HER2* amplification by fluorescence *in situ* hybridization (PathVysion, Abbott, Des Plaines, IL, USA) and were designated as positive or negative. Ki-67 expression was classified as low ($< 14\%$) or high ($\geq 14\%$).²³ Based on the IHC results, molecular subtypes were

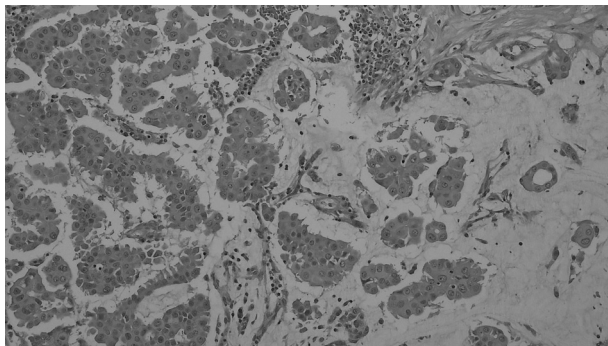


Fig. 1. Micropapillary features were found in more than 50% of the mucinous carcinoma cases.

defined as follow: luminal A (ER⁺ and/or PR⁺, HER2⁻, Ki-67 low), luminal B (ER⁺ and/or PR⁺, HER2⁺/ ER⁺ and/or PR⁺, HER2⁻, Ki-67 high), HER2-positive (ER⁻, PR⁻, HER2⁺), and basal-like (ER⁻, PR⁻, HER2⁻, EGFR⁺ and/or CK5/6⁺).²³ Patients underwent either mastectomy or breast conserving surgery with lymph node dissection. Adjuvant chemotherapy or hormonal therapy was routinely considered. All patients underwent mammography, physical examination, chest X-ray, and breast ultrasonography during follow-up of 6 to 96 months. This study was approved by the Institutional Review Board of our hospital (SGPAIK 2016-04-002).

The following clinical and pathological factors were assessed: age at diagnosis, nuclear grade (a one-level increase on a 1–3 scale), mitotic rate (a one-level increase on a 1–3 scale), ER expression (positive vs negative), PR expression (positive vs negative), HER2 amplification (positive vs negative) and the Ki-67 proliferation index (high vs low). Molecular tumor subtypes were categorized as luminal A, luminal B, basal-like, or HER2 positive. The clinicopathological features of MUC, MUMPC, IMPC, and IDMPC cases were compared. Pearson's chi-square test, Student's t test, and ANOVA were used to evaluate discrete and quantitative variables. Among the clinicopathological variables, the potential risk factors for overall survival (OS) were examined using univariate and multivariate logistic regression analyses. Statistical analyses were performed using IBM SPSS Statistics ver. 20 software (IBM Corp., Armonk, NY, USA). Statistical significance was determined using the likelihood ratio test and accepted at values of $p < .05$.

RESULTS

The 64 cases comprised 19 (29.7%) with MUC, 17 (26.6%) with MUMPC, 15 (23.4%) with IMPC, and 13 (20.3%) with IDMPC. All cases were female and aged 29–79 years (mean, 51.8 ± 12.8 years).

Both MUC and MUMPC showed low nuclear grades and low mitotic rates. In both groups, all tumor cells were positive for ER, irrespective of the presence of micropapillary features. All but one of the MUC cases revealed strong PR expression but no *HER2* amplification. All but one of the MUMPC cases were positive for PR and negative for *HER2* amplification. A high Ki-67 proliferation index was noted in eight cases of MUC (42.1%) and 10 cases of MUMPC (58.8%). Among the MUC and MUMPC cases, 11 (57.9%) and seven cases (41.2%) were luminal A, respectively, and eight (42.1%) and 10 cases (58.8%) were luminal B. Neither the HER2 nor basal-like subtype was detected in MUC or MUMPC. Among the MUC cases, 11 cases (57.5%)

were T1, seven cases (36.8%) were T2, and a case (5.3%) was T3. Among the MUMPC, six cases (35.3%) were T1, seven cases (41.2%) were T2, and four cases (23.5%) were T3. Metastasis to the axillary lymph node was detected in two cases of MUC (10.5%) and four cases of MUMPC (23.5%). The surrounding breast parenchyma showed changes suggestive of ductal carcinoma *in situ* in 13 cases (36.1%), comprising eight cases of MUC and five of MUMPC (Table 1).

Compared with IMPC and IDMPC, nuclear grade and mitotic rate were lower in MUMPC ($p < .01$). MUMPC showed lower frequency of ER and PR negativity ($p = .04$) and HER2 positivity ($p = .01$). The Ki-67 proliferation index of the MUMPC cases was lower than that of the IMPC and IDMPC cases ($p < .01$). Upon comparison of MUC and MUMPC, IMPC and IDMPC revealed less frequent luminal A and more frequent HER2 and basal-like subtypes ($p < .01$). Among the MUMPC cases, six cases (35.3%) were T1, seven cases (41.2%) were T2, and four cases (23.5%) were T3. Among the IMPC and IDMPC cases, six cases (40.0%) and four cases (30.8%) were T1, six cases (40.0%) and seven cases (53.8%) were T2, and three cases (20.0%) and

two cases (15.4%) were T3, respectively. Four of the MUMPC cases (23.5%) exhibited lymph node involvement, while metastasis to the axillary lymph node was detected in 12 (80.0%) and nine (69.2%) cases of IMPC and IDMPC, respectively ($p < .01$) (Table 1). The surrounding breast parenchyma showed changes suggested of ductal carcinoma *in situ* in 19 cases (67.9%), comprising eight cases of IMPC and 11 of IDMPC.

Mean follow-up duration was 83 ± 51 months. Overall, PR and HER2 statuses, T-stage, and lymph node metastasis were correlated with death (Table 2). Univariate analysis using a logistic regression model revealed that OS was significantly associated with PR and HER2 statuses, T-stage, and lymph node metastasis (Table 3). However, on multivariate analysis, only T-stage was significantly associated with OS (Table 3).

DISCUSSION

Pure mucinous carcinoma of the breast has a good prognosis with a low rate of regional lymph node metastasis and excellent survival, in contrast to invasive ductal carcinoma of no special

Table 1. Comparisons of clinicopathological parameters among MUC, MUMPC, IMPC, and IDMPC

Parameter	MUC (n=19)	MUMPC (n=17)	IMPC (n=15)	IDMPC (n=13)	p-value ^a	
Age, mean (yr)	52.7 ± 14.0	53.9 ± 11.8	45.9 ± 11.7	54.3 ± 12.6	.22 ^b	
NG	Low	6 (31.6)	1 (5.9)	0	<.01	
	Intermediate	11 (57.9)	14 (82.4)	4 (26.7)		
	High	2 (10.5)	2 (11.8)	11 (73.3)	9 (69.2)	
Mitosis	Low	16 (84.2)	13 (76.5)	2 (13.3)	2 (15.4)	<.01
	Intermediate	1 (5.3)	4 (23.5)	3 (20.0)	3 (23.1)	
	High	2 (10.5)	0	10 (66.7)	8 (61.5)	
ER	Negative	0	0	5 (33.3)	4 (30.8)	.04
	Positive	19 (100)	17 (100)	10 (66.7)	9 (69.2)	
PR	Negative	1 (5.3)	1 (5.9)	7 (46.7)	5 (38.5)	.04
	Positive	18 (94.7)	16 (94.1)	8 (53.3)	8 (61.5)	
HER2	Negative	18 (94.7)	16 (94.1)	9 (60.0)	8 (61.5)	.01
	Positive	1 (5.3)	1 (5.9)	6 (40.0)	5 (38.5)	
Ki-67	Low	11 (57.9)	7 (41.2)	1 (6.7)	1 (7.7)	<.01
	High	8 (42.1)	10 (58.8)	14 (93.3)	12 (92.3)	
MS	LA	11 (57.9)	6 (35.3)	1 (6.7)	1 (7.7)	<.01
	LB	8 (42.1)	11 (64.7)	9 (60.0)	8 (61.5)	
	HER2	0	0	2 (13.3)	2 (15.4)	
	Basal-like	0	0	3 (20.0)	2 (15.4)	
T-stage	1	11 (57.9)	6 (35.3)	6 (40.0)	4 (30.8)	.62
	2	7 (36.8)	7 (41.2)	6 (40.0)	7 (53.8)	
	3	1 (5.3)	4 (23.5)	3 (20.0)	2 (15.4)	
LNM	Absence	17 (89.5)	13 (76.5)	3 (20.0)	4 (30.8)	<.01
	Presence	2 (10.5)	4 (23.5)	12 (80.0)	9 (69.2)	

Values are presented as number (%).

MUC, mucinous carcinoma without micropapillary feature; MUMPC, mucinous carcinoma with micropapillary feature; IMPC, invasive micropapillary carcinoma; IDMPC, mixed invasive ductal and micropapillary carcinoma; NG, nuclear grade; ER, estrogen receptor; PR, progesterone receptor; HER2, human epidermal growth factor receptor 2; MS, molecular subtype; LA, luminal A; LB, luminal B; LNM, lymph node metastasis.

^aChi-square test; ^bANOVA test.

Table 2. Clinicopathological parameters related to death

Parameter		Alive	Dead	p-value ^a
Age, mean (yr)		51.6±12.3	53.0±16.0	.75 ^b
Category	MUC	19 (100)	0	.20
	MUMPC	14 (82.4)	3 (17.6)	
	IMPC	12 (80.0)	3 (20.0)	
	IDMPC	10 (76.9)	3 (23.1)	
MUC vs MUMPC	MUC	19 (100)	0	.06
	MUMPC	14 (82.4)	3 (17.6)	
NG	Low	7 (100)	0	.34
	Intermediate	29 (87.9)	4 (12.1)	
	High	19 (79.2)	5 (20.8)	
Mitosis	Low	31 (93.9)	2 (6.1)	.14
	Intermediate	8 (72.7)	3 (27.3)	
	High	16 (80.0)	4 (20.0)	
ER	Negative	6 (66.7)	3 (33.3)	.07
	Positive	49 (89.1)	6 (10.9)	
PR	Negative	9 (64.3)	5 (35.7)	.01
	Positive	46 (92.0)	4 (8.0)	
HER2	Negative	47 (92.2)	4 (7.8)	.01
	Positive	8 (61.5)	5 (38.5)	
Ki-67	Low	19 (95.0)	1 (5.0)	.16
	High	36 (81.8)	8 (18.2)	
MS	LA	20 (82.9)	0	.05
	LB	29 (82.9)	6 (17.1)	
	HER2	2 (50.0)	2 (50.0)	
	Basal-like	4 (80.0)	1 (20.0)	
T-stage	1	27 (100)	0	<.01
	2	24 (88.9)	3 (11.1)	
	3	4 (40.0)	6 (60.0)	
LNM	Absence	36 (97.3)	1 (2.7)	<.01
	Presence	19 (70.4)	8 (29.6)	

MUC, mucinous carcinoma without micropapillary feature; MUMPC, mucinous carcinoma with micropapillary feature; IMPC, invasive micropapillary carcinoma; IDMPC, mixed invasive ductal and micropapillary carcinoma; NG, nuclear grade; ER, estrogen receptor; PR, progesterone receptor; HER2, human epidermal growth factor receptor 2; MS, molecular subtype; LA, luminal A; LB, luminal B; LNM, lymph node metastasis.

^aChi-square test; ^bt test (2-tailed).

type.² In this study, pure mucinous carcinoma showed a low rate of nodal involvement (16.7%) and a high rate of OS (91.7%). This indolent behavior is associated with a relatively low level of genomic instability, low proliferative activity, positivity for hormone receptors, and low *HER2* amplification.^{2,24,25} In the present study, pure mucinous carcinoma showed a low nuclear grade, diffuse and strong expression of hormone receptors, and very low expression of *HER2*.

A micropapillary architecture in breast carcinoma has been reported to result in a poor prognosis.^{17,18,26,27} In one study, 86% of mucinous carcinomas had a micropapillary pattern.²⁸ The micropapillary architecture can be ignored in tumors with a large quantity of extracellular mucin as detected by low-power microscopy.¹⁶ A

micropapillary pattern has been identified in pure mucinous carcinoma, although its prognostic significance is unclear. In this study, 17 of 36 cases of mucinous carcinoma (47.2%) had micropapillary features. As reported in a previous study, these micropapillary subtypes of mucinous carcinoma impact patient survival via their propensity for nodal metastases, depending on the amount of mucin within the tumor.^{16,28} The study also demonstrated that even tumors classified as MUMPC can lead to IMPC-type metastasis. Prior studies have reported that mucinous carcinomas result in nonmucinous or ductal metastasis.²⁹ However, the results are conflicting. In the current study, four of 17 MUMPC cases (23.5%) had lymph node metastases of the ductal, micropapillary, or mucinous type. MUC and MUMPC were not significantly influenced by the presence of micropapillary features. It has been demonstrated in both types that abundant extracellular mucin contributes to the slower spread of pure mucinous carcinoma by functioning as a physical barrier between the neoplastic cells and surrounding stroma.^{30,31} This suggests that abundant mucin is a more important prognostic factor than is the presence of micropapillary features. The micropapillary pattern in mucinous carcinoma indicates a possible histogenetic association with IMPC. Indeed, the ability of IMPC to undergo at least partial mucinous differentiation has been reported.^{8,9,14}

We separately reviewed 45 cases of breast carcinoma with micropapillary features, of which 17 cases were MUMPC, 15 IMPC, and 13 IDMPC, and found that nuclear grade; mitotic rate; ER, PR, *HER2*, and *Ki-67* expression; and lymph node status differed significantly among the subtypes ($p < .05$). MUMPC and IMPC have been reported to have similar high nuclear grades, with 70%–80% having florid mitotic activity.^{10,11,18,32-34} This suggests that MUMPC and IMPC are components of the same spectrum; they show similar nuclear grades and vary only in their mucin content. In contrast, compared with patients with IMPC, those with MUMPC have a better prognosis irrespective of tumor stage.¹⁶ In the present study, MUMPC cases had lower and intermediate nuclear grades and a lower mitotic rate than those of IMPC cases. These results indicate that MUMPC exhibits a level of aggressiveness intermediate to those of pure mucinous carcinoma and IMPC.

Previous studies have reported high *HER2* expression and low hormone receptor expression in IMPC of the breast.^{6,15,17,27,32} IMPC has a high propensity for lymph node metastasis and more frequent involvement of the lymph nodes compared with invasive ductal carcinoma.³⁵ In this study, four cases of MUMPC (23.5%) had lymph node metastasis; however, synchronous lymph node metastasis was detected in 12 cases of IMPC (80.0%) and nine

Table 3. Univariate and multivariate analyses of the associations between clinicopathological parameters and overall survival using logistic regression model

Category		Univariate	p-value	Multivariate	p-value
		RR (95% CI)		RR (95% CI)	
Category	MUMPC	1.0	Reference	-	-
	IMPC vs MUMPC	1.2 (0.2–6.9)	.87	-	-
	IDMPC vs MUMPC	1.4 (0.2–8.4)	.71	-	-
NG		2.5 (0.7–8.7)	.15	-	-
Mitosis		1.9 (0.8–4.1)	.13	-	-
ER		0.3 (0.1–1.2)	.09	-	-
PR		0.2 (0.1–0.7)	.02	0.7 (0.1–6.6)	.78
HER2		7.3 (1.6–33.0)	.01	1.1 (0.1–11)	.92
Ki-67		4.2 (0.5–36.0)	.19	-	-
MS	LA	1.0	Reference	-	-
	LB vs LA	0.0	.10	-	-
	HER2 vs LA	4.8 (0.6–41.0)	.15	-	-
	Basal-like vs LA	1.2 (0.1–13.0)	.88	-	-
T-stage		15 (3.2–72.0)	.001	14 (2.1–88)	.006
LNM		15 (1.8–130.0)	.01	9 (0.6–149)	.11

RR, relative risk; 95% CI, 95% confidence interval; MUMPC, mucinous carcinoma with micropapillary feature; IMPC, invasive micropapillary carcinoma; IDMPC, mixed invasive ductal and micropapillary carcinoma; NG, nuclear grade; ER, estrogen receptor; PR, progesterone receptor; HER2, human epidermal growth factor receptor 2; MS, molecular subtype; LA, luminal A; LB, luminal B; LNM, lymph node metastasis.

cases of IDMPC (69.2%). In IMPC, histologic grade, lymphatic vessel density, and lymphocyte infiltration might influence lymph node metastasis.^{9,16,33,35,36} In the present study, MUMPC tumors showed high rates of hormone receptor expression: ER and PR were expressed in 17 (100%) and 16 (94.1%) of 17 cases, respectively; one case (5.9%) was positive for *HER2* amplification. A high rate of hormone receptor expression and a low rate of *HER2* suggested good prognosis. Hsu and Shaw³⁷ reported no *HER2* amplification in mucinous breast cancer, suggesting that *HER2* is rarely involved in its tumorigenesis; low *HER2* amplification might also contribute to a better prognosis of this cancer.

Most cases of IMPC are associated with nodal metastases and a poor prognosis.^{12,13,34,38,39} There were typically multiple metastases, with 51% of cases having three or more positive lymph nodes.^{13,35} The average number of metastatic lymph nodes was shown to be 10.7.³⁸ In addition, lymphatic and vascular invasion has been reported in 33%–67% of cases.^{5,8,12} In this study, 12 of 15 IMPC cases (80.0%) exhibited synchronous axillary lymph node metastasis. Of these 12 cases, multiple lymph node metastases (>4) were noted in five cases (41.7%). The mechanism underlying the high incidence of lymph node metastasis in IMPC is unclear, and the intrinsic subtype is considered an important prognostic factor.^{40,41}

The prognosis of luminal A type breast cancer is markedly superior to that of *HER2*-positive and triple-negative breast cancers. A previous study reported that MUMPC revealed more prevalent luminal B or *HER2* subtypes than MUC.⁴² However, we could not identify the clinical significance of breast carcinoma

molecular subtype since there was no *HER2* positivity in either MUC or MUMPC cases in this study.

In conclusion, our findings suggest heterogeneous biological behavior among tumors with a micropapillary architecture. Morphologically, MUMPC shares features with both mucinous carcinoma and IMPC, which could result in its intermediate clinical behavior. Although IMPC and IDMPC are aggressive tumors, the presence of micropapillary features in MUMPC was not associated with poorer prognosis. It can be postulated that MUMPC has a more favorable prognosis than that of IMPC, and that the micropapillary pattern in mucinous carcinoma does not contribute to its aggressive behavior. However, further analyses involving a larger cohort are required to clarify the pathogenetic relationships among these tumor types. Furthermore, the classical tumor stage was the strongest predictor of prognosis.

Conflicts of Interest

No potential conflict of interest relevant to this article was reported.

Acknowledgments

This work was supported by the 2012 Inje University research grant for Kyeongmee Park.

REFERENCES

1. Barkley CR, Ligibel JA, Wong JS, Lipsitz S, Smith BL, Golshan M. Mucinous breast carcinoma: a large contemporary series. *Am J Surg* 2008; 196: 549-51.
2. Di Saverio S, Gutierrez J, Avisar E. A retrospective review with long term follow up of 11,400 cases of pure mucinous breast carcinoma. *Breast Cancer Res Treat* 2008; 111: 541-7.
3. Diab SG, Clark GM, Osborne CK, Libby A, Allred DC, Elledge RM. Tumor characteristics and clinical outcome of tubular and mucinous breast carcinomas. *J Clin Oncol* 1999; 17: 1442-8.
4. Louwman MW, Vriezen M, van Beek MW, *et al.* Uncommon breast tumors in perspective: incidence, treatment and survival in the Netherlands. *Int J Cancer* 2007; 121: 127-35.
5. Siriaunkgul S, Tavassoli FA. Invasive micropapillary carcinoma of the breast. *Mod Pathol* 1993; 6: 660-2.
6. Pettinato G, Manivel CJ, Panico L, Sparano L, Petrella G. Invasive micropapillary carcinoma of the breast: clinicopathologic study of 62 cases of a poorly recognized variant with highly aggressive behavior. *Am J Clin Pathol* 2004; 121: 857-66.
7. Tavassoli FA, Devilee P. World Health Organization classification of tumours: pathology and genetics of tumours of the breast and female genital organs. Lyon: IARC Press, 2003; 35-6.
8. Walsh MM, Bleiweiss IJ. Invasive micropapillary carcinoma of the breast: eighty cases of an underrecognized entity. *Hum Pathol* 2001; 32: 583-9.
9. Zekioglu O, Erhan Y, Ciris M, Bayramoglu H, Ozdemir N. Invasive micropapillary carcinoma of the breast: high incidence of lymph node metastasis with extranodal extension and its immunohistochemical profile compared with invasive ductal carcinoma. *Histopathology* 2004; 44: 18-23.
10. Paterakos M, Watkin WG, Edgerton SM, Moore DH 2nd, Thor AD. Invasive micropapillary carcinoma of the breast: a prognostic study. *Hum Pathol* 1999; 30: 1459-63.
11. Middleton LP, Tressera F, Sobel ME, *et al.* Infiltrating micropapillary carcinoma of the breast. *Mod Pathol* 1999; 12: 499-504.
12. Luna-Moré S, Gonzalez B, Acedo C, Rodrigo I, Luna C. Invasive micropapillary carcinoma of the breast: a new special type of invasive mammary carcinoma. *Pathol Res Pract* 1994; 190: 668-74.
13. Nassar H, Wallis T, Andea A, Dey J, Adsay V, Visscher D. Clinicopathologic analysis of invasive micropapillary differentiation in breast carcinoma. *Mod Pathol* 2001; 14: 836-41.
14. Luna-Moré S, Casquero S, Pérez-Mellado A, Rius F, Weill B, Gornemann I. Importance of estrogen receptors for the behavior of invasive micropapillary carcinoma of the breast. Review of 68 cases with follow-up of 54. *Pathol Res Pract* 2000; 196: 35-9.
15. Barbashina V, Corben AD, Akram M, Vallejo C, Tan LK. Mucinous micropapillary carcinoma of the breast: an aggressive counterpart to conventional pure mucinous tumors. *Hum Pathol* 2013; 44: 1577-85.
16. Liu F, Yang M, Li Z, *et al.* Invasive micropapillary mucinous carcinoma of the breast is associated with poor prognosis. *Breast Cancer Res Treat* 2015; 151: 443-51.
17. Ng WK. Fine-needle aspiration cytology findings of an uncommon micropapillary variant of pure mucinous carcinoma of the breast: review of patients over an 8-year period. *Cancer* 2002; 96: 280-8.
18. Madur B, Shet T, Chinoy R. Cytologic findings in infiltrating micropapillary carcinoma and mucinous carcinomas with micropapillary pattern. *Acta Cytol* 2007; 51: 25-32.
19. Yang YL, Liu BB, Zhang X, Fu L. Invasive micropapillary carcinoma of the breast: an update. *Arch Pathol Lab Med* 2016; 140: 799-805.
20. Edge SB, Byrd DR, Compton CC, Fritz AG, Greene FL, Trotti A. *AJCC cancer staging manual*. 7th ed. New York: Springer, 2009; 589-628.
21. Hammond ME, Hayes DF, Dowsett M, *et al.* American Society of Clinical Oncology/College of American Pathologists guideline recommendations for immunohistochemical testing of estrogen and progesterone receptors in breast cancer. *Arch Pathol Lab Med* 2010; 134: 907-22.
22. Wolff AC, Hammond ME, Hicks DG, *et al.* Recommendations for human epidermal growth factor receptor 2 testing in breast cancer: American Society of Clinical Oncology/College of American Pathologists clinical practice guideline update. *Arch Pathol Lab Med* 2014; 138: 241-56.
23. Goldhirsch A, Wood WC, Coates AS, *et al.* Strategies for subtypes: dealing with the diversity of breast cancer: highlights of the St. Gallen International Expert Consensus on the Primary Therapy of Early Breast Cancer 2011. *Ann Oncol* 2011; 22: 1736-47.
24. Fujii H, Anbazhagan R, Bornman DM, Garrett ES, Perlman E, Gabrielson E. Mucinous cancers have fewer genomic alterations than more common classes of breast cancer. *Breast Cancer Res Treat* 2002; 76: 255-60.
25. Lacroix-Triki M, Suarez PH, MacKay A, *et al.* Mucinous carcinoma of the breast is genomically distinct from invasive ductal carcinomas of no special type. *J Pathol* 2010; 222: 282-98.
26. Bal A, Joshi K, Sharma SC, Das A, Verma A, Wig JD. Prognostic significance of micropapillary pattern in pure mucinous carcinoma of the breast. *Int J Surg Pathol* 2008; 16: 251-6.
27. Ranade A, Batra R, Sandhu G, Chitale RA, Balderacchi J. Clinicopathological evaluation of 100 cases of mucinous carcinoma of breast with emphasis on axillary staging and special reference to a micropapillary pattern. *J Clin Pathol* 2010; 63: 1043-7.
28. Shet T, Chinoy R. Presence of a micropapillary pattern in mucinous

- carcinomas of the breast and its impact on the clinical behavior. *Breast J* 2008; 14: 412-20.
29. Rasmussen BB, Rose C, Christensen IB. Prognostic factors in primary mucinous breast carcinoma. *Am J Clin Pathol* 1987; 87: 155-60.
 30. Akiyoshi T, Nagaie T, Tokunaga M, *et al.* Invasive micropapillary carcinoma of the breast with minimal regional lymph node metastasis regardless of the huge size: report of a case. *Breast Cancer* 2003; 10: 356-60.
 31. Anan K, Mitsuyama S, Tamae K, *et al.* Pathological features of mucinous carcinoma of the breast are favourable for breast-conserving therapy. *Eur J Surg Oncol* 2001; 27: 459-63.
 32. Kuroda H, Sakamoto G, Ohnisi K, Itoyama S. Clinical and pathological features of invasive micropapillary carcinoma. *Breast Cancer* 2004; 11: 169-74.
 33. Guo X, Chen L, Lang R, Fan Y, Zhang X, Fu L. Invasive micropapillary carcinoma of the breast: association of pathologic features with lymph node metastasis. *Am J Clin Pathol* 2006; 126: 740-6.
 34. Tresserra F, Grases PJ, Fàbregas R, Fernández-Cid A, Dexeus S. Invasive micropapillary carcinoma: distinct features of a poorly recognized variant of breast carcinoma. *Eur J Gynaecol Oncol* 1999; 20: 205-8.
 35. Chen AC, Paulino AC, Schwartz MR, *et al.* Prognostic markers for invasive micropapillary carcinoma of the breast: a population-based analysis. *Clin Breast Cancer* 2013; 13: 133-9.
 36. De la Cruz C, Moriya T, Endoh M, *et al.* Invasive micropapillary carcinoma of the breast: clinicopathological and immunohistochemical study. *Pathol Int* 2004; 54: 90-6.
 37. Hsu YH, Shaw CK. Expression of p53, DCC, and HER-2/neu in mucinous carcinoma of the breast. *Kaohsiung J Med Sci* 2005; 21: 197-202.
 38. Tsumagari K, Sakamoto G, Akiyama F, Kasumi F. The clinicopathological study of invasive micropapillary carcinoma of the breast. *Jpn J Breast Cancer* 2001; 16: 341-8.
 39. Ide Y, Horii R, Osako T, *et al.* Clinicopathological significance of invasive micropapillary carcinoma component in invasive breast carcinoma. *Pathol Int* 2011; 61: 731-6.
 40. Perou CM, Sorlie T, Eisen MB, *et al.* Molecular portraits of human breast tumours. *Nature* 2000; 406: 747-52.
 41. Sorlie T, Perou CM, Tibshirani R, *et al.* Gene expression patterns of breast carcinomas distinguish tumor subclasses with clinical implications. *Proc Natl Acad Sci U S A* 2001; 98: 10869-74.
 42. Min SY, Jung EJ, Seol H, Park IA. Cancer subtypes of breast carcinoma with micropapillary and mucinous component based on immunohistochemical profile. *Korean J Pathol* 2011; 45: 125-31.

The Use of the Bethesda System for Reporting Thyroid Cytopathology in Korea: A Nationwide Multicenter Survey by the Korean Society of Endocrine Pathologists

Mimi Kim · Hyo Jin Park¹ · Hye Sook Min
Hyeong Ju Kwon^{2,3} · Chan Kwon Jung⁴
Seoung Wan Chae⁵ · Hyun Ju Yoo⁶
Yoo Duk Choi⁷ · Mi Ja Lee⁸ · Jeong Ja Kwak⁹
Dong Eun Song¹⁰ · Dong Hoon Kim¹¹
Hye Kyung Lee¹² · Ji Yeon Kim¹³
Sook Hee Hong¹⁴ · Jang Sihm Sohn¹⁵
Hyun Seung Lee¹⁶ · So Yeon Park¹
Soon Won Hong¹⁷ · Mi Kyung Shin¹⁸

Department of Pathology, Seoul National University Hospital, Seoul; ¹Department of Pathology, Seoul National University Bundang Hospital, Seongnam; ²Department of Pathology, Severance Hospital, Yonsei University College of Medicine, Seoul; ³Department of Pathology, Wonju Severance Christian Hospital, Yonsei University Wonju College of Medicine, Wonju; ⁴Department of Hospital Pathology, College of Medicine, The Catholic University of Korea, Seoul; ⁵Department of Pathology, Kangbuk Samsung Hospital, Sungkyunkwan University School of Medicine, Seoul; ⁶Department of Pathology, Thyroid Center, Daerim St. Mary's Hospital, Seoul; ⁷Department of Pathology, Chonnam National University Medical School, Gwangju; ⁸Department of Pathology, Chosun University School of Medicine, Gwangju; ⁹Department of Pathology, Soon Chun Hyang University Hospital, Bucheon; ¹⁰Department of Pathology, Asan Medical Center, University of Ulsan College of Medicine, Seoul; ¹¹Department of Pathology, Hallym University Sacred Heart Hospital, Anyang; ¹²Department of Pathology, Eulji University School of Medicine, Daejeon; ¹³Department of Pathology, Inje University Haeundae Paik Hospital, Busan; ¹⁴Department of Pathology, Seegene Medical Foundation, Busan; ¹⁵Department of Pathology, Konyang University Hospital, Daejeon; ¹⁶Department of Pathology, Yangji General Hospital, Seoul; ¹⁷Department of Pathology, Thyroid Cancer Center, Gangnam Severance Hospital, Yonsei University College of Medicine, Seoul; ¹⁸Department of Pathology, Hallym University Kangnam Sacred Heart Hospital, Seoul, Korea

Received: January 6, 2017

Revised: April 3, 2017

Accepted: April 5, 2017

Corresponding Author

Mi Kyung Shin, MD, PhD
Department of Pathology, Hallym University
Kangnam Sacred Heart Hospital, Hallym University
College of Medicine, 1 Singil-ro, Yeongdeungpo-gu,
Seoul 07441, Korea
Tel: +82-2-2639-5114
Fax: +82-2-2633-7571
E-mail: smk0103@yahoo.co.kr

Hyo Jin Park, MD, PhD
Department of Pathology, Seoul National University
Bundang Hospital, 82 Gumi-ro 173beon-gil,
Bundang-gu, Seongnam 13620, Korea and Sheikh Khalifa
Specialty Hospital, P.O. Box 6365 Ras Al Khaimah, UAE
Tel: +971-7-201-2602
Fax: +82-31-787-4012
E-mail: hjparkmd92@gmail.com

Background: The Bethesda System for Reporting Thyroid Cytopathology (TBSRTC) has standardized the reporting of thyroid cytology specimens. The objective of the current study was to evaluate the nationwide usage of TBSRTC and assess the malignancy rates in each category of TBSRTC in Korea. **Methods:** Questionnaire surveys were used for data collection on the fine needle aspiration (FNA) of thyroid nodules at 74 institutes in 2012. The incidences and follow-up malignancy rates of each category diagnosed from January to December, 2011, in each institute were also collected and analyzed. **Results:** Sixty out of 74 institutes answering the surveys reported the results of thyroid FNA in accordance with TBSRTC. The average malignancy rates for resected cases in 15 institutes were as follows: nondiagnostic, 45.6%; benign, 16.5%; atypical of undetermined significance, 68.8%; suspicious for follicular neoplasm (SFN), 30.2%; suspicious for malignancy, 97.5%; malignancy, 99.7%. **Conclusions:** More than 80% of Korean institutes were using TBSRTC as of 2012. All malignancy rates other than the SFN and malignancy categories were higher than those reported by other countries. Therefore, the guidelines for treating patients with thyroid nodules in Korea should be revisited based on the malignancy rates reported in this study.

Key Words: Thyroid; Biopsy, Fine-needle; Bethesda system; Cytopathology; Korea

The Bethesda System for Reporting Thyroid Cytopathology (TBSRTC) was developed to provide uniform terminology and diagnostic criteria for reporting thyroid fine needle aspiration (FNA) and to relate these cytologic diagnoses to clinical management.¹ TBSRTC describes six categories for the diagnosis and reporting of thyroid FNAs, each with an assigned “risk of malignancy” and associated recommendations for clinical management.¹ Since its implementation, many studies have demonstrated that TBSRTC has improved the quality of reporting by decreasing the number of ambiguous reports, increasing the positive predictive value of malignancy in thyroid glands that are operated, and decreasing the rates of surgery for benign thyroid nodules.²⁻⁵

TBSRTC terminology was incorporated into the 2009 guidelines of the Korean Thyroid Association (KTA) for management of patients with thyroid nodules and thyroid cancer.⁶ Several studies in Korea have demonstrated that TBSRTC well stratifies the malignancy risk by diagnostic categories and provides clinicians with useful information on the management of thyroid nodules.⁷⁻¹⁰ However, a wide variation in the incidence and malignant risk of each diagnostic category (DC; from here on, we will use DC as the abbreviation of diagnostic category), especially of the atypia of undetermined significance/follicular lesion of undetermined significance (AUS/FLUS) categories, has been reported.^{11,12} Moreover, the malignant risk of the categories has been reported to be higher than the implied risk of malignancy in TBSRTC.^{7,9,13-15}

In the current study, we aimed to evaluate the extent of implementation of TBSRTC for reporting thyroid FNAs and its impact on managing patients with thyroid nodules by assessing the incidence and malignancy rate in each category of TBSRTC in Korea.

MATERIALS AND METHODS

Design and data collection

A questionnaire designed by the Endocrine Pathology Study Group of the Korean Society of Pathologists to gather data concerning the extent of implementation of TBSRTC and its impact on clinical practice was mailed to 211 pathology laboratories in the year 2012. Participants were asked questions related to the year of implementation of TBSRTC, number of thyroid aspiration cases in 2010 and 2011, usage of liquid-based cytology, types of liquid-based cytology used, and usage of core needle biopsy. Subsequently, a questionnaire was mailed to 41 institutions that had agreed to provide the statistics of thyroid FNA including the incidence, operation rate and malignancy rate of each diagnostic categories of TBSRTC. All the participants' answers were collated.

Among them, sixteen institutes reported the incidence of each category (unsatisfactory, benign, AUS, follicular neoplasm [FN], suspicious for malignancy [SM], and malignancy) in TBSRTC diagnosed from January to December, 2011. In total, 42,132 cases were analyzed. Follow-up malignancy rates of each category in 15 institutes were also collected and analyzed. Malignancy rate of each category was estimated based on surgically resected specimens. This survey was approved by the Institutional Review Board of Seoul National University Bundang Hospital, waiving the requirement for informed consent (IRB No. B-1212/182-304).

Statistics

The statistical significance of the data was assessed using SPSS ver. 21.0 for Windows (IBM Corp., Armonk, NY, USA). The sensitivity, specificity, positive predictive value, and negative predictive value were calculated in two different settings considering thyroid FNA as a “screening test.” First, we calculated these parameters in malignant thyroid tumors. Surgical specimens which had been cytologically classified in the DC II of TBSRTC and diagnosed histologically as benign were considered to be true-negative samples. Surgical specimens whose cytologic diagnoses were in the remaining diagnostic categories (DC V, DC VI) and histologically proved to be malignant neoplasms were considered to be true-positives. The false-positive category included cases that had been diagnosed as SM or malignant (DC V, DC VI), but later confirmed histologically as benign (normal, non-neoplastic benign lesion, or benign neoplasm). The false-negative cases included those diagnosed as benign on FNA but confirmed as malignant upon surgical excision. In addition, those parameters were calculated for thyroid neoplasms including benign (such as follicular adenoma) and malignant. For this calculation, follow-up surgical specimens diagnosed as non-neoplastic benign disease or normal, which were interpreted as the DC II of TBSRTC, were considered to be true-negative samples, and the remaining diagnostic categories (DC IV, DC V, and DC VI), which proved to be either benign or malignant neoplasms by histologic examination of the surgical specimens, were considered to be true-positive. The false-positive category included cases that were diagnosed as FN, SM, and malignant but later confirmed histologically as benign non-neoplastic or normal. The false-negative cases included those diagnosed as DC II on FNA but confirmed as a true neoplasm upon surgical excision. The DC I and DC III (AUS/FLUS) categories were excluded from the statistical analysis because these diagnoses usually led to a repeat FNA rather than to surgical excision; moreover, these cases could not be categorized as either positive or negative.

RESULTS

General survey questions

Questionnaire surveys were sent out to 77 institutes of pathology with controlled quality authorized by the Korean Cytopathology Conference. Three institutes were excluded because they were sending out their cytology specimens to consultants for the diagnosis, and answers from 74 institutes were included in the assessment. The survey results are summarized in Table 1.

Among the 74 institutes, 60 used TBSRTC for their diagnostic categorization of thyroid FNA at the time of survey. The starting year of using this classification varied from 2008 to 2012. The usage increased particularly from 2010 to 2012, 3 to 5 years after the conference in Bethesda. In Korea, the corresponding guidelines of the KTA for management of patients with thyroid nodules

Table 1. Summary of the survey

	No. of institutions (%)
No. of institutions using TBSRTC	60/74 (81)
The starting year using TBSRTC	60
2008	1
2009	5
2010	17
2011	20
2012	17
Methods of fine needle aspiration	74
Conventional	41
Liquid base	11
Both	22
The starting year using liquid based cytology	33
2000	1
2002	1
2006	1
2007	2
2008	5
2009	5
2010	10
2011	3
2012	3
Others	2
Types of liquid based cytology	33
Thin-prep	16
Sure-path	16
Others	1
Main department performing FNA on patients	74
Radiology	38 (51.4)
Pathology	2 (2.7)
Internal medicine	21 (28.4)
Surgery	12 (16.2)
Thyroid clinician	1 (1.4)

TBSRTC, The Bethesda System for Reporting Thyroid Cytopathology; FNA, fine needle aspiration.

and thyroid cancer were introduced in 2009, which might attribute in the subsequent sharp rise in the usage of TBSRTC.^{6,16} Forty-one out of the 74 institutes used conventional method for FNA, whereas 11 institutes used liquid-based method; the remaining 22 adopted both. Out of the 33 institutes using liquid-based preparation, 10 had started doing so in 2010. Regarding the preparation method for liquid-based FNA, two representative commercial methods, Thin-prep and Sure-path, were predominant: almost every institute chose one or the other method. Core needle biopsy was being done in 21 institutes (27% of the 77). Among them, four institutes (5% of the 77) used both core needle biopsy and FNA as the primary investigation method of thyroid nodules. In thirty-eight institutes (51.4%), FNA was done by radiologists, followed by clinicians of internal medicine, surgeons, pathologists, and thyroid-specialized clinicians.

The survey indicated that the majority of the FNA specimens in Korea (60/74, 81%) were being diagnosed as per TBSRTC as of 2007. Moreover, the preparation method also shifted from conventional to liquid-based, the latter adopted in about 43% (33/77) including the institutes performing both.

Incidence and malignancy rate of each DC of TBSRTC in Korea

Sixteen out of 74 institutes answering the survey reported the results of thyroid FNA by TBSRTC. The mean distribution of six categories from 42,132 cases of 16 institutes was as follows: 11.1% nondiagnostic, 62.3% benign, 9.7% AUS, 0.9% FN, 6.7% SM, and 9.1% malignancy (Table 2). The mean operation rates of each category were as follows: 7.5% nondiagnostic, 2.4% benign, 20.2% AUS, 43.7% FN, 59.9% SM, and 69.2% malignancy (Table 3).

The average of malignancy rates for resected cases of 15 institutes are shown in Table 4: nondiagnostic, 45.6%; benign, 16.5%; AUS, 68.7%; FN, 30.2%; SM, 97.5%; and malignancy, 99.7%. Relatively high malignancy rates were noted in nondiagnostic and benign categories, which might have resulted from false-negative results of clinically suspicious nodules. Overall, the false-positive rate of the SM and malignancy category combined was 1.23%.

Follow-up histologic diagnosis of each categories of TBSRTC

The final histological diagnoses upon resection are listed in Table 5. Each DC is sub-classified according to the recommendation of TBSRTC and follow-up histologic diagnoses are summarized by the sub-classification of each DC.

Of 4,599 cases, 247 were operated in the non-DC (DC I) and

128 cases (51.8%) were revealed as malignant nodules. The malignant cases mainly consisted of papillary thyroid carcinoma (121 cases), followed by five cases of follicular carcinoma, one case of poorly differentiated carcinoma, and one case of lymphoma. The benign category (DC II) had 422 cases of follow-up operation out of 21,399 cases. Among them, 320 (75.8%) were revealed as benign nodules and 102 cases (24.2%) were malignant: 89 papillary thyroid carcinomas, 12 follicular carcinomas, and one medullary carcinoma. Out of the 3,708 AUS-categorized cases, 722 had follow-up surgical resection (Table 3). The 514 cases (71.2%) with malignant histologic diagnoses consisted of 471 cases of papillary carcinoma, 25 cases of follicular carcinoma, 13 of medullary carcinoma, four of Hurthle cell carcinoma, and one of poorly differentiated carcinoma. The remaining 208 (28.8%) cases were proved to be benign lesions. In DC VI (FN), 121 out of 283 cases had surgical resection. Forty-six cases out of 121 cases (38%) were malignant: 23 cases of follicular carcinoma, 20 of papillary carcinoma, and three of Hurthle cell carcinoma. The remaining cases (75 cases, 61.9%) that were proved to be benign included 36 follicular adenomas, 19 nodular hyperplasia, 16 Hurthle cell adenomas, and four lymphocytic

thyroiditis (Table 5). A total of 1,133 cases of DC V were histologically confirmed as benign nodules in 32 cases (2.8 %) and malignancy in 1,101 cases (97.2%): 1,094 cases of papillary carcinoma and seven cases of medullary carcinoma (Table 5). Lastly, DC VI (malignancy) had 2,439 resected cases out of 3,343 FNAs. Overall, the final histologic diagnoses were well correlated with preoperative FNA diagnoses. Out of 2,439 cases, 2,419 (99.6%) with a preoperative diagnosis of papillary carcinoma on FNA sub-classification were proved to be papillary carcinoma upon resection. Only 20 out of 2,439 resected cases were non-papillary thyroid carcinoma lesions including one follicular carcinoma, three medullary carcinomas, two poorly differentiated carcinomas, one undifferentiated carcinoma, one metastatic carcinoma, and 12 various benign lesions (Table 5).

Diagnostic values for TBSRTC in Korea

Through the data obtained by the survey summarized above, sensitivity, specificity, positive predictive value, and negative predictive value were analyzed in two ways. First, we included only those in the benign category (DC II) as negative and malignant

Table 2. The distribution of each diagnostic category of TBSRTC from 16 institutions

	Diagnostic category																Total	Range (%)	Mean ± SD (%)
	1	2	3	4	5	6	7	8	9	10	11	12	13	14	15	16			
UNS/ND	1,040 (14.7)	386 (21.2)	865 (16.6)	199 (10.7)	513 (11.7)	185 (10.0)	285 (7.5)	64 (8.0)	315 (17.2)	400 (13.1)	154 (6.8)	208 (10.4)	522 (16.9)	39 (6.4)	7 (0.9)	97 (5.8)	5,279 (12.5)	0.9–21.2	11.1 ± 5.3
Benign	3,397 (47.9)	1,045 (57.4)	2,791 (53.5)	978 (52.5)	2,825 (64.6)	1,099 (59.7)	2,611 (68.5)	409 (50.9)	1,087 (56.3)	2,218 (72.7)	1,904 (83.9)	1,512 (75.2)	1,290 (41.7)	441 (72.4)	615 (78.2)	1,014 (60.8)	25,236 (59.9)	41.7–83.9	62.3 ± 12.0
AUS	893 (12.9)	190 (10.4)	360 (6.9)	369 (19.8)	275 (6.3)	159 (8.6)	367 (9.6)	117 (14.6)	188 (10.3)	248 (8.1)	87 (3.8)	81 (4.0)	551 (17.8)	55 (9.0)	43 (5.5)	117 (7.0)	4,100 (9.7)	3.8–19.8	9.7 ± 4.6
FN/SFN	55 (0.7)	5 (0.3)	38 (0.7)	28 (1.5)	93 (2.1)	8 (0.4)	14 (0.4)	5 (0.6)	55 (3.0)	11 (0.4)	0 (0)	4 (0.2)	49 (1.6)	1 (0.2)	10 (1.3)	17 (1.0)	393 (0.9)	0–2.1	0.9 ± 0.8
SFM	1,178 (16.6)	63 (3.5)	269 (5.2)	54 (2.9)	124 (2.8)	122 (6.6)	204 (5.4)	74 (9.2)	87 (4.7)	100 (3.3)	46 (2.0)	183 (9.1)	193 (6.2)	68 (11.2)	48 (6.1)	219 (13.1)	3,032 (7.2)	2.0–16.6	6.7 ± 4.1
Malignant	521 (7.4)	133 (7.3)	889 (17.1)	236 (12.7)	546 (12.5)	269 (14.6)	329 (8.6)	135 (16.8)	102 (5.6)	73 (2.4)	79 (3.5)	22 (1.1)	486 (15.7)	5 (0.8)	63 (8.0)	204 (12.2)	4,092 (9.7)	0.8–17.1	9.1 ± 5.5
Total	7,084	1,822	5,212	1,864	4,376	1,842	3,810	804	1,834	3,050	2,270	2,010	3,091	609	786	1,668	42,132		

Values are presented as number (%).

TBSRTC, The Bethesda System for Reporting Thyroid Cytopathology; SD, standard deviation; UNS, unsatisfactory; ND, non-diagnostic; AUS, atypia of undetermined significance; FN, follicular neoplasm; SFN, suspicious for follicular neoplasm; SFM, suspicious for malignancy.

Table 3. Operation rate by each diagnostic category of TBSRTC

	Diagnostic category															Range (%)	Mean ± SD (%)
	1	2	3	4	6	7	8	9	10	11	12	13	14	15			
UNS/ND	1.6	6.5	10.2	2.5	3.2	5.3	42.2	1.9	0.5	3.9	2.9	10.2	0	14.3	0–42.2	7.5 ± 10.8	
Benign	0.9	1.8	4.3	1.1	1.8	1.4	11.7	1.8	0.1	1.5	3	1.6	1.1	2.4	0.1–11.7	2.4 ± 2.8	
AUS	10.5	23.2	28.1	9.5	16.4	38.7	23.9	16.5	13.3	13.8	25.9	24.5	5.5	32.6	5.5–38.7	20.2 ± 9.5	
FN/SFN	45.5	60	71.1	32.1	37.5	35.7	100.0	29.1	54.5		50	42.9	0	10	0–100	43.7 ± 25.6	
SFM	9.9	63.5	82.5	90.7	63.9	74	75.7	46	75	23.9	59	67.9	25	81.3	9.9–90.7	59.9 ± 24.6	
Malignant	52.2	72.9	86.5	69.5	73.2	73.3	90.4	54.9	80.8	39.2	68.2	72.8	40	95.2	40–95.2	69.2 ± 17.2	

Values are presented as percentage.

TBSRTC, The Bethesda System for Reporting Thyroid Cytopathology; SD, standard deviation; UNS, unsatisfactory; ND, non-diagnostic; AUS, atypia of undetermined significance; FN, follicular neoplasm; SFN, suspicious for follicular neoplasm; SFM, suspicious for malignancy.

categories (DC V and VI) as positive. In this analysis, the sensitivity, specificity, positive predictive value and negative predictive value for malignant thyroid tumors were 97.19%, 87.91%, 98.76%, and 75.83%, respectively. Second, we included FN (DC

IV) cases as positive and calculated each parameter for the neoplasm including both benign and malignant. In this case, the sensitivity, specificity, positive predictive value, and negative predictive value for neoplasm of thyroid were 97.14%, 72.89%,

Table 4. The malignancy rate by each diagnostic category of TBSRTC

	Diagnostic category															Range (%)	Mean ± SD (%)
	1	2	3	4	6	7	8	9	10	11	12	13	14	15			
UNS/ND	12/17 (70.6)	13/25 (52)	51/88 (58)	4/5 (80)	4/6 (66.7)	10/15 (66.7)	4/27 (14.8)	0/6 (0)	0/2 (0)	2/6 (33.3)	0/6 (0)	27/43 (62.8)	NE ^a	1/1 (100)	0–100	46.5 ± 33.5	
Benign	10/32 (31.3)	2/19 (10.5)	43/119 (36.1)	2/11 (18.2)	1/20 (5)	12/37 (32.4)	5/48 (10.4)	3/20 (15)	0/2 (0)	8/28 (28.6)	14/46 (30.4)	0/20 (0)	0/5 (0)	2/15 (13.3)	0–36.1	16.5 ± 13.1	
AUS	53/94 (56.4)	33/44 (75)	80/101 (79.2)	28/35 (80)	12/26 (46.2)	123/142 (86.6)	14/28 (50)	19/31 (61.3)	28/33 (84.8)	5/12 (41.7)	18/21 (85.7)	87/138 (63.0)	2/3 (66.7)	12/14 (85.7)	41.7–86.6	68.7 ± 15.8	
FN/SFN	16/25 (64)	1/3 (33.3)	12/27 (44.4)	5/9 (55.6)	0/3 (0)	0/5 (0)	0/5 (0)	8/16 (50)	0/6 (0)	NE ^a	0/2 (0)	3/19 (15.8)	NE ^a	1/1 (100)	0–100	30.2 ± 33.1	
SFM	115/117 (98.3)	40/40 (100)	213/222 (95.9)	49/49 (100)	72/78 (92.3)	148/151 (98)	47/56 (83.9)	40/40 (100)	74/75 (98.7)	11/11 (100)	106/108 (98.1)	131/131 (100)	17/17 (100)	39/39 (100)	83.9–100	97.5 ± 4.5	
Malignant	271/272 (99.6)	97/97 (100)	760/769 (98.8)	164/164 (100)	197/197 (100)	241/241 (100)	120/122 (98.4)	56/56 (100)	59/59 (100)	31/31 (100)	15/15 (100)	354/354 (100)	2/2 (100)	60/60 (100)	98.4–100	99.7 ± 0.5	

Values are presented as number (mal/op) (%).

TBSRTC, The Bethesda System for Reporting Thyroid Cytopathology; SD, standard deviation; UNS, unsatisfactory; ND, non-diagnostic; AUS, atypia of undetermined significance; FN, follicular neoplasm; SFN, suspicious for follicular neoplasm; SFM, suspicious for malignancy.

^aNot evaluated due to no case of operation.

Table 5. Follow up surgical diagnosis by each DC of TBSRTC

DC		No. of FNA	No. of operation	Surgical diagnosis															
				PTC	FTC	HTC	MTC	PDC	UC	SCC	MC	Lym	FA	HA	NH	LT	GT	O	
I	Cyst	796	35	7	1	-	-	-	-	-	-	-	1	3	-	22	-	-	1
	Acellular	3,803	212	114	4	-	-	1	-	-	-	-	-	17	1	64	5	1	5
	Total	4,599	247	121	5	-	-	1	-	-	-	-	1	20	1	86	5	1	6
II	Be	19,179	375	73	11	-	1	-	-	-	-	-	-	34	2	240	7	-	7
	LT	1,148	25	9	-	-	-	-	-	-	-	-	-	-	-	-	16	-	-
	GT	49	0	-	-	-	-	-	-	-	-	-	-	-	-	-	-	-	-
	O	1,023	22	7	1	-	-	-	-	-	-	-	-	4	-	9	1	-	-
	Total	21,399	422	89	12	-	1	-	-	-	-	-	-	38	2	249	24	-	7
III	AUS	3,708	722	471	25	4	13	1	-	-	-	-	52	13	124	11	1	7	
IV	FN	283	121	20	23	3	-	-	-	-	-	-	36	16	19	4	-	-	
V	PTC	1,715	1,123	1,093	-	-	-	-	-	-	-	-	1	-	19	10	-	-	
	MTC	11	8	-	-	-	7	-	-	-	-	-	-	-	-	-	1	-	
	MC	2	0	-	-	-	-	-	-	-	-	-	-	-	-	-	-	-	
	Lym	1	0	-	-	-	-	-	-	-	-	-	-	-	-	-	-	-	
	O	12	2	1	-	-	-	-	-	-	-	-	-	-	-	-	-	1	
	Total	1,741	1,133	1,094	-	-	7	-	-	-	-	-	-	1	-	19	10	2	
VI	PTC	3,313	2,429	2,419	1	-	-	1	-	-	-	-	-	-	4	4	-	-	
	PDC	2	2	-	-	-	-	1	-	-	-	-	-	-	1	-	-	-	
	MTC	5	3	-	-	-	3	-	-	-	-	-	-	-	-	-	-	-	
	UC	5	1	-	-	-	-	-	1	-	-	-	-	-	-	-	-	-	
	SCC	1	0	-	-	-	-	-	-	-	-	-	-	-	-	-	-	-	
	MC	8	3	-	-	-	-	-	-	-	1	-	-	-	-	-	-	2	
	Lym	2	0	-	-	-	-	-	-	-	-	-	-	-	-	-	-	-	
	O	7	1	-	-	-	-	-	-	-	-	-	-	-	-	-	-	1	
	Total	3,343	2,439	2,419	1	-	3	2	1	-	1	-	-	-	1	4	4	-	3

DC, diagnostic category; TBSRTC, The Bethesda System for Reporting Thyroid Cytopathology; PTC, papillary thyroid carcinoma; FTC, follicular thyroid carcinoma; HTC, Hurthle cell thyroid carcinoma; MTC, medullary thyroid carcinoma; UC, undifferentiated carcinoma; SCC, squamous cell carcinoma; MC, metastatic carcinoma; Lym, lymphoma; FA, follicular adenoma; HA, Hurthle cell adenoma; NH, nodular hyperplasia; LT, lymphocytic thyroiditis; GT, granulomatous thyroiditis; O, others; Be, benign; AUS, atypia of undetermined significance; FN, follicular neoplasm; PDC, poorly differentiated carcinoma.

96.78%, and 75.83%, respectively.

DISCUSSION

TBSRTC was proposed in October 2007 in Bethesda, Maryland, and published in 2009,¹ TBSRTC was then immediately introduced in the 2009 guidelines of the KTA.^{6,16} Despite the information about TBSRTC having been globally disseminated, the status of its usage in clinical practice in Korea has been unknown. This questionnaire provides a cross-sectional view, based on the collective data from participating pathology laboratories, of the degree of implementation of TBSRTC in Korea and evaluates its impact on daily practice by assessing the incidence and malignant risk of each DC at each pathology laboratory using TBSRTC.

Overall, the data shows that TBSRTC is well implemented in Korea. As of July 2012 (when the questionnaire was mailed), 81% (60 out of 74) of the participating pathology laboratories were already using TBSRTC, which is higher than the rate given in published data from the College of American Pathologists.¹⁷ In addition, the data demonstrates interesting technical points. Fifty-seven percent of the laboratories are using conventional alcohol-fixed direct smears as a preparatory method for thyroid FNA; in contrast, 14.9% of the laboratories are using liquid-based cytology and 29.7% are using both. Overall, 44.6% of the laboratories are using liquid based cytology. Twenty-one out of 74 pathology laboratories (27%) received thyroid core needle biopsies; among them, four institutes used both core needle biopsy and FNA as the primary diagnostic test for thyroid nodules. Although core needle biopsy of thyroid nodules is emerging as an effective alternative method, the primary use of core needle biopsy in a thyroid nodule is quite unusual. For example, current American Thyroid Association thyroid nodule management guidelines and the Society of Radiologists in Ultrasound Consensus Statement have not included core biopsy as an evaluation tool of thyroid nodule, and some other studies suggest that after several non-diagnostic FNA, surgical excision should be considered appropriate.^{18,19}

More importantly, our data showed some differences in the incidence and malignant risk of certain categories between TBSRTC1 or published studies from other countries^{7,12} and the current results. As shown in Table 2, lower incidence of DC IV (0.9 ± 0.8%) and higher incidence of DC III (9.7 ± 4.6%), DC V (6.7 ± 4.1%), and DC VI (9.1 ± 5.5%) were demonstrated. Moreover, the malignancy rates of DC I, II, III, and V (mean of malignancy rates: 46.5 ± 33.5, 16.5 ± 13.1, 68.7 ± 15.8, and 97.5 ± 4.5, re-

spectively) in our study were higher than the risk of malignancy indicated by the original TBSRTC (1%–4%, DC I; 0%–3%, DC II; 5%–15%, DC III, and 60%–75%, DC V)¹ and other previous studies.^{11,18-24} However, these findings are consistently shown in previous reports from Korea.^{8,9} These can be explained by several reasons. First, in Korea, the prevalence of papillary thyroid carcinoma is more than 95%, whereas that of follicular carcinoma is very low, at 3.2%,⁶ which has resulted in the lower incidence of DC IV and higher incidence of DC III, V, and VI. In addition, higher prevalence of papillary thyroid carcinoma might influence higher malignant rates of DC II, DC III, and DC V. Second, most institutes submitting their details of TBSRTC are university-based tertiary centers. In tertiary referral institutes, the patients who had been diagnosed with suspicious or malignant nodules at primary care centers were more likely to receive an operation despite a DC III or DC V diagnosis of FNA, especially those whose imaging studies strongly suggest malignancy. In the present study, malignancy rates were calculated based on the resected cases. The malignancy rate assessed either in the total fine needle aspiration cytology cases or in the resected cases cannot be said to represent the exact malignancy rate of each DC of TBSRTC. The former can miss unresected malignant tumors, and the latter can be exaggerated by selection bias, which may occur in this type of retrospective study. Therefore, our malignancy rates cannot be directly compared with the malignant risk recommended in TBSRTC. Lastly, because Korean citizens tend to consider false-positive results more significantly than false-negative results, cytopathologists in Korea may have a tendency to under-diagnose FNA of thyroid nodules.¹⁰

There are some limitations in the data derived from this questionnaire, especially those evaluating the incidence and malignancy rate of each DC in TBSRTC, as mentioned above. First, 14 out of 16 institutes submitting the incidence and malignancy rate of TBSRTC are university-based centers. Therefore, the results of this survey may not be truly representative of all kinds of practices; from community to academic. Second, all data are self-reported and not verified. Third, the data might not reflect the current status in certain aspects because the questionnaire was mailed in July 2012. The implementation of TBSRTC is more widespread in Korea at present, and liquid-based cytology and core needle biopsy are likely to have been adopted more widely. The usage of core needle biopsy in thyroid nodules has been actively studied in Korea.²⁵

In conclusion, overall, TBSRTC has been well adopted in Korea, with more than 80% of institutes using TBSRTC as of 2012. However, ongoing education is still necessary to reduce

the variation of incidence and malignant rates of TBSRTC. Moreover, it would be better to modify reference values of malignancy rate of each category of TBSRTC and revisit the guidelines for treating patients with thyroid nodules in Korea based on the results of this study. Finally, it is highly recommended that each institute review their report of thyroid aspiration and have their own incidence and malignant rates for each DC.

Conflicts of Interest

No potential conflict of interest relevant to this article was reported.

Acknowledgments

This research was supported by The Korean Society for Cytopathologists Grant No. 2012-01.

REFERENCES

- Cibas ES, Ali SZ; NCI Thyroid FNA State of the Science Conference. The Bethesda System For Reporting Thyroid Cytopathology. *Am J Clin Pathol* 2009; 132: 658-65.
- Bongiovanni M, Krane JF, Cibas ES, Faquin WC. The atypical thyroid fine-needle aspiration: past, present, and future. *Cancer Cytopathol* 2012; 120: 73-86.
- Crowe A, Linder A, Hameed O, *et al.* The impact of implementation of the Bethesda System for Reporting Thyroid Cytopathology on the quality of reporting, "risk" of malignancy, surgical rate, and rate of frozen sections requested for thyroid lesions. *Cancer Cytopathol* 2011; 119: 315-21.
- Ozlu Y, Pehlivan E, Gulluoglu MG, *et al.* The use of the Bethesda terminology in thyroid fine-needle aspiration results in a lower rate of surgery for nonmalignant nodules: a report from a reference center in Turkey. *Int J Surg Pathol* 2011; 19: 761-71.
- Horne MJ, Chheng DC, Theoharis C, *et al.* Thyroid follicular lesion of undetermined significance: Evaluation of the risk of malignancy using the two-tier sub-classification. *Diagn Cytopathol* 2012; 40: 410-5.
- Yi KH, Park YJ, Koong SS, *et al.* Revised Korean Thyroid Association management guidelines for patients with thyroid nodules and thyroid cancer. *Endocrinol Metab* 2010; 25: 270-97.
- Kim SK, Hwang TS, Yoo YB, *et al.* Surgical results of thyroid nodules according to a management guideline based on the *BRAF* (V600E) mutation status. *J Clin Endocrinol Metab* 2011; 96: 658-64.
- Lee YB, Cho YY, Jang JY, *et al.* Current status and diagnostic values of the Bethesda system for reporting thyroid cytopathology in a papillary thyroid carcinoma-prevalent area. *Head Neck* 2017; 39: 269-74.
- Park JH, Yoon SO, Son EJ, Kim HM, Nahm JH, Hong S. Incidence and malignancy rates of diagnoses in the Bethesda system for reporting thyroid aspiration cytology: an institutional experience. *Korean J Pathol* 2014; 48: 133-9.
- Lee K, Jung CK, Lee KY, Bae JS, Lim DJ, Jung SL. Application of Bethesda system for reporting thyroid aspiration cytology. *Korean J Pathol* 2010; 44: 521-7.
- Bongiovanni M, Spitale A, Faquin WC, Mazzucchelli L, Baloch ZW. The Bethesda System for Reporting Thyroid Cytopathology: a meta-analysis. *Acta Cytol* 2012; 56: 333-9.
- Ohuri NP, Schoedel KE. Variability in the atypia of undetermined significance/follicular lesion of undetermined significance diagnosis in the Bethesda System for Reporting Thyroid Cytopathology: sources and recommendations. *Acta Cytol* 2011; 55: 492-8.
- Mathur A, Najafian A, Schneider EB, Zeiger MA, Olson MT. Malignancy risk and reproducibility associated with atypia of undetermined significance on thyroid cytology. *Surgery* 2014; 156: 1471-6.
- Ho AS, Sarti EE, Jain KS, *et al.* Malignancy rate in thyroid nodules classified as Bethesda category III (AUS/FLUS). *Thyroid* 2014; 24: 832-9.
- VanderLaan PA, Marqusee E, Krane JF. Clinical outcome for atypia of undetermined significance in thyroid fine-needle aspirations: should repeated fna be the preferred initial approach? *Am J Clin Pathol* 2011; 135: 770-5.
- Yi KH, Park YJ, Koong SS, *et al.* Revised Korean Thyroid Association Management Guidelines for patients with thyroid nodules and thyroid cancer. *Korean J Otorhinolaryngol-Head Neck Surg* 2011; 54: 8-36.
- Auger M, Nayar R, Khalbuss WE, *et al.* Implementation of the Bethesda System for Reporting Thyroid Cytopathology: observations from the 2011 thyroid supplemental questionnaire of the College of American Pathologists. *Arch Pathol Lab Med* 2013; 137: 1555-9.
- Haugen BR, Alexander EK, Bible KC, *et al.* 2015 American Thyroid Association management guidelines for adult patients with thyroid nodules and differentiated thyroid cancer: The American Thyroid Association Guidelines Task Force on Thyroid Nodules and Differentiated Thyroid Cancer. *Thyroid* 2016; 26: 1-133.
- Samir AE, Vij A, Seale MK, *et al.* Ultrasound-guided percutaneous thyroid nodule core biopsy: clinical utility in patients with prior nondiagnostic fine-needle aspirate. *Thyroid* 2012; 22: 461-7.
- Yang J, Schnadig V, Logrono R, Wasserman PG. Fine-needle aspiration of thyroid nodules: a study of 4703 patients with histologic and clinical correlations. *Cancer* 2007; 111: 306-15.
- Yassa L, Cibas ES, Benson CB, *et al.* Long-term assessment of a mul-

- tidisciplinary approach to thyroid nodule diagnostic evaluation. *Cancer* 2007; 111: 508-16.
22. Mufti ST, Molah R. The Bethesda system for reporting thyroid cytopathology: a five-year retrospective review of one center experience. *Int J Health Sci (Qassim)* 2012; 6: 159-73.
 23. Baloch ZW, Hendreen S, Gupta PK, *et al.* Interinstitutional review of thyroid fine-needle aspirations: impact on clinical management of thyroid nodules. *Diagn Cytopathol* 2001; 25: 231-4.
 24. Wu HH, Rose C, Elsheikh TM. The Bethesda system for reporting thyroid cytopathology: An experience of 1,382 cases in a community practice setting with the implication for risk of neoplasm and risk of malignancy. *Diagn Cytopathol* 2012; 40: 399-403.
 25. Yi KS, Kim JH, Na DG, *et al.* Usefulness of core needle biopsy for thyroid nodules with macrocalcifications: comparison with fine-needle aspiration. *Thyroid* 2015; 25: 657-64.

Metaplastic Carcinoma with Chondroid Differentiation Arising in Microglandular Adenosis

Ga-Eon Kim · Nah Ihm Kim
Ji Shin Lee · Min Ho Park¹

Departments of Pathology and ¹Surgery,
Chonnam National University Medical School,
Gwangju, Korea

Received: August 3, 2016
Revised: October 3, 2016
Accepted: October 5, 2016

Corresponding Author

Ji Shin Lee, MD
Department of Pathology, Chonnam National
University Hwasun Hospital, 322 Seoyang-ro,
Hwasun 58128, Korea
Tel: +82-61-379-7072
Fax: +82-61-379-7079
E-mail: jshinlee@hanmail.net

Microglandular adenosis (MGA) of the breast is a rare, benign proliferative lesion but with a significant rate of associated carcinoma. Herein, we report an unusual case of metaplastic carcinoma with chondroid differentiation associated with typical MGA. Histologically, MGA showed a direct transition to metaplastic carcinoma without an intervening atypical MGA or ductal carcinoma *in situ* component. The immunohistochemical profile of the metaplastic carcinoma was mostly similar to that of MGA. In both areas, all the epithelial cells were positive for S-100 protein, but negative for estrogen receptor, progesterone receptor, HER2/neu, and epidermal growth factor receptor. An increase in the Ki-67 and p53 labelling index was observed from MGA to invasive carcinoma. To the best of our knowledge, this is the first case of metaplastic carcinoma with chondroid differentiation arising in MGA in Korea. This case supports the hypothesis that a subset of MGA may be a non-obligate morphologic precursor of breast carcinoma, especially the triple-negative subtype.

Key Words: Breast; Metaplastic carcinoma; Fibrocystic breast disease

Microglandular adenosis (MGA) of the breast is a rare benign proliferative lesion that is often difficult to differentiate clinicopathologically from invasive carcinoma.^{1,2} Breast carcinomas arising in MGA have occasionally been reported and metaplastic carcinoma is an extremely rare subtype of breast carcinoma-associated MGA.³⁻⁹ In Korea, Choi and Bae⁹ previously reported the first two cases of invasive carcinoma arising in MGA. Invasive carcinomas arising in MGA usually show a transition from typical MGA through atypical MGA to carcinoma. Herein, we report an unusual case of metaplastic carcinoma with chondroid differentiation associated with typical MGA. To the best of our knowledge, this is the first case of metaplastic carcinoma arising in MGA reported in Korea.

CASE REPORT

A 60-year-old female presented with a palpable breast mass in the left breast. Ultrasound-guided core needle biopsy revealed invasive carcinoma. Preoperative breast magnetic resonance imaging showed an irregular solid mass approximately 1.5 cm in size in the upper outer quadrant of the left breast, which showed good contrast enhancement. A conserving operation

was performed. Grossly, a grey to white colored, hard mass with ill-defined borders measuring 1.5 cm × 1.2 cm × 1 cm was observed. Microscopically, the tumor was composed of an invasive carcinoma area and MGA area (Fig. 1A). Invasive carcinoma of no special type, grade 2 with an abrupt transition to chondroid matrix without an intervening spindle cell sarcomatoid component was observed (Fig. 1B). The chondroid matrix comprised 70% of the invasive area. Focal chondroid differentiation in the chondroid matrix area was found, thus the patient was diagnosed with metaplastic carcinoma with chondroid differentiation. In the MGA area, small round glands lined by a single layer of cuboidal epithelial cells were diffused throughout the fibrous or adipose breast tissues (Fig. 1C). Some of the glands were filled with a colloid-like secretion. No obvious architectural complexity or cytological atypia was present. MGA showed direct transition to metaplastic carcinoma without an intervening atypical MGA or ductal carcinoma *in situ* area. The glands in MGA were surrounded by a basement membrane, which was clearly demonstrated by reticulin staining. However, the basement membrane was disrupted around the invasive nests of the metaplastic carcinoma (Fig. 1D). The immunohistochemical profile of metaplastic carcinoma was nearly identical to that of MGA. In both

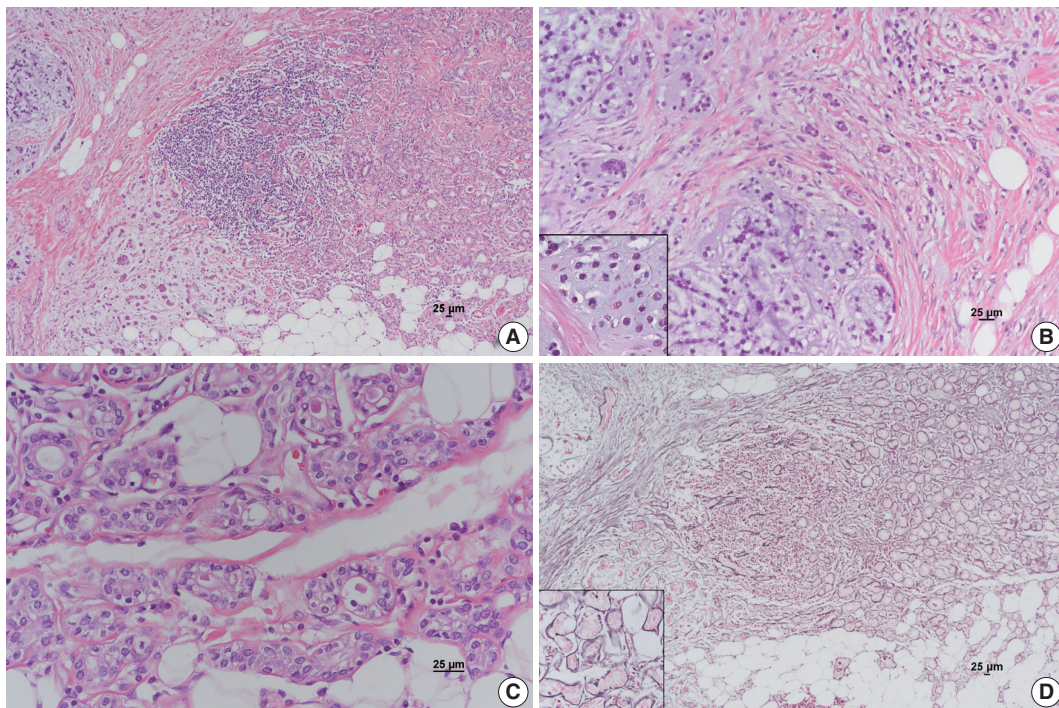


Fig. 1. Metaplastic carcinoma with mesenchymal differentiation arising in microglandular adenosis (MGA). (A) MGA on the right shows direct transition to invasive carcinoma on the left. (B) Invasive carcinoma primarily composed of cord-like cells scattered in the chondromyxoid matrix with focal chondroid differentiation (inset). (C) Typical glands in MGA are lined by uniform cuboidal cells regularly spaced around a lumen containing a colloid-like secretion. (D) Basement membranes highlighted by the reticulin stain are preserved in the MGA area (inset) but disrupted in the invasive carcinoma area.

instances, the epithelial cells were positive for cytokeratin (CK) 7 and S-100 protein, but negative for estrogen receptor (ER), progesterone receptor (PR), HER2/neu, and epidermal growth factor receptor (EGFR) (Fig. 2A, B). Other basal-like markers such as CK 5/6 and nestin were negative. No myoepithelial cells were demonstrated on immunohistochemical stainings for both smooth muscle myosin heavy chain and p63 (Fig. 2C). Ki-67 and p53 were positive in MGA and metaplastic carcinoma but tended to show a more intense staining in metaplastic carcinoma (Fig. 2D). The percentage of p53 and Ki-67 positive cells was 5% and 3% in MGA and 90% and 45% in metaplastic carcinoma, respectively. This case was finally diagnosed as metaplastic carcinoma with chondroid differentiation arising in MGA.

No metastasis was found in the sentinel lymph nodes. After surgery, the patient received adjuvant chemoradiotherapy. After 14 months of follow-up, no evidence of recurrence was observed.

DISCUSSION

MGA of the breast is a rare, benign glandular proliferative lesion that mimics invasive carcinoma clinicopathologically.^{1,2} Carcinoma arising in MGA has previously been reported.³⁻⁸ The

incidence of invasive carcinoma ranges from 23%–64% in patients with MGA,^{3,8} the high upper limit may be due to referral bias at institutions.⁵

Invasive breast carcinomas arising in MGA have various histological features.¹ Invasive carcinoma of no special type is the most common type of carcinoma arising in MGA. Specialized variants of carcinoma, including carcinoma with secretory differentiation, carcinoma with squamous differentiation, acinic cell carcinoma, and adenoid cystic carcinoma, have also been reported.³⁻⁸ Metaplastic carcinoma of the breast represents 0.2%–5% of all invasive carcinomas.⁶ Metaplastic carcinoma with mesenchymal differentiation is an extremely rare subtype of breast carcinoma arising in MGA.⁸ Structural transitions from MGA to atypical MGA and intraductal carcinoma and to invasive carcinoma are usually observed in invasive carcinomas arising in MGA.³⁻⁸

In the present case, invasive carcinoma showed abrupt transition to chondroid matrix without an intervening spindle cell component. An intervening atypical MGA or ductal carcinoma *in situ* component between MGA and invasive carcinoma was not observed. Histologically, this case was consistent with metaplastic carcinoma with chondroid differentiation associated

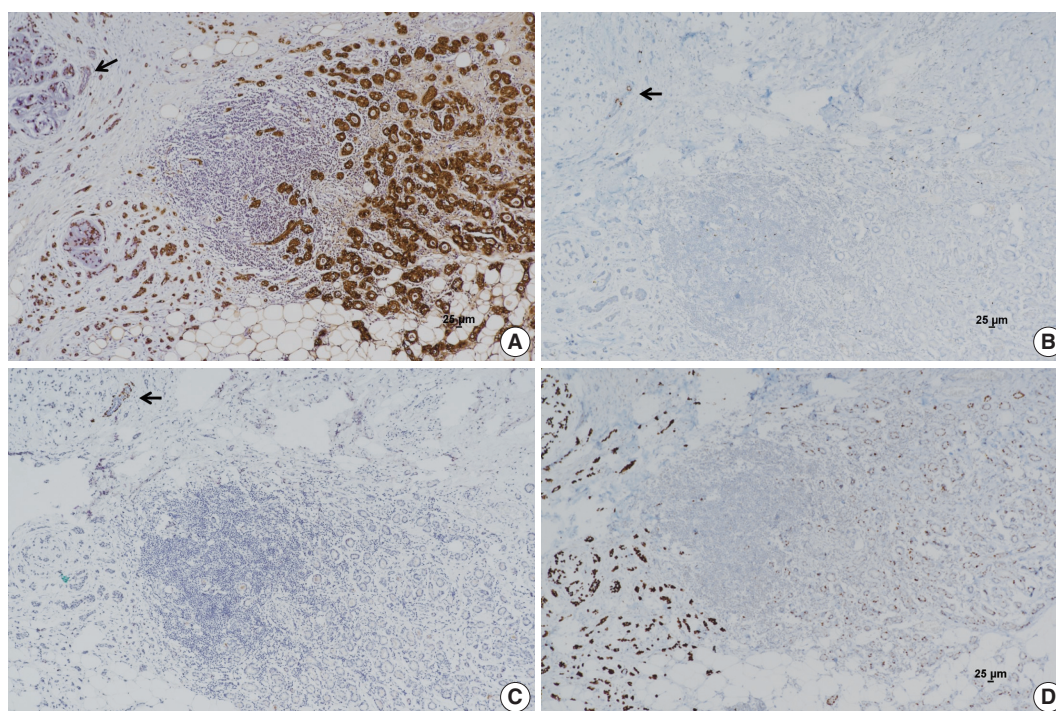


Fig. 2. Immunohistochemical stains. (A) S-100 protein is strongly positive in microglandular adenosis (MGA) and invasive carcinoma. Entrapped normal mammary gland is negative for S-100 protein (arrow). (B) Estrogen receptor (ER) is positive in entrapped normal mammary glands (arrow); however, MGA and invasive carcinoma are negative for ER. (C) No immunoreactivity for p63 is observed in the MGA area or invasive carcinoma area. Normal mammary glands are stained positively in myoepithelial cells (arrow). (D) An increase in p53 labelling index is observed from MGA to invasive carcinoma.

with typical MGA.

The main histological difference between MGA and MGA-associated invasive carcinoma is the presence of a basement membrane. The glands in MGA are surrounded by a basement membrane that can be highlighted using reticulin staining, periodic acid-Schiff staining, and immunohistochemical stains for type IV collagen and laminin. However, the basement membrane in MGA-associated carcinoma is disrupted around invasive nests.

The immunohistochemical profile of invasive carcinoma arising in MGA is similar to that of MGA.^{3-6,8} No myoepithelial cells are found in MGA and related lesions. The epithelial cells are usually positive for CK 7 and S-100 protein, but negative for ER, PR, and HER2/neu. In the present case, all the epithelial cells in MGA and invasive carcinoma were strongly immunoreactive for S-100 protein and negative for ER, PR, and HER2/neu, which was consistent with a triple-negative immunoprofile. Although the positivity for basal-like markers such as EGFR, CK 5/6, and nestin has been described in MGA and associated lesions,⁸ epithelial cells in the present case lacked these markers. Several studies have reported a trend toward increased positivity for the p53 and proliferation marker Ki-67 together with increased severity of the lesions.^{4,5} In the present case, metaplastic carcinoma

showed a higher percentage of staining for p53 and Ki-67 than MGA. The identification of MGA and its direct transition to invasive lesions and the maintenance of the characteristic immunoprofile of MGA and invasive carcinoma associated with MGA in this study provided strong evidence suggesting that an MGA subset may constitute a non-obligate morphological precursor of invasive breast carcinoma, especially the triple-negative subtype.

Recent molecular genetic studies including massively parallel sequencing approaches provide further evidence to support the hypothesis that MGA is, at least in several cases, a neoplastic, clonal lesion and may be a non-obligate precursor for triple-negative or basal-like breast carcinomas.^{10,11}

The treatment of carcinomas arising in MGA follows the same general guidelines for breast carcinomas. The prognosis of invasive carcinoma arising in MGA varies in the literature. Some authors reported that patients with invasive carcinoma arising in MGA have a relatively favorable prognosis.^{3,7} Another study, however, showed that the outcome for patients with invasive carcinoma arising in MGA ranged from favorable to unfavorable.⁵ In our patient, no axillary lymph node metastasis was found. Metaplastic carcinoma, the subtype of invasive carcinoma

found in the present case, has lower response rates to conventional adjuvant chemotherapy and a worse clinical outcome than other forms of triple-negative breast cancers. Because metaplastic carcinoma arising in MGA is extremely rare, the prognosis of the lesion requires further characterization with more cases and longer follow-up.

Conflicts of Interest

No potential conflict of interest relevant to this article was reported.

REFERENCES

1. Shin SJ, Gobbi H. Microglandular adenosis, atypical microglandular adenosis and microglandular adenosis with carcinoma. In: Lakhani SR, Ellis IO, Schnitt SJ, Tan PH, van de Vijver MJ, eds. WHO classification of tumours of the breast. 4th ed. Lyon: IARC Press, 2012; 113-4.
2. Brogi E. Adenosis and microglandular adenosis. In: Hoda SA, Brogi E, Koerner FC, Rosen PP, eds. Rosen's breast pathology. 4th ed. Philadelphia: Lippincott Williams & Wilkins, 2014; 183-212.
3. James BA, Cranor ML, Rosen PP. Carcinoma of the breast arising in microglandular adenosis. *Am J Clin Pathol* 1993; 100: 507-13.
4. Koenig C, Dadmanesh F, Bratthauer GL, Tavassoli FA. Carcinoma arising in microglandular adenosis: an immunohistochemical analysis of 20 intraepithelial and invasive neoplasms. *Int J Surg Pathol* 2000; 8: 303-15.
5. Khalifeh IM, Albarracin C, Diaz LK, *et al.* Clinical, histopathologic, and immunohistochemical features of microglandular adenosis and transition into *in situ* and invasive carcinoma. *Am J Surg Pathol* 2008; 32: 544-52.
6. Shui R, Bi R, Cheng Y, Lu H, Wang J, Yang W. Matrix-producing carcinoma of the breast in the Chinese population: a clinicopathological study of 13 cases. *Pathol Int* 2011; 61: 415-22.
7. Zhong F, Bi R, Yu B, *et al.* Carcinoma arising in microglandular adenosis of the breast: triple negative phenotype with variable morphology. *Int J Clin Exp Pathol* 2014; 7: 6149-56.
8. Liu LY, Sheng SH, Zhang ZY, Xu JH. A case of matrix-producing carcinoma of the breast with micoglandular adenosis and review of literature. *Int J Clin Exp Pathol* 2015; 8: 8568-72.
9. Choi JE, Bae YK. Invasive breast carcinoma arising in microglandular adenosis: two case reports. *J Breast Cancer* 2013; 16: 432-7.
10. Shin SJ, Simpson PT, Da Silva L, *et al.* Molecular evidence for progression of microglandular adenosis (MGA) to invasive carcinoma. *Am J Surg Pathol* 2009; 33: 496-504.
11. Guerini-Rocco E, Piscuoglio S, Ng CK, *et al.* Microglandular adenosis associated with triple-negative breast cancer is a neoplastic lesion of triple-negative phenotype harbouring TP53 somatic mutations. *J Pathol* 2016; 238: 677-88.

Mammary Carcinoma Arising in Microglandular Adenosis: A Report of Five Cases

Mimi Kim¹ · Milim Kim^{1,2}
Yul Ri Chung¹ · So Yeon Park^{1,2}

¹Department of Pathology, Seoul National University College of Medicine, Seoul;

²Department of Pathology, Seoul National University Bundang Hospital, Seongnam, Korea

Received: October 11, 2016

Revised: November 8, 2016

Accepted: November 11, 2016

Corresponding Author

So Yeon Park, MD, PhD

Department of Pathology, Seoul National University Bundang Hospital, 82 Gumi-ro 173beon-gil, Bundang-gu, Seongnam 13620, Korea

Tel: +82-31-787-7712

Fax: +82-31787-4012

E-mail: syprd@snu.ac.kr

Mammary carcinoma arising in microglandular adenosis (MGA) is extremely rare, and MGA is regarded as a non-obligate precursor of triple-negative breast cancer. We report five cases of carcinoma arising in MGA of the breast. All cases showed a spectrum of proliferative lesions ranging from MGA to atypical MGA, ductal carcinoma in situ or invasive carcinoma. Immunohistochemically, all cases were triple-negative and expression of S-100 protein gradually decreased as the lesions progressed from MGA to atypical MGA and carcinoma. Three cases showed acinic cell differentiation with reactivity to α 1-antitrypsin, and one case was metaplastic carcinoma. During clinical follow-up, one patient developed local recurrence. Carcinoma arising in MGA is a rare but distinct subset of triple-negative breast cancer with characteristic histologic and immunohistochemical findings.

Key Words: Microglandular adenosis; Breast; Carcinoma

Microglandular adenosis (MGA) is a rare benign breast lesion, and it often mimics invasive carcinoma due to the lack of myoepithelium and the infiltrative growth pattern in the stroma.¹ The unique immunohistochemical characteristic of MGA is the positivity for S-100 protein which is not generally positive in normal breast ductal and glandular cells.

Carcinomas arising in MGA (MGACA) are reported to comprise 27% of all MGA cases.² They are well known for its various histologic manifestations, showing apparent tumor heterogeneity as in the mixed carcinomas.³⁻⁵ The other proliferative entity related to MGA, whose atypia is insufficient to be classified as carcinoma, is classified as atypical MGA (AMGA). Whether AMGA is a precursor of the MGACA is still under discussion and the evidences from molecular and genetic analyses for this topic are being accumulated.

This case report presents five cases of MGACA focusing on some of the interesting histologic features and immunohistochemical findings to further clarify the clinicopathologic characteristics of this rare entity.

CASE REPORT

By searching the electronic database, we found five cases of MGACA (including an *in situ* lesion). The clinical characteristics of these five are summarized in Table 1. The median age of the patients at the time of the diagnosis was 47 years (range, 40 to 60 years). All patients underwent breast conserving surgery. Two patients had lymph node metastasis on pathologic examination and four received adjuvant chemo-radiation therapy. During follow-up, one patient (case 1) developed recurrence in the ipsilateral breast and axillary lymph nodes 1 year after the surgery. The rest of the patients had no evidence of disease and are being regularly followed up. This study was approved by the Institutional Review Board of Seoul National University Bundang Hospital (protocol # B-1609-364-701), and informed consent was waived.

The pathologic findings and the results of the immunohistochemical studies are shown in the Table 2. One patient (case 5) was diagnosed as ductal carcinoma *in situ* (DCIS) and the rest of the cases were all invasive carcinomas. The lesions in these five cases displayed the histologic spectrum ranging from MGA to

Table 1. Clinical characteristics of the five cases of MGACA

Characteristic	Case 1	Case 2	Case 3	Case 4	Case 5
Age (yr)	40	38	47	46	60
Location	Left	Left	Left	Left	Left
T stage (size of tumor, cm)	T1c (2.0)	T2 (2.3)	T1c (1.2)	T2 (2.5)	Tis (4.5)
N stage	N1a	N0	N1a	N0	N0
Type of surgery	BCS	BCS	BCS	BCS	BCS
Adjuvant CRTx	Received	Received	Received	Received	Not received
Disease status	Local recurrence	NED	NED	NED	NED

MGACA, carcinoma arising in microglandular adenosis; BCS, breast-conserving surgery; CRTx, chemo-radiation therapy; NED, no evidence of disease.

Table 2. Pathologic and immunohistochemical features of the five cases of MGACA

Characteristic	Case 1	Case 2	Case 3	Case 4	Case 5
Histologic subtype	Invasive carcinoma, NST	Invasive carcinoma, NST	Invasive carcinoma, NST	Metaplastic carcinoma	Ductal carcinoma <i>in situ</i>
Acinic cell differentiation	Absent	Present	Present	Absent	Present
Estrogen receptor	Negative	Negative	Negative	Negative	Negative
Progesterone receptor	Negative	Negative	Negative	Negative	Negative
HER-2	Negative	Negative	Negative	Negative	Negative
S-100 protein	Decreased	Decreased	Decreased	Decreased	Intact
Cytokeratin 5/6	Positive	Positive	Positive	Negative	Positive
p53	Negative	Negative	Negative	Positive	Negative
Ki-67 index (%)	50	20	30	80	5
α 1-Antitrypsin	Negative	Positive	Positive	Negative	Positive
Chymotrypsin	Negative	Negative	Negative	Negative	Negative

MGACA, carcinoma arising in microglandular adenosis; NST, no special type; HER-2, human epidermal growth factor receptor 2.

AMGA and finally to MGACA (Fig. 1). The MGA areas had the typical structure: groups of small round glands infiltrating the stroma of the breast and adipose tissue. Glands were single layered and lined by an intact basement membrane, which can be highlighted by periodic acid–Schiff (PAS) and reticulin stains. However, myoepithelium was absent, as revealed by the absence of immunohistochemical reactivity for calponin. In the lumens of the glands, eosinophilic secretions were common.

In areas diagnosed as AMGA, glands became irregular in shape and cytologically, the nuclear pleomorphism or atypism increased as the amount of eosinophilic secretions decreased. Furthermore, the proliferating atypical cells filled the lumens completely to form carcinoma *in situ* lesions and finally grew to break the basement membrane to invade the stroma which can be visualized as interrupted and discontinued strands of fibers on PAS and reticulin stains.

Even though this histological spectrum occurred in all four cases of the invasive cancers, the invasive components of some cases had unique morphologic features to be sub-classified separately. Cases 2 and 3 had some characteristic features in the glands, which were similar to those of the pancreas or of the salivary gland. These specific glands tend to make acinar structures with abundant eosinophilic cytoplasmic granules. Case 5, the

DCIS lesion, also showed acinic cell differentiation. The acinic cell differentiation in these three cases was confirmed by the immunohistochemical staining for α 1-antitrypsin and chymotrypsin (Table 2, Fig. 2). Case 4 was diagnosed as metaplastic carcinoma, specifically a matrix-producing carcinoma showing an abrupt transition from the typical invasive carcinoma to spindle cell carcinoma with chondromyxoid matrix.

All tumor cells of MGACA in our cases were negative to estrogen receptor, progesterone receptor, and human epidermal growth factor receptor 2, that is, triple-negative. For the immunohistochemical study with S-100 protein, which is the most well-known immunohistochemical marker for MGA lesions, we used a polyclonal antibody which is mainly reactive to S-100b subunit. The reactivity gradually decreased as the lesions progressed from MGA to AMGA and MGACA, showing near negativity in some areas of invasive carcinoma (Fig. 3). On the other hand, Ki-67 index increased from MGA to AMGA and finally to MGACA, as expected. p53 reactivity was negative in four cases except for case 4. For cytokeratin 5/6, four cases including one DCIS case demonstrated at least focal positivity (Table 2).

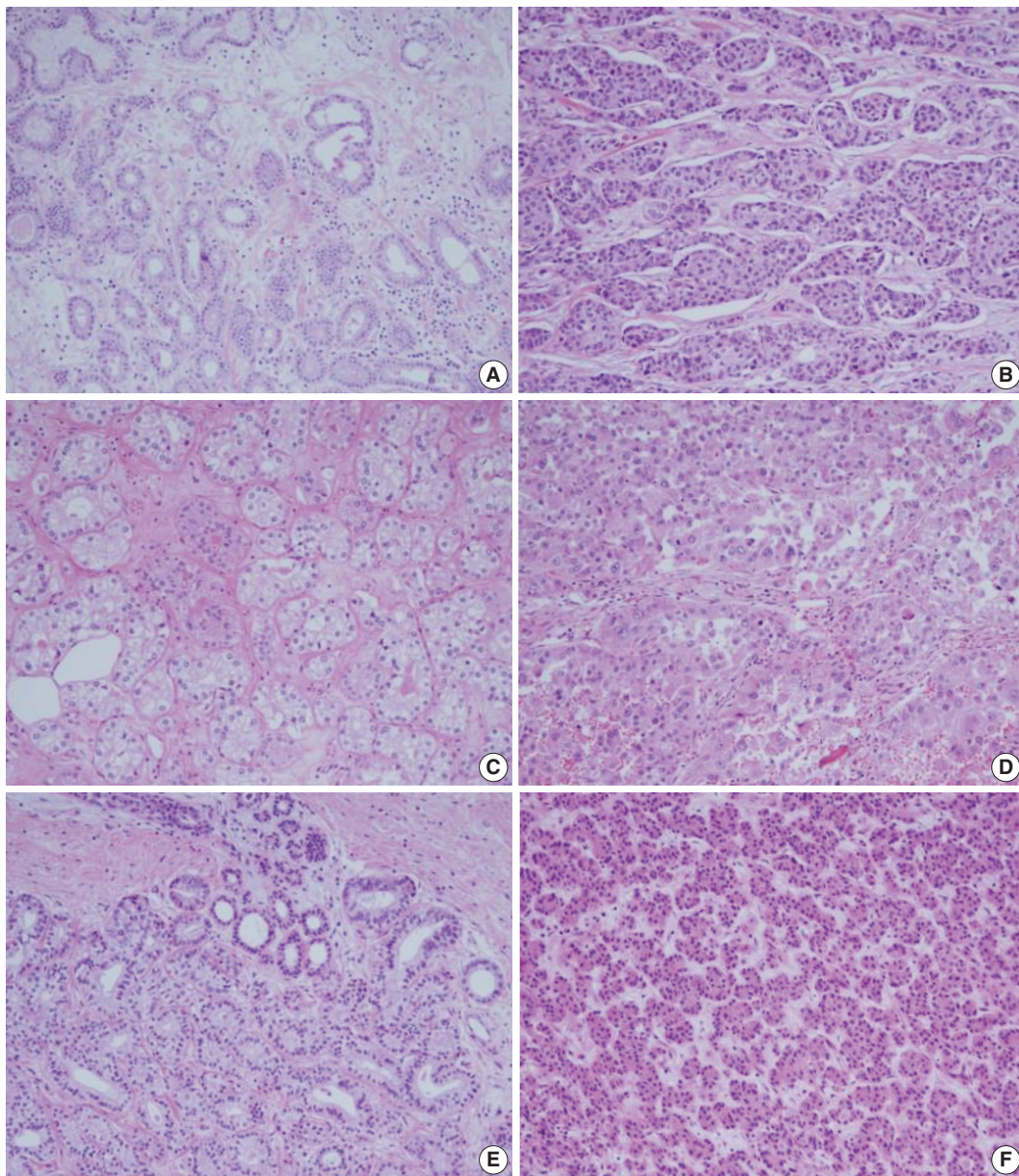


Fig. 1. Representative histologic features of the five cases. (A, C, E, G, I) Microglandular adenosis (MGA) or atypical MGA component. (B, D, F, H, J) Carcinoma component arising in MGA in each case. (H) Histologic features of matrix forming metaplastic carcinoma. (J) Ductal carcinoma *in situ* (A, B, case 1; C, D, case 2; E, F, case 3; G, H, case 4; I, J, case 5). (Continued to the next page)

DISCUSSION

The MGA differs substantially from other adenosis lesions in many aspects including the immunohistochemical properties. The myoepithelial linings, which disappear in MGA, resulted in negative reactivity to the myoepithelial markers such as calponin and p63. In our case, calponin was all negative in the MGA lesions as well as in the associated carcinoma. The PAS and reticulin staining instead revealed the intact and regular linings of the

basement membranes of MGA. These staining patterns therefore could be used to distinguish the invasive portion from the DCIS or other AMGA lesions. The invasive cancers showed the irregular and discontinuous stromal fibers around tumor cell nests.

Through the immunohistochemical studies, we could detect some phenotypic changes from MGA to MGACA. Ki-67 index increased in a stepwise manner as the diseases progressed. Especially in case 4, p53 overexpression gradually increased during transition from AMGA to MGACA. In contrast, the positivity

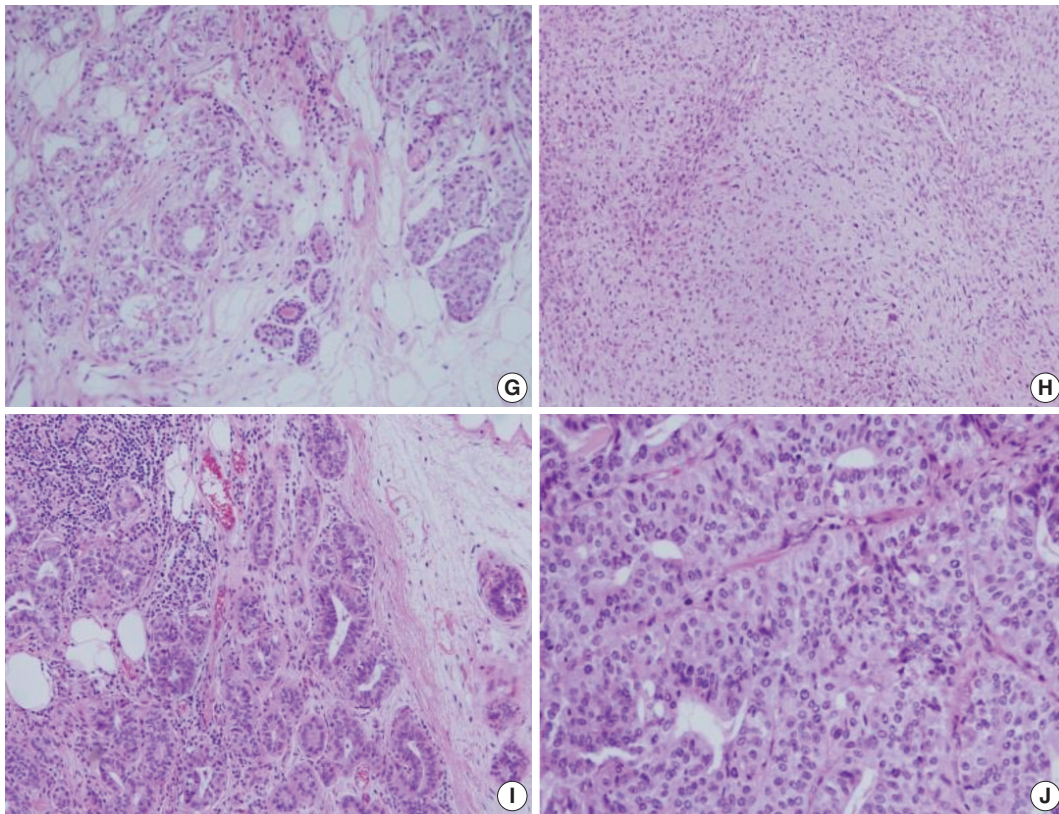


Fig. 1. (Continued from the previous page)

of S-100 protein, the most unique immunohistochemical property of MGA, diminished gradually as the disease progressed to MGACA.

However, some studies reported positive results with S-100 protein in carcinoma portions as strong as in the pure MGA lesions.^{5,6} This discordance may have resulted from the use of different members of S-100 protein, which is known to have at least 21 types currently.⁷ In a study of MGACA, Koenig *et al.*³ used two separate antibodies of S-100 protein, S-100a and S-100b for immunohistochemical characterization of MGACA, and reported that S-100b protein showed decreased reactivity, which is similar to our result. They suggested that this finding might be derived from the different localizations of the S-100a and S-100b, which are ductal cytoplasm and myoepithelium, respectively.³ However, as MGA shows immunoreactivity to S-100b, it is plausible that epithelial cells of MGA pose myoepithelial cell features and this characteristic may be lost during the progression from MGA to MGACA.

The various histologic and immunohistochemical features of MGACA in our cases have some points of interest. Among the various molecular subtypes of the triple-negative breast cancer,⁸ the metaplastic carcinoma case resembles mainly the mesenchy-

mal subtype because it had chondromyxoid and spindle cell areas and was highly proliferative (Ki-67 index, 80%). Several MGA-CAs of our cases demonstrated acinic cell differentiation. Interestingly, two invasive cancers with acinic cell differentiation were all positive for α 1-antitrypsin and totally negative for chymotrypsin. The DCIS case with acinic cell differentiation showed weak positivity for α 1-antitrypsin. These findings are reminiscent of acinic cell carcinoma of the salivary gland rather than that of the pancreas, which is usually positive for chymotrypsin and α 1-antichymotrypsin and almost always negative for α 1-antitrypsin. It is also consistent with the fact that the traditional acinic cell carcinomas of the breast look similar to that of the salivary gland. Large proportions of the acinic cell carcinomas of the breast reported in articles share many aspects in common with our cases both histologically and immunohistochemically; this suggests that most acinic cell carcinomas originated in breast may arise from MGA lesions.

The molecular characteristics of MGA and MGACA are currently being investigated⁹⁻¹² and one study reported some shared genetic mutations between MGA and MGACA in four out of 12 cases.¹¹ The overlapped sequences included recurrent gains on 1q, 2q, and 8q and losses in 14q. They suggested that MGA

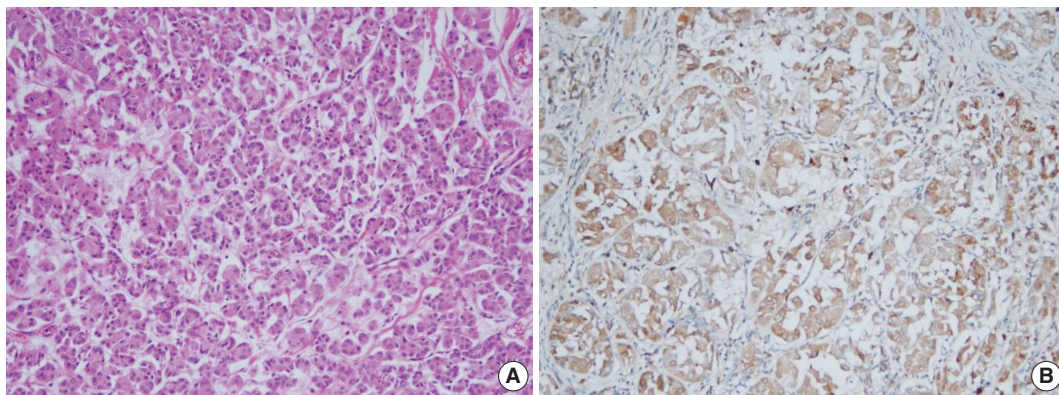


Fig. 2. Acinic cell differentiation in case 3. Tumor cells have eosinophilic granular cytoplasm (A) and show immunoreactivity to α 1-antitrypsin (B).

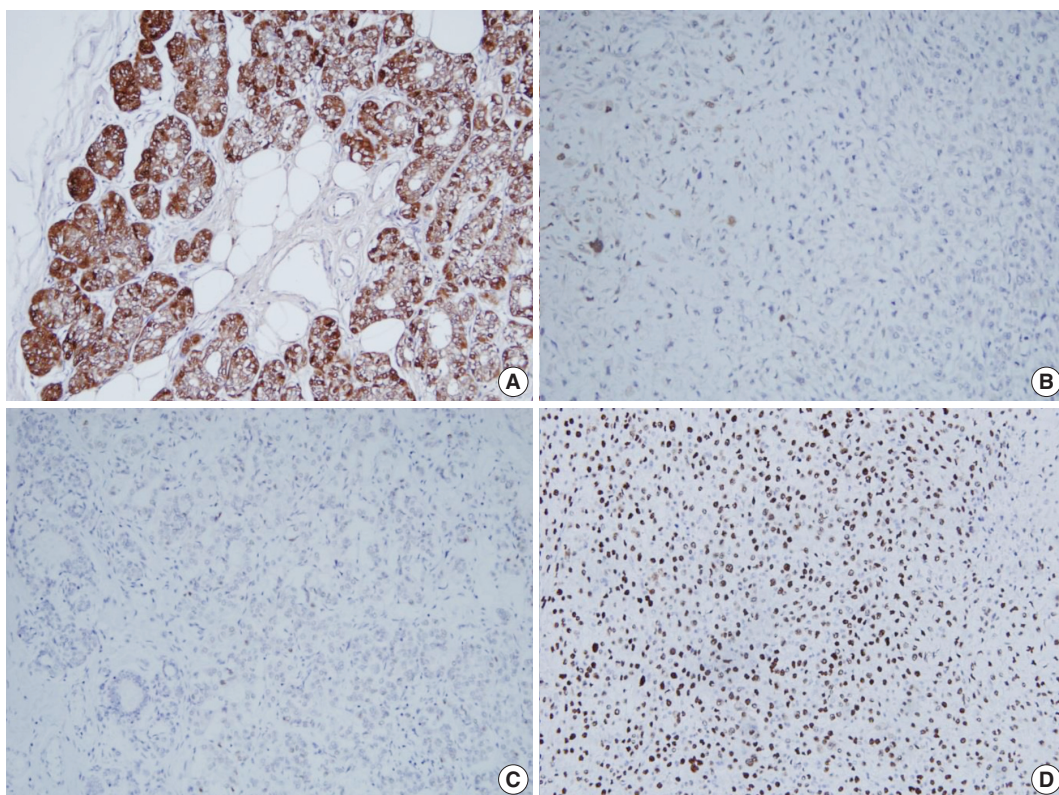


Fig. 3. S-100 protein and p53 expression in case 4. (A, B) Atypical microglandular adenosis (AMGA) shows diffuse strong positivity to S-100 protein (A), while carcinoma arising in microglandular adenosis (MGACA) shows decreased expression to S-100 protein (B). (C, D) p53 staining is evident in MGACA (D), but not in AMGA (C).

might be a non-obligate precursor to a specific subgroup of high grade triple-negative breast carcinomas.¹¹

As the histologic spectrum of the MGA associated lesions (from the MGA to AMGA and MGACA) becomes a frequent finding, some researchers suggested a new term, “microglandular adenoma” instead of “microglandular adenosis” for its potential to become a cancer.⁹ According to their opinions, MGA seems to be more similar to the adenoma of the gastrointestinal tract

rather than other adenosis lesions of the breast in terms of the possibility to progress to malignancies.

In conclusion, MGACA is one of the rare breast cancers and has many unique features that are worth classifying. Further studies will be needed to find the association between the genetic backgrounds and the characteristics of the lesions.

Conflicts of Interest

No potential conflict of interest relevant to this article was reported.

REFERENCES

1. Rosen PP. Rosen's breast pathology. 2nd ed. Philadelphia: Lippincott Williams & Wilkins, 2001.
2. Rosenblum MK, Purrazzella R, Rosen PP. Is microglandular adenosis a precancerous disease? A study of carcinoma arising therein. *Am J Surg Pathol* 1986; 10: 237-45.
3. Koenig C, Dadmanesh F, Bratthauer GL, Tavassoli FA. Carcinoma arising in microglandular adenosis: an immunohistochemical analysis of 20 intraepithelial and invasive neoplasms. *Int J Surg Pathol* 2000; 8: 303-15.
4. Khalifeh IM, Albarracin C, Diaz LK, *et al.* Clinical, histopathologic, and immunohistochemical features of microglandular adenosis and transition into in situ and invasive carcinoma. *Am J Surg Pathol* 2008; 32: 544-52.
5. Shui R, Bi R, Cheng Y, Lu H, Wang J, Yang W. Matrix-producing carcinoma of the breast in the Chinese population: a clinicopathological study of 13 cases. *Pathol Int* 2011; 61: 415-22.
6. Shui R, Yang W. Invasive breast carcinoma arising in microglandular adenosis: a case report and review of the literature. *Breast J* 2009; 15: 653-6.
7. Marenholz I, Heizmann CW, Fritz G. S100 proteins in mouse and man: from evolution to function and pathology (including an update of the nomenclature). *Biochem Biophys Res Commun* 2004; 322: 1111-22.
8. Lehmann BD, Bauer JA, Chen X, *et al.* Identification of human triple-negative breast cancer subtypes and preclinical models for selection of targeted therapies. *J Clin Invest* 2011; 121: 2750-67.
9. Geyer FC, Kushner YB, Lambros MB, *et al.* Microglandular adenosis or microglandular adenoma? A molecular genetic analysis of a case associated with atypia and invasive carcinoma. *Histopathology* 2009; 55: 732-43.
10. Shin SJ, Simpson PT, Da Silva L, *et al.* Molecular evidence for progression of microglandular adenosis (MGA) to invasive carcinoma. *Am J Surg Pathol* 2009; 33: 496-504.
11. Geyer FC, Lacroix-Triki M, Colombo PE, *et al.* Molecular evidence in support of the neoplastic and precursor nature of microglandular adenosis. *Histopathology* 2012; 60: E115-30.
12. Tsang JY, Tse GM. Microglandular adenosis: a prime suspect in triple-negative breast cancer development. *J Pathol* 2016; 239: 129-32.

Perivascular Epithelioid Cell Tumor in the Stomach

Sun Ah Shin · Jiwoon Choi
Kyung Chul Moon · Woo Ho Kim

Department of Pathology, Seoul National University Hospital, Seoul, Korea

Received: August 15, 2016
Accepted: September 16, 2016

Corresponding Author

Woo Ho Kim, MD, PhD
Department of Pathology, Seoul National University College of Medicine, 103 Daehak-ro, Jongno-gu, Seoul 03080, Korea
Tel: +82-2-740-8269
Fax: +82-2-765-5600
E-mail: woohokim@snu.ac.kr

Perivascular epithelioid cell tumors or PEComas can arise in any location in the body. However, a limited number of cases of gastric PEComa have been reported. We present two cases of gastric PEComas. The first case involved a 62-year-old woman who presented with a 4.2 cm gastric subepithelial mass in the prepyloric antrum, and the second case involved a 67-year-old man with a 5.0 cm mass slightly below the gastroesophageal junction. Microscopic examination revealed that both tumors were composed of perivascular epithelioid cells that were immunoreactive for melanocytic and smooth muscle markers. Prior to surgery, the clinical impression of both tumors was gastrointestinal stromal tumor (GIST), and the second case was erroneously diagnosed as GIST even after microscopic examination. Although gastric PEComa is a very rare neoplasm, it should be considered in the differential diagnosis of gastric submucosal lesions.

Key Words: Perivascular epithelioid cell neoplasms; Stomach neoplasms; HMB-45 protein, human; MART-1 antigen; Gastrointestinal stromal tumors

In the early 1990s, Pea *et al.*¹ reported that renal angiomyolipomas demonstrated positive immunoreactivity for human melanoma black (HMB)-45, which recognize the premelanosome protein encoded by the *PMEL* gene.² Subsequently, the same group asserted that cells of renal angiomyolipomas and clear cell tumors of the lung demonstrated similar morphology and had identical immunohistochemical profiles.³ Bonetti *et al.*⁴ proposed the term perivascular epithelioid cell to describe the aforementioned tumor cells. Zamboni *et al.*⁵ used the term PEComa to describe tumor containing perivascular epithelioid cells with immunoreactivity for melanocytic markers when they detected a clear cell “sugar” tumor arising in the pancreas. In 2002, the World Health Organization classified PEComa as a distinct disease entity, a mesenchymal neoplasm composed of distinctive cells that partly show an association with blood vessel walls and usually express melanocytic and smooth muscle markers.⁶

PEComa predominantly arises in the kidney, lung, falciform ligament, ligamentum teres, uterus, or gastrointestinal tract.⁷⁻⁹ PEComas located in the gastrointestinal tract predominantly affect the colon and small intestine,^{9,11} and only a limited number of cases of gastric PEComa have been reported in the English literature. Here, we present two cases of gastric PEComa encountered in our hospital.

CASE REPORT

The first patient was a 62-year-old woman. She underwent a routine check-up due to a minor injury to her foot. Elevated liver enzyme levels were noted, and subsequent abdomen ultrasonography revealed a submucosal mass in the stomach. She had neither signs of tuberous sclerosis complex nor any family history of it. An abdomen computed tomography image showed a 4.2-cm subepithelial mass with broad base in the prepyloric antrum (Fig. 1A). Endoscopic ultrasound revealed a hypoechoic mass involving the proper muscle layer, and laparoscopic wedge resection of stomach was performed. Lymph node enlargement or peritoneal metastasis was not detected. The patient was discharged after the surgery without any complication.

On gross examination, the subepithelial mass measured 4.2 × 3.2 × 2.0 cm and demonstrated fleshy cut surface with a well-defined border (Fig. 1B). Microscopically, the tumor displayed a nested pattern of epithelioid tumor cells with abundant granular eosinophilic cytoplasm and round to oval nuclei (Fig. 1C). The nests were surrounded by thin walled capillaries and a radial arrangement of tumor cells was found around the vascular lumens. The tumor cells showed mild pleomorphism, but coagulation necrosis was not observed. The mitotic count was 1 in 50 high power fields (HPF). Lymphovascular or perineural invasion was

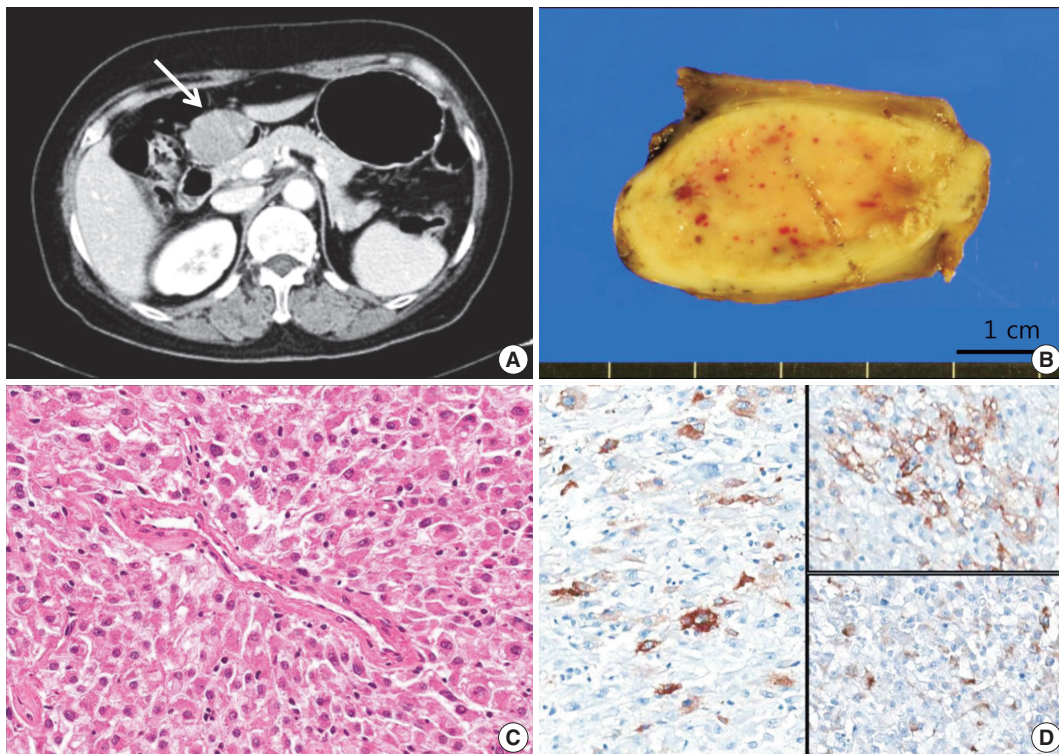


Fig. 1. Case 1. (A) Abdomen computed tomography shows a 4.2-cm-sized mass (arrow) with broad base in the prepyloric antrum. (B) On gross examination, the mass shows fleshy cut surface with a well-defined border. (C) Microscopically, the tumor displays a nested pattern, and the tumor cells were epithelioid with abundant granular eosinophilic cytoplasm and round nuclei. (D) Immunohistochemistry shows positive staining for human melanoma black 45 (left), smooth muscle actin (upper right), and desmin (lower right).

not found. The tumor was focally positive for human melanoma black 45 (HMB-45), smooth muscle actin (SMA), and desmin (Fig. 1D), and negative for Melan A, vimentin, CD117, CD34, S100, pancytokeratin, and transcription factor E3 (TFE3). The Ki-67 labeling index was 1%.

The second case was detected when we evaluated the expression of melanocytic and smooth muscle markers on our 343 gastrointestinal stromal tumor (GIST) cases. The patient was a 67-year-old man who was transferred to our hospital for further evaluation of low hemoglobin levels. Endoscopic examination revealed a 5.0-cm ulcerofungating mass with spontaneous bleeding below the gastroesophageal junction, and a subtotal gastrectomy was performed. The subepithelial mass measured 5.0 × 4.7 × 1.6 cm (Fig. 2A). Microscopically, the lesion was composed of radially arranged epithelioid cells, involving mucosa to subserosa (Fig. 2B, C). The nuclei showed marked pleomorphism and the mitotic counts were high (45/50 HPF). Direct sequencing of the *KIT* and *PDGFRA* genes revealed no mutations. The tumor showed focal positivity for SMA (Fig. 2D) and faint positivity for CD117. Thus, the tumor was initially diagnosed as epithelioid GIST. However, during the re-evaluation of GIST cases with

melanocytic markers, this case was positive for Melan-A as well as SMA, and therefore, the diagnosis was revised to PEComa. The patient did not receive any further treatment, and he did not show any evidence of recurrence for 7 years.

DISCUSSION

PEComa involving the gastrointestinal tract is rare, and the most common site within the gastrointestinal tracts is the colon.⁹⁻¹¹ Only six cases of gastric PEComa have been reported in English literature,^{9,12-15} and two cases among them were included in the case series of gastrointestinal PEComas. Thus, detailed information regarding these tumors is insufficient (Table 1).

Microscopically, PEComa shows perivascular epithelioid cells arranged radially around the vascular lumens. Spindle cells are usually located at the periphery compared with epithelioid cells. Perivascular epithelioid cells contain a large amount of lipids, and thus, are morphologically similar to lipocyte or lipoblast. Perivascular epithelioid cells have clear to slightly eosinophilic cytoplasm compared with smooth muscle cells. The aforementioned cells demonstrated small, centrally placed, round to oval

nuclei and small nucleoli,¹⁶ as in our cases.

Upon immunohistochemical analysis, PEComas are positive for melanocytic markers such as HMB-45, Melan A, and microph-

themia-associated transcription factor. Among them, HMB-45 is considered to be the most sensitive marker.⁸ In our two cases, the first case was positive for HMB-45, and the second was positive

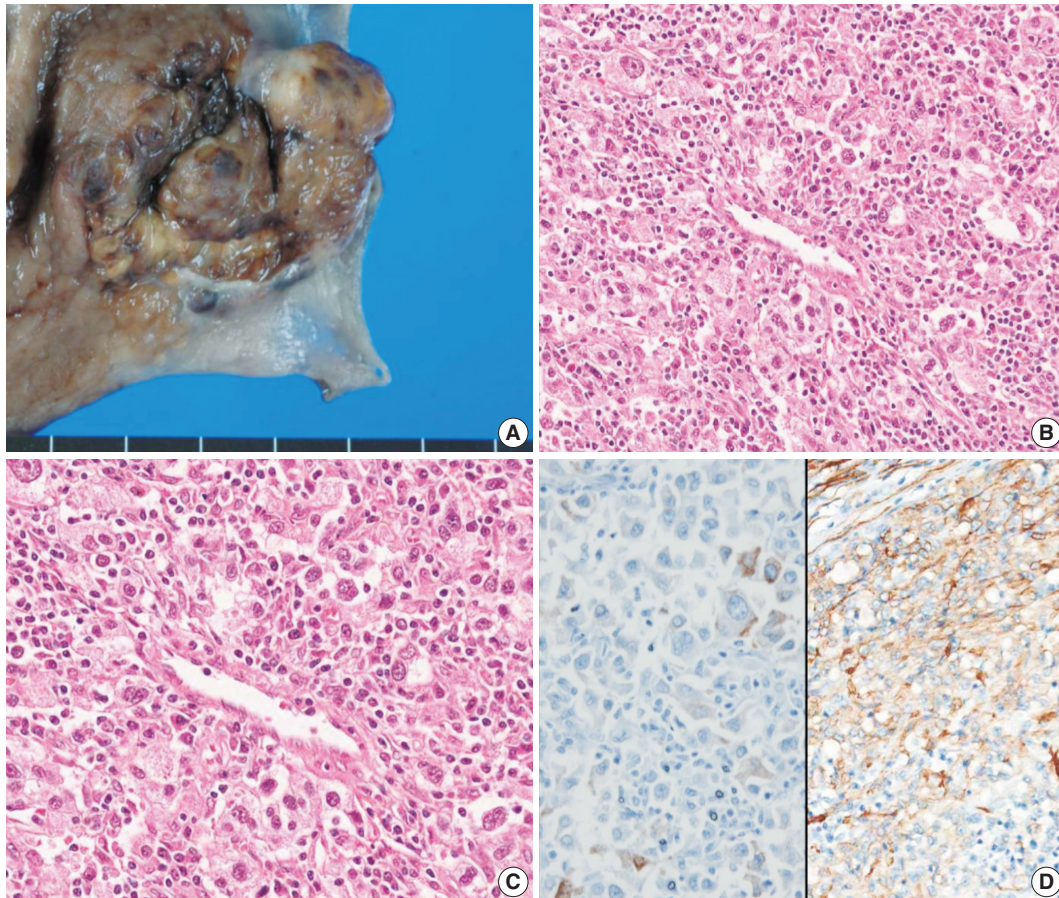


Fig. 2. Case 2. (A) The tumor was a subepithelial lesion involving gastroesophageal junction. (B, C) Microscopically, the tumor was composed of perivascular epithelioid cells with heavy lymphoid cell infiltration. (D) Immunohistochemistry reveals positivity for Melan-A (left) and smooth muscle actin (right).

Table 1. Summary of gastric PEComa cases

Case	Reference	Age (yr)	Sex	Size (cm)	Microscopic feature					Recurrence or metastasis	IHC			
					Infiltrative border	Nuclear grade	Mitotic activity	Necrosis	Cellularity		HMB-45	Melan-A	SMA	Desmin
1	Mitteldorf et al. ¹²	71	F	3.0	-	Moderate	Low (1/50 HPF)	-	NR	NED for 19 mo	-	+	+	+
2	Waters et al. ¹³	42	M	10.0	NR	NR	NR	NR	NR	Metastasis to liver	NR	+	NR	+
3	Yamada et al. ¹⁴	39	M	7.3	+	High	High (>2/50 HPF)	+	NR	NED for 6 mo	+	+	+	+
4	Kumar et al. ¹⁵	48	F	11.5	NR	High	High (20/10 HPF)	+	NR	-	-	+	+	NR
5	Case 1	62	F	4.2	-	Low	Low (1/50 HPF)	-	Low	NED for 8 mo	+	-	+	+
6	Case 2	67	M	5.0	-	High	High (45/50 HPF)	-	High	NED for 7 yr	-	+	+	-

Case 2–4: malignant gastric PEComas.

IHC, immunohistochemistry; HMB-45, human melanoma black 45; SMA, smooth muscle actin; F, female; HPF, high power fields; NR, not recorded; NED, no evidence of disease; M, male.

for Melan-A. The majority of PEComas are positive for smooth muscle markers, including SMA, desmin, and calponin, and among them, SMA is considered to be the most sensitive, whilst desmin is less sensitive.¹⁷ Both cases in our study demonstrated positivity for SMA, and the first case showed positivity for desmin. The first case was negative for CD117 and TFE3; these markers are known to show positivity in a small proportion of PEComas.¹⁸

Clinically and microscopically, PEComa can be misdiagnosed as epithelioid GIST. Therefore, we re-analyzed 343 cases diagnosed as GIST between 2005 and 2011 in our hospital, including 20 c-kit negative cases.¹⁹ Of the 343 cases, we found that only a single case showed positivity for Melan-A, and we believe that this case should have been classified as PEComa. Malignant melanoma or clear cell sarcoma should also be considered in the differential diagnosis; however, our second case did not show immunopositivity for S100, which is characteristic for malignant melanoma or clear cell sarcoma.

A consensus regarding the prognostic factors of PEComa has yet to be established because of its rarity. Folpe *et al.*⁸ concluded that malignant behavior, including recurrence or metastasis of PEComa involving soft tissue and gynecologic organs, is associated with a large size (> 5 cm), frequent mitosis (> 1/50HPF), necrosis, infiltrative growth pattern, high cellularity, and high nuclear grade. Hornick and Fletcher¹⁷ ascertained that malignant behavior was associated with nuclear atypia and pleomorphism. In addition, Doyle *et al.*⁹ revealed that the aggressive behavior of PEComa of the gastrointestinal tract is associated with a large size (> 6 cm), mitotic count (> 2/10HPF), marked cellular atypia, and diffuse pleomorphism.

Among the previously reported four cases of gastric PEComas, three cases displayed histologically malignant features.¹²⁻¹⁵ In our first case, the tumor size was 4.2 cm and the mitotic count was 1 in 50 HPF. Microscopically, the tumor showed mild pleomorphism. Since there was no evidence of malignant features, the surgeon decided to follow-up without additional treatment. In our second case, the tumor measured 5.0 cm and the mitotic count was 45 in 50 HPF. Microscopically, the tumor showed marked pleomorphism and high cellularity, and it should have been categorized as a high risk PEComa. However, it was erroneously diagnosed as epithelioid GIST and the patient underwent curative resection only without adjuvant therapy. Fortunately, there was no adverse event during the 7 years of follow-up.

In conclusion, gastric PEComa is a rare neoplasm, but some gastric PEComas show malignant behavior. Therefore, pathologists should include PEComa in the differential diagnosis for gastric subepithelial tumors with epithelioid cell features. Since

PEComas may display faint CD117 immunoreactivity,⁹ CD117 immunoreactivity alone cannot justify the exclusion of PEComa during the diagnostic process. Its tendency to manifest immunopositivity for melanocytic and smooth muscle markers should warrant pathologists to make a diagnosis with correlation of the patient's clinical information.

Conflicts of Interest

No potential conflict of interest relevant to this article was reported.

REFERENCES

1. Pea M, Bonetti F, Zamboni G, *et al.* Melanocyte-marker-HMB-45 is regularly expressed in angiomyolipoma of the kidney. *Pathology* 1991; 23: 185-8.
2. Adema GJ, de Boer AJ, Vogel AM, Loenen WA, Figdor CG. Molecular characterization of the melanocyte lineage-specific antigen gp100. *J Biol Chem* 1994; 269: 20126-33.
3. Pea M, Bonetti F, Zamboni G, Martignoni G, Fiore-Donati L, Doglioni C. Clear cell tumor and angiomyolipoma. *Am J Surg Pathol* 1991; 15: 199-202.
4. Bonetti F, Pea M, Martignoni G, Zamboni G. PEC and sugar. *Am J Surg Pathol* 1992; 16: 307-8.
5. Zamboni G, Pea M, Martignoni G, *et al.* Clear cell "sugar" tumor of the pancreas: a novel member of the family of lesions characterized by the presence of perivascular epithelioid cells. *Am J Surg Pathol* 1996; 20: 722-30.
6. Hornick JL, Pan CC. PEComa. In: Fletcher CD, Bridge JA, Hogendoorn PC, Mertens F, eds. *WHO classification of tumours of soft tissue and bone*. 4th ed. Lyon: IARC Press, 2013; 230-1.
7. Folpe AL, Goodman ZD, Ishak KG, *et al.* Clear cell myomelanocytic tumor of the falciform ligament/ligamentum teres: a novel member of the perivascular epithelioid clear cell family of tumors with a predilection for children and young adults. *Am J Surg Pathol* 2000; 24: 1239-46.
8. Folpe AL, Mentzel T, Lehr HA, Fisher C, Balzer BL, Weiss SW. Perivascular epithelioid cell neoplasms of soft tissue and gynecologic origin: a clinicopathologic study of 26 cases and review of the literature. *Am J Surg Pathol* 2005; 29: 1558-75.
9. Doyle LA, Hornick JL, Fletcher CD. PEComa of the gastrointestinal tract: clinicopathologic study of 35 cases with evaluation of prognostic parameters. *Am J Surg Pathol* 2013; 37: 1769-82.
10. Im S, Yoo C, Jung JH, Choi HJ, Yoo J, Kang CS. Primary perivascular epithelioid cell tumor in the rectum: a case report and review of

- the literature. *Pathol Res Pract* 2013; 209: 244-8.
11. Shi HY, Wei LX, Sun L, Guo AT. Clinicopathologic analysis of 4 perivascular epithelioid cell tumors (PEComas) of the gastrointestinal tract. *Int J Surg Pathol* 2010; 18: 243-7.
 12. Mitteldorf CA, Birolini D, da Camara-Lopes LH. A perivascular epithelioid cell tumor of the stomach: an unsuspected diagnosis. *World J Gastroenterol* 2010; 16: 522-5.
 13. Waters PS, Mitchell DP, Murphy R, McKenna M, Waldron RP. Primary malignant gastric PEComa: diagnostic and technical dilemmas. *Int J Surg Case Rep* 2012; 3: 89-91.
 14. Yamada S, Nabeshima A, Noguchi H, *et al.* Coincidence between malignant perivascular epithelioid cell tumor arising in the gastric serosa and lung adenocarcinoma. *World J Gastroenterol* 2015; 21: 1349-56.
 15. Kumar M, Kumar V, Abrina V, Kaur S, Kumar A, Maroules M. Malignant gastric PEComa: a rare malignancy. *Am J Cancer Case Rep* 2015; 3: 209-14.
 16. Folpe AL, Kwiatkowski DJ. Perivascular epithelioid cell neoplasms: pathology and pathogenesis. *Hum Pathol* 2010; 41: 1-15.
 17. Hornick JL, Fletcher CD. PEComa: what do we know so far? *Histopathology* 2006; 48: 75-82.
 18. Argani P, Aulmann S, Illei PB, *et al.* A distinctive subset of PEComas harbors *TFE3* gene fusions. *Am J Surg Pathol* 2010; 34: 1395-406.
 19. Lee HE, Kim MA, Lee HS, Lee BL, Kim WH. Characteristics of KIT-negative gastrointestinal stromal tumours and diagnostic utility of protein kinase C theta immunostaining. *J Clin Pathol* 2008; 61: 722-9.

A Rare Case of Intramural Müllerian Adenosarcoma Arising from Adenomyosis of the Uterus

Sun-Jae Lee · Ji Y. Park

Department of Pathology, Catholic University of Daegu School of Medicine, Daegu, Korea

Received: May 29, 2017

Revised: June 7, 2017

Accepted: June 11, 2017

Corresponding Author

Sun-Jae Lee, MD, PhD

Department of Pathology, Catholic University of Daegu School of Medicine, 33 Duryugongwon-ro 17-gil, Nam-gu, Daegu 42472, Korea

Tel: +82-53-650-4629

Fax: +82-53-650-4834

E-mail: pathosjlee@cu.ac.kr

Müllerian adenosarcomas usually arise as polypoid masses in the endometrium of post-menopausal women. Occasionally, these tumors arise in the cervix, vagina, broad and round ligaments, ovaries and rarely in extragenital sites; these cases are generally associated with endometriosis. We experienced a rare case of extraendometrial, intramural adenosarcoma arising in a patient with adenomyosis. A 40-year-old woman presented with sudden-onset suprapubic pain. The imaging findings suggested leiomyoma with cystic degeneration in the uterine fundus. An ill-defined ovoid tumor with hemorrhagic degeneration, measuring 7.5 cm in diameter, was detected. The microscopic findings showed glandular cells without atypia and a sarcomatous component with pleomorphism and high mitotic rates. There was no evidence of endometrial origin. To recognize that adenosarcoma can, although rarely, arise from adenomyosis is important to avoid overstaging and inappropriate treatment.

Key Words: Uterus; Müllerian adenosarcoma; Adenomyosis

Müllerian adenosarcoma is a relatively uncommon variant of Müllerian mixed tumor with distinctive clinical and histologic characteristics.¹ The term Müllerian adenosarcoma was first used in 1974 to describe an unusual variant of Müllerian mixed tumor of the uterus, characterized by a mixture of benign or occasionally mildly atypical glandular components and malignant, usually low-grade, stromal components.² The morphologic features of these neoplasms distinguish them from other biphasic (epithelial and mesenchymal) tumors, both benign and malignant.¹ Müllerian adenosarcoma is generally of low malignant potential, except when accompanied by sarcomatous overgrowth and myoinvasion.¹ Patients with Müllerian adenosarcoma lacking these two histopathologic features have an excellent prognosis;¹ these tumors may recur locally but only rarely metastasize.²

Müllerian adenosarcomas generally arise from the eutopic endometrium in the uterine corpus and grow as polypoid masses in post-menopausal women who present with abnormal vaginal bleeding.^{2,3} These neoplasms, however, may also arise in ectopic foci of endometriosis, such as the uterine cervix, vagina, broad and round ligaments, and ovaries or even at extragenital sites in rare cases.^{4,5} For example, among 41 previously reported Müllerian adenosarcomas, 29 (71%) were extrauterine,⁶ with the sites including the ovaries, cervix, peritoneum, pelvis, gastrointestinal tract,

bladder, perirectal tissue, rectovaginal septum, pouch of Douglas, and liver.⁷ Some studies have reported that adenosarcomas arising in extrauterine and extragenital area may be associated with more aggressive clinical behavior, probably due to an increasing tendency for peritoneal spread.²

Extraendometrial uterine adenosarcomas, that is, tumors originating from adenomyosis or an adenomyoma and not from the eutopic endometrium, are rare, with no specific staging guidelines for these tumors provided in the new International Federation of Gynecology and Obstetrics (FIGO) staging system of uterine sarcomas.^{8,9} In fact, only a few prior cases of primary adenosarcoma arising from adenomyosis have been reported in the English literature.^{2,5,8,10} The present report describes the clinical and pathologic findings of a rare case of extraendometrial, intramural adenosarcoma arising from adenomyosis without eutopic endometrial involvement in a 40-year-old woman and briefly reviews the literature describing the clinical and pathologic characteristics of adenosarcoma arising from adenomyosis.

Because this is a descriptive case report and literature review, institutional review board approval was waived and personal information of the patient was de-identified.

CASE REPORT

A 40-year-old woman (gravida 2, para 2) presented in July 2015 with sudden-onset suprapubic pain and initial low back pain. Gynecologic examination detected a round soft fist-sized mass in the right fundic area accompanied by bloody vaginal discharge. Laboratory examination of serum tumor markers showed that the concentration of carbohydrate antigen (CA) 125 was markedly elevated (5,000 IU/mL; normal, < 16 IU/mL), while the concentration of CA19-9 was slightly elevated (39 IU/mL; normal, < 37 IU/mL). In contrast, the serum concentrations of β -human chorionic gonadotropin (1.34 mIU/mL) and α -fetoprotein (0.90 ng/mL) were within normal limits.

Pelvic ultrasonography showed an enlarged uterus with a 7 cm solid and cystic mass (Fig. 1A). T2-weighted magnetic resonance imaging (MRI) demonstrated an enlarged uterus with a mass, measuring 71 × 59 × 72 mm in size, arising from the uterine fundus (Fig. 1B). An exophytic multilocular cystic lesion, measuring 43 × 39 × 31 mm, was also present in the cranial portion of the mass. These findings suggested peripheral intramural leiomyoma with cystic degeneration and cranial rupture.

The patient underwent laparoscopically-assisted total vaginal hysterectomy without nodal dissection and without oophorectomy. Laparoscopic examination revealed a hemorrhagic friable mass arising from the uterine fundus. The tumor was attached to the bowel and omentum. There was no evidence of peritoneal endometriosis or other peritoneal lesions.

Gross examination showed that the uterus measured 14 × 7.5 × 5.5 cm in size and weighed 54 g. The uterine fundus contained an ill-defined, rubbery ovoid tumor, measuring 7.5 cm in diameter,

with hemorrhagic degeneration and rupture (Fig. 2A). The remaining endometrium and cervix were unremarkable. The cut surface of the lesion was tan-brown in color, multicystic and solid (Fig. 2B).

Microscopic examination revealed a biphasic tumor composed of both dilated glandular elements and abundant, hypercellular stromal elements (Fig. 3A, B). The tumor revealed expansile growth within the myometrium with extensive myometrial invasion and focal infiltration with expansile margins into the subserosa (Fig. 3C).

The glands were lined by benign endometrioid cells that were columnar or cuboidal in shape, with focal secretion (Fig. 3D). Some of these glands showed mild hyperplasia with rare mitosis (0–1/10 high power fields [HPFs]) of the lining; however, the glandular epithelium showed no indications of malignancy.

The benign endometrial glands were surrounded by hypercellular spindle cell proliferation, with cells growing in a fascicular pattern. The stromal cells showed mild to moderate focal atypia with occasional mitotic figures (Fig. 3D, E). The mitotic count was 5/10 HPFs, which was higher than that of the glandular cells. Diffuse hemorrhagic necrosis was present at the center of the mass.

Immunohistochemical analysis, performed with appropriate controls, showed that both the glandular and stromal cells were positive for estrogen and progesterone receptors (Fig. 3F) and focally positive for TP53 in the tumor tissue (Fig. 3G). The stromal cells were immunohistochemically positive for CD10 (Fig. 3H) and smooth muscle actin (Fig. 3I), and their Ki-67 proliferation index was mildly increased (Fig. 3J).

These microscopic findings suggested that the tumor was a mixed epithelial-stromal tumor consisting of glandular cells without atypia (benign endometrial hyperplasia) and sarcomatous stromal cells with mild pleomorphism and a high mitotic rate



Fig. 1. Radiologic findings. (A) Pelvic ultrasonography, showing an enlarged uterus with a 7-cm solid and cystic mass. (B) T2-weighted magnetic resonance imaging, showing an enlarged uterus with a mass, measuring 71 × 59 × 72 mm, arising from the uterine fundus.

(low-grade endometrial stromal sarcoma). There was no evidence of sarcomatous overgrowth, a heterologous (i.e., muscle, cartilage, bone) or sex-cord element, or lymphovascular invasion.

The endometrium was unremarkable and the background myometrium showed focal involvement of adenomyosis. There was no evidence of serosal endometriosis or other tumors intrinsic or extrinsic to the uterus. Although the specimen was submitted in a ruptured state, there was no distinct evidence of serosal involvement of the tumor. The adenosarcoma was limited to the myometrium and was not detected on the serosal surface.

Taken together, these histologic findings indicated a low-grade Müllerian adenosarcoma arising from adenomyosis.

The patient underwent follow-up evaluation 2 weeks after surgery. Further clinical workup included a whole body bone scan and positron emission tomography/computed tomography (PET-CT) scan. There was no evidence of regional or distant metastasis. One month later, the patient underwent an additional bilateral salpingo-oophorectomy, omental biopsy, and cul de sac washing cytology. There was no residual adenosarcoma in the specimen.

To date, regular follow-up evaluation has shown no evidence

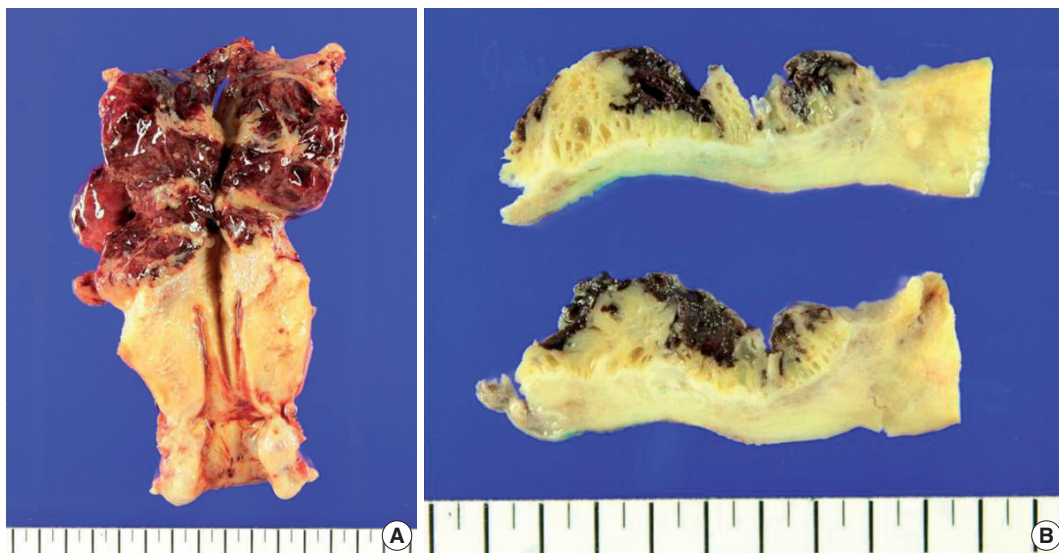


Fig. 2. Macroscopic findings of the hysterectomy specimen. (A) View showing an ill-defined ovoid tumor, 7.5 cm in diameter, together with hemorrhagic degeneration in the uterine fundus. (B) View showing that the cut surface of the lesion was tan-brown in color, multicystic, and solid.

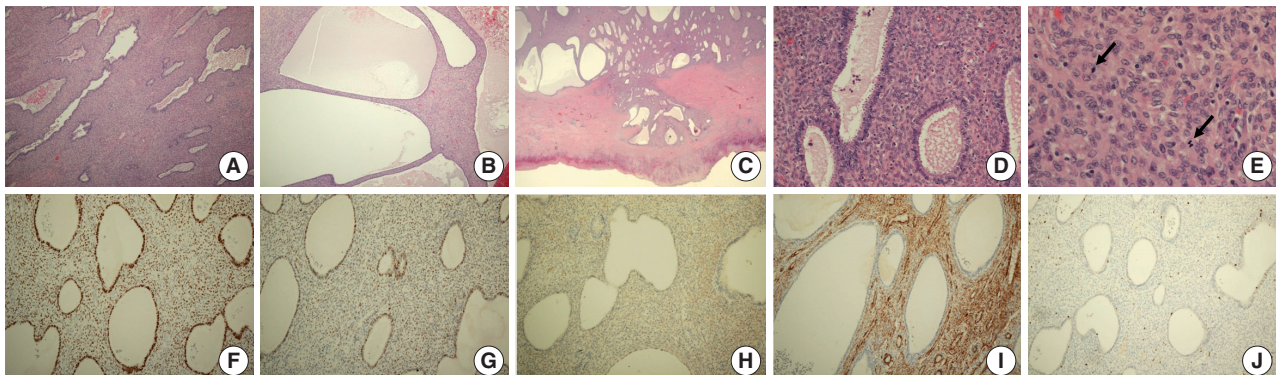


Fig. 3. Histologic and immunohistochemical findings. (A, B) Microscopic examination showing a biphasic tumor composed of both dilated glandular elements and abundant, hypercellular stromal elements. (C) The tumor shows expansile growth within the myometrium, with extensive myometrial invasion and focal infiltrates into the subserosa with expansile margins. (D) Proliferation of hypercellular spindle cells growing in a fascicular pattern, around benign endometrial glands. (E) The stromal cells show mild and focal moderate cytological atypia with occasional mitotic figures (arrows). (F–J) Immunohistochemical analysis showing that the glandular and stromal cells in tumor tissue are positive for estrogen receptor (F) and focally positive for p53 (G); that the stromal cells are positive for CD10 (H) and smooth muscle actin (I); and that the Ki-67 proliferation index is higher in the stromal component than in the epithelium (J).

of tumor recurrence, with negative radiologic findings, including transvaginal ultrasonography, chest and pelvic computed tomography, and whole body PET-CT. Her elevated serum CA125 level resolved immediately after surgery and has continued to remain in the normal range.

DISCUSSION

Uterine sarcomas of any type are rare when compared with uterine epithelial malignancies. Especially, Müllerian adenosarcomas are highly rare, accounting for only 3%–7% of all uterine sarcomas.^{11,12}

Despite their rarity, these tumors affect women of all age groups.¹ Although most adenosarcomas of the female genital tract occur in post-menopausal women (median age, 58 years), these tumors have been reported in perimenopausal women as well as in children as young as 10 years old.¹² Clinically, the patients usually present with vaginal bleeding, but may also present with other nonspecific symptoms, such as pelvic pain and vaginal discharge; a large percentage of patients are asymptomatic.^{1,2}

Although the eutopic endometrium of the uterus is the most common primary site, adenosarcomas may arise in the ovaries, fallopian tubes, cervix, or vagina, as well as at extragenital sites in rare cases.³ Adenosarcomas occurring outside the female genital tract likely represent tumors arising from preexisting endometriosis.³ In fact, approximately 1%–10% of these tumors are thought to arise from the malignant transformation of endometriosis.⁴ Endometrioid adenocarcinomas and clear cell carcinomas are the most common tumor types, occurring in 70% and 14% of patients, respectively.⁴ Only a limited number of stromal tumors including adenosarcoma have been reported to date.⁴

Furthermore, these tumors are thought to arise from the endometrial stroma, they can implant into the myometrium and coexist with diffuse adenomyosis or focal adenomyoma; however, only a few cases of intramural adenosarcoma arising from adenomyosis have previously been reported in the English literature.^{2,5,8,10,13-15} These include intramural adenosarcomas originating in the foci of adenomyosis,⁵ intramural adenomyoma,⁸ and deep subserosal adenomyoma² with no evidence of eutopic endometrial origin. The detailed clinicopathologic characteristics of previously described patients are summarized in Table 1.

An essential feature of these adenosarcomas is their mixed nature, including both benign and neoplastic epithelial and malignant stromal elements.³ The epithelium, which may be dilated or slit-like in appearance, is mostly endometrioid type, usually composed of cuboidal or low columnar cells, although ciliated, mucinous, and

occasionally squamous type epithelial cells have also been identified.³ Abundant eosinophilic cytoplasm may also be present in the epithelial cells.³ The epithelial cells are usually in active phase, showing mitoses or subnuclear vacuolation, in spite of the adjacent atrophic endometrium.³ Focal crowded glands with nuclear atypia may occur, which are indicators of atypical hyperplasia.³

The stromal component, which is usually low grade, is composed of spindle and/or round cells.³ In a minority of patients, including ours, the stromal component is uniformly cellular.³ The formation of a “periglandular cuffing” or “cambium” layer, in which the stroma surrounds the glandular elements, is one of the most characteristic features of adenosarcoma.³ This cellular zone is characterized by variable degrees of nuclear atypia and mitosis.³ Although most of these tumors have a mitotic count of $\geq 2/10$ HPFs, some tumors have a lower count.³ The World Health Organization criteria consider stromal mitotic activity $> 1/10$ HPFs diagnostic of adenosarcoma, whereas other classification systems use a cutoff of $4/10$ HPFs.³ Moreover, many adenosarcomas include large areas of stromal fibrosis without mitotic activity.³ Stromal components of adenosarcomas are exclusively homologous, that are normally seen in the uterus.³ The most common mesenchymal elements consist of low-grade endometrial stromal or nonspecific fibroblastic components; the stromal cells in the periglandular area are often endometrial stromal type whereas that located away from the glands are typically of nonspecific fibrous type.³ Approximately one quarter of adenosarcomas show heterologous stromal components, comprising predominantly rhabdomyosarcoma; however, chondrosarcoma and liposarcoma may also be seen.¹⁶ Sex cord-like components, such as cords, solid nests, and/or hollow tubules, may be found within the stromal component.³ Occasionally, marked decidualization of the stroma may also be present, secondary to hormonal usage.³

Adenosarcoma is one of the mixed Müllerian tumors of the female genital tract, located between adenofibroma and carcinosarcoma (so called malignant mixed Müllerian tumor) on the spectrum.³ Because these tumors are rare, the precise molecular mechanism associated with their tumorigenesis is not fully understood.¹ Some studies have reported low rates of *TP53* mutations, and low-level amplification of *MDM2* and other genes on chromosome band 12q14-15.¹⁷ Recently described alterations in adenosarcoma include *MYBL1* amplification and *ATRX* mutation, each of which has been detected in 50% of adenosarcomas with sarcomatous overgrowth.¹⁷ Immunohistochemical analysis of the tumor in our patient showed an overexpression of TP53 in both epithelial and stromal cells. In a previous study, an adenosarcoma with sarcomatous overgrowth was found to have a hyperdiploid karyotype with multiple structural and numerical abnormalities involving

Table 1. Clinicopathologic features of adenosarcomas arising from adenomyosis

Case No. (ref No.)	Clinical feature	Pathology	Treatment	Outcome	Remarks
1 ¹⁵	Age: 51 yr Gyn hx: unknown Clinical sign: unknown Tumor marker: unknown	Size: 4 cm Location: lateral wall of the uterine body Micro: Glands with no epithelial cell atypia Sarcomatous component with cell pleomorphism and a high mitotic count Accompanied by adenomyosis	Unknown	Unknown	-
2 ¹³	Age: 20 yr Gyn hx: null Clinical sign: a long-standing history of menorrhagia and vaginal bleeding Tumor marker: β -hCG 50–80 mIU/mL	Size: unknown Location: right anterolateral portion Micro: Florid adenomyosis with extensive myometrial invasion, expansile growth within the myometrium, and intravascular invasion in the myometrium	Hysterectomy	Two years after surgery, no evidence of recurrent disease	Stromal overgrowth
3 ²	Age: 46 yr Gyn hx: para 1 Clinical sign: vaginal bleeding Tumor marker: unknown	Size: unknown Location: subserosal mass arising from the posterior surface of the uterus Micro: Adenomyoma with focal predominant endometrial stroma and periglandular cuffs Endometrial stromal cells in the periglandular cuffs showing mild and focal moderate cytological atypia with sparse mitotic figures, including an occasional atypical form	Myomectomy Additional TAH, BSO, and bilateral pelvic lymphadenectomy	Unknown	-
4 ⁵	Age: 38 yr Gyn hx: gravida 1, para 0 Clinical sign: chronic pelvic pain and dysmenorrhea Tumor marker CEA and AFP: normal CA125: 45 U/mL	Size: 1.5 cm Location: right cornual area Micro: Irregular glands with benign epithelium surrounded by a hypercellular spindle cell stroma showing rare mitoses, mild nuclear hyperchromasia, and pleomorphism	Exploratory laparotomy, TAH, LSO, and omentectomy Adjuvant cisplatin, ifosfamide, and mesna 5,500 cGy to the abdominal wall	Disease-free 30 mo after treatment	Heterologous element (rhabdomyosarcoma)
5 ¹⁰	Age: 52 yr Gyn hx: gravida 3, para 3 Peri-menopausal	Size: uncheckable (no distinct mass formation) Location: uterine fundus Micro: Diffuse adenomyosis with focal stromal expansion, consisting of a hypercellular proliferation of moderately atypical spindle cells with mitotic activity around benign endometrial glands and infiltrating the anterior myometrium	Radical hysterectomy with BSO and lymph node dissection and debulking of the pelvic mass	Unknown	Extrauterine pelvic mass (19 cm in diameter) diagnosed as adenosarcoma with rhabdomyosarcomatous differentiation and stromal overgrowth

(Continued to the next page)

Table 1. Continued

Case No. (ref No.)	Clinical feature	Pathology	Treatment	Outcome	Remarks
6 ¹⁴	Clinical sign: none Tumor marker CA125: 258 U/mL Age: 53 yr	Size: unknown	Unknown	Unknown	Developed breast carcinoma and received adjuvant chemotherapy including tamoxifen
	Gyn hx: unknown Clinical sign: unknown Tumor marker: unknown	Location: unknown Micro: Uterine adenosarcoma following an adenomyoma			
7	Age: 40 yr	Size: 7.5 cm	Laparoscopically assisted TVH	No evidence of recurrence to date	This case
	Gyn hx: gravida 2, para 2 Clinical sign: sudden-onset suprapubic pain and initial low back pain Tumor marker CA125: 5,000 U/mL CA19-9: 39 U/mL β -hCG, AFP: normal	Location: uterine fundus Micro: Dilated glandular elements and abundant, hypercellular stromal elements Expansile growth within the myometrium with extensive myometrial invasion and focal infiltration with expansile margin into the subserosa Focal involvement of adenomyosis	Additional BSO		

Gyn Hx, gynecological history; hCG, human chorionic gonadotropin; Micro, microscopic findings; TAH, total abdominal hysterectomy; BSO, bilateral salpingo-oophorectomy; LSO, left salpingo-oophorectomy; CEA, carcinoembryonic antigen; AFP, α -fetoprotein; CA, carbohydrate antigen; TVH, total vaginal hysterectomy.

chromosomes 2, 8, 10, 13, 19, and 21.¹⁸ Finally, studies have also suggested that the use of tamoxifen may have a role in the pathogenesis of adenosarcoma.^{1,14}

Several types of uterine tumors, including adenofibroma, adenosarcoma, and carcinosarcoma, consist of mixtures of epithelial and stromal components.¹³ Because they include large hypocellular areas and infrequent mitoses, adenosarcomas are difficult to histologically differentiate from adenofibromas, endometriosis and adenomyosis. Especially on a background of adenomyosis, a conclusive pathologic differential diagnosis may be more difficult, because florid adenomyosis can prevent an accurate initial diagnosis. In typical adenomyosis, the volume of the endometrial stromal component is low relative to the volume of smooth muscle.² Moreover, although endometrial stromal cells have mitotic activity, they show no evidence of significant cytological atypia.² Similarly, stromal mitoses of ≥ 2 per 10 HPFs, marked stromal cellularity, and significant stromal cell atypia can differentiate Müllerian adenosarcoma from Müllerian adenofibroma.¹⁶ In one study, the diagnoses of eight adenomyomas were revised as adenofibroma, atypical polypoid adenomyoma, adenocarcinoma, and adenosarcoma.¹⁹ The adenofibroma contains variably cellular fibrous tissue in stroma,

Table 2. The 2009 FIGO staging system for uterine adenosarcoma

Stage	Definition
I	Tumor limited to uterus
IA	Tumor limited to endometrium/endocervix with no myometrial invasion
IB	$\leq 50\%$ myometrial invasion
IC	$> 50\%$ myometrial invasion
II	Tumor extension beyond the uterus, within the pelvis
IIA	Adnexal involvement
IIB	Involvement of other pelvic tissues
III	Tumor invasion of abdominal tissues (not just protruding into the abdomen)
IIIA	1 site
IIIB	> 1 site
IIIC	Metastasis to pelvic and/or para-aortic lymph nodes
IV	
IVA	Tumor invasion of bladder and/or rectum
IVB	Distant metastasis

FIGO, International Federation of Gynecology and Obstetrics.

but lacks the smooth muscle and endometrial stromal tissue present in adenomyoma.² In adenosarcoma, the endometrial stromal tissue predominates, not the smooth muscle component, and the glands are no longer evenly distributed but are more widely

separated due to stromal expansion.² Smooth muscle may be found in the stroma of adenosarcomas, but it is rarely prominent.² Typically, cambium layer is not found in adenomyoma, which is characteristic for adenosarcomas.² Although mitotic activities in stroma have been reported in a few cases of adenomyomas, the stromal atypia is not found in these tumors.² Finally, adenosarcoma may show myometrial and vascular invasion.² Evidences that the tumor in our patient was a low-grade Müllerian adenosarcoma included an extensive expansile growth pattern of stromal and glandular tissue throughout the myometrium with involvement of the uterine serosal surface, the presence of epithelial metaplasia within the glandular components of the tissue, and frequent mitoses.

Müllerian adenosarcoma has been regarded as a low-grade tumor with a fair prognosis. Most tumors can be cured with surgery, but recurrence is associated with poor outcomes.⁷ Müllerian adenosarcomas rarely give rise to distant metastasis. The outcome of uterine adenosarcomas is associated with many factors, including the grade and mitotic activity of the stromal component; however, the presence of sarcomatous overgrowth and invasion into the myometrium, the key factors of the FIGO staging system, are the most important.² Unlike most adenosarcomas, those comprising more than 25% of the sarcomatous component are considered high-grade.¹³ These tumors are more aggressive than most Müllerian adenosarcomas, which are usually of low malignant potential.¹⁶ One study found that 38% of patients had recurrent disease, with histologic sarcomatous overgrowth being a predictor of poor prognosis ($p = .03$).⁶ A second study reported recurrence in 36% of patients with adenosarcoma with myometrial invasion, and the risk of recurrence in the absence of myoinvasion was only 7%.²⁰ Tumors that arise in the ovaries and extrauterine sites tend to have a higher recurrence rate, perhaps due to the lack of a physical barrier preventing spread within the pelvis and abdomen.¹

Because adenosarcomas occasionally show an aggressive clinical behavior, despite benign or low-grade microscopic appearance, an aggressive therapeutic approach has been recommended.⁷ However, caution should be exercised, as it may lead to overtreatment of some patients.⁷ The current treatment of choice is hysterectomy and bilateral salpingo-oophorectomy; however, some patients have undergone selective myomectomies, with variable results.^{2,10,13} Tumors showing a pattern of sarcomatous overgrowth require more aggressive surgery.¹³ Imaging with PET-CT and MRI may be helpful for preoperative planning, monitoring the treatment response, and postoperative surveillance and restaging.¹³ Platin-based adjuvant chemotherapy and radiotherapy have been used to treat patients with aggressive prognostic factors, such as deep myometrial invasion and sarcomatous overgrowth.²⁷

The lack of a staging system for uterine adenosarcoma led to development of the FIGO staging system for endometrial carcinomas.³ The new FIGO staging system for uterine adenosarcoma, published in 2009, is identical to that for endometrial stromal sarcoma⁹ (Table 2) and is an improvement on the earlier generic application of the 1988 FIGO staging system for endometrial cancer to adenosarcoma.⁸

Because of tumor involvement of the outer half of the myometrium, the tumor in our case would be staged as IC (deeply myoinvasive) according to the new FIGO staging system for uterine sarcomas.⁹ Stage IC tumors would normally be considered for adjuvant treatment.² However, the FIGO staging applies to adenosarcomas that arise in the endometrium and invade into the myometrium.² Thus, use of a staging system that does not consider adenosarcomas that arise *ab initio* within the myometrium, and are confined to this layer, would have resulted in overstaging of the adenosarcoma in our patient.²

To date, there are no specific staging guidelines for tumors arising from adenomyosis. In a series of case reports, two previous cases of adenosarcomas were reported to be problematic in staging.⁸ The first was a tumor that arose in the eutopic endometrium with involvement of underlying adenomyosis but without myometrial invasion. The second was a tumor located in an intramural adenomyoma with no evidences of a primary lesion in the eutopic endometrium. It was suggested that these tumors should be noted as adenosarcoma, intramural stage I am1 or am2, whether the involved adenomyosis/adenomyoma was located in the inner or outer half of the myometrium. Such a classification system would facilitate reliable data collection, allowing the formulation of an evidence-based staging system for these tumors.⁸

In conclusion, this report describes the clinical and pathologic findings of a rare extraendometrial, intramural adenosarcoma arising from adenomyosis without eutopic endometrial involvement in a 40-year-old woman. Malignant transformation of adenomyosis should be considered in the differential diagnosis of a huge solid and cystic uterine mass. To avoid overstaging and inappropriate treatment, it is important to recognize that adenosarcomas can, although rarely, arise from adenomyosis. Collection of additional data and prospective studies will provide a clearer understanding of the malignant transformation of adenomyosis and may provide more evidences for an upgraded staging system.

Conflicts of Interest

No potential conflict of interest relevant to this article was reported.

Acknowledgments

This research was supported by Basic Science Research Program through the National Research Foundation of Korea (NRF) funded by the Ministry of Education (NRF-2017R1D1A1B03036519).

REFERENCES

- Pinto A, Howitt B. Uterine adenosarcoma. *Arch Pathol Lab Med* 2016; 140: 286-90.
- Elshafie M, Rahimi S, Ganesan R, Hirschowitz L. Müllerian adenosarcoma arising in a subserosal adenomyoma. *Int J Surg Pathol* 2013; 21: 186-9.
- McCluggage WG. Müllerian adenosarcoma of the female genital tract. *Adv Anat Pathol* 2010; 17: 122-9.
- Raffaelli R, Piazzola E, Zanconato G, Fedele L. A rare case of extra-uterine adenosarcoma arising in endometriosis of the rectovaginal septum. *Fertil Steril* 2004; 81: 1142-4.
- Gollard R, Kosty M, Bordin G, Wax A, Lacey C. Two unusual presentations of mullerian adenosarcoma: case reports, literature review, and treatment considerations. *Gynecol Oncol* 1995; 59: 412-22.
- Verschraegen CF, Vasuratna A, Edwards C, *et al.* Clinicopathologic analysis of Müllerian adenosarcoma: the M.D. Anderson Cancer Center experience. *Oncol Rep* 1998; 5: 939-44.
- Liu L, Davidson S, Singh M. Müllerian adenosarcoma of vagina arising in persistent endometriosis: report of a case and review of the literature. *Gynecol Oncol* 2003; 90: 486-90.
- Clarke BA, Mulligan AM, Irving JA, McCluggage WG, Oliva E. Müllerian adenosarcomas with unusual growth patterns: staging issues. *Int J Gynecol Pathol* 2011; 30: 340-7.
- Prat J. FIGO staging for uterine sarcomas. *Int J Gynaecol Obstet* 2009; 104: 177-8.
- Jha P, Ansari C, Coakley FV, *et al.* Case report: Imaging of Müllerian adenosarcoma arising in adenomyosis. *Clin Radiol* 2009; 64: 645-8.
- Major FJ, Blessing JA, Silverberg SG, *et al.* Prognostic factors in early-stage uterine sarcoma: a Gynecologic Oncology Group study. *Cancer* 1993; 71(4 Suppl): 1702-9.
- Abeler VM, Royne O, Thoresen S, Danielsen HE, Nesland JM, Kristensen GB. Uterine sarcomas in Norway: a histopathological and prognostic survey of a total population from 1970 to 2000 including 419 patients. *Histopathology* 2009; 54: 355-64.
- Early HM, McGahan JP, Naderi S, Lamba R, Fananapazir G. Mullerian adenosarcoma: a malignant progression of adenomyosis? Pictorial review with multimodality imaging. *J Ultrasound Med* 2015; 34: 2109-13.
- Bocklage T, Lee KR, Belinson JL. Uterine Müllerian adenosarcoma following adenomyoma in a woman on tamoxifen therapy. *Gynecol Oncol* 1992; 44: 104-9.
- Oda Y, Nakanishi I, Tateiwa T. Intramural Müllerian adenosarcoma of the uterus with adenomyosis. *Arch Pathol Lab Med* 1984; 108: 798-801.
- Clement PB, Scully RE. Müllerian adenosarcoma of the uterus: a clinicopathologic analysis of 100 cases with a review of the literature. *Hum Pathol* 1990; 21: 363-81.
- Howitt BE, Sholl LM, Dal Cin P, *et al.* Targeted genomic analysis of Müllerian adenosarcoma. *J Pathol* 2015; 235: 37-49.
- Chen Z, Hong B, Drozd-Borysiuk E, Coffin C, Albritton K. Molecular cytogenetic characterization of a case of Müllerian adenosarcoma. *Cancer Genet Cytogenet* 2004; 148: 129-32.
- Gilks CB, Clement PB, Hart WR, Young RH. Uterine adenomyomas excluding atypical polypoid adenomyomas and adenomyomas of endocervical type: a clinicopathologic study of 30 cases of an under-emphasized lesion that may cause diagnostic problems with brief consideration of adenomyomas of other female genital tract sites. *Int J Gynecol Pathol* 2000; 19: 195-205.
- Gallardo A, Prat J. Müllerian adenosarcoma: a clinicopathologic and immunohistochemical study of 55 cases challenging the existence of adenofibroma. *Am J Surg Pathol* 2009; 33: 278-88.

Metastatic Squamous Cell Carcinoma from Lung Adenocarcinoma after Epidermal Growth Factor Receptor Tyrosine Kinase Inhibitor Therapy

Hyung Kyu Park · Youjeong Seo · Yoon-La Choi · Myung-Ju Ahn¹ · Jounggho Han

Department of Pathology and Translational Genomics, ¹Division of Hematology and Oncology, Department of Medicine, Samsung Medical Center, Sungkyunkwan University School of Medicine, Seoul, Korea

Inhibition of mutated epidermal growth factor receptor (EGFR), EGFR tyrosine kinase inhibitor (TKI), is one of the most successful cancer targeted therapies.¹ While this therapy has been beneficial for many non-small cell lung cancer (NSCLC) patients with activated *EGFR* mutations, almost all patients inevitably develop acquired resistance which limits the median response duration to around 1 year.² Most of the mechanisms leading to EGFR TKI resistance are additional mutation or amplification of alternative pathways, and morphological transformation to small cell lung cancer (SCLC).³

Recently, several authors reported another type of morphologic transformation for EGFR TKI resistance, namely, transformation from adenocarcinoma to squamous cell carcinoma.⁴⁻⁶ However, the reports were of limited value because they were based only on biopsied specimens. This report describes a case of lung adenocarcinoma with transformation to squamous cell carcinoma that was established histological evaluation of lobectomy specimen.

CASE REPORT

A 40-year-old man with a 23-year smoking history received a medical check-up, which revealed a solitary pulmonary nodule. Chest computed tomography revealed a 17-mm-sized tumor at

the peripheral posterior segment of the right upper lobe (clinically T1aN0M0). The patient underwent a right upper lobectomy with mediastinal lymph node dissection. Histological examination showed a 1.3-cm-sized poorly differentiated adenocarcinoma with solid and acinar growth patterns with visceral pleural invasion and no lymph node metastasis (pT2aN0). The tumor cells showed marked nuclear atypia, numerous mitoses (23/10 high power field [HPF]) and multifocal microscopic necrosis. The tumor was dissected and entirely embedded. We morphologically and immunohistochemically evaluated all tumor sections to rule out the possibility of adenosquamous carcinoma (Fig. 1A–E). The patient received adjuvant chemotherapy with combined vinorelbine and cisplatin.

Four years later, multiple metastatic lesions were found at the right lower lobe, right pleura, right fifth rib, and right femoral head. *EGFR* mutation analysis, using a previously resected lobectomy specimen, revealed a deletion at exon 19 of the *EGFR* gene. The patient was treated with afatinib, which is an EGFR TKI and radiation therapy. The patient showed partial remission of the tumor.

Two years later, the patient developed multiple metastatic lesions throughout the body, including a telangiectatic nodule on the scalp. A punch biopsy was performed and histologic evaluation of the biopsied specimen showed a tumorous lesion in the deep dermis. This tumor showed squamoid appearance with sheet-like growth patterns and evident intercellular bridges. Compared to the previous lobectomy specimen, the tumor cells were more bland with moderate nuclear atypia, some mitotic activity (13/10 HPF) and no necrosis. Immunohistochemical staining showed diffuse and strong p63 immunoreactivity and no thyroid transcription factor 1 immunoreactivity (Fig. 1F–J).

Corresponding Author

Jounggho Han, MD
Department of Pathology and Translational Genomics, Samsung Medical Center, Sungkyunkwan University School of Medicine, 81 Irwon-ro, Gangnam-gu, Seoul 06351, Korea
Tel: +82-2-3410-2765, Fax: +82-2-3410-0025, E-mail: hanjho@skku.edu

Received: August 24, 2016 Revised: October 16, 2016

Accepted: October 17, 2016

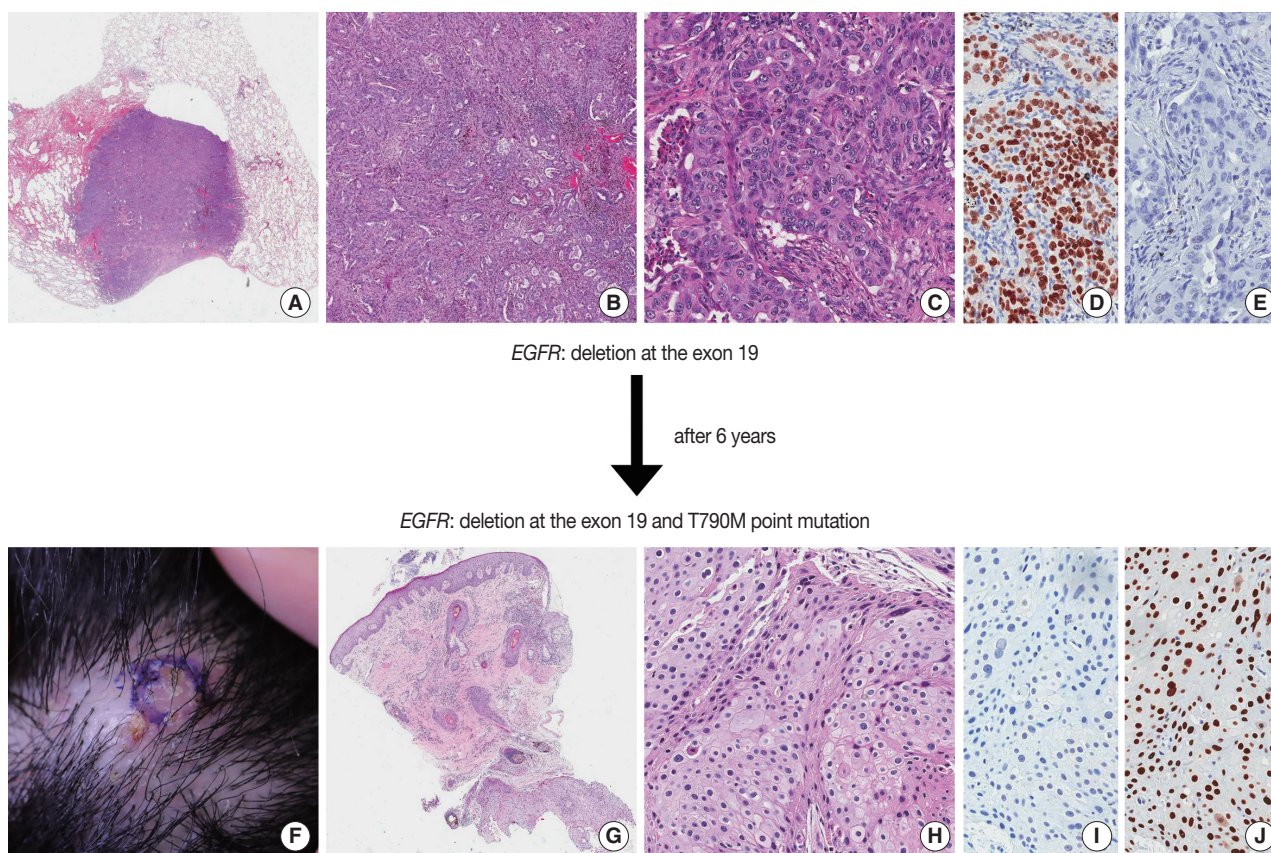


Fig. 1. Squamous metastasis from lung adenocarcinoma. Initial lobectomy specimen (A–E) and punch biopsy specimen of the scalp (F–J). (A–C) The well-demarcated adenocarcinoma with solid and acinar growth patterns was found in the lobectomy specimen. The tumor shows thyroid transcription factor 1 immunoreactivity (D) and no p63 immunoreactivity (E). Punch biopsy specimen of the telangiectatic nodule on scalp (F) shows a tumorous lesion at the deep dermis (G). (H) This tumor shows a squamoid appearance with a sheet-like growth pattern. The tumor shows no TTF-1 immunoreactivity (I) and diffuse p63 immunoreactivity (J). EGFR, epidermal growth factor receptor.

EGFR mutation analysis, using a biopsied specimen, revealed a deletion at exon 19 of the *EGFR* gene and an additional T790M point mutation. After several special and immunohistochemical stainings, this tumor was diagnosed as a metastatic carcinoma from the lung with squamous differentiation. The patient informed consent was waived by the Institutional Review Board of the Samsung Medical Center (2016-08-109).

DISCUSSION

Lung cancer is the most common cause of cancer deaths in Korea.⁷ Traditional therapy, including resection, platinum-based chemotherapy and radiation therapy, have only limited therapeutic value. Therefore, the 5-year survival rate of lung cancer has not changed significantly in the past 30 years.⁸

EGFR TKI therapy, which specifically targets EGFR, was recently introduced and provided guidance in this situation. Targeting EGFR in patients with activating *EGFR* mutations

has shown initial and significant success in practice.¹ Unfortunately, the vast majority of patients develop resistance to the treatment, typically in less than 1 year. In this situation, understanding the mechanism of the resistance became very important.

Most of the mechanisms that lead to EGFR TKI resistance involve an additional mutation, such as a T790M mutation, or amplification of alternative pathways. In addition, morphological transformation is also a well-known mechanism. The most well known example of this interesting phenomenon is the transformation from NSCLC to SCLC.⁹

Recently, several authors have described histologic transformation from lung adenocarcinoma to squamous cell carcinoma as a mechanism of resistance to EGFR TKI therapy.⁴⁻⁶ In four previously reported cases, all four patients were female and three of them had never been smokers. The most common *EGFR* mutation was an L858R point mutation and the most common acquired gene alteration was a T790M point mutation. All cases showed the same *EGFR* mutation in both primary

and metastatic carcinomas.

The mechanism of this morphologic transformation is still poorly understood. Possible explanations include (1) small population of squamous cell carcinoma phenotype cells are already present before the EGFR TKI therapy and selectively survive during EGFR TKI therapy; or (2) carcinoma cells acquire a different morphologic phenotype during EGFR TKI therapy.⁶

Considering that primary adenosquamous carcinoma shows the same mutations in both adenocarcinoma and squamous cell carcinoma components, additional studies are needed and a solution is beyond the scope of this report.

In conclusion, lung primary adenocarcinoma can transform into squamous cell carcinoma after EGFR TKI therapy. We should be aware of this phenomenon to avoid misdiagnosis in practice.

Conflicts of Interest

No potential conflict of interest relevant to this article was reported.

REFERENCES

1. Stewart EL, Tan SZ, Liu G, Tsao MS. Known and putative mechanisms of resistance to EGFR targeted therapies in NSCLC patients with EGFR mutations-a review. *Transl Lung Cancer Res* 2015; 4: 67-81.
2. Choi CM, Lee JC. Mechanisms of acquired resistance to epidermal growth factor receptor inhibitors and overcoming strategies in lung cancer. *J Lung Cancer* 2012; 11: 59-65.
3. Yu HA, Arcila ME, Rekhtman N, *et al.* Analysis of tumor specimens at the time of acquired resistance to EGFR-TKI therapy in 155 patients with *EGFR*-mutant lung cancers. *Clin Cancer Res* 2013; 19: 2240-7.
4. Jukna A, Montanari G, Mengoli MC, *et al.* Squamous cell carcinoma "transformation" concurrent with secondary T790M mutation in resistant *EGFR*-mutated adenocarcinomas. *J Thorac Oncol* 2016; 11: e49-51.
5. Kuiper JL, Ronden MI, Becker A, *et al.* Transformation to a squamous cell carcinoma phenotype of an *EGFR*-mutated NSCLC patient after treatment with an EGFR-tyrosine kinase inhibitor. *J Clin Pathol* 2015; 68: 320-1.
6. Levin PA, Mayer M, Hoskin S, Sailors J, Oliver DH, Gerber DE. Histologic transformation from adenocarcinoma to squamous cell carcinoma as a mechanism of resistance to EGFR inhibition. *J Thorac Oncol* 2015; 10: e86-8.
7. Jung KW, Won YJ, Kong HJ, *et al.* Cancer statistics in Korea: incidence, mortality, survival, and prevalence in 2012. *Cancer Res Treat* 2015; 47: 127-41.
8. Cagle PT, Chirieac LR. Advances in treatment of lung cancer with targeted therapy. *Arch Pathol Lab Med* 2012; 136: 504-9.
9. Ahn S, Hwang SH, Han J, *et al.* Transformation to small cell lung cancer of pulmonary adenocarcinoma: clinicopathologic analysis of six cases. *J Pathol Transl Med* 2016; 50: 258-63.

Bronchial Washing Cytology of Pulmonary Langerhans Cell Histiocytosis: A Case Report

Taeyeong Kim · Hyeong Ju Kwon · Minseob Eom · Sang Wook Kim · Min Hi Sin · Soon-Hee Jung

Department of Pathology, Yonsei University Wonju College of Medicine, Wonju, Korea

Pulmonary Langerhans cell histiocytosis (PLCH) is a rare histiocytic interstitial lung disease, characterized by abnormal infiltration of Langerhans cells (LCs) with lung parenchyma destruction. PLCH can occur at any age, but is reported mainly in adults (between 20 and 40 years), especially those with a history of cigarette smoking. The clinical presentation can vary from no symptoms to severe respiratory symptoms.¹ PLCH is regarded as a reactive lesion rather than a neoplastic process, even though the proliferation of LCs is found in the lesion.²

PLCH is normally diagnosed from resected lung specimens. Cytological diagnostic methods such as bronchial washing or bronchoalveolar lavage (BAL) are used as a less invasive technique through bronchoscopy.³ Reports have indicated that BAL cytology can be helpful for diagnosing PLCH.⁴ However, the diagnosis of PLCH by bronchial washing cytology has not yet been reported. Herein, we present a case of PLCH diagnosed through bronchial washing cytology.

CASE REPORT

The 41-year-old male patient visited our hospital due to a cough that had persisted for 7 months. He had a history of 20 pack-year smoking and diabetes mellitus. Physical examination of the chest revealed fine crackle of both upper lung fields. There was no skin rash or palpable lymph node. The chest computed tomography (CT) showed multiple, irregularly-shaped cysts and

centrilobular nodules of variable sizes in both lungs (Fig. 1).

Bronchial washing cytology, BAL, and wedge resection of the lung were performed. The BAL slides revealed a fraction rate of 59.6% monocytes and 9.4% eosinophils with about 6.5% LCs. The bronchial washing slides showed scattered non-cohesive large cells with abundant, granular, and eosinophilic cytoplasm. These cells had grooved or convoluted nuclei with fine chromatin, delicate nuclear membranes, and prominent nucleoli. Immunohistochemical staining for CD1a was positive in these cells (Fig. 2).

The cut surface of the wedge-resected lung specimen revealed numerous cystic spaces with whitish gray stellate fibrous scars. Microscopic examination indicated multiple cystic spaces of variable sizes with diffuse alveolar wall thickening, cellular infiltration, and fibrosis. The infiltrated cells had eosinophilic cytoplasm and grooved or infolded nuclei. These cells were proven to be LCs based on immunohistochemical staining, showing strong positive reaction for CD1a and S-100 protein (Fig. 3).

Bronchial washing cytology was performed again during follow-up. Some cells with the features described above were detected on the bronchial washing cytology. Therefore, we used the same approach to determine that the PLCH was still present.

DISCUSSION

When patients with ongoing PLCH present at a hospital, non- or less-invasive pulmonological approaches, such as chest CT, pulmonary function test, and fiberoptic bronchoscopy, are usually performed. The cytological specimens obtained from fiberoptic bronchoscopy are then sent to the pathology department, and these cytological specimens can be challenging for pathologists to diagnose. The cytological diagnosis of PLCH with bronchial washing can be difficult because it is a rare disease with unfamiliar

Corresponding Author

Soon-Hee Jung, MD, PhD
Department of Pathology, Yonsei University Wonju College of Medicine, 20 Ilsan-ro, Wonju 26426, Korea
Tel: +82-33-741-1551, Fax: +82-33-731-6590, E-mail: soonheej@yonsei.ac.kr

Received: September 2, 2016 Revised: February 3, 2017

Accepted: February 15, 2017

features. Therefore, in this report, we focused on bronchial washing cytology findings of PLCH.

Some reports have presented cytological findings of Langerhans cell histiocytosis (LCH) that have arisen in various organs. Lee *et al.*⁵ reported a case of LCH in the mandible diagnosed with fine needle aspiration cytology and indicated that the smear revealed



Fig. 1. Chest computed tomography findings. There are multiple, variable-sized, irregularly-shaped cysts and centrilobular nodules in both lungs.

high cellularity, and that the LCs had abundant vacuolated cytoplasm with round or occasionally folded nuclei. The LC nuclei showed a fine granular chromatin pattern with prominent nucleoli. Ha *et al.*⁶ reported a case of LCH in lymph nodes using aspiration cytology similar to the case reported by Lee *et al.*⁵ In their study, the LCs had wrinkled or grooved nuclei with thin nuclear membranes and a delicate chromatin pattern. Multinucleated cells were also identified. In another report that applied fine needle aspiration LCH cytology, many of the cytological findings were similar, but the nucleoli were absent.⁷

Another cytological method applied fiberoptic bronchoscopy for diagnosing PLCH is BAL fluid analysis. Takizawa *et al.*³ conducted BAL fluid analysis in PLCH and found a high mean cell fraction rate for macrophages (75.2%) and a variable eosinophil fraction rate (1% to 16%). The LCs revealed chromatin-poor nuclei with well-developed nucleoli. Previously described cytological findings with quantitative analysis of PLCH in BAL fluid are summarized in Table 1. In two studies with CD1a-positive cells in PLCH, BAL fluid obtained from patients with PLCH revealed more than 5% CD1a-positive cells.^{8,9} In the present case, BAL

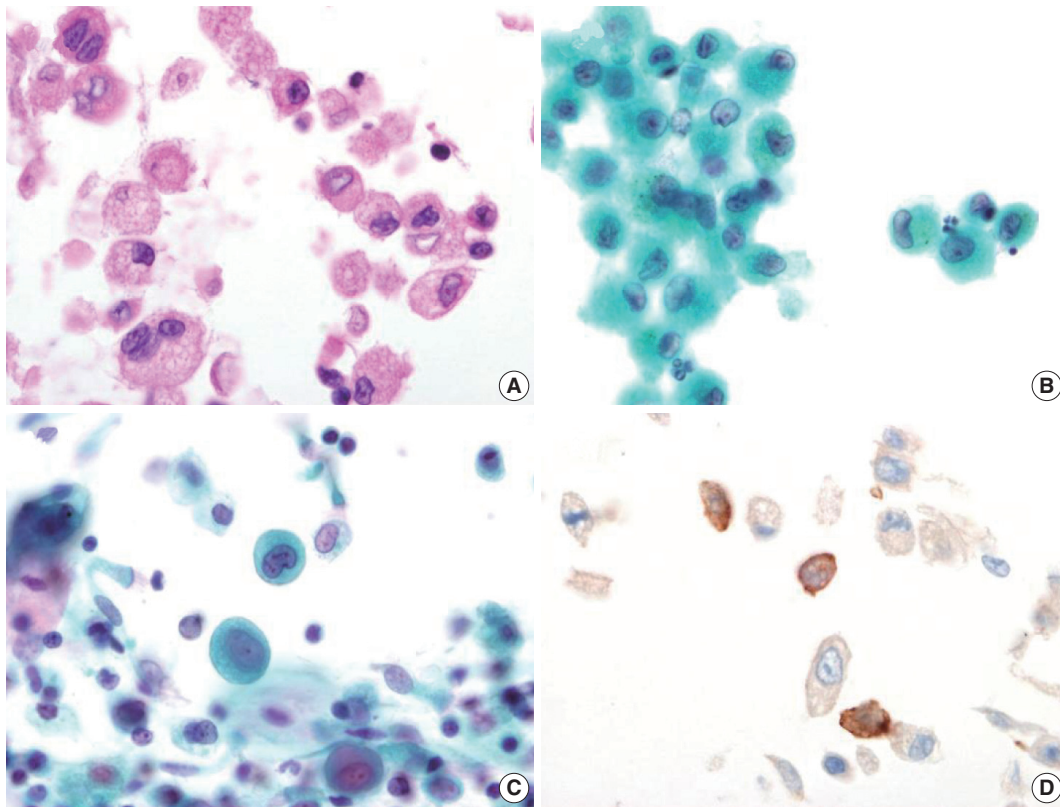


Fig. 2. Bronchial washing cytology. Bronchial washing cytology reveals many Langerhans cells. (A–C) The cells have abundant pale granular cytoplasm with a convoluted irregular nucleus and fine chromatin pattern (A, cell block; B, Thin prep; C, conventional smear). (D) Immunohistochemical staining for CD1a is positive in the Langerhans cells.

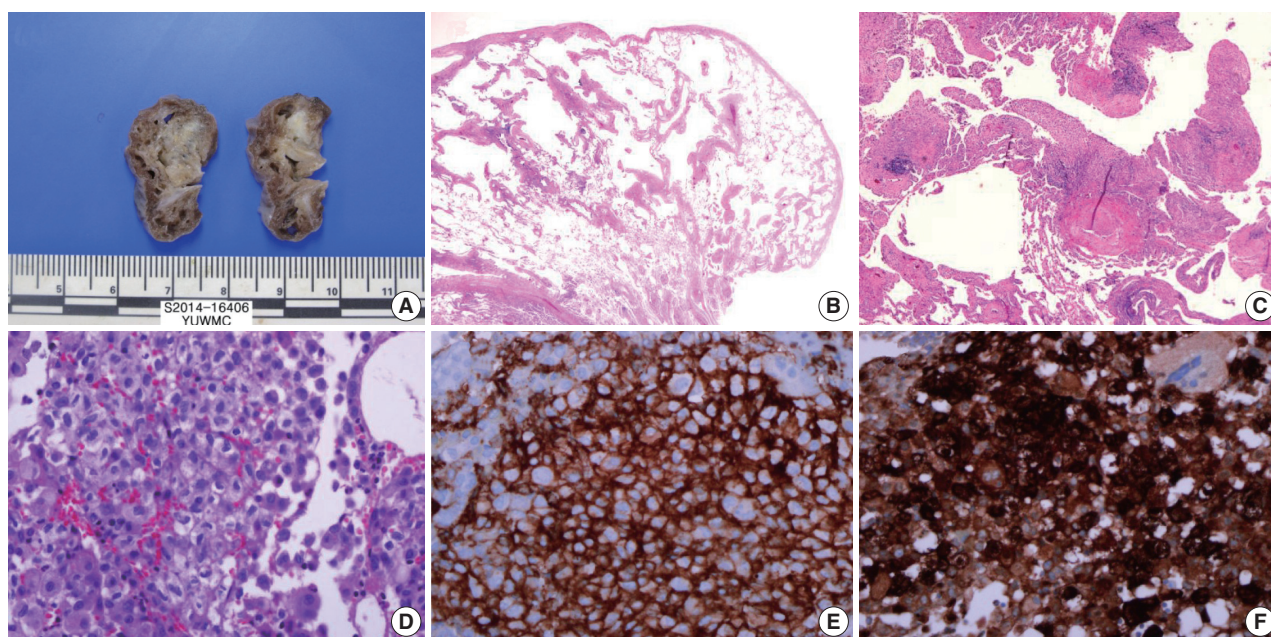


Fig. 3. Wedge resected lung via video-assisted thoracoscopic surgery. (A) The cut surface of the wedge-resected lung shows multiple numerous cystic spaces with white gray stellate fibrous scars. (B, C) There are multiple cystic spaces with diffuse thickening, cellular infiltration, and fibrous tissue. (D) The infiltrated cells have pale eosinophilic cytoplasm with grooved or infolded nuclei. (E, F) Immunohistochemical staining for CD1a and S-100 protein is positive in the proliferating cells.

Table 1. Summary of previously reported cytological findings of pulmonary Langerhans cell histiocytosis in bronchoalveolar lavage fluid

Study	Cytological finding	Langerhans cells (%)
Takizawa et al. ³	Clear and velvety cytoplasm	8.0 ± 1.3
	Oval or kidney-shaped, vesicular nuclei with irregular shapes	
	Nucleoli	
	Frequent groove and indentations	
Sharma and Dey ⁴	Nuclear grooving	16.5 (CD1a-positive cells)
	Bi-nucleation	
	Multinucleation	
This case	Pale and granular cytoplasm	6.5
	Indistinct cell border	
	Occasional binucleation or multinucleation	
	Grooved or convoluted nuclei	
	Prominent nucleoli	

fluid cytology showed similar fraction rates and cytological features. The percentage of LCs was about 6.5%. Based on these results, the 5% cut-off value of CD1a-positive cells or LCs could be postulated in BAL fluid cytology to make a PLCH diagnosis.

In this report, we described bronchial washing cytology findings of PLCH. These findings are similar to other studies describing aspiration cytology and BAL. A common finding in all of the previous reports indicates that grooved or infolded nuclei with abundant cytoplasm could be used as diagnostic features for LCs.

The difference in the present case compared with other reports could be that prominent nucleoli were observed only in some cells. The Birbeck granules are known as diagnostic LCH structures on electron microscopy (EM). However, EM study requires additional time and costs. We did not perform EM to detect Birbeck granules since other authors have suggested that it is not essential for diagnosing LCH.¹⁰

In conclusion, the possibility of LCH can be considered when bronchial washing cytology is mainly composed of Langerhans cells and eosinophils. In addition, more than 5% CD1a-positive cells in BAL fluid could be helpful for diagnosing PLCH. However, to date, there is no quantitative guideline for diagnosing PLCH. Therefore, additional cytological studies of PLCH, including quantitative analysis, are required to further identify and improve diagnostic approaches.

Conflicts of Interest

No potential conflict of interest relevant to this article was reported.

REFERENCES

1. Tazi A. Adult pulmonary Langerhans' cell histiocytosis. *Eur Respir J* 2006; 27: 1272-85.

2. Yousem SA, Colby TV, Chen YY, Chen WG, Weiss LM. Pulmonary Langerhans' cell histiocytosis: molecular analysis of clonality. *Am J Surg Pathol* 2001; 25: 630-6.
3. Takizawa Y, Taniuchi N, Ghazizadeh M, *et al.* Bronchoalveolar lavage fluid analysis provides diagnostic information on pulmonary Langerhans cell histiocytosis. *J Nippon Med Sch* 2009; 76: 84-92.
4. Sharma S, Dey P. Childhood pulmonary langerhans cell histiocytosis in bronchoalveolar lavage: a case report along with review of literature. *Diagn Cytopathol* 2016; 44: 1102-6.
5. Lee SR, Suh JH, Cha HJ, Kim YM, Choi HJ. Fine needle aspiration cytology of Langerhans cell histiocytosis of mandible: a case report. *Korean J Pathol* 2010; 44: 106-9.
6. Ha SY, Kim MJ, Kim GY, Cho HY, Chung DH, Kim NR. Fine needle aspiration cytology of Langerhans cell histiocytosis in a lymph node: a case report. *Korean J Cytopathol* 2007; 18: 87-91.
7. Kumar N, Sayed S, Vinayak S. Diagnosis of Langerhans cell histiocytosis on fine needle aspiration cytology: a case report and review of the cytology literature. *Patholog Res Int* 2011; 2011: 439518.
8. Auerswald U, Barth J, Magnussen H. Value of CD-1-positive cells in bronchoalveolar lavage fluid for the diagnosis of pulmonary histiocytosis X. *Lung* 1991; 169: 305-9.
9. Refabert L, Rambaud C, Mamou-Mani T, Scheinmann P, de Blic J. Cd1a-positive cells in bronchoalveolar lavage samples from children with Langerhans cell histiocytosis. *J Pediatr* 1996; 129: 913-5.
10. Kilpatrick SE. Fine needle aspiration biopsy of Langerhans cell histiocytosis of bone: are ancillary studies necessary for a "definitive diagnosis"? *Acta Cytol* 1998; 42: 820-3.

